ICSOBA 2014 Workshop

Hall-Héroult Cell Advanced Modelling Development

Dr. Marc Dupuis GENISIM

Introduction

In general, we can fit Hall-Héroult cell mathematical models into three broad categories:

- **Stress models which are generally associated with cell shell deformation and cathode heaving issues.**
- **Magneto-hydro-dynamic (MHD) models which are generally associated with the problem of cell stability.**
- **Thermal-electric models which are generally associated with the problem of cell heat balance.**

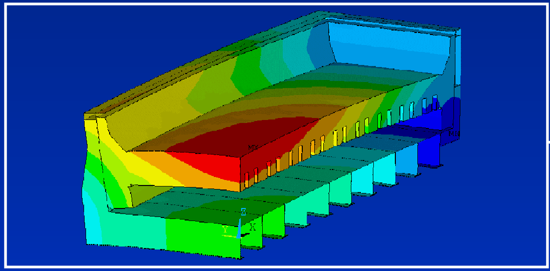

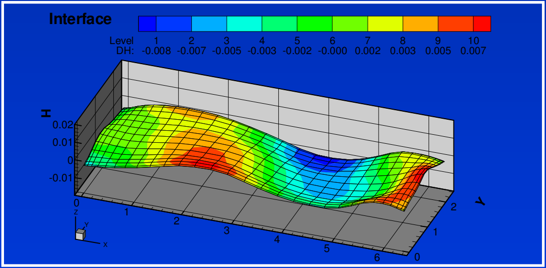

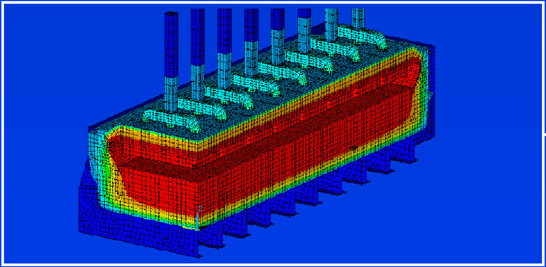

Cell Design

GENISIM

Introduction

The design of the smelter potroom building requires a forth categorie of models:

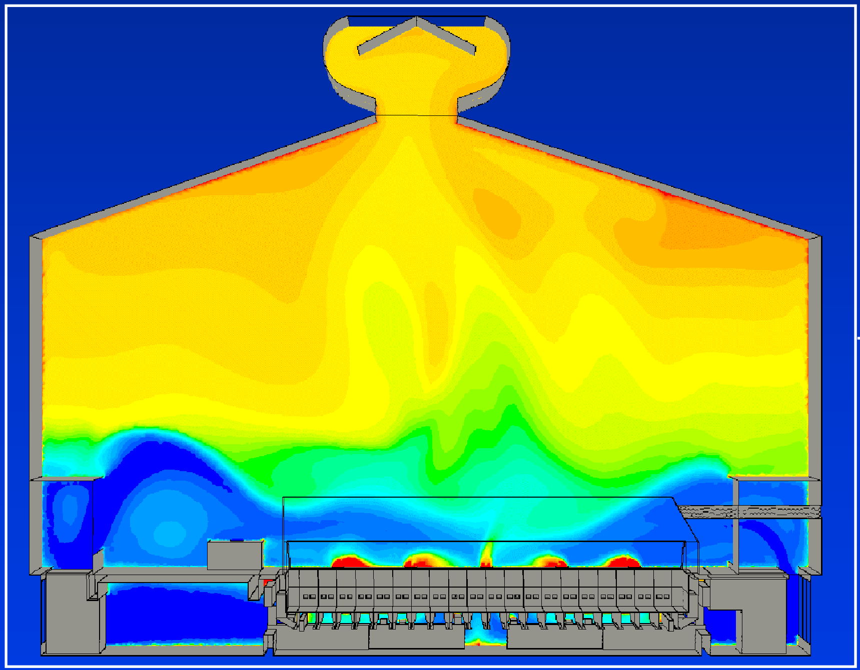

Potroom Design

1980-84, 2D potroom ventilation model

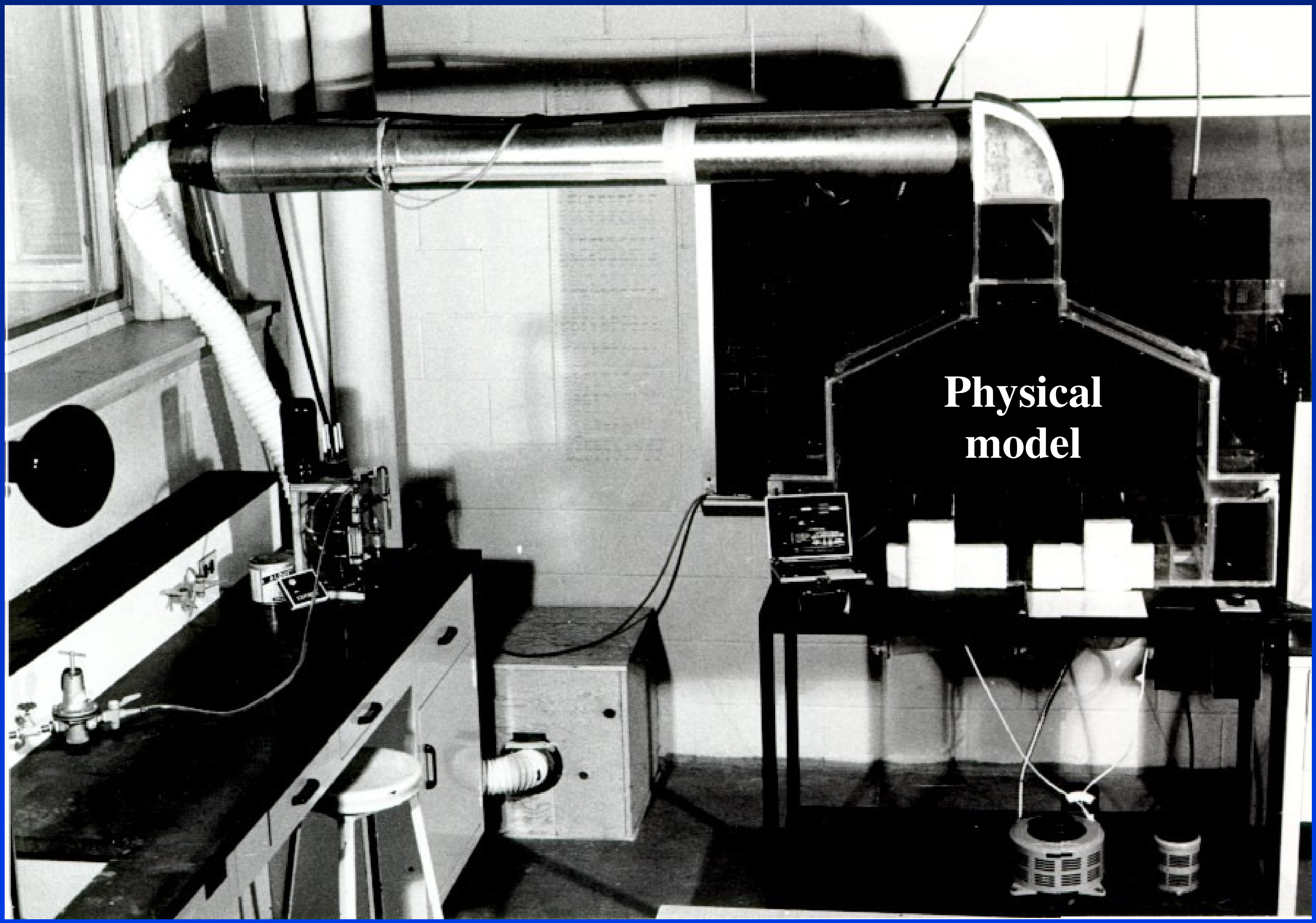

GENISIM

1980-84, 2D potroom ventilation model

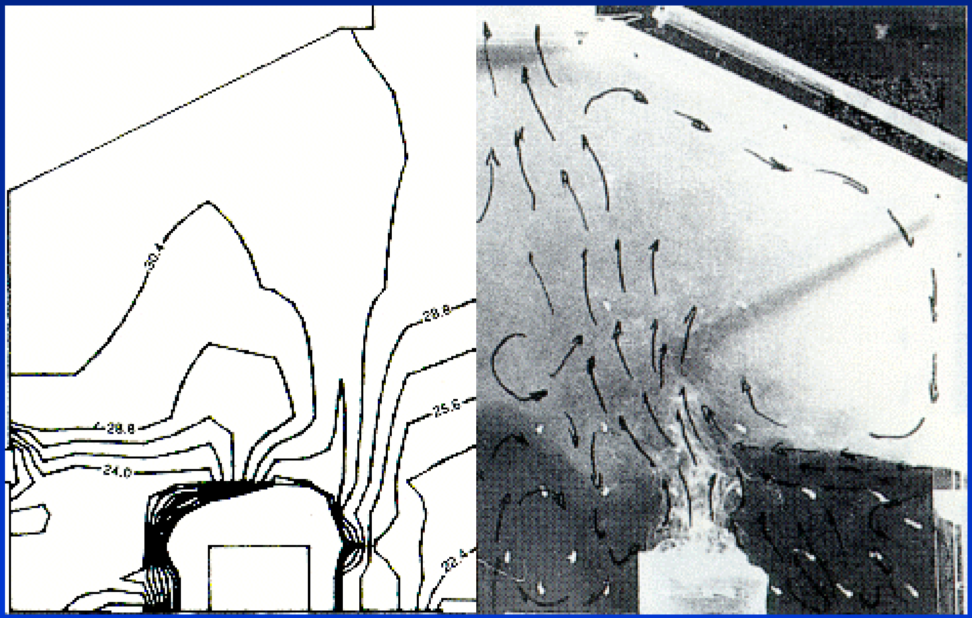

Experimental results

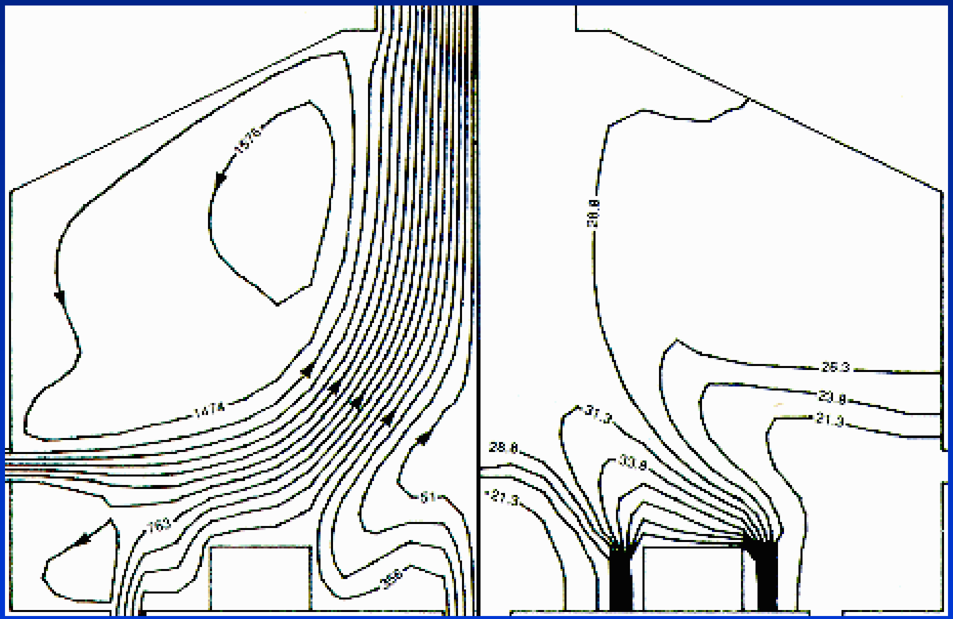

Best model results

The best results of my Ph.D. work: the 2D finite difference vorticity-stream function formulated model could not reproduces well the observed air flow regardless of the turbulence model used.

1984, 3D thermo-electric half anode model

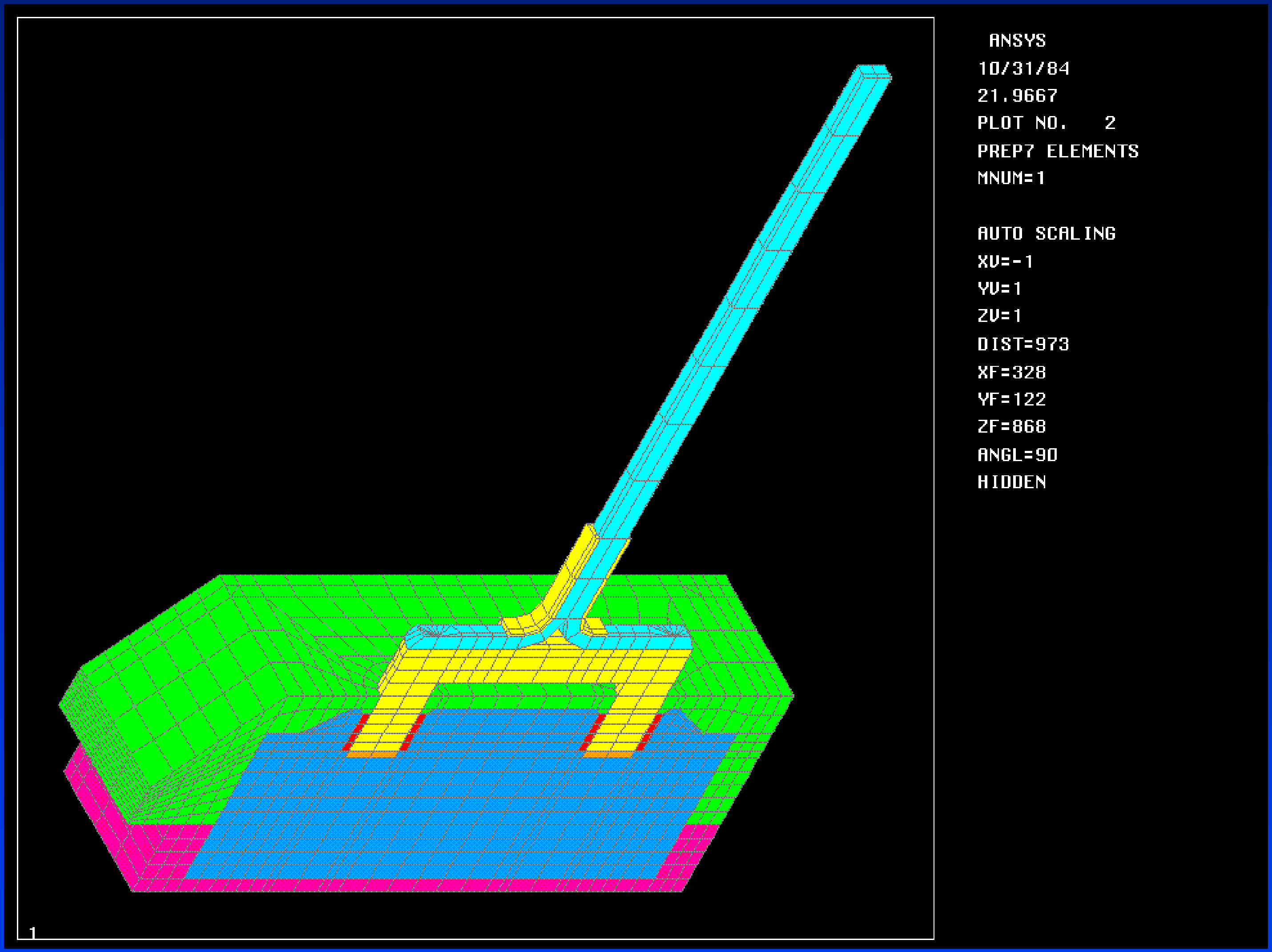

That model was developed on ANSYS 4.1 installed on a shaded VAX 780 platform.

That very first 3D half anode model of around 4000 Solid 69 thermo-electric elements took 2 weeks elapse time to compute on the VAX.

GENISIM

1986, 3D thermo-electric cathode side slice and cathode corner model

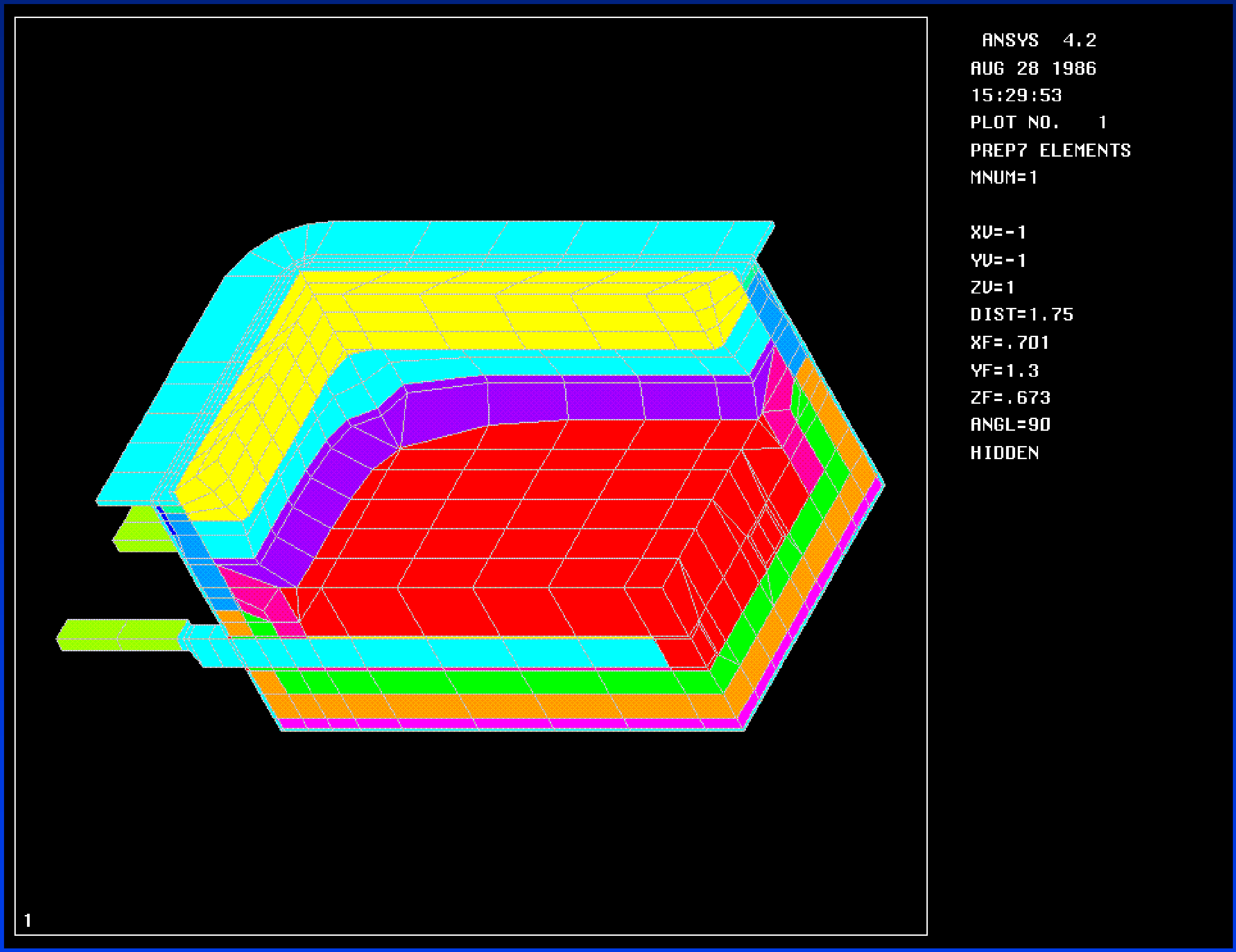

The next step was the development of a 3D cathode side slice thermo-electric model that included the calculation of the thickness of the solid electrolyte phase on the cell side wall .

Despite the very serious limitations on the size of the mesh, a full cathode corner was built next .

GENISIM

1988, 3D cathode potshell plastic deformation mechanical model

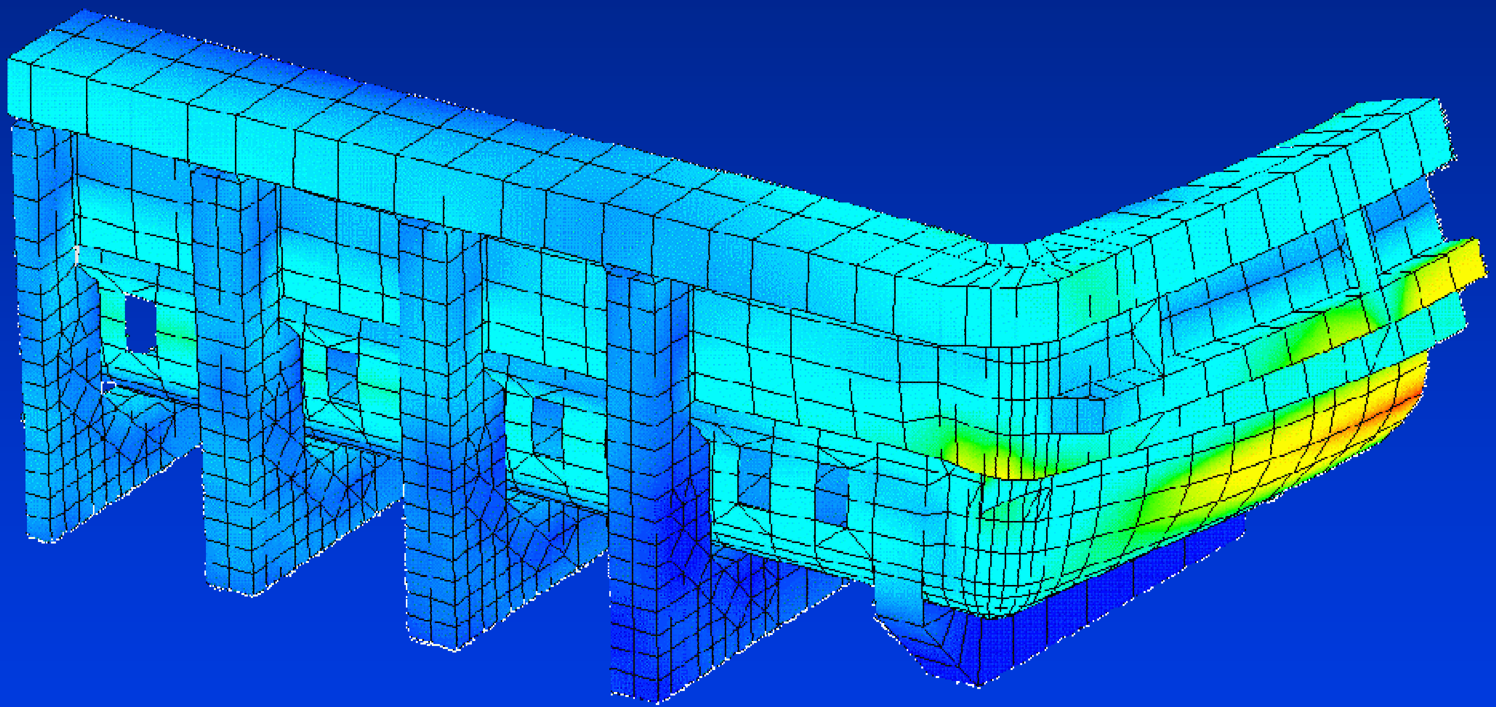

The new model type addresses a different aspect of the physic of an aluminum reduction cell, namely the mechanical deformation of the cathode steel potshell under its thermal load and more importantly its internal pressure load .

1988, 3D cathode potshell plastic deformation mechanical model

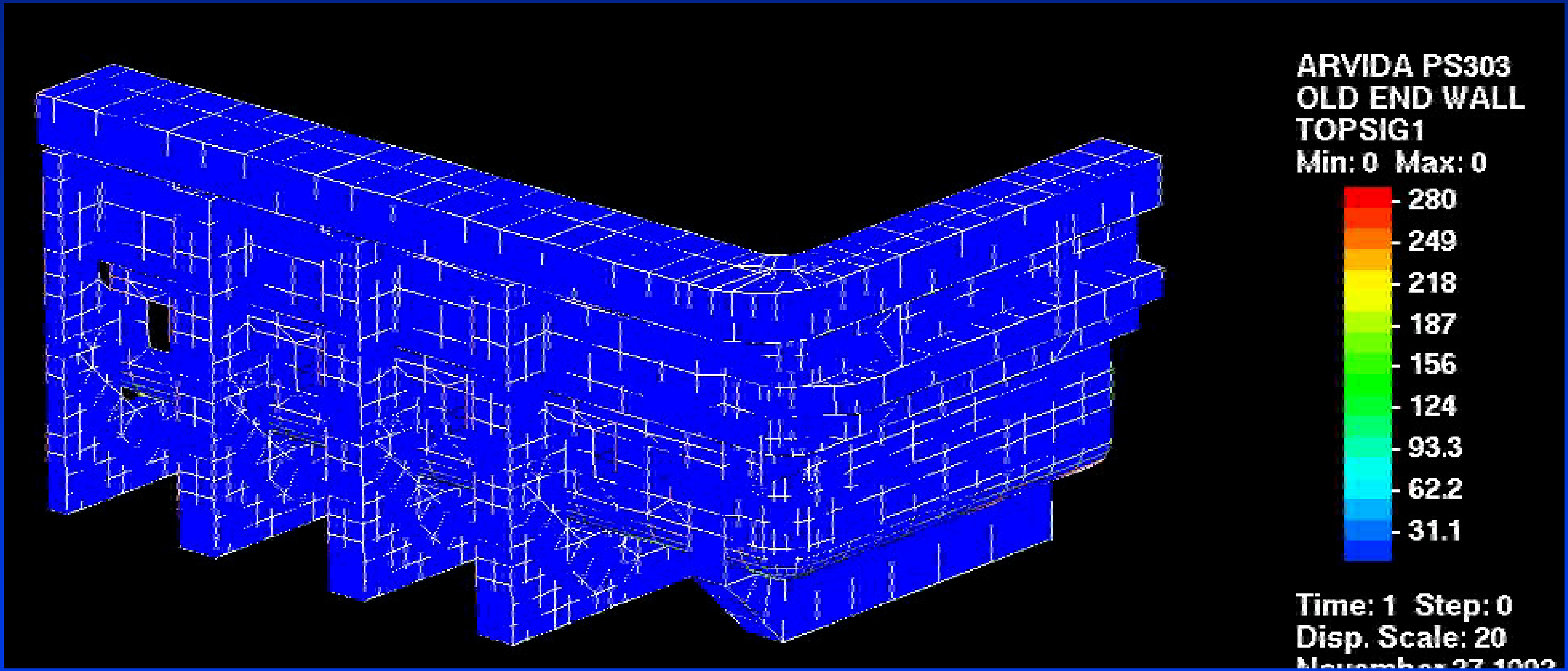

GENISIM

1989, 3D cathode potshell plastic deformation and lining swelling mechanical model

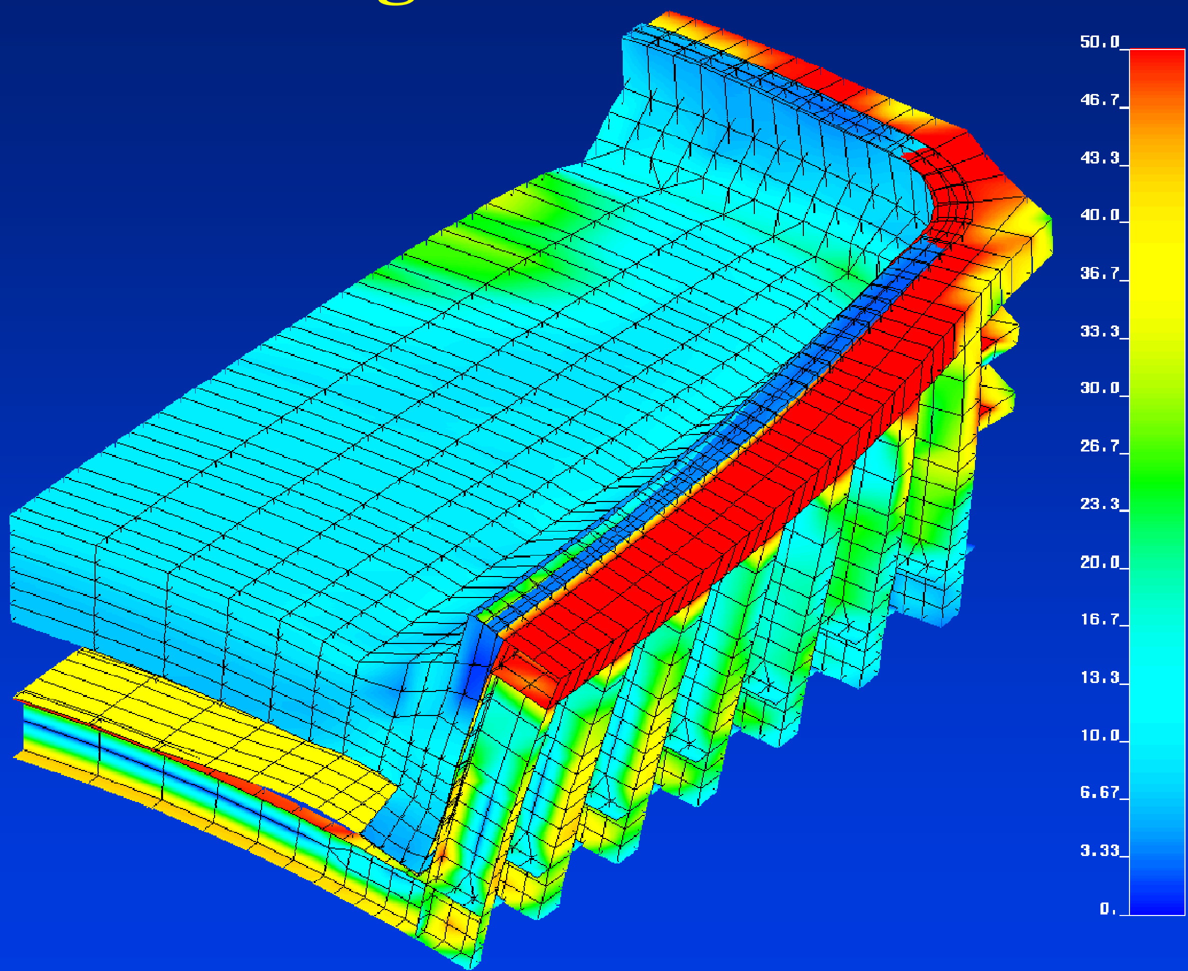

First "Half Empty shell" potshell model developed in 1989 and presented at a CRAY Supercomputing Symposium in 1990

GENISIM

1992, 3D thermo-electric quarter cathode model

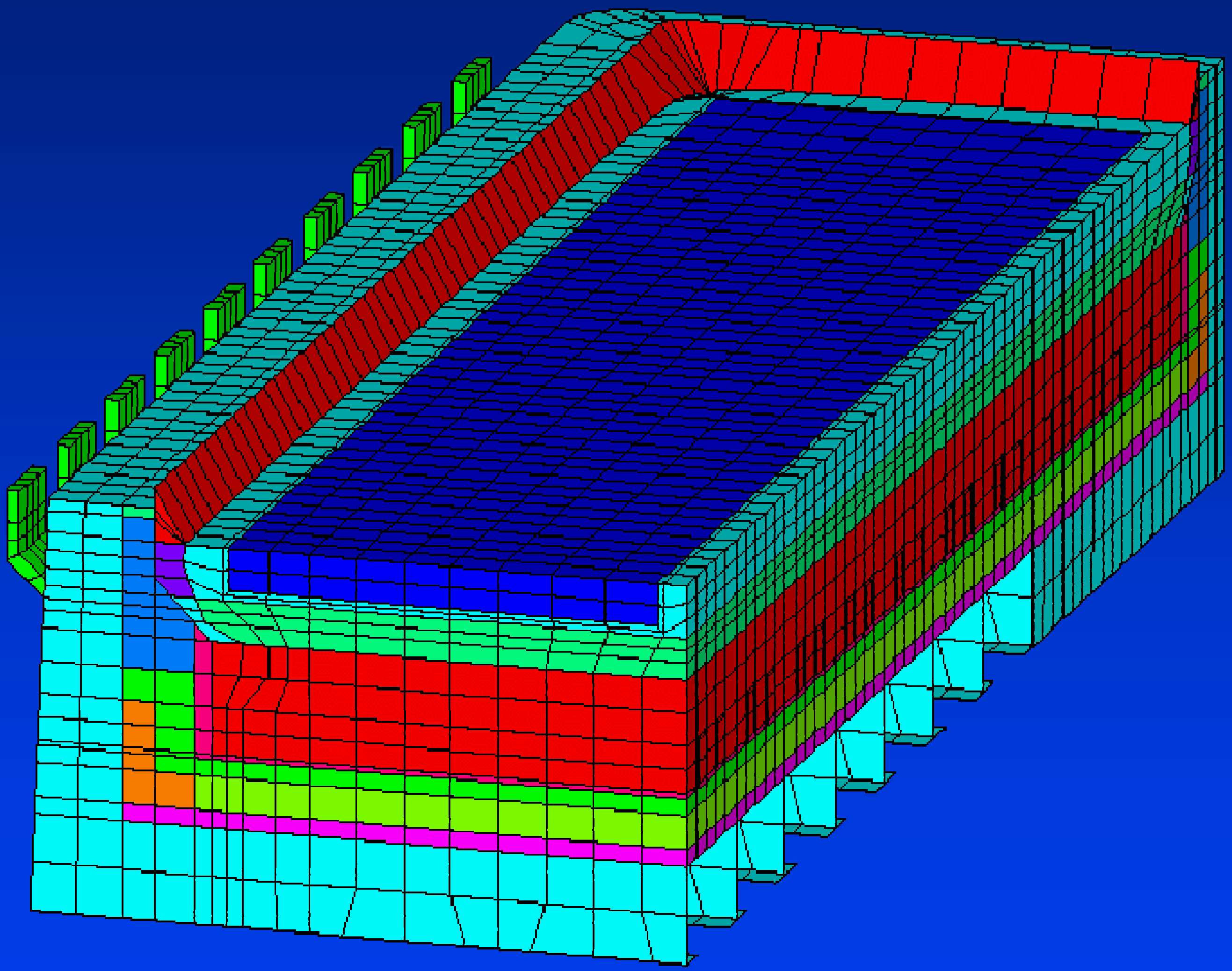

With the upgrade of the P-IRIS to 4D/35 processor, and the option to run on a CRAY XMP supercomputer, the severe limitations on the CPU usage were finally partially lifted.

This opened the door to the possibility to develop a full 3D thermo-electric quarter cathode model.

Full Cell Quarter Thermo-Electric Model

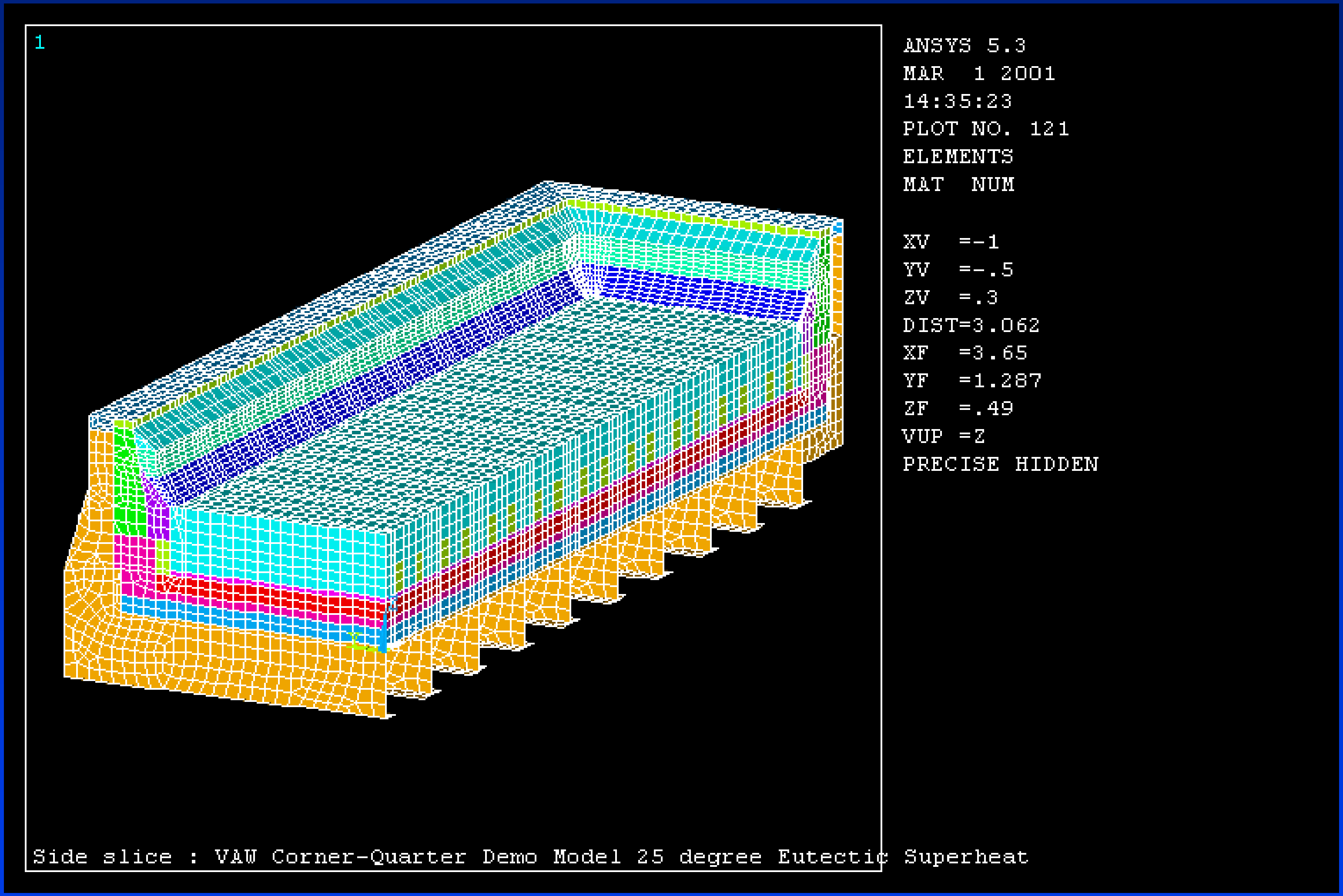

GENISIM

1992, 3D thermo-electric “pseudo” full cell and external busbars model

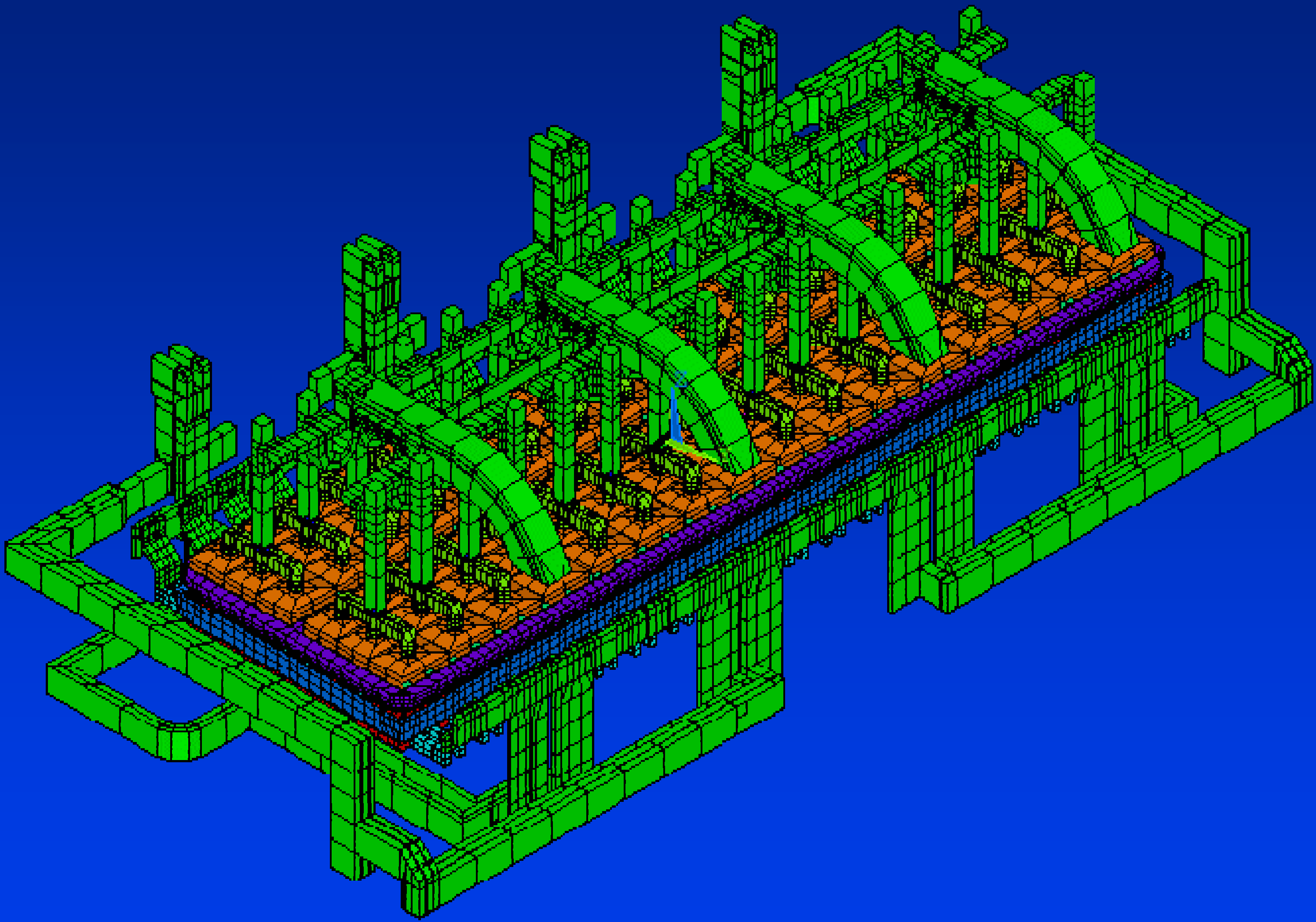

As a first step toward the development of a first thermo-electro-magnetic model, a 3D thermo-electric “pseudo” full cell and external busbars model was developed.

That model was really at the limit of what could be built and solved on the available hardware at the time both in terms of RAM memory and disk space storage.

1992, 3D cathode potshell plastic deformation and lining swelling mechanical model

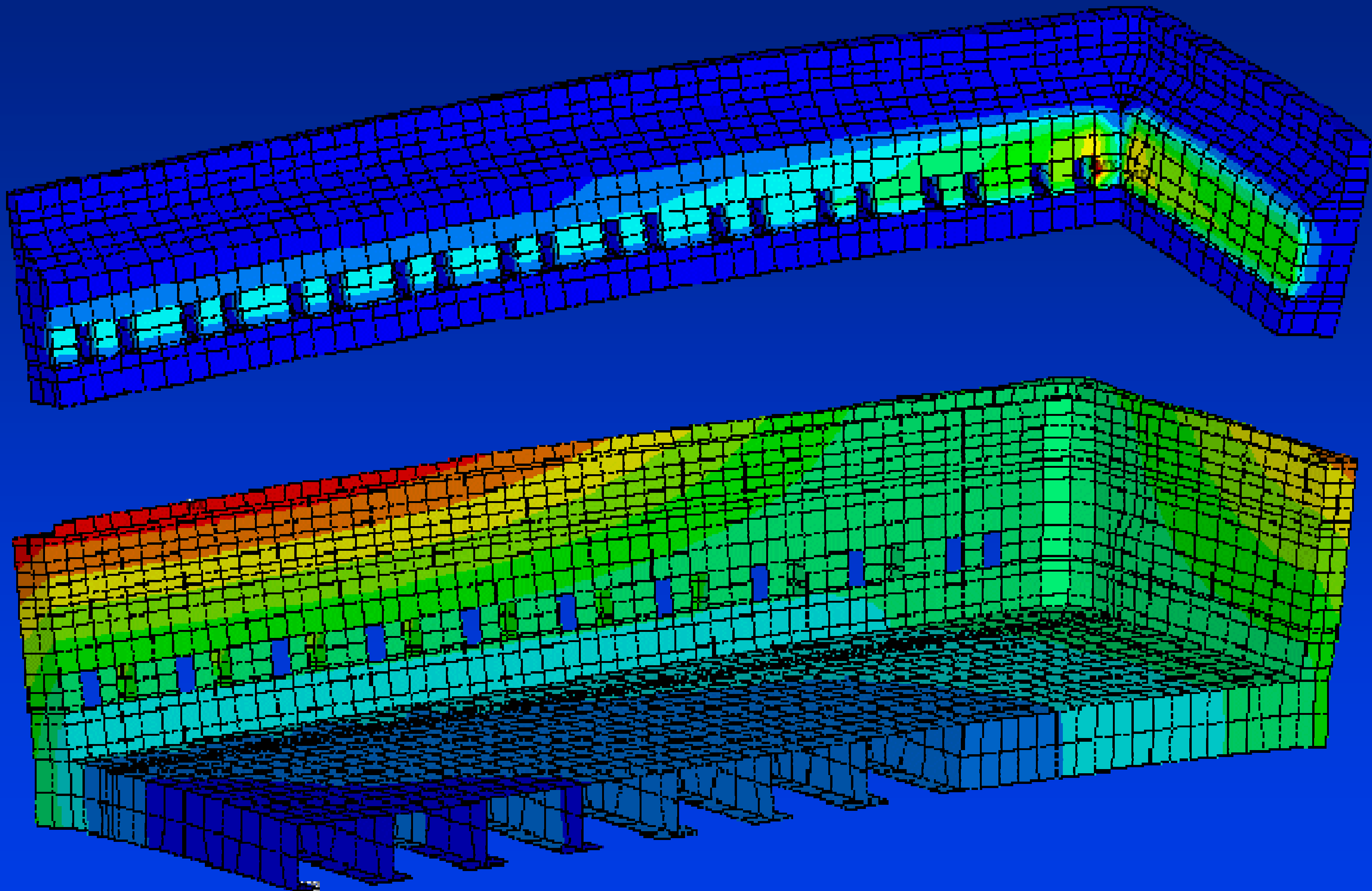

The empty quarter potshell mechanical model was extended to take into account the coupled mechanical response of the swelling lining and the restraining potshell structure.

That coupling was important to consider as a stiffer, more restraining potshell will face more internal pressure from the swelling lining material.

GENISIM

1992, 3D cathode potshell plastic deformation and lining swelling mechanical model

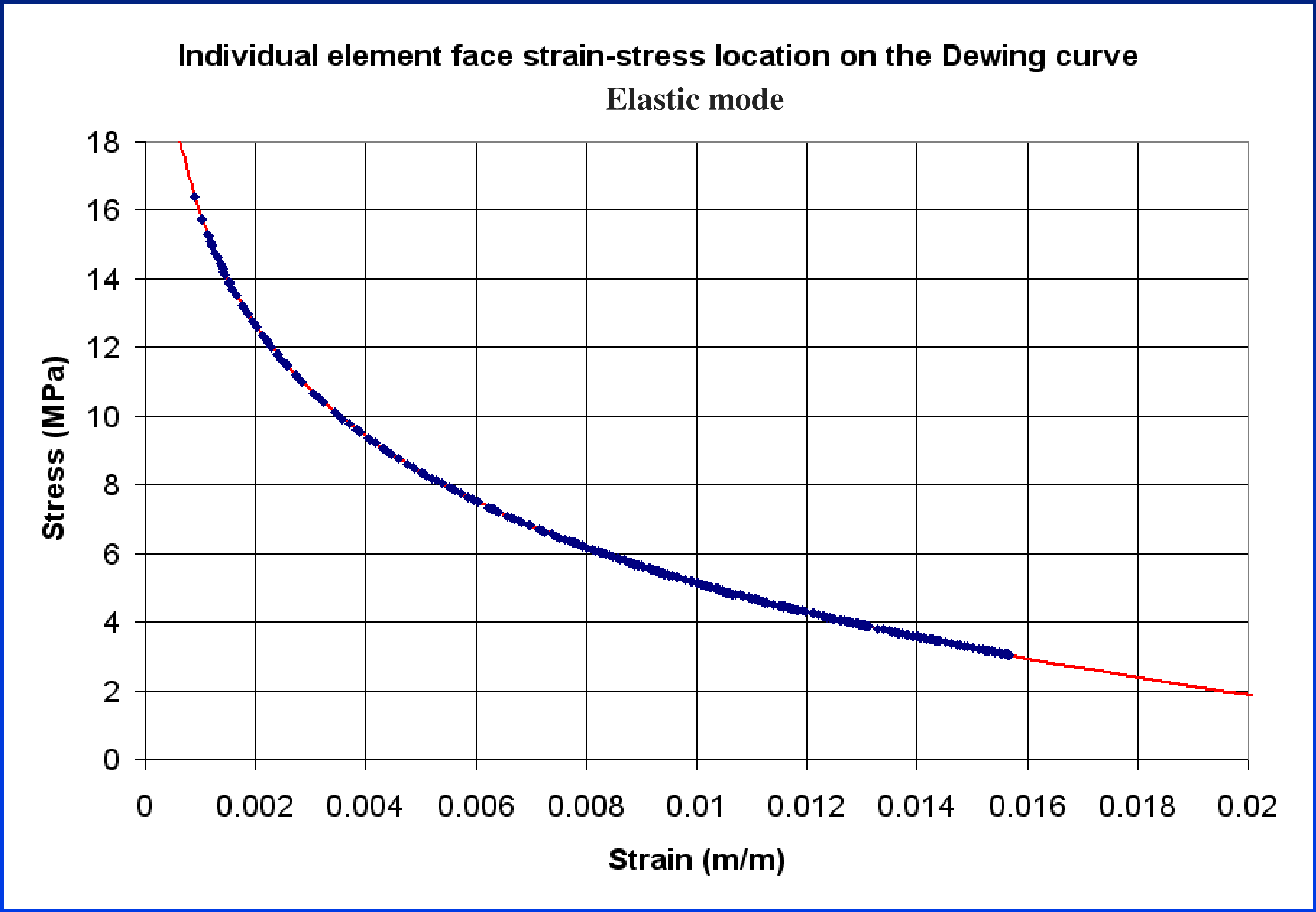

A numerical scheme external to the ANSYS solver must be setup, starting from an assumed initial internal load. The task of that external numerical scheme is to converge toward that cathode block equilibrium condition pressure loading for each element face of the carbon block/side lining interface.

1992, 3D cathode potshell plastic deformation and lining swelling mechanical model

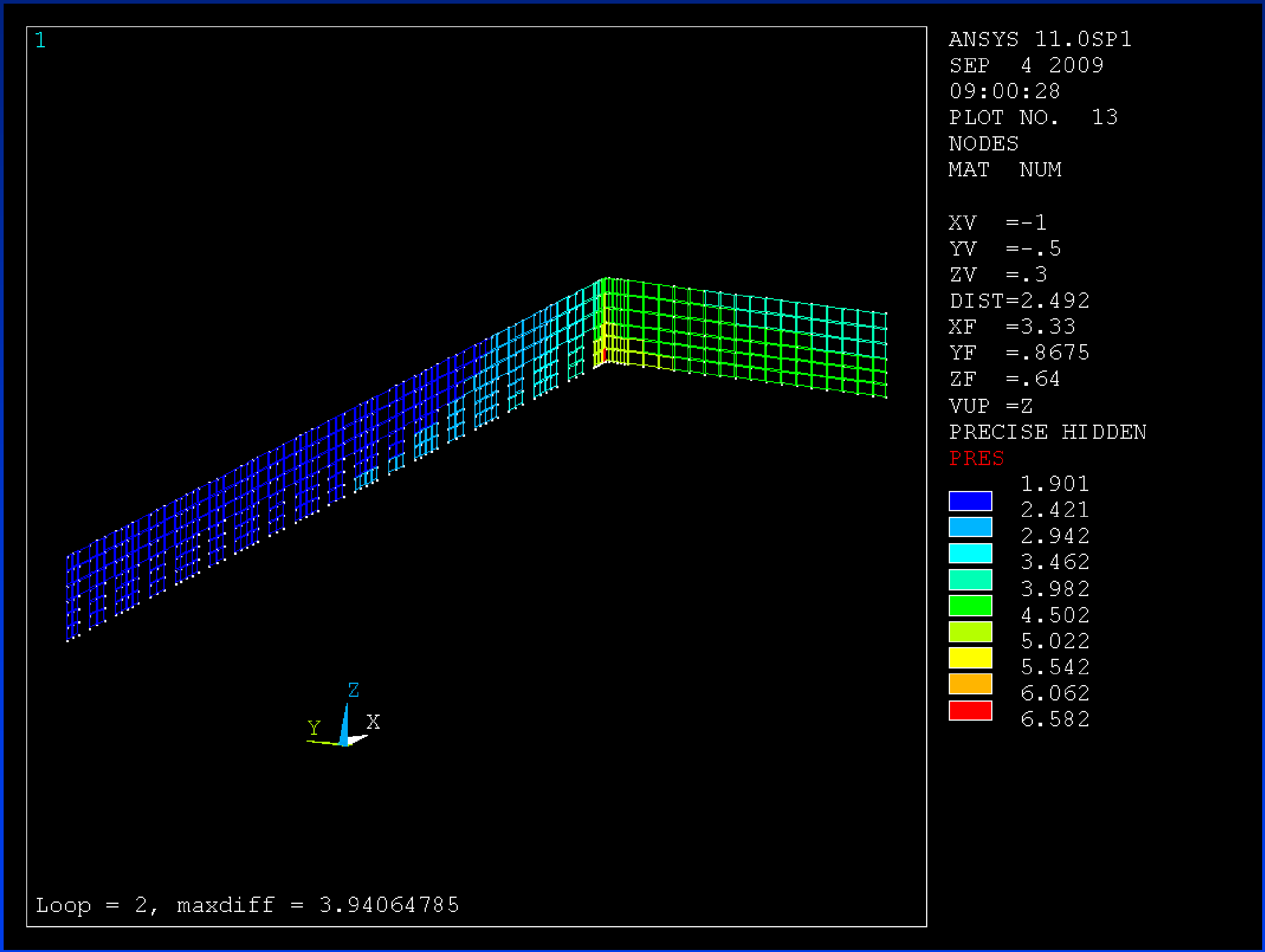

1993, 3D electro-magnetic full cell model

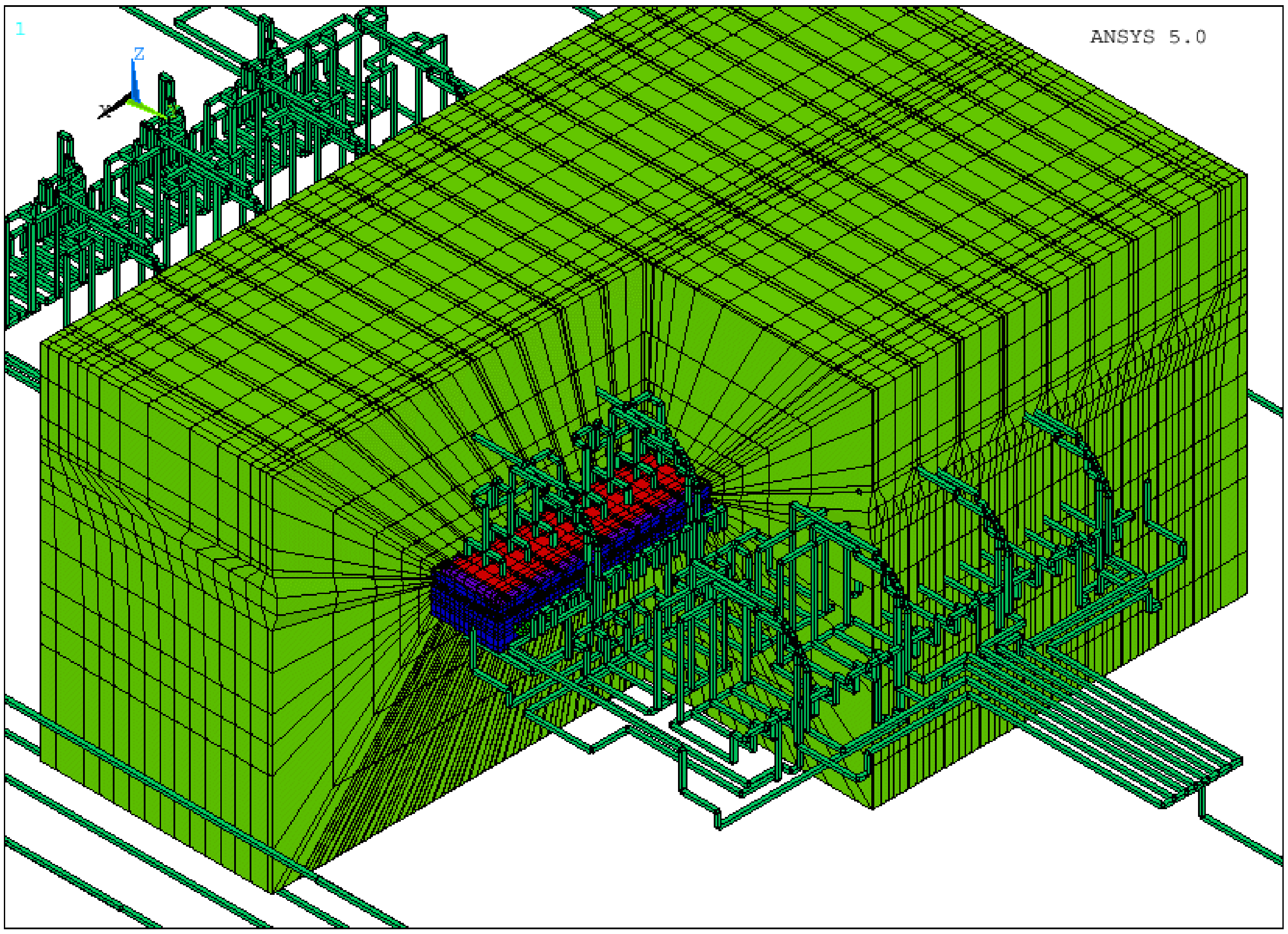

The development of a finite element based aluminum reduction cell magnetic model clearly represented a third front of model development.

Because of the presence of the ferro-magnetic shielding structure, the solution of the magnetic problem cannot be reduced to a simple Biot-Savard integration scheme.

1993, 3D electro-magnetic full cell model

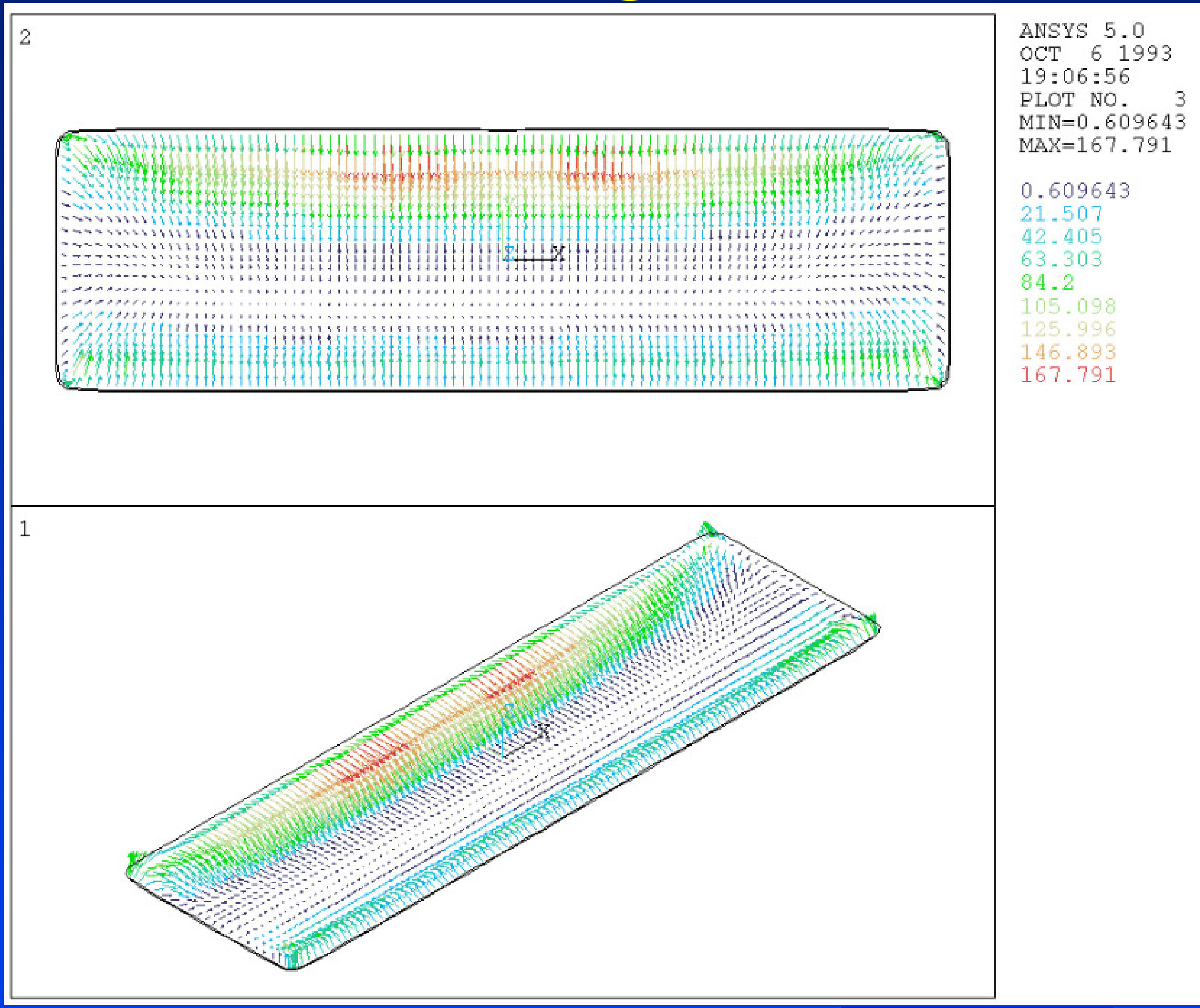

GENISIM

1993, 3D electro-magnetic full cell model

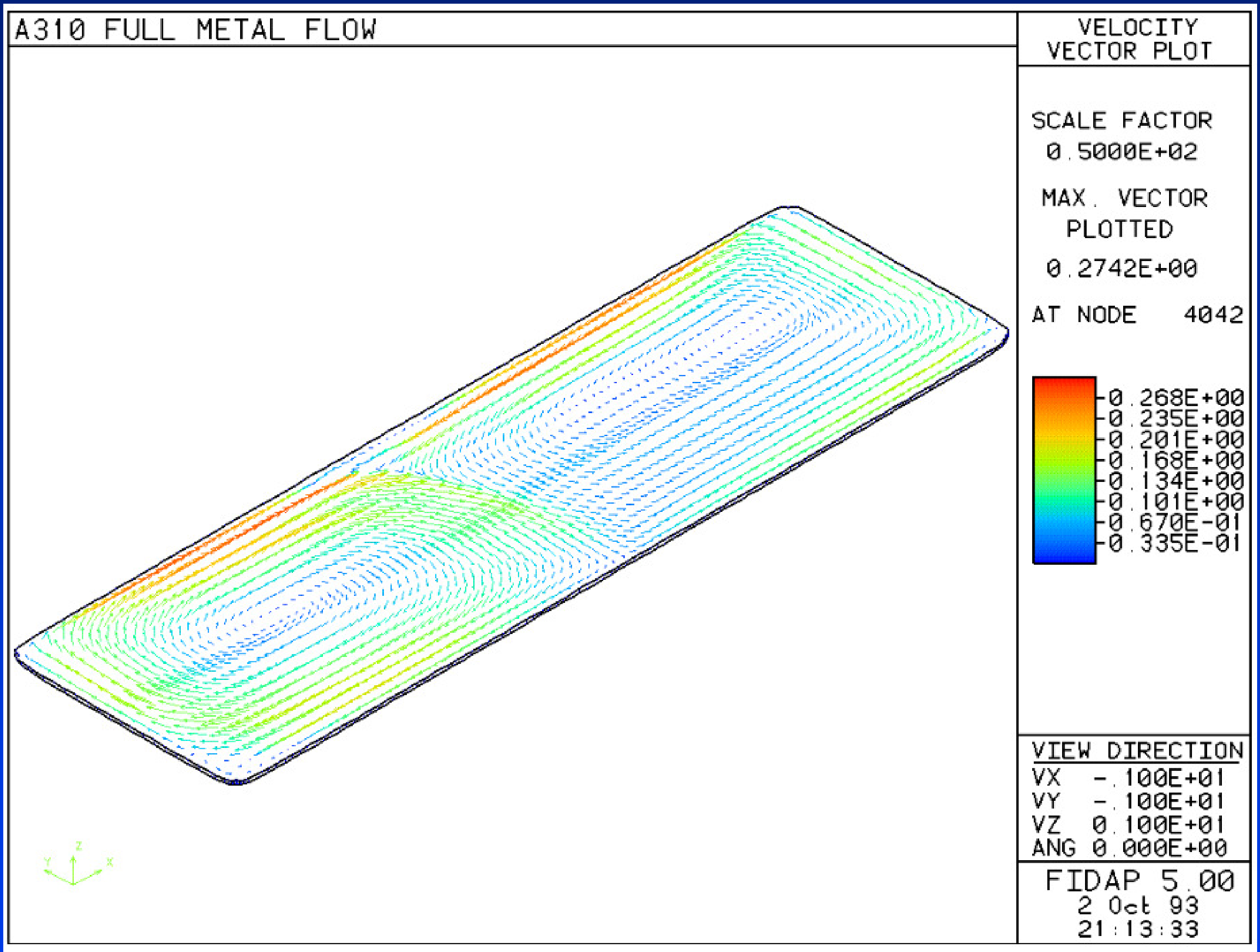

GENISIM

1993, 3D transient thermo-electric full quarter cell preheat model

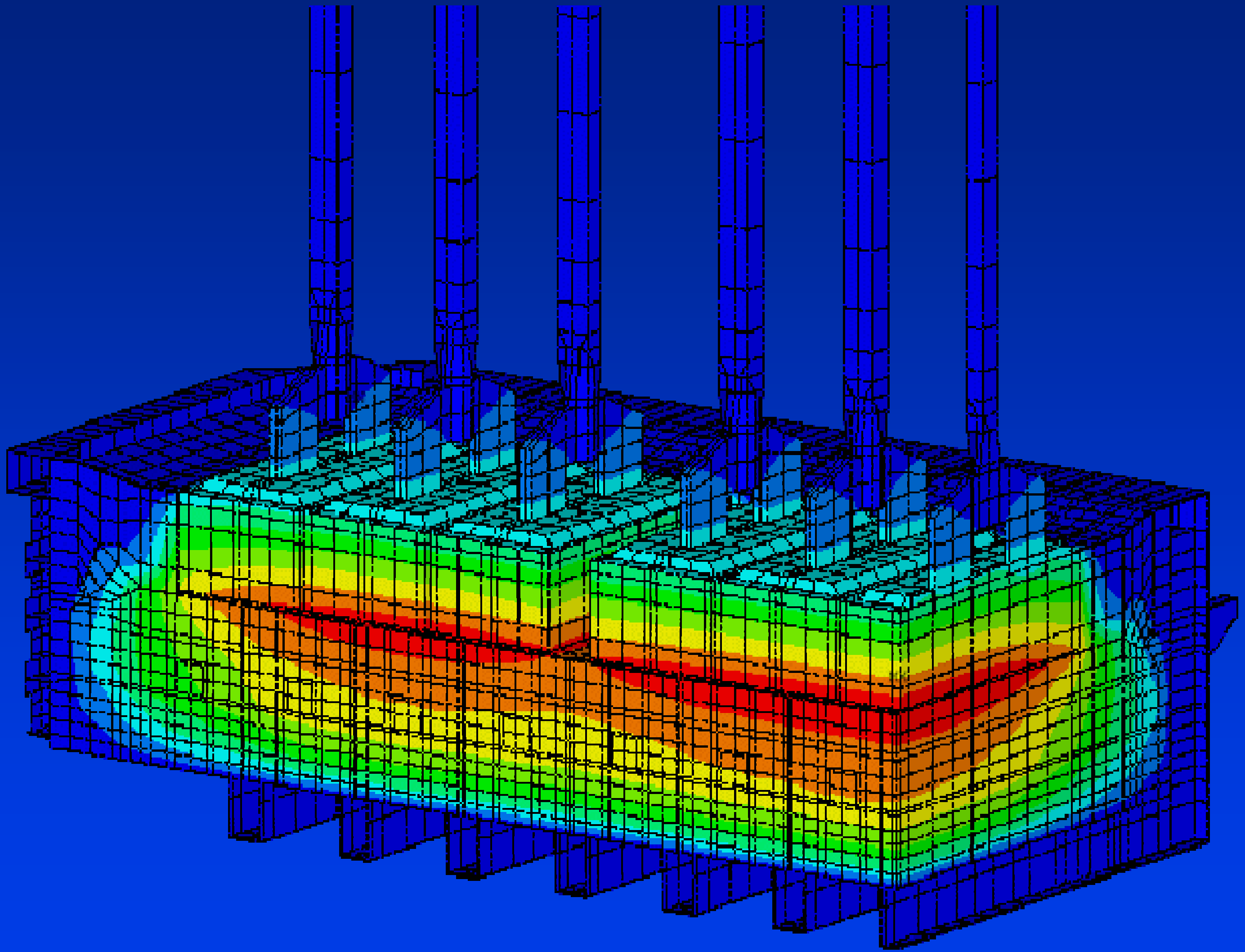

The cathode quarter thermo-electric model was extended into a full quarter cell geometry in preheat configuration and ran in transient mode in order to analyze the cell preheat process .

The need was urgent, but due to its huge computing resources requirements, the model was not ready in time to be used to solve the plant problem at the time.

Transient Thermal Model Solution

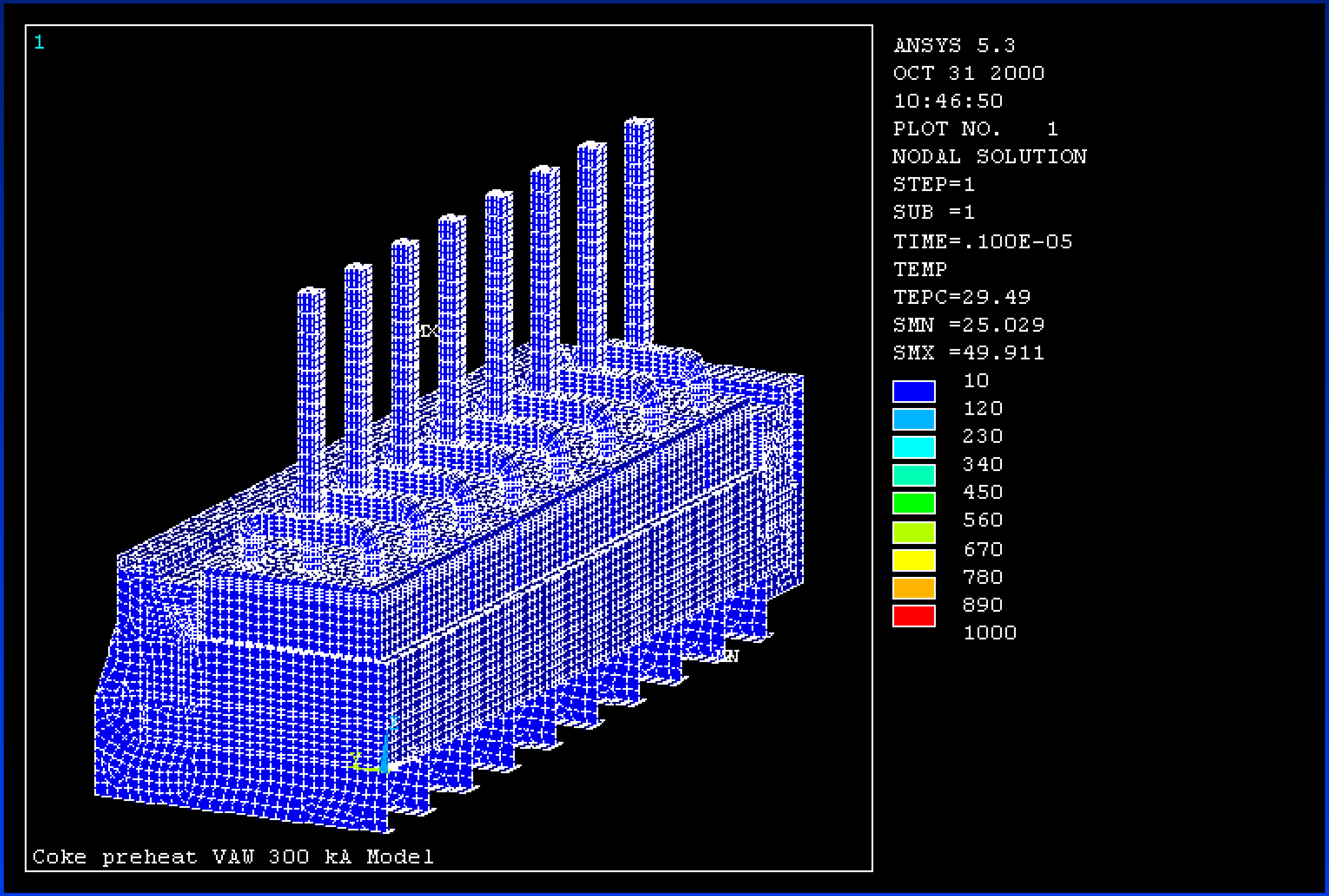

GENISIM

1993's Model Extension to Stress Analysis

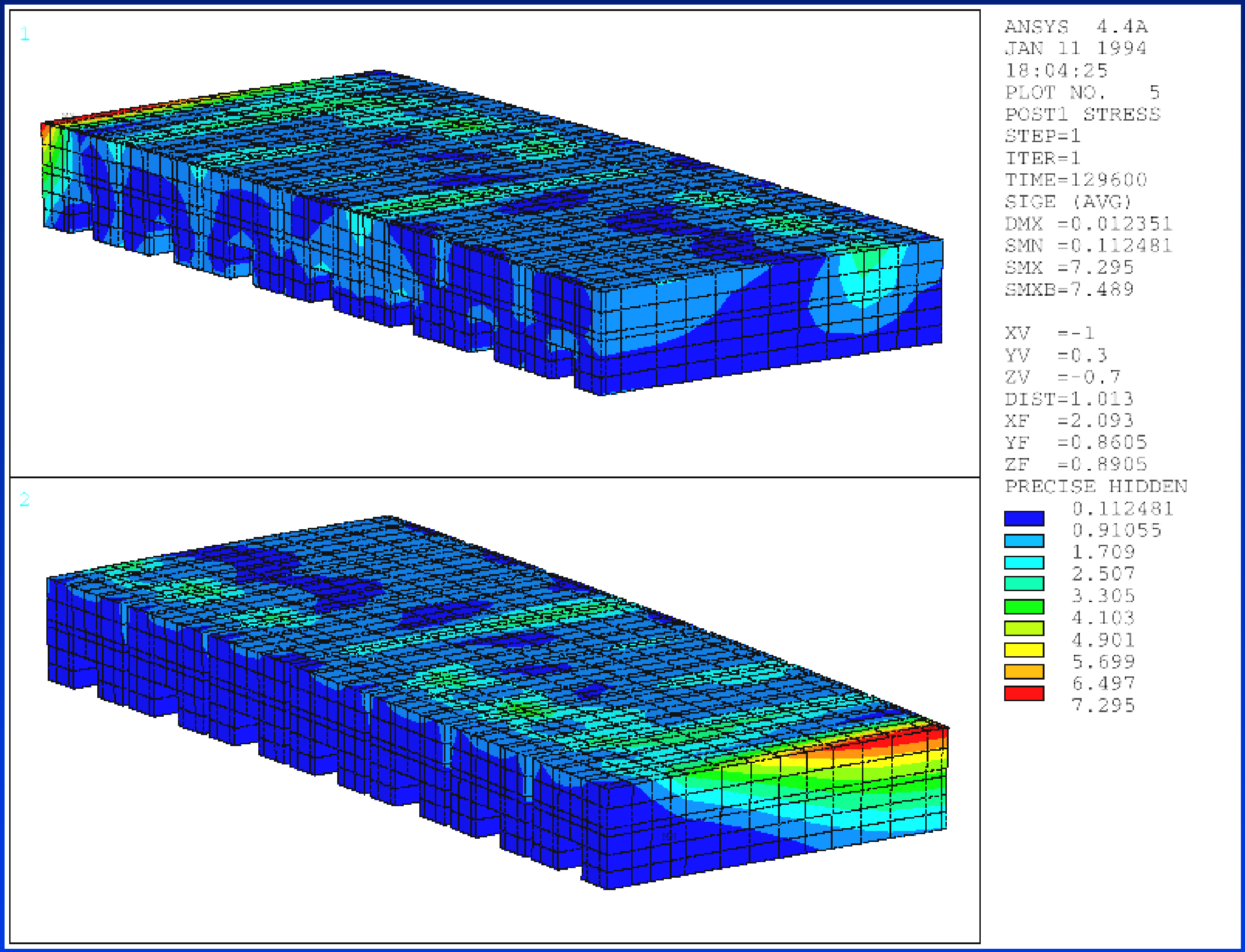

Equivalent stress in the cathode panel at 36 hours – standard coke bed

GENISIM

1993, 2D CFDS-Flow3D potroom ventilation model

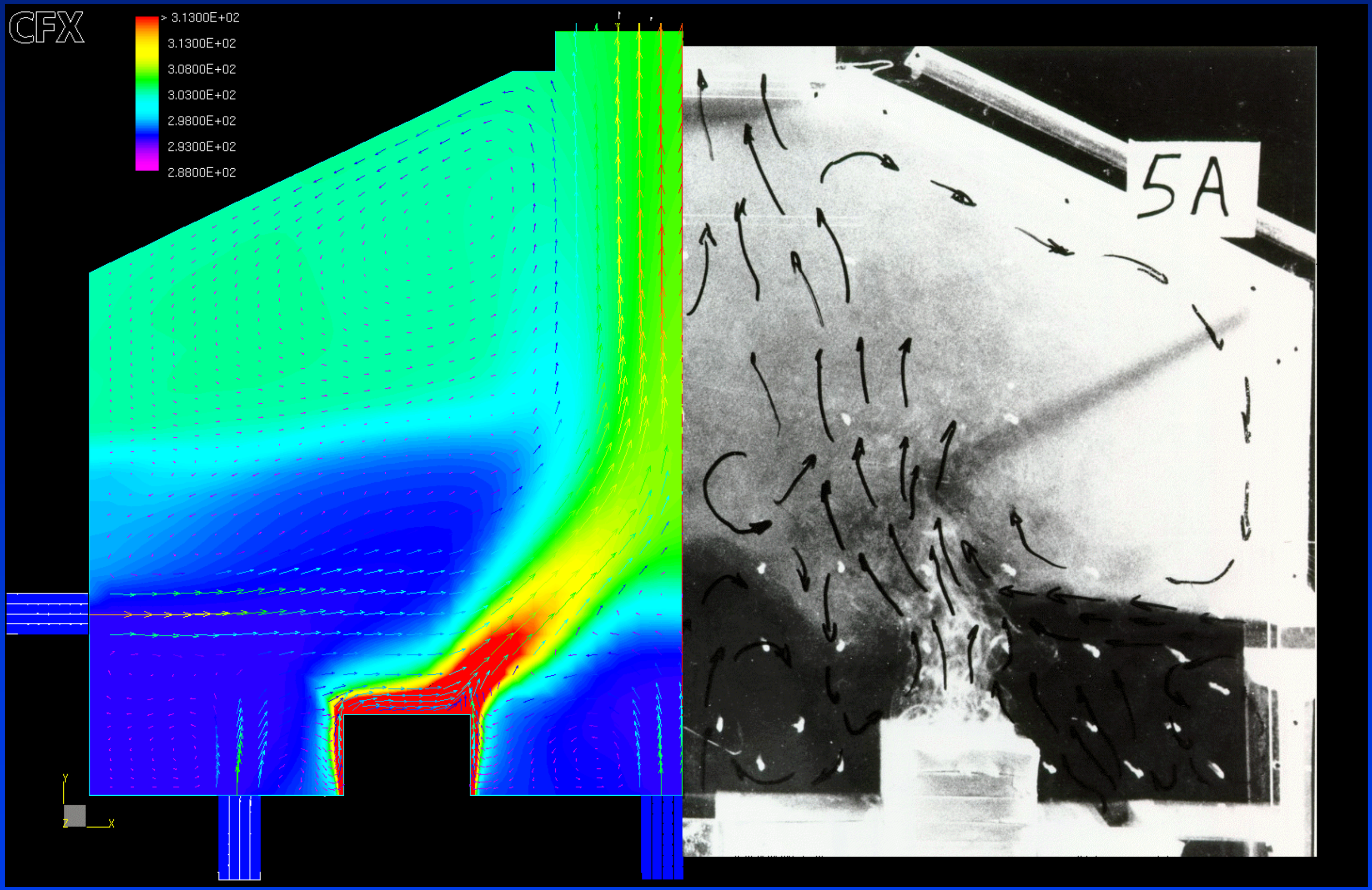

GENISIM

1993, 2D CFDS-Flow3D potroom ventilation model

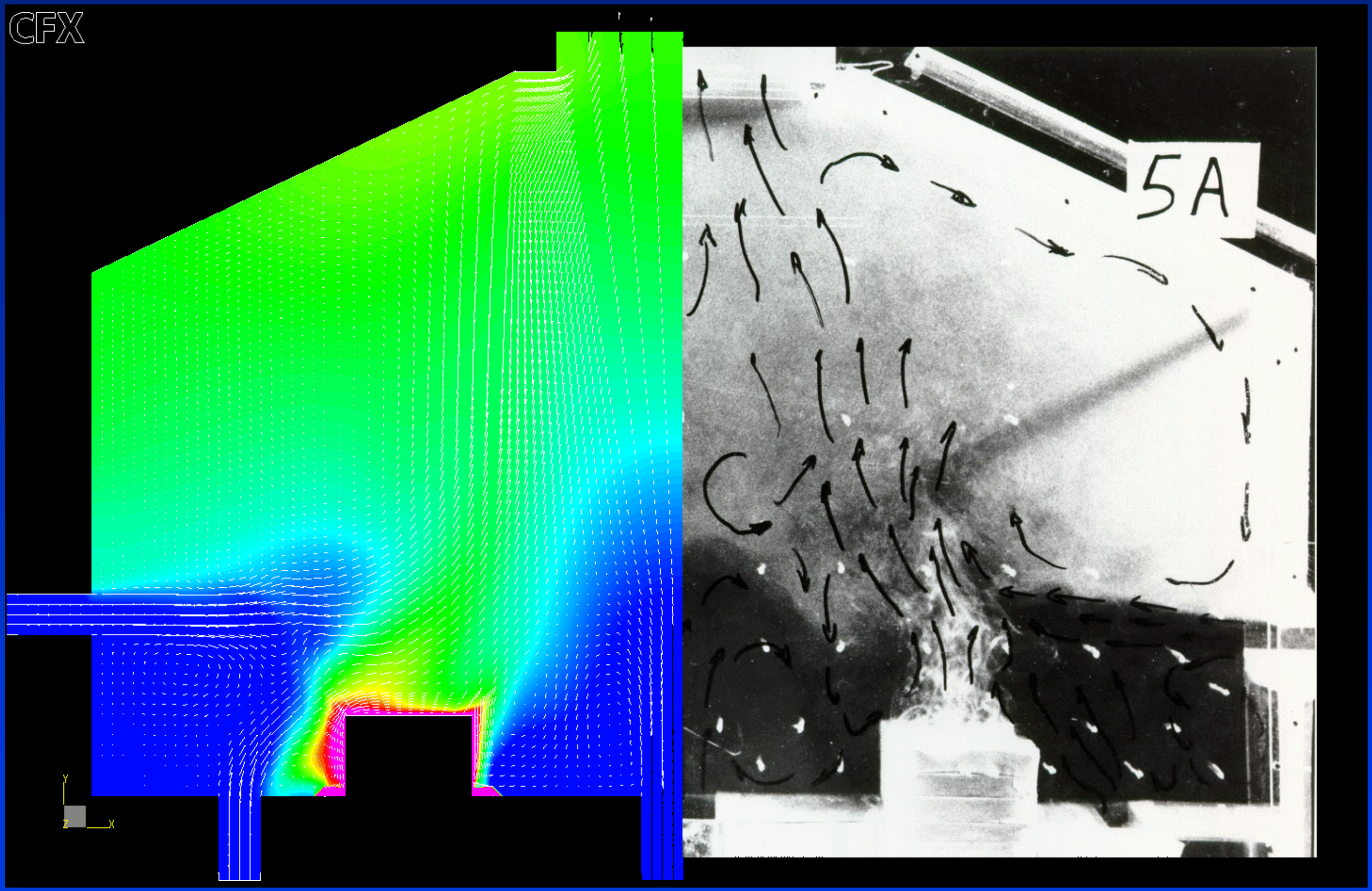

2D "Reynolds flux" model results vs. physical model results

1995, Dyna/Marc Lump Parameters+ Model

DYNA/MARC (DYNAmic Model of Aluminum Reduction Cells) is a dynamic simulator of the behavior of aluminum reduction cells.

DYNA/MARC is composed of three different models.

The first is the <u>Process model</u>, that solves the heat and mass balance in the cell. It also takes into account the evolution of the ACD (anode to cathode distance) and the line amperage fluctuation.

The second model is the <u>Controller model</u>. This reproduces the plant controller response based on all the programmed algorithms taking into account the current cell state.

Finally, the <u>Operator model</u> allows the software to simulate the actions undertaken by the operator on his schedule or when the controller requires his intervention.

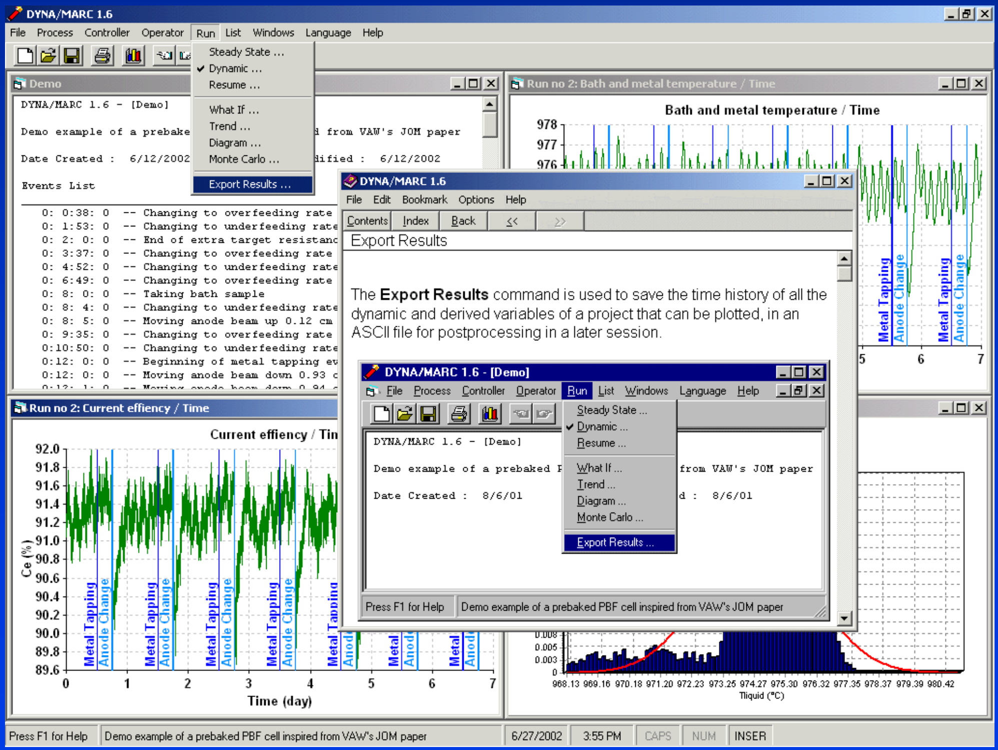

1995, Dyna/Marc Lump Parameters+ Model

Dyna/Marc can be used to illustrate the behavior of the Hall-Héroult process in the context of a general purpose aluminium electrolysis training course.

For example, it can illustrate the impact of undesirable alumina feeding from the cover material during an anode change on the cell current efficiency.

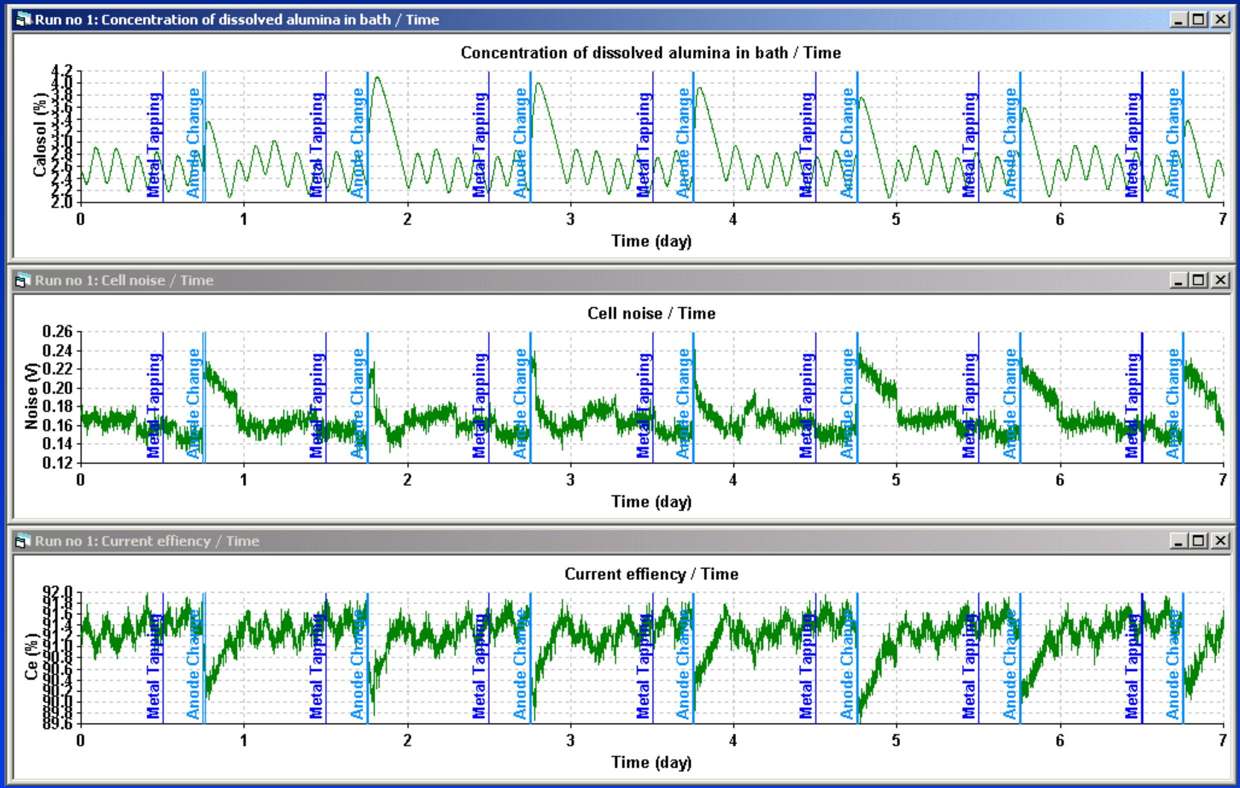

With undesirable alumina feeding

GENISIM

1998, 3D thermo-electric full cell slice model

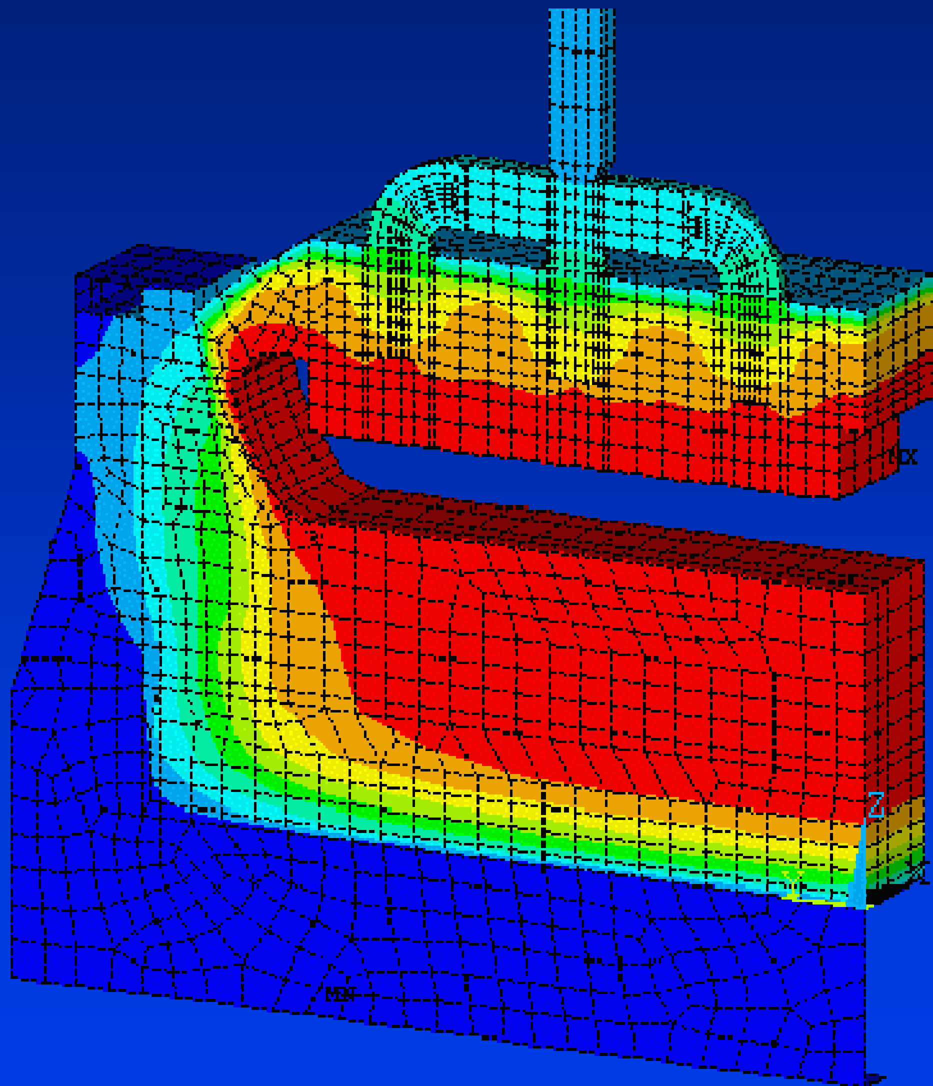

As described previously, the 3D half anode model and the 3D cathode side slice model have been developed in sequence, and each separately required a fair amount of computer resources.

Merging them together was clearly not an option at the time, yet it would have been a natural thing to do. Many years later, the hardware limitation no longer existed so they were finally merged.

1998, 2D+ thermo-electric full cell slice model

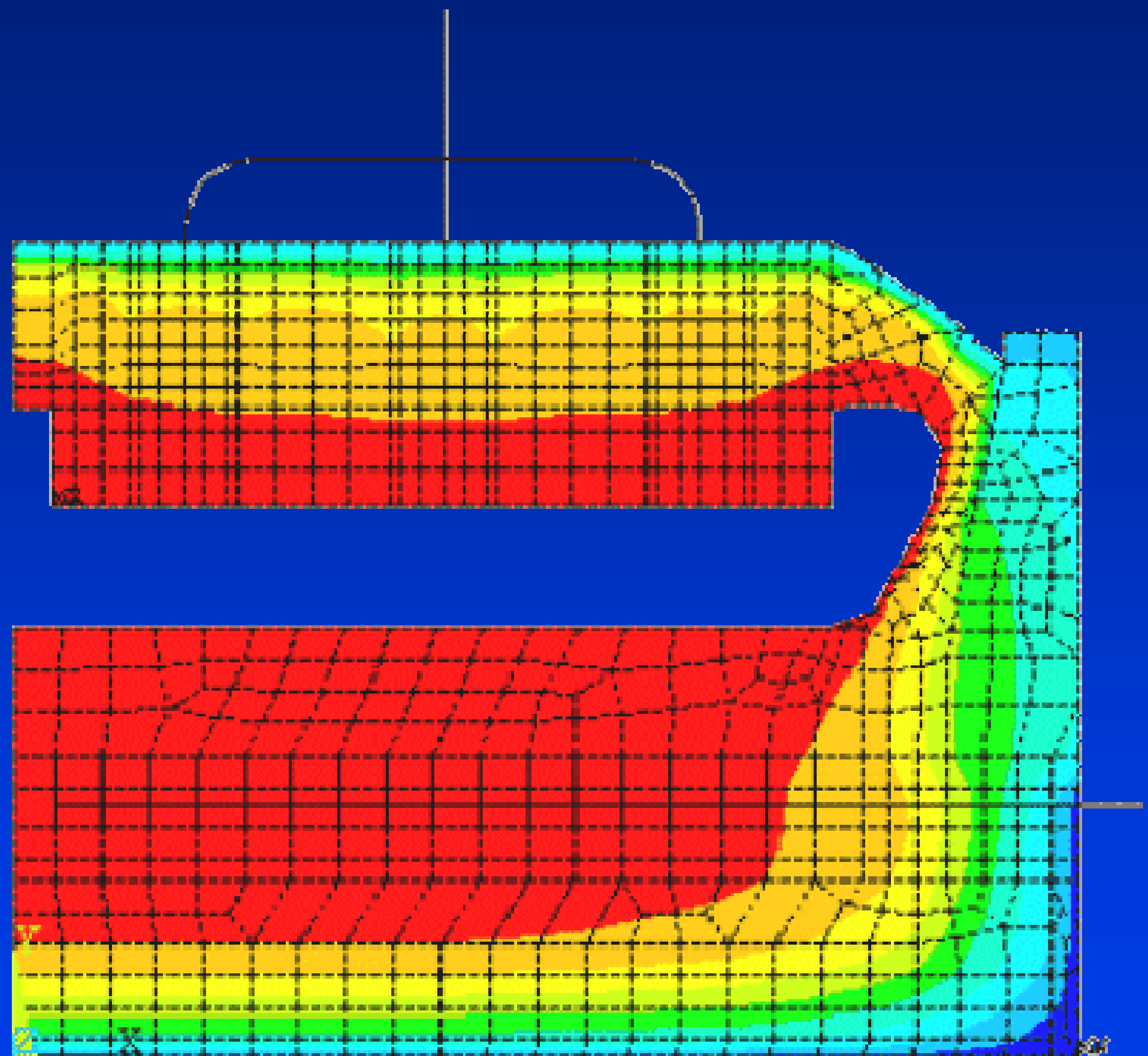

2D+ version of the same full cell slice model was developed. Solving a truly three dimensional cell slice geometry using a 2D model may sound like a step in the wrong direction, but depending on the objective of the simulation, sometimes it is not so.

The 2D+ model uses beam elements to represent geometric features lying in the third dimension (the + in the 2D+ model).

1999, 2D+ transient thermo-electric full cell slice model

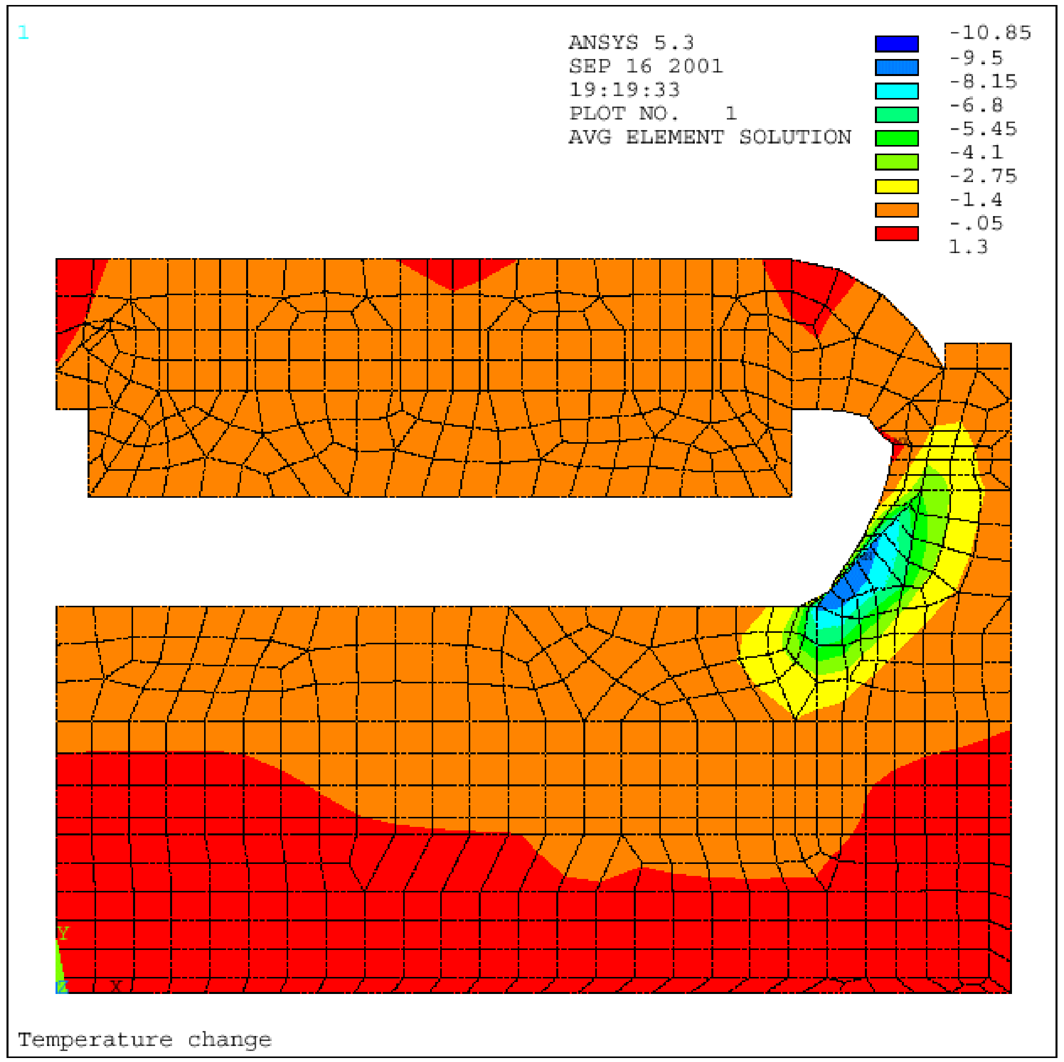

An interesting feature of that model is the extensive APDL coding that computes other aspects of the process related to the different mass balances like the alumina dissolution, the metal production etc.

As that type of model has to compute the dynamic evolution of the ledge thickness, there is a lot more involved than simply activating the ANSYS transient mode option.

Modeling Total Power Failure

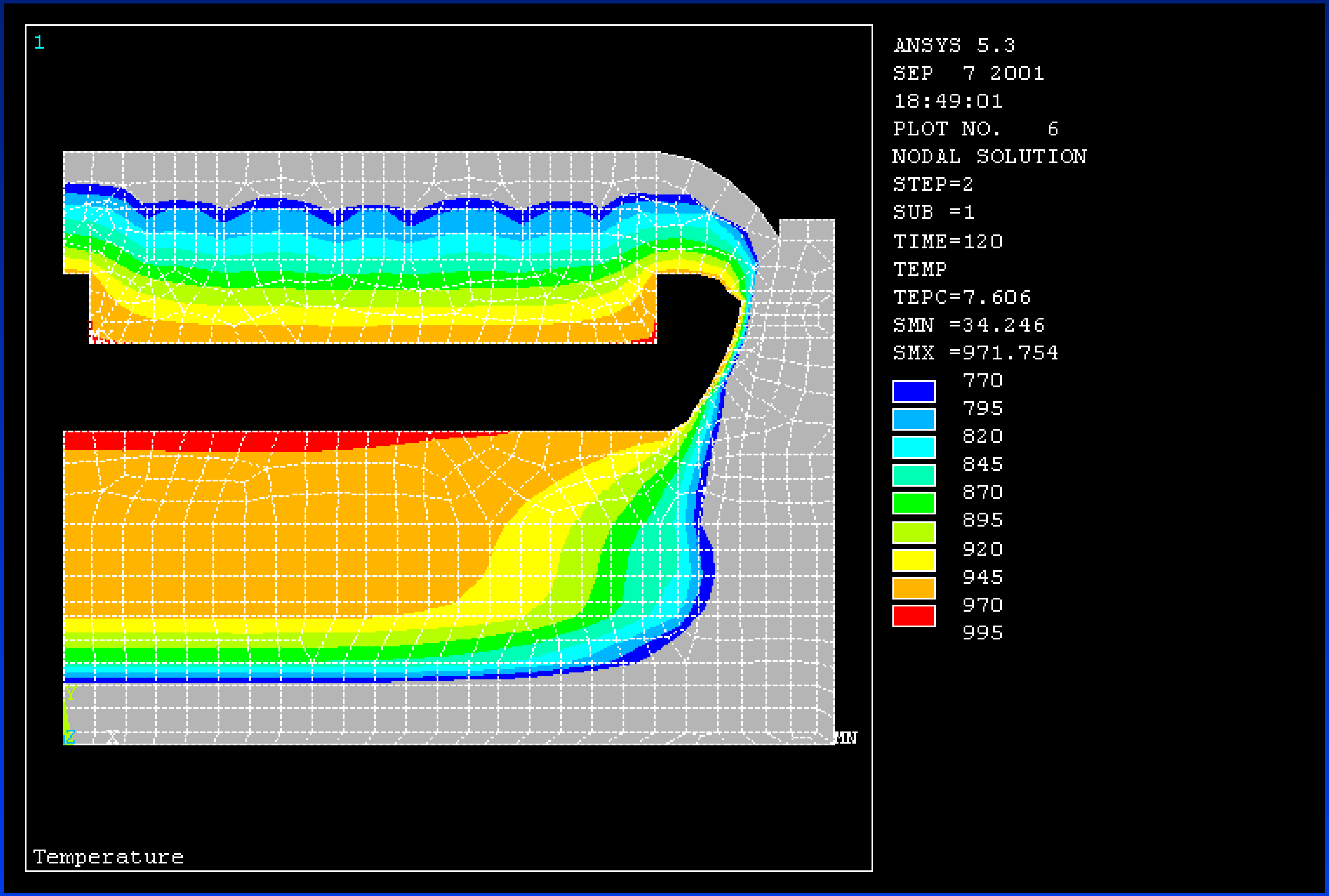

GENISIM

VAW aluminium technology

Technology key to competitive smelting vaw aluminium today

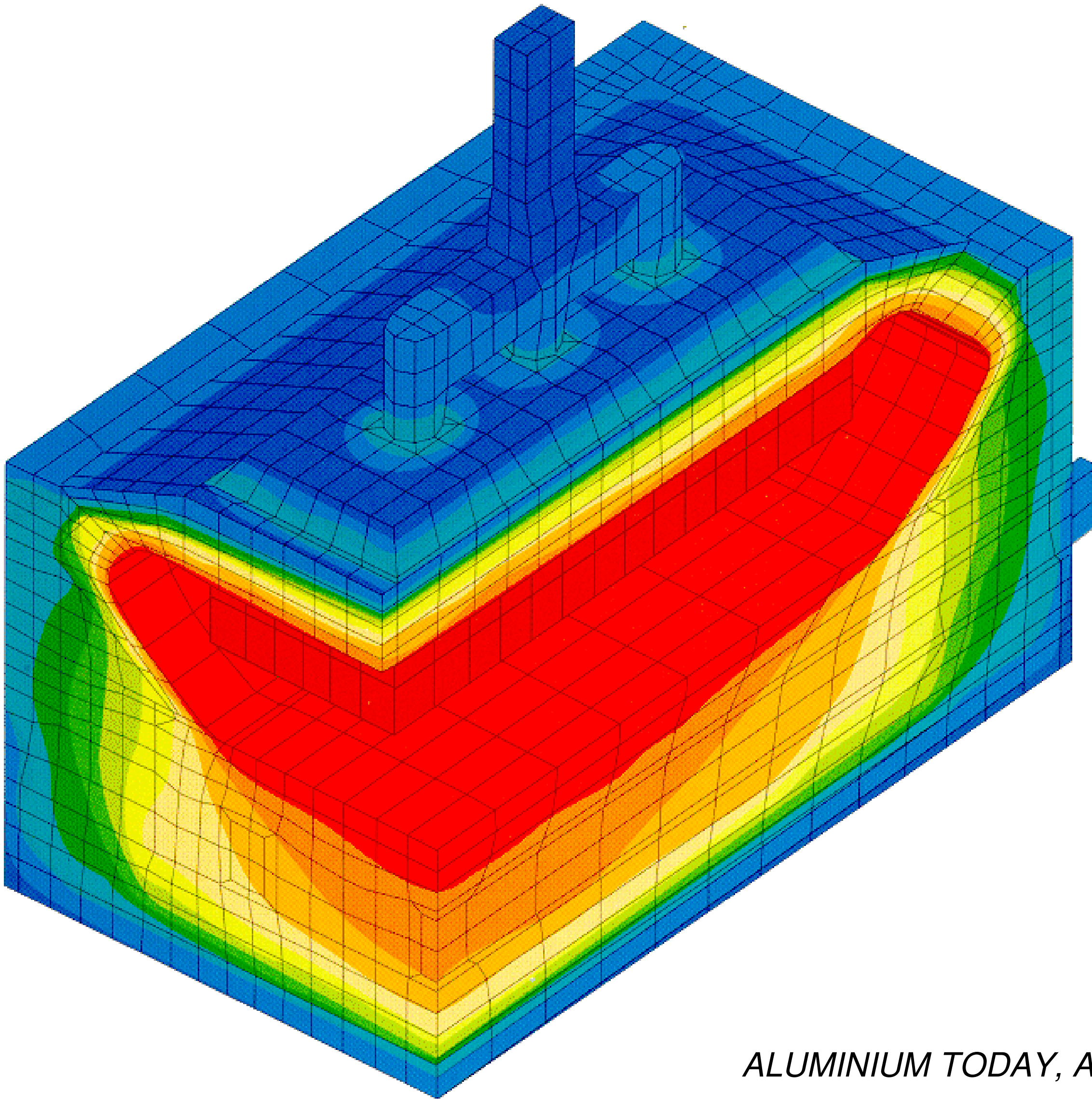

ALUMINIUM TODAY, AUGUST/SEPTEMBER 1999

2000, 3D thermo-electric cathode slice erosion model

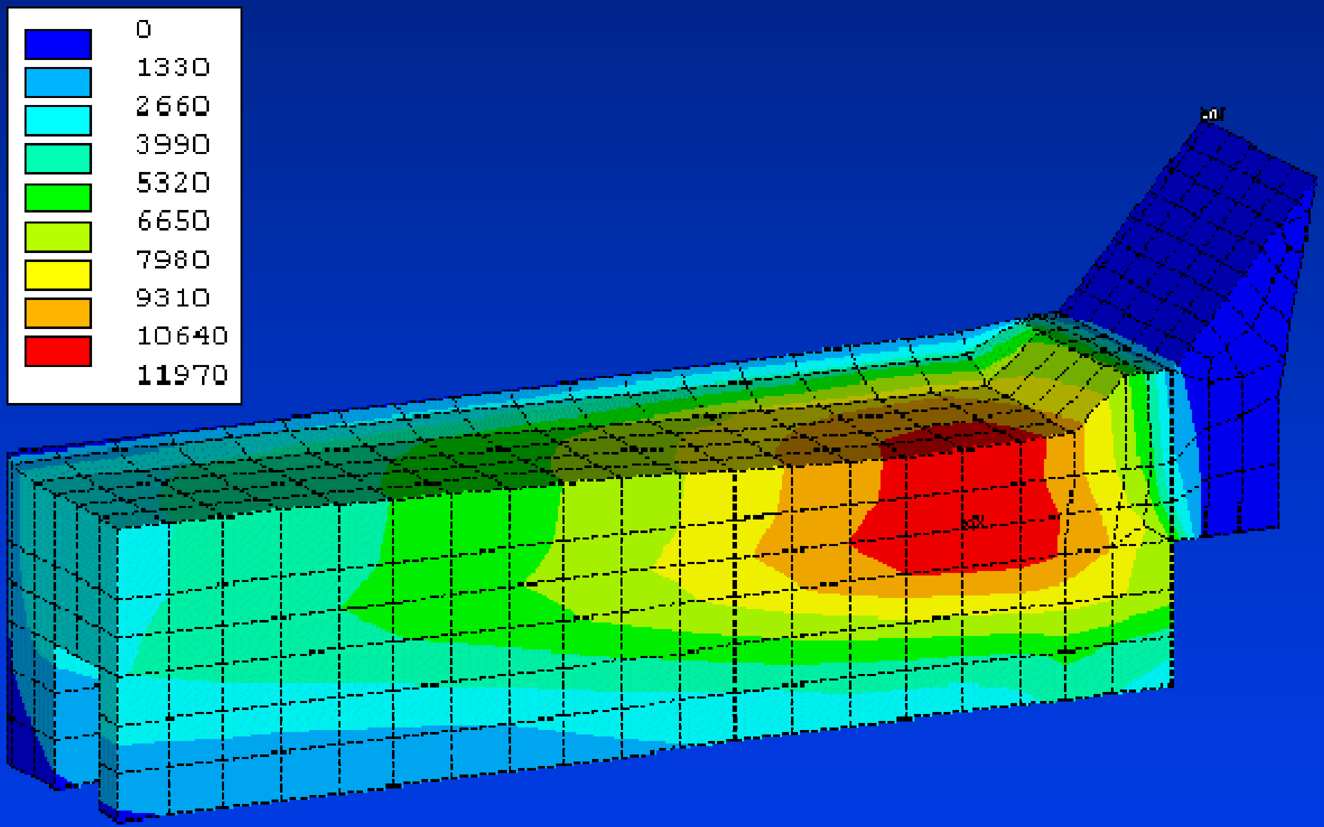

Cathode erosion rate is proportional to the cathode surface current density and that the initial surface current density is not uniform, the erosion profile will not be uniform.

Furthermore, that initial erosion profile will promote further local concentration of the surface current density that in turn will promote a further intensification of the non-uniformity of the erosion rate.

Base Case Model Solution

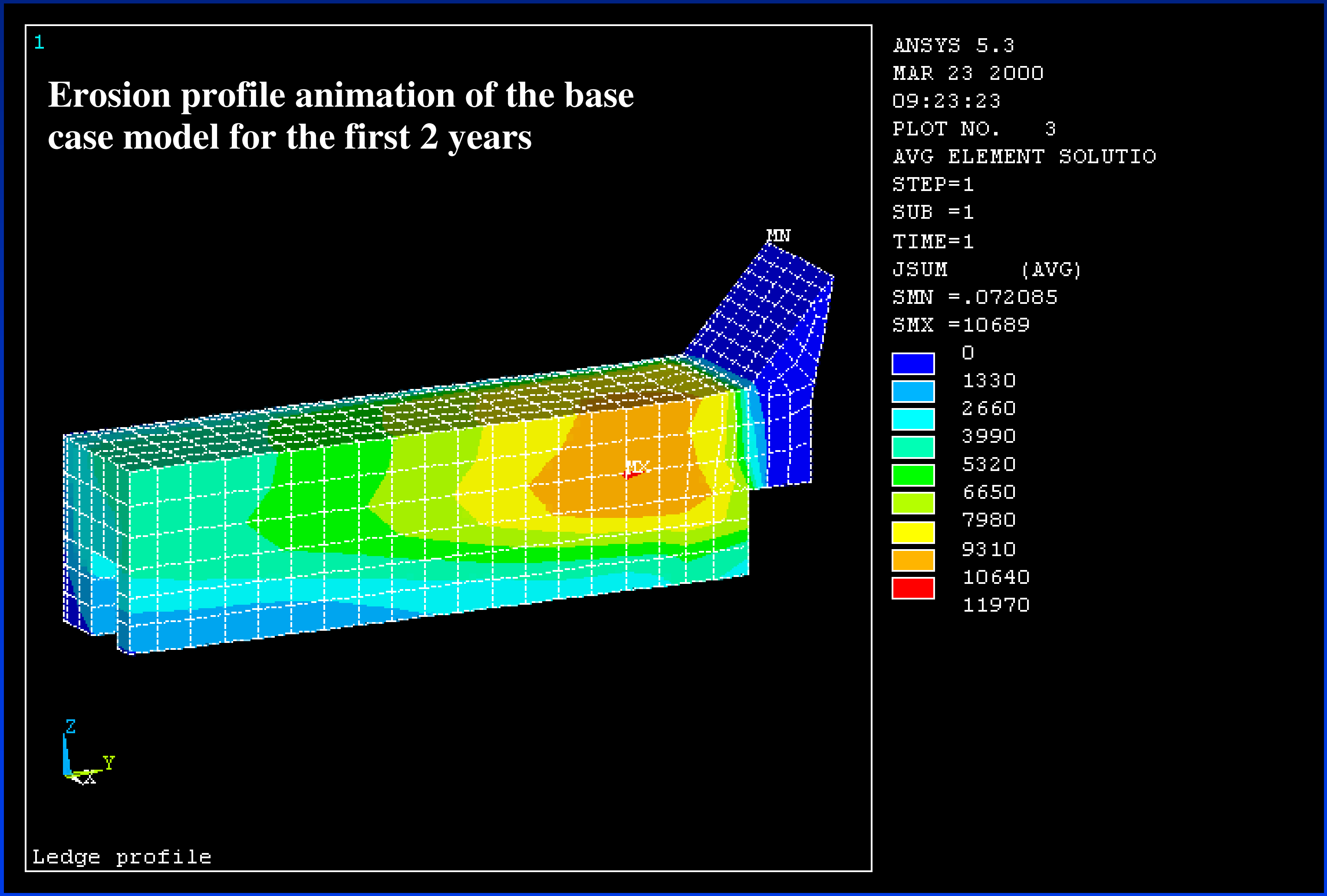

GENISIM

ENVIRONMENTAL IMPROVEMENTS IN A SØDERBERG POTLINE

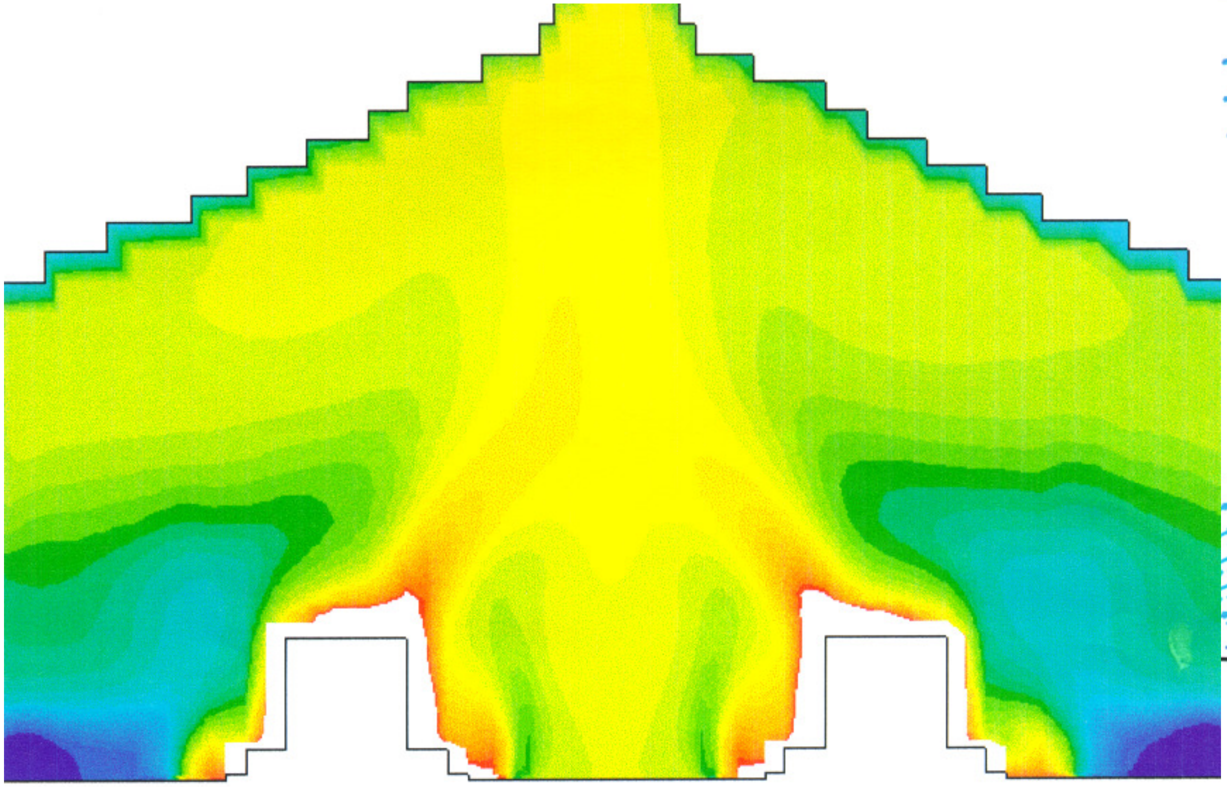

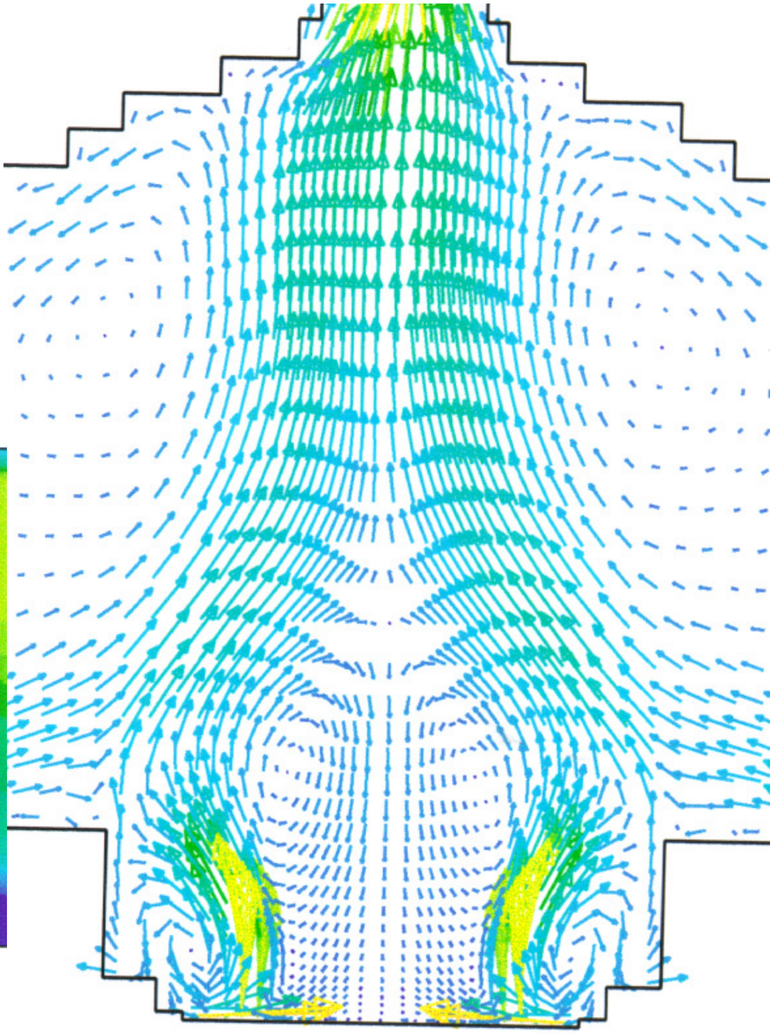

CFD simulations (velocity vectors and temperature distribution plot).

UNIVERSITÉ LAVAL

THERMO-ELECTRO-MECHANICAL MODELLING OF THE CONTACT BETWEEN STEEL AND CARBON CYLINDERS USING THE FINITE ELEMENT METHOD

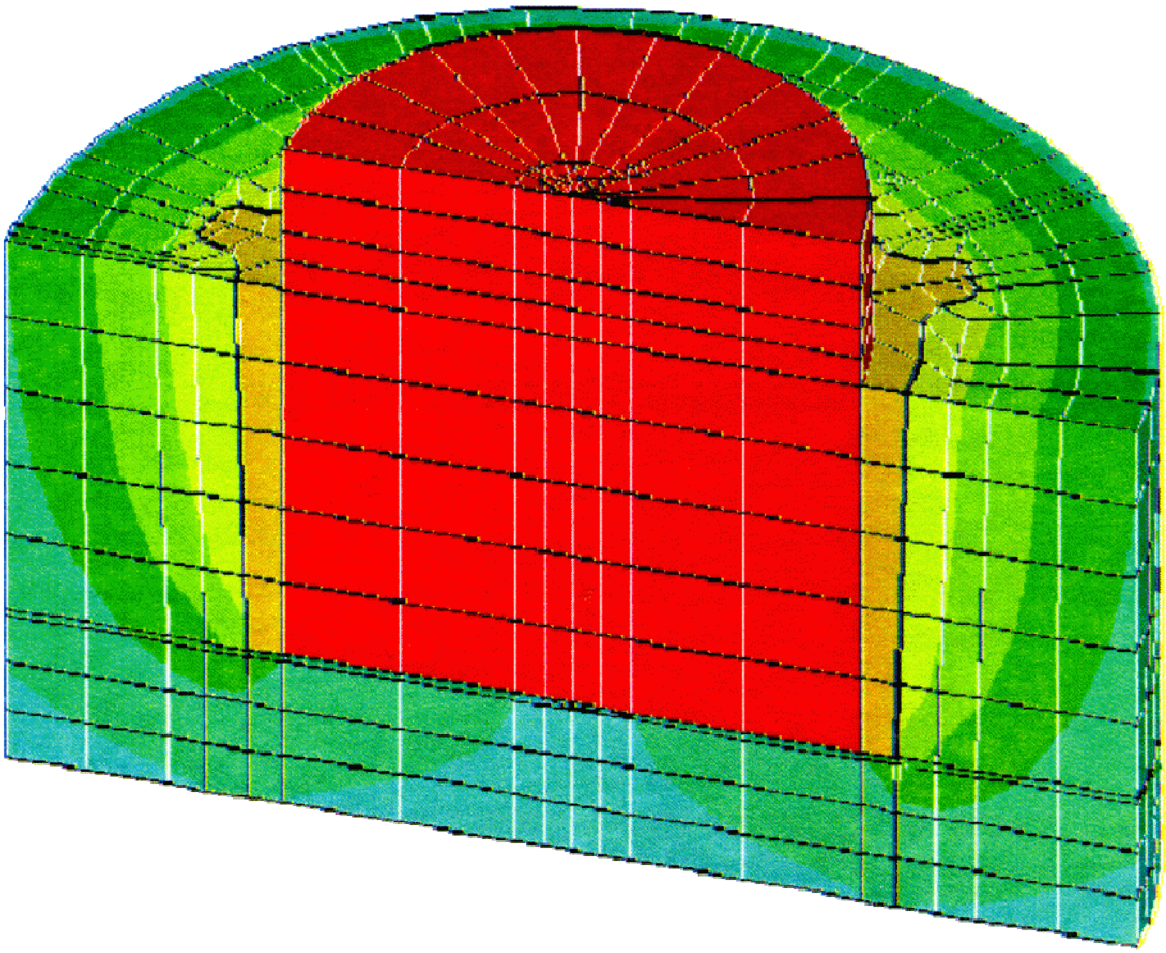

Richard was also the first to develop an ANSYS® based TEM anode stub hole model and to use such a model to do some stub hole design optimization work.

Unfortunately, the ANSYS® version available at the time was not supporting thermo-electro-mechanical contact elements preventing the development of a fully coupled model.

2001, 3D CFX-4 potroom ventilation model

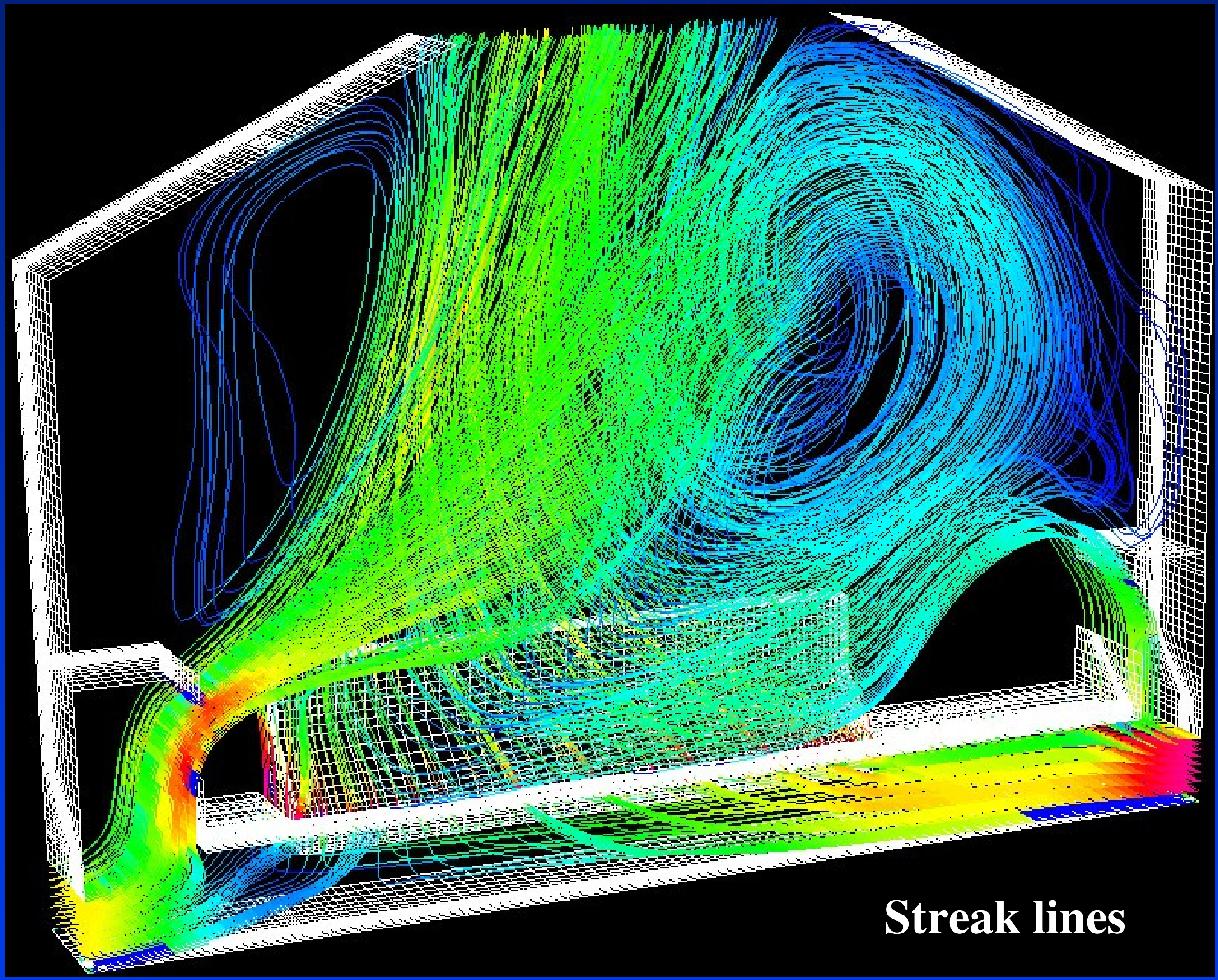

GENISIM

2001, 3D CFX-4 potroom ventilation model

Temperature fringe plot, back plane

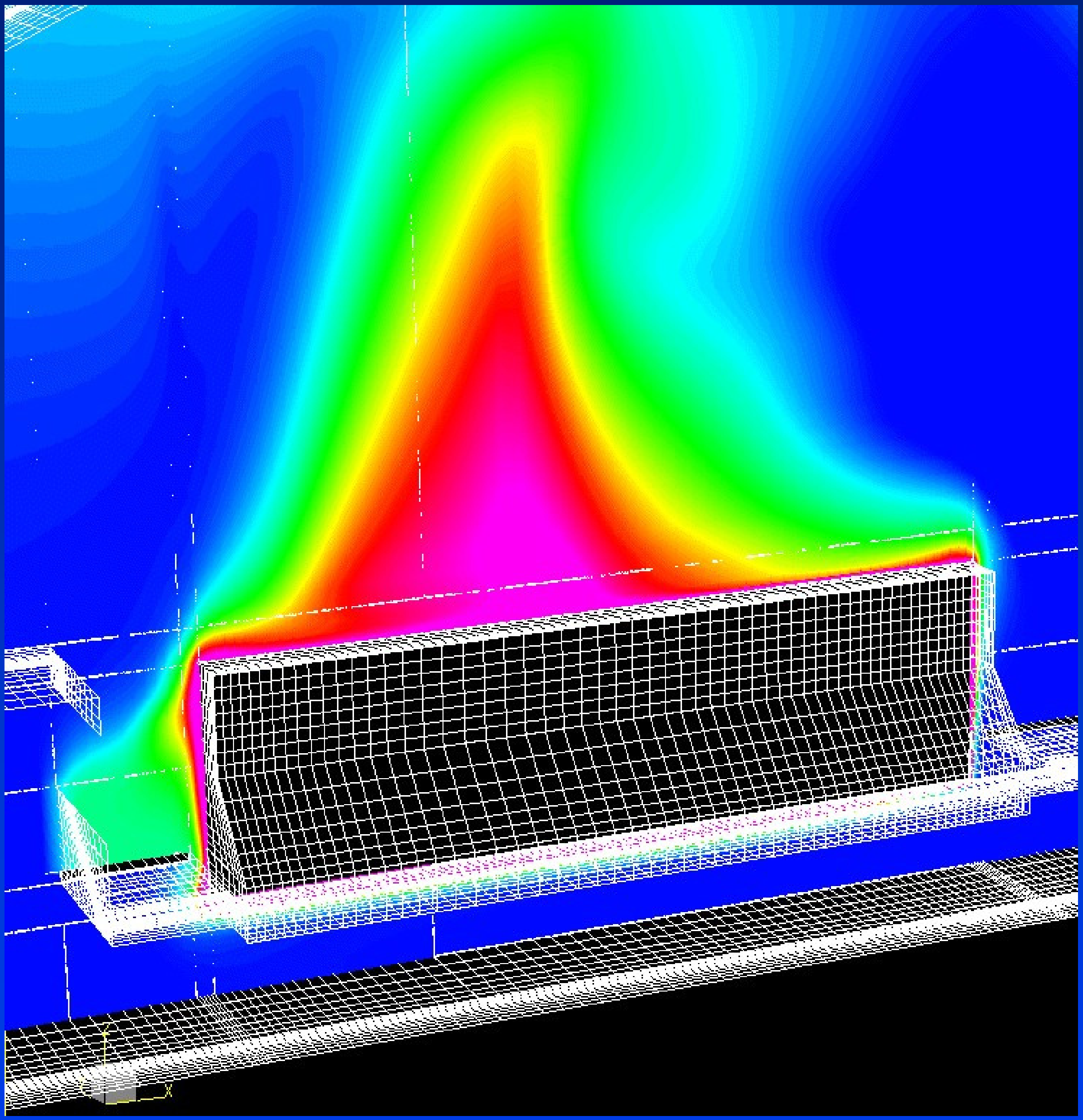

2002, 3D thermo-electric half cathode and external busbar model

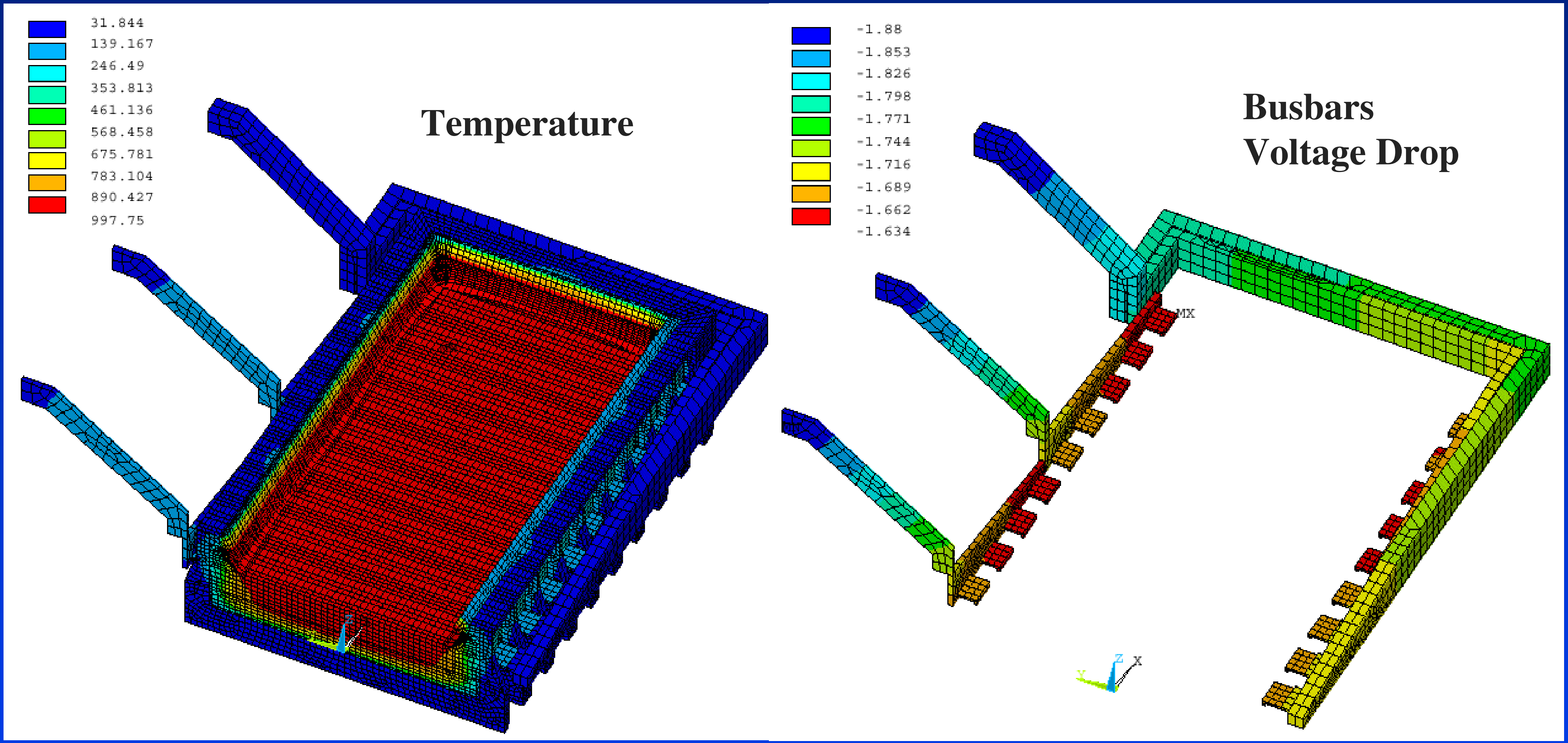

GENISIM

Relationship between Local Heat Transfer Coefficient of the Liquid/Ledge Interface and the Velocity Field

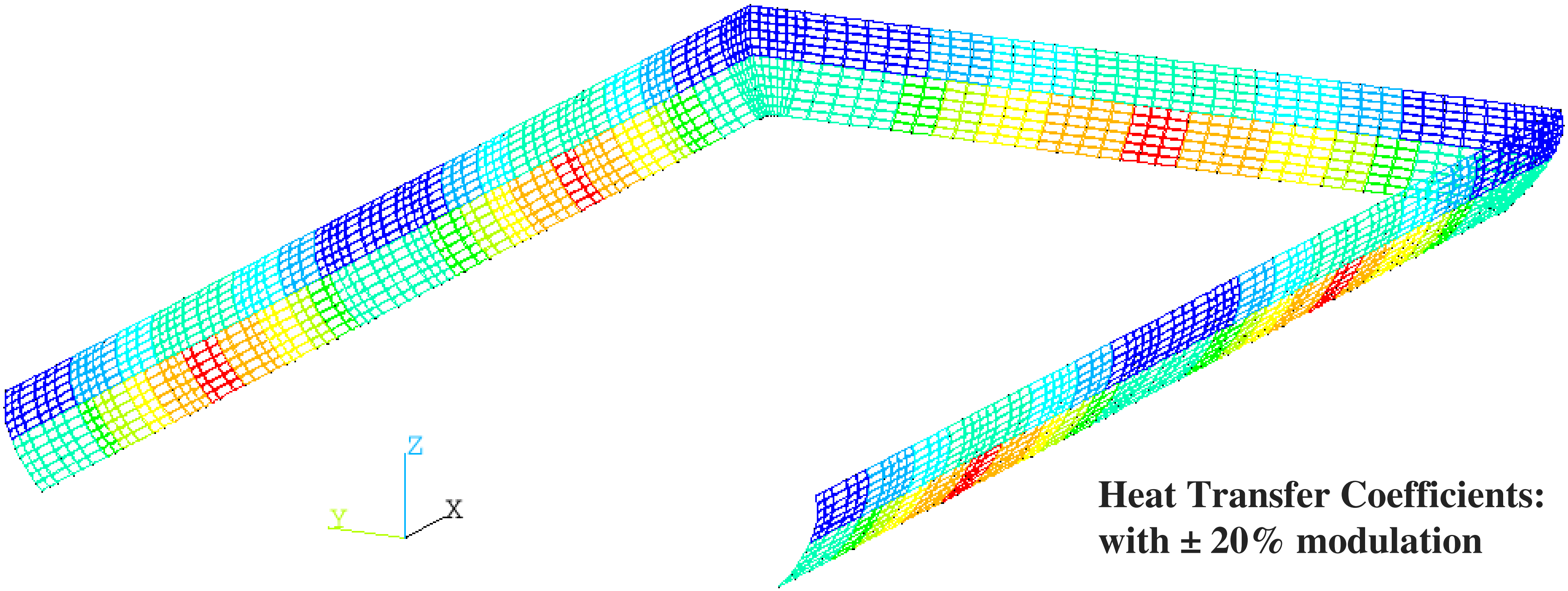

Heat Transfer Coefficients: with ± 20% modulation

GENISIM

2002, 3D thermo-electric half cathode and external busbar model

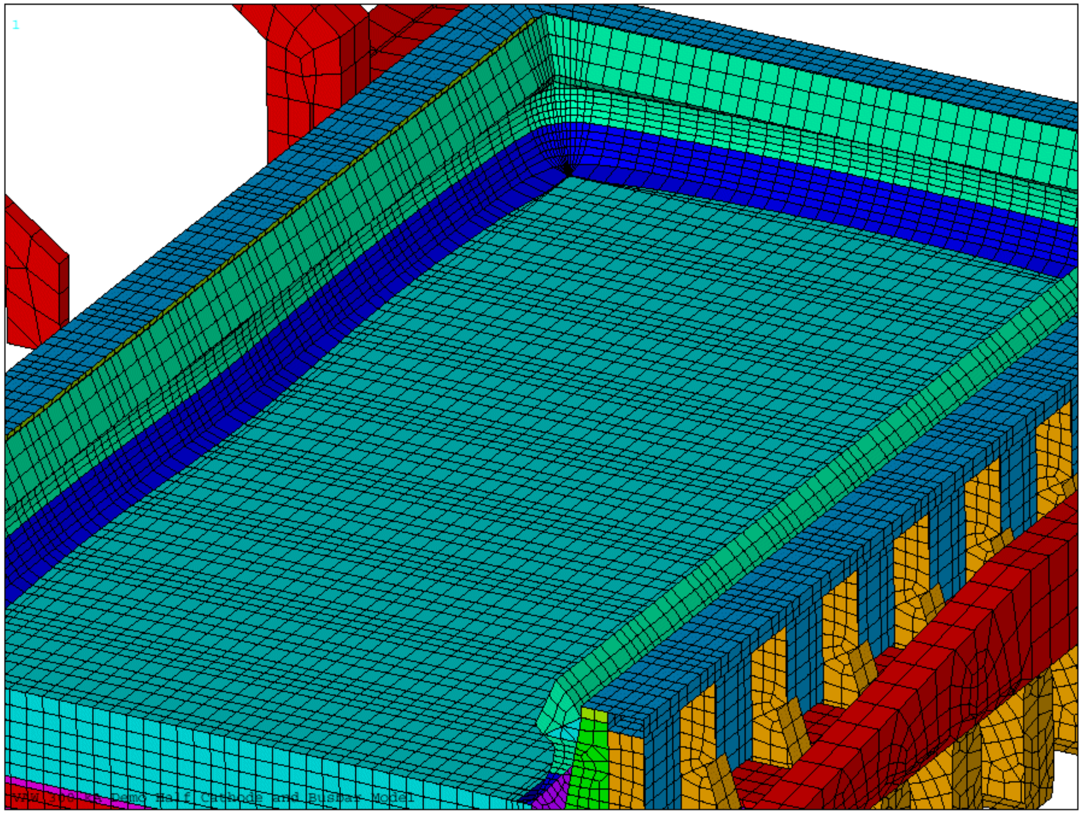

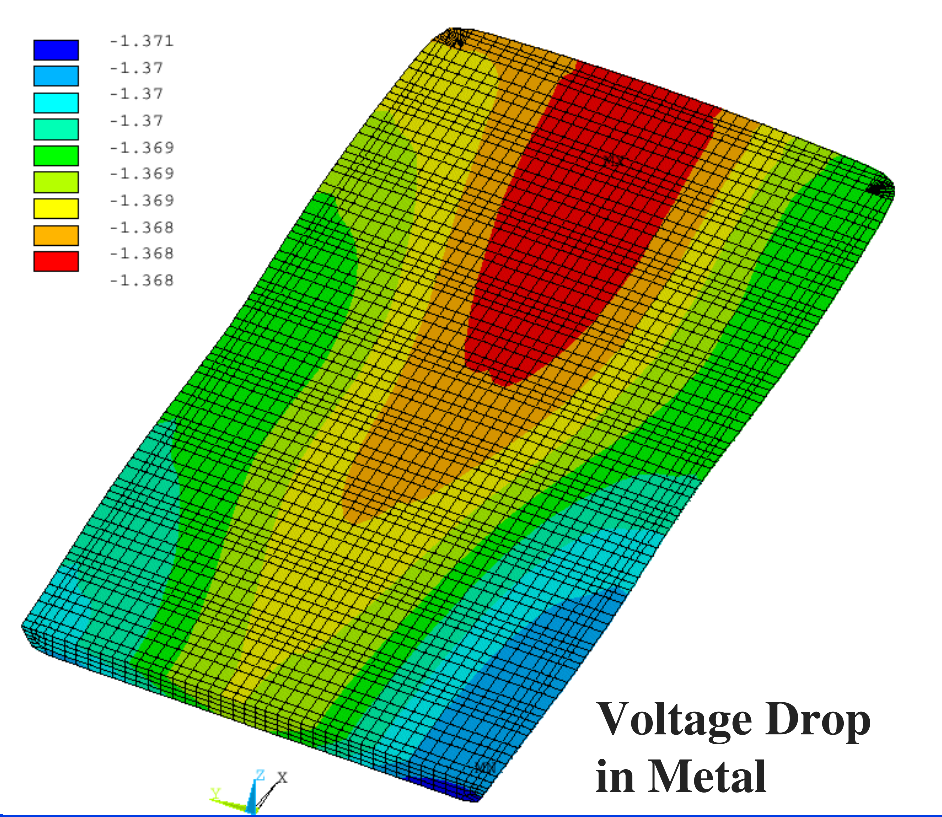

Voltage Drop in Metal

Experience of Improvements of Vertical Stud Soderberg Operation at the Largest Aluminium Smelters of Russia.

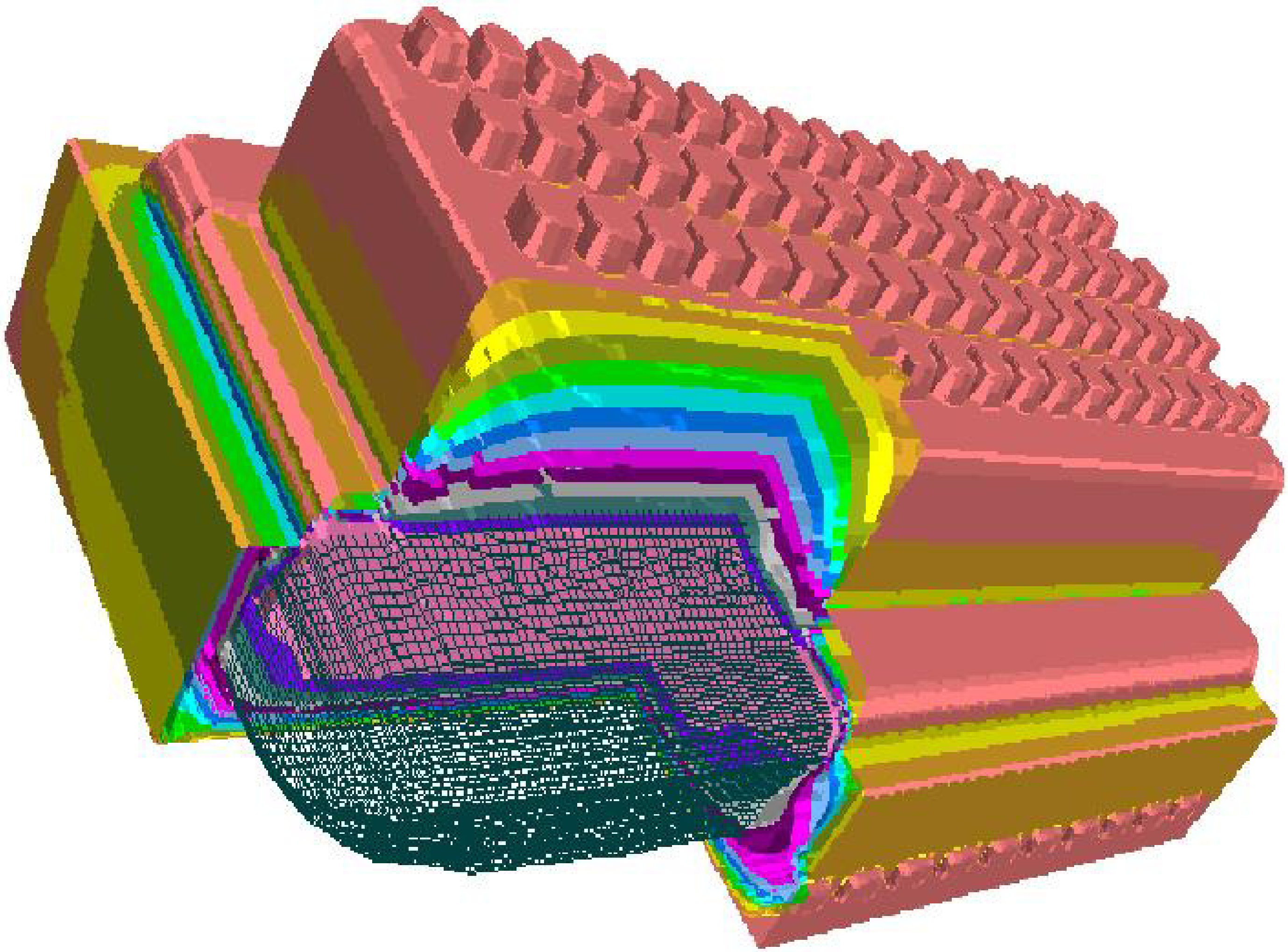

Electrical field and Energy balance

February 17-21, 2002, Seattle, WA

Experience of Improvements of Vertical Stud Soderberg Operation at the Largest Aluminium Smelters of Russia.

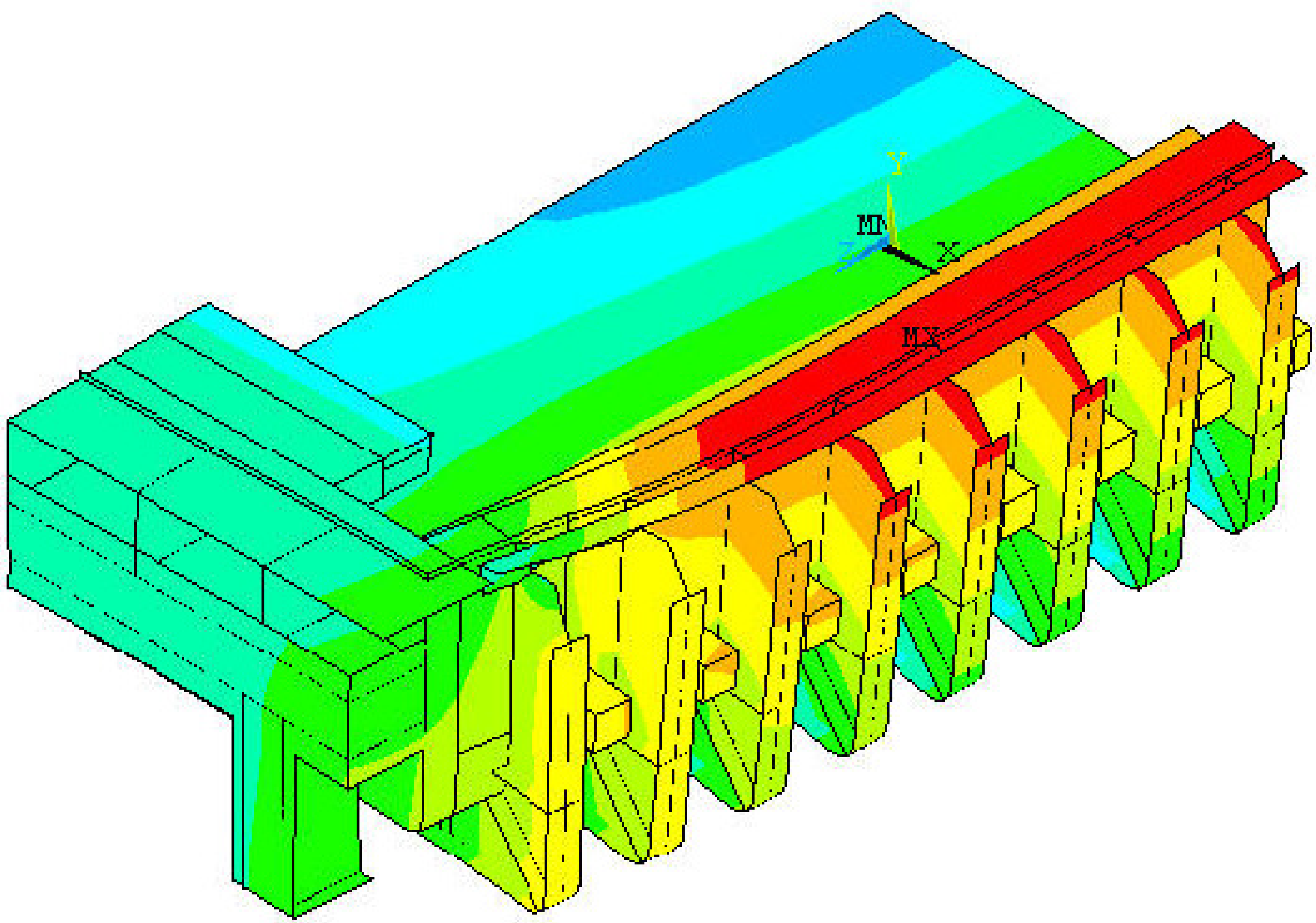

Stress-deformed state

Norðurál, the Icelandic Saga Continues

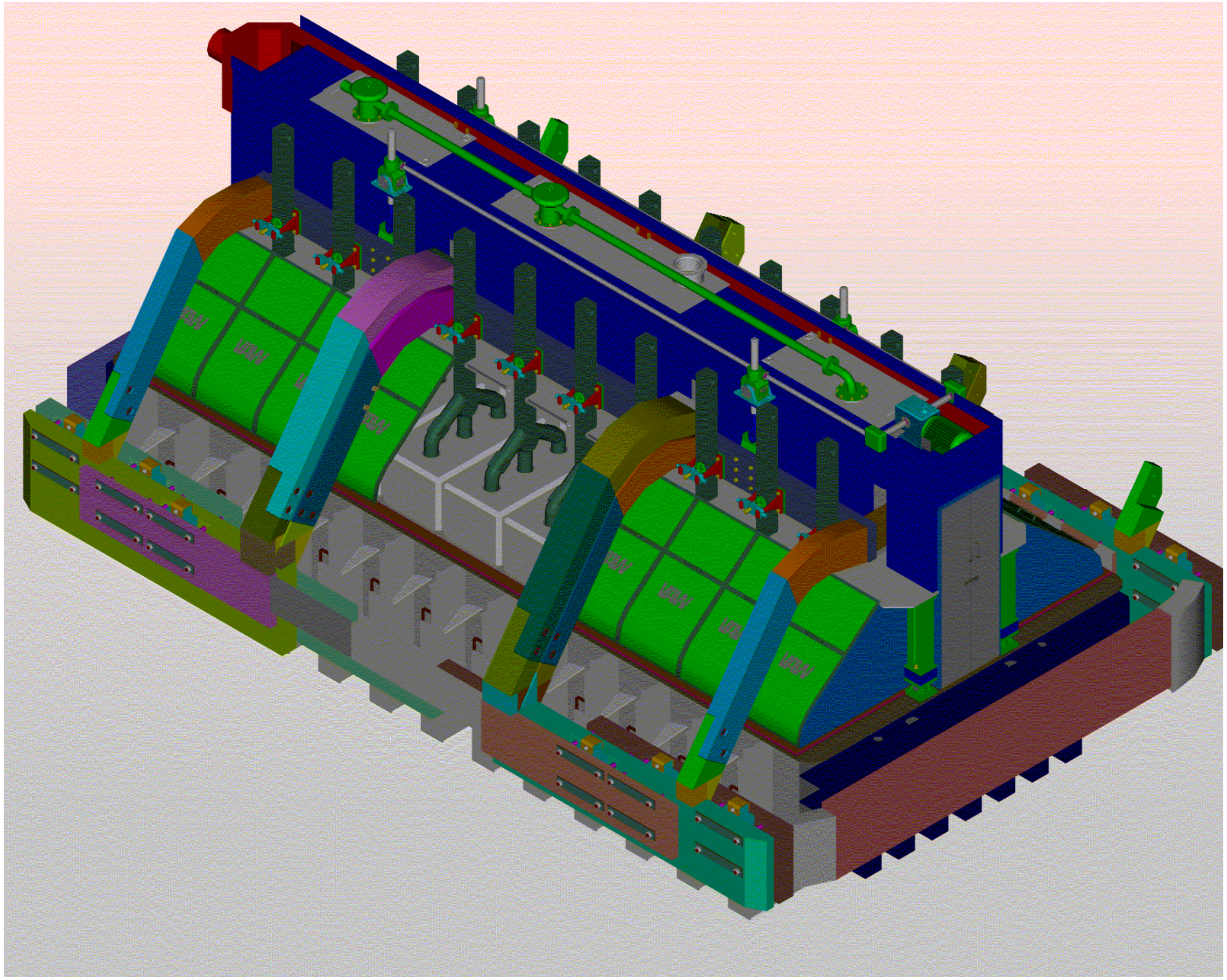

Computer model of the CA180/2 cell

Norðurál, the Icelandic Saga Continues

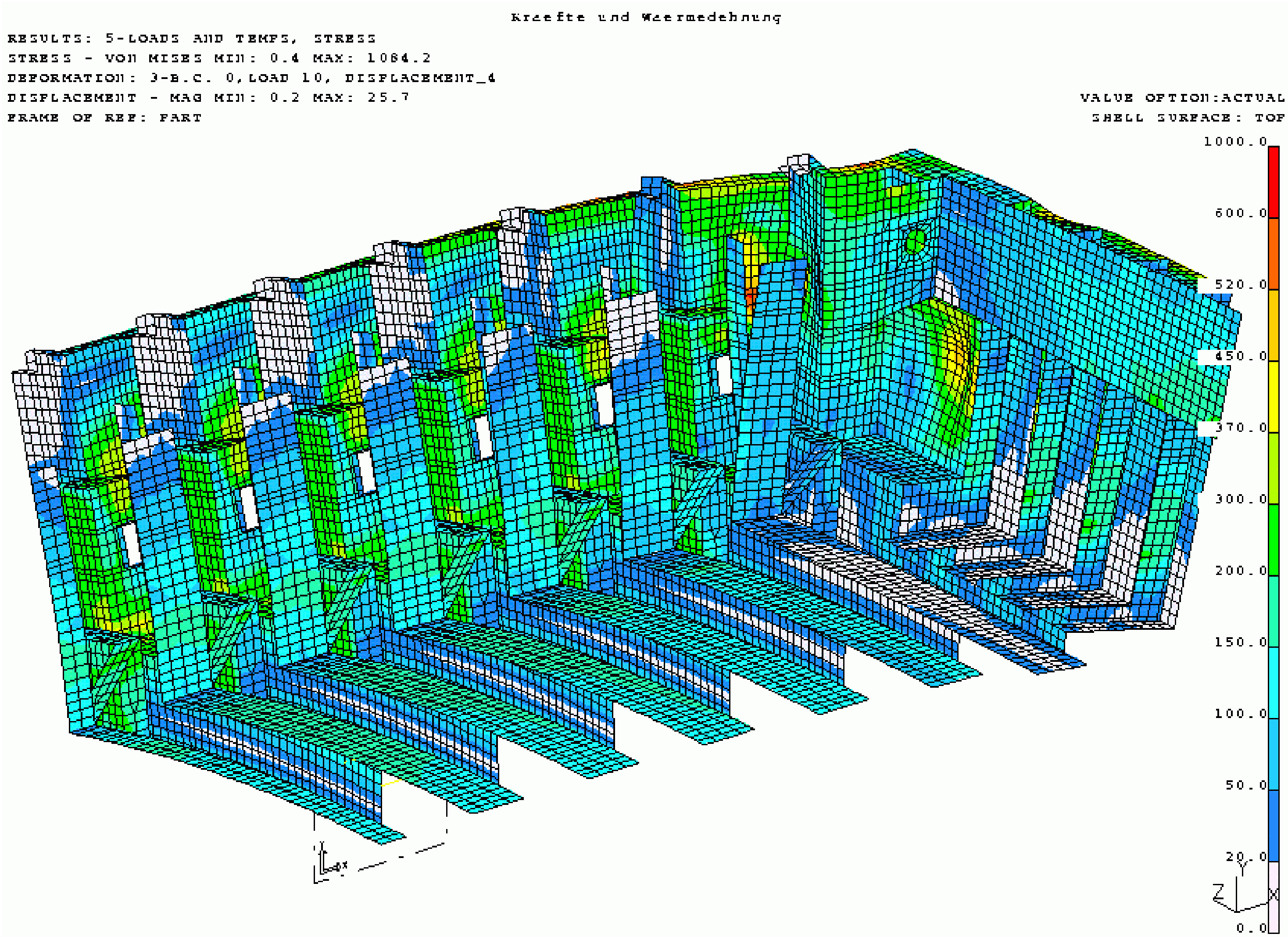

Loading forces for the CA180/2 pot shell

February 17-21, 2002, Seattle, WA

USING A MAGNETOHYDRODYNAMIC MODEL TO ANALYZE POT STABILITY IN ORDER TO IDENTIFY AN ABNORMAL OPERATING CONDITION

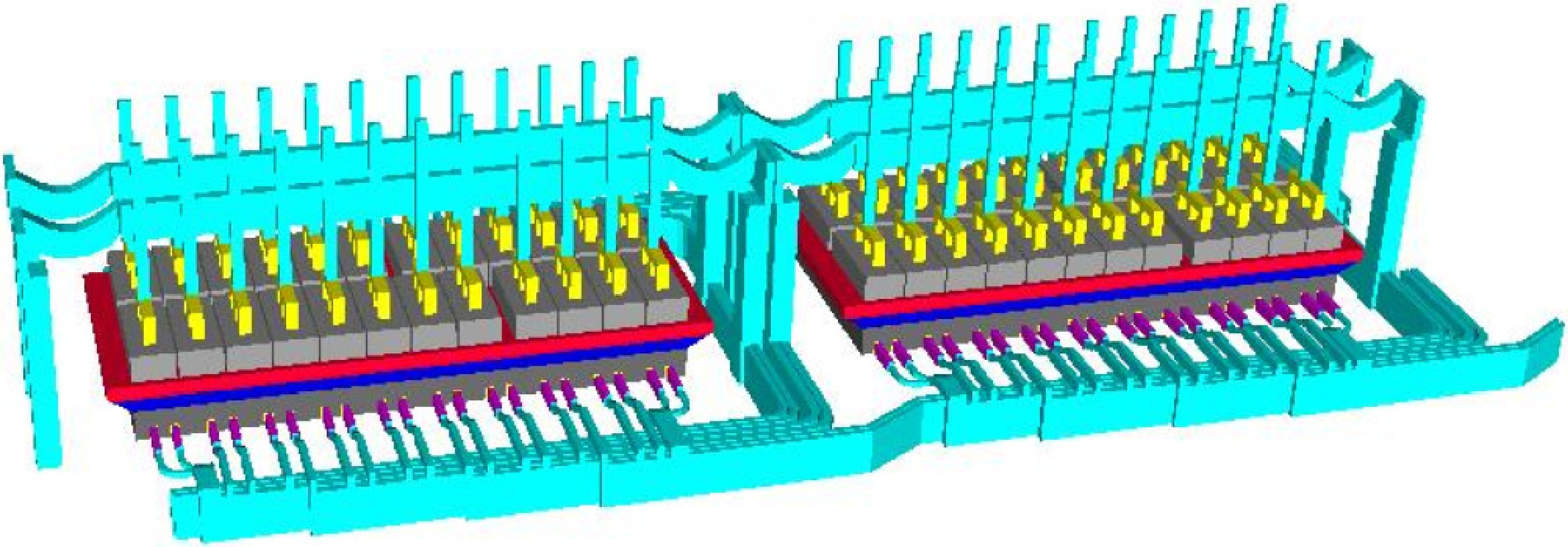

The 3D representation of the pot and its downstream neighbor

February 17-21, 2002, Seattle, WA

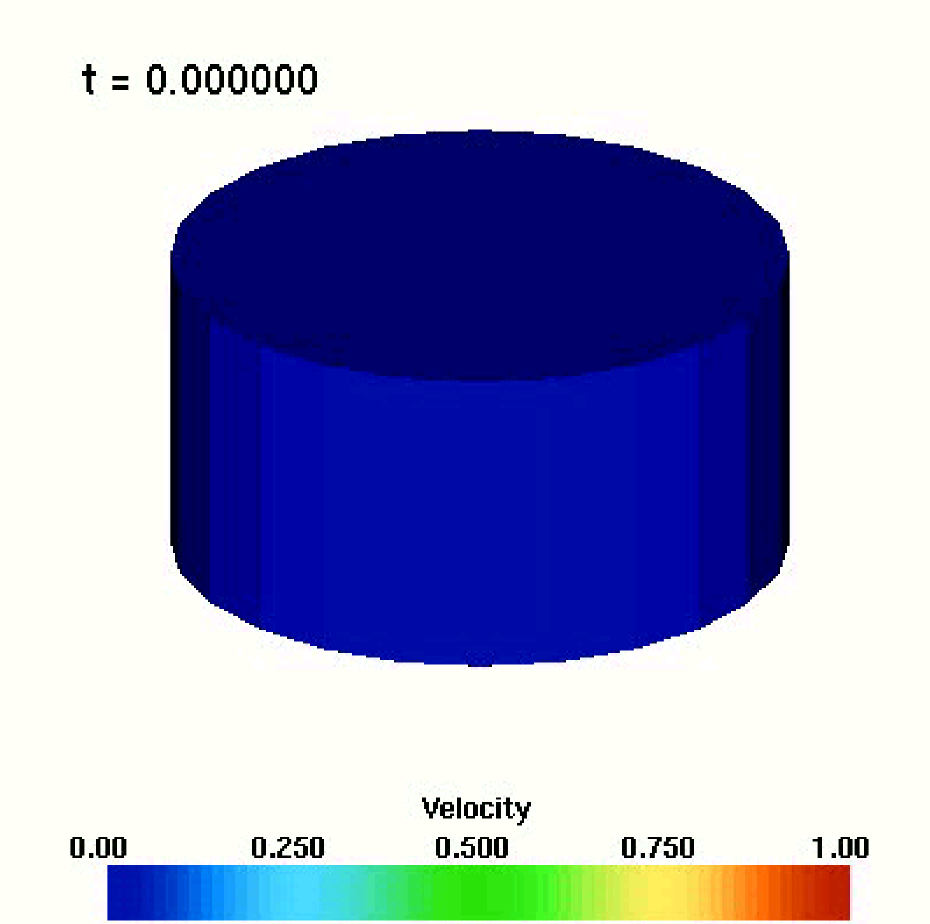

METAL PAD ROLL INSTABILITIES

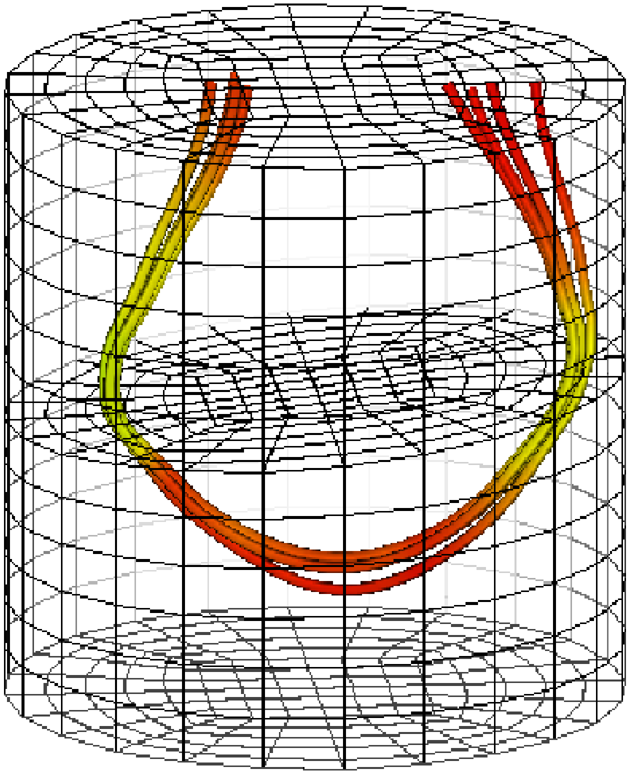

Existence of a vertical magnetic field value beyond which the cell becomes unstable

The physical explanation of the phenomenon is checked by computing the disturbed currents j = curl (B)

PROCESS MODELLING AS A KEY FACTOR IN AP14 RETROFIT AT ALUMINIJ D.D. MOSTAR

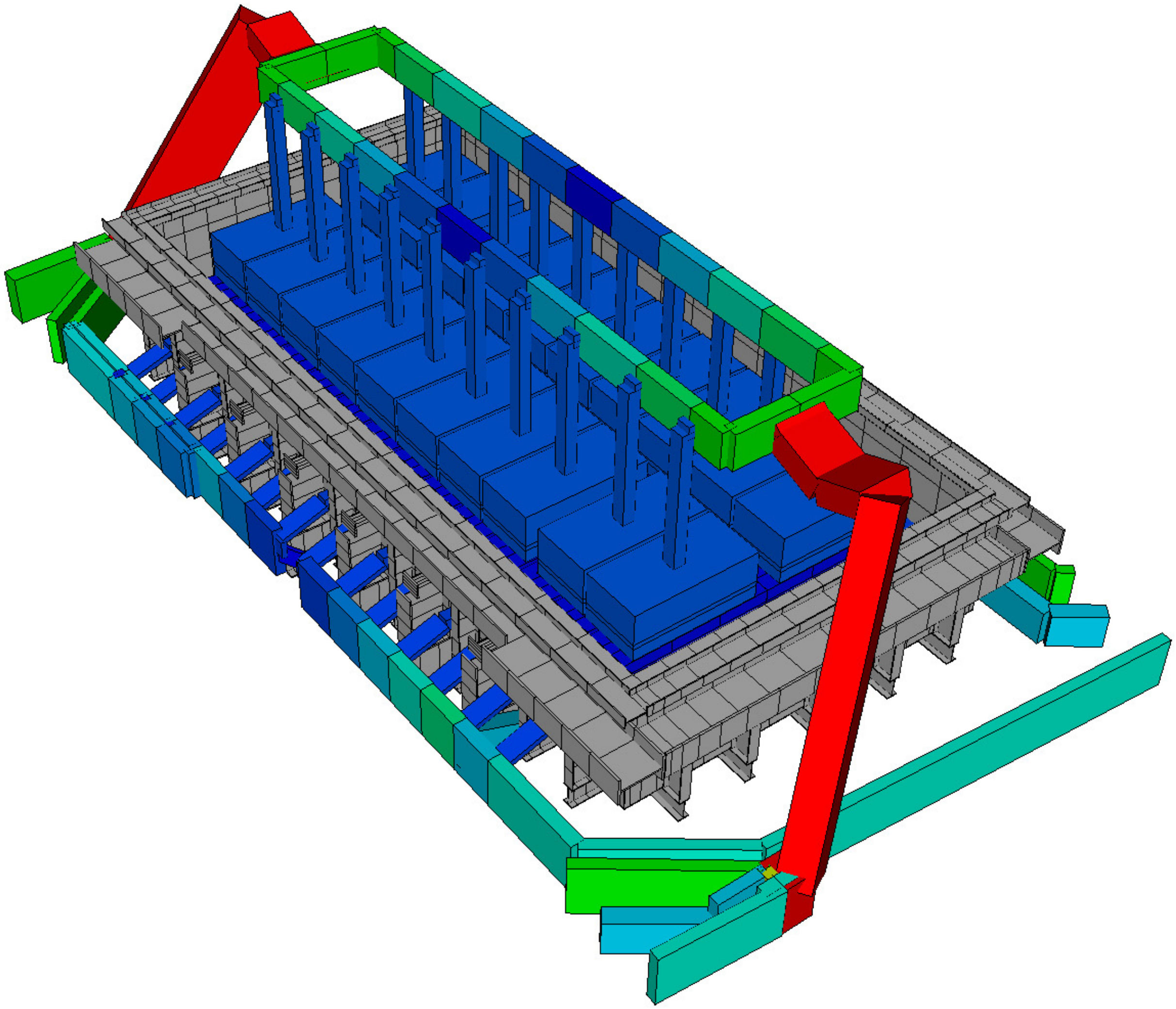

Geometrical cell model

PROCESS MODELLING AS A KEY FACTOR IN AP14 RETROFIT AT ALUMINIJ D.D. MOSTAR

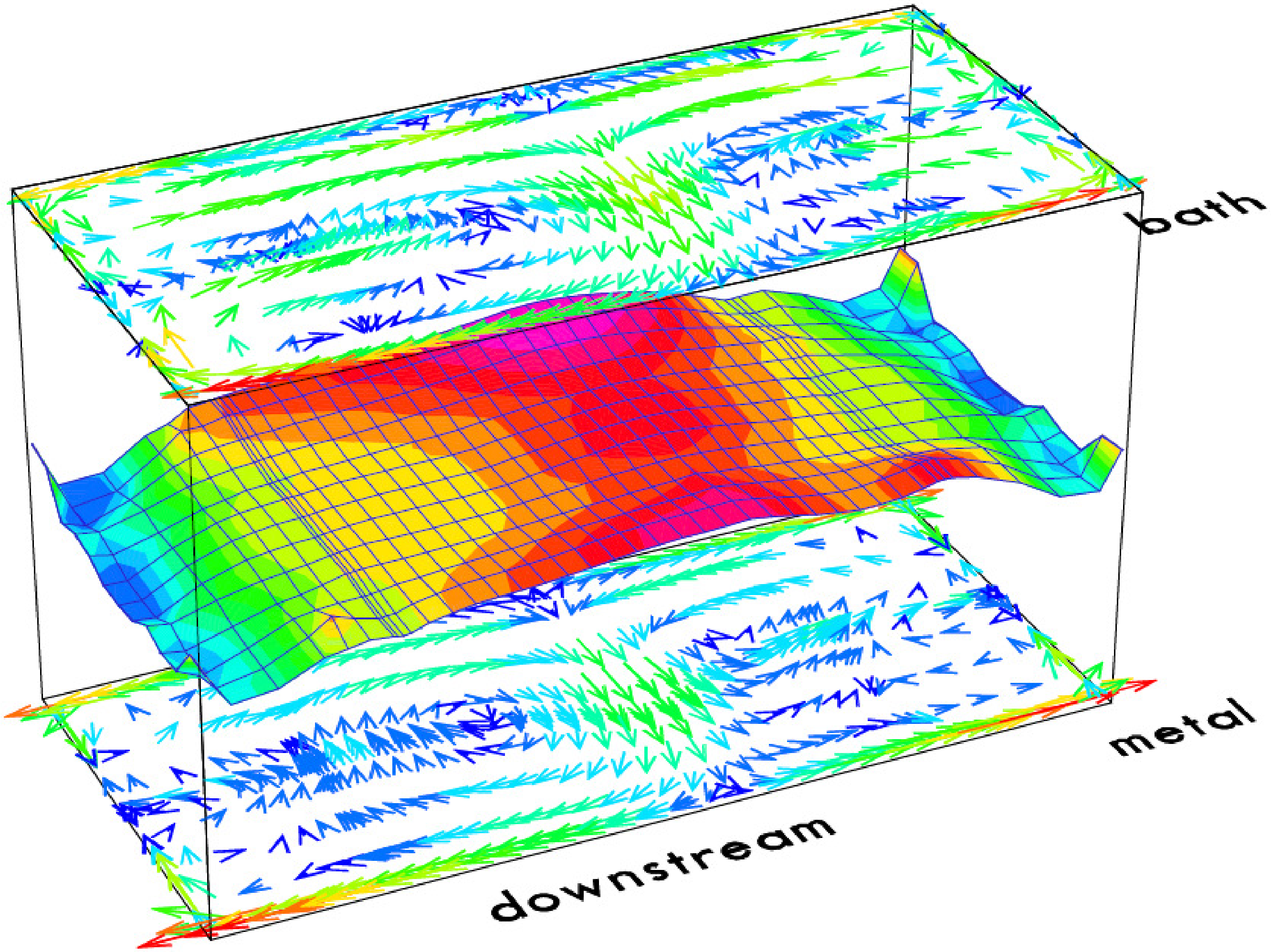

Fluid flow of the liquid metal and bath and metal heaving

March 2-6, 2003, San Diego, CA

PROCESS MODELLING AS A KEY FACTOR IN AP14 RETROFIT AT ALUMINIJ D.D. MOSTAR

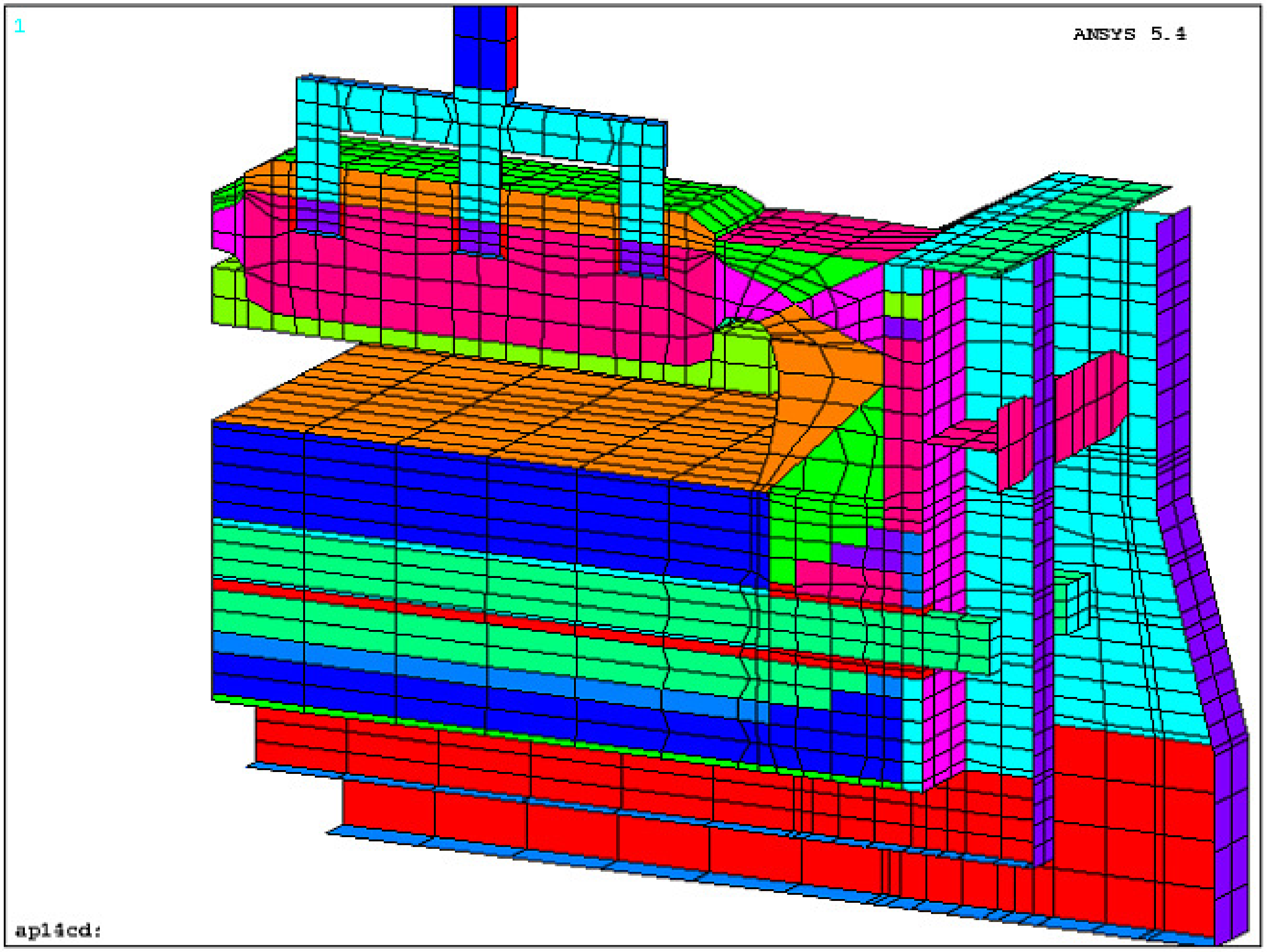

Thermo-electric slice model

2003, 3D thermo-electric full cathode and external busbar model

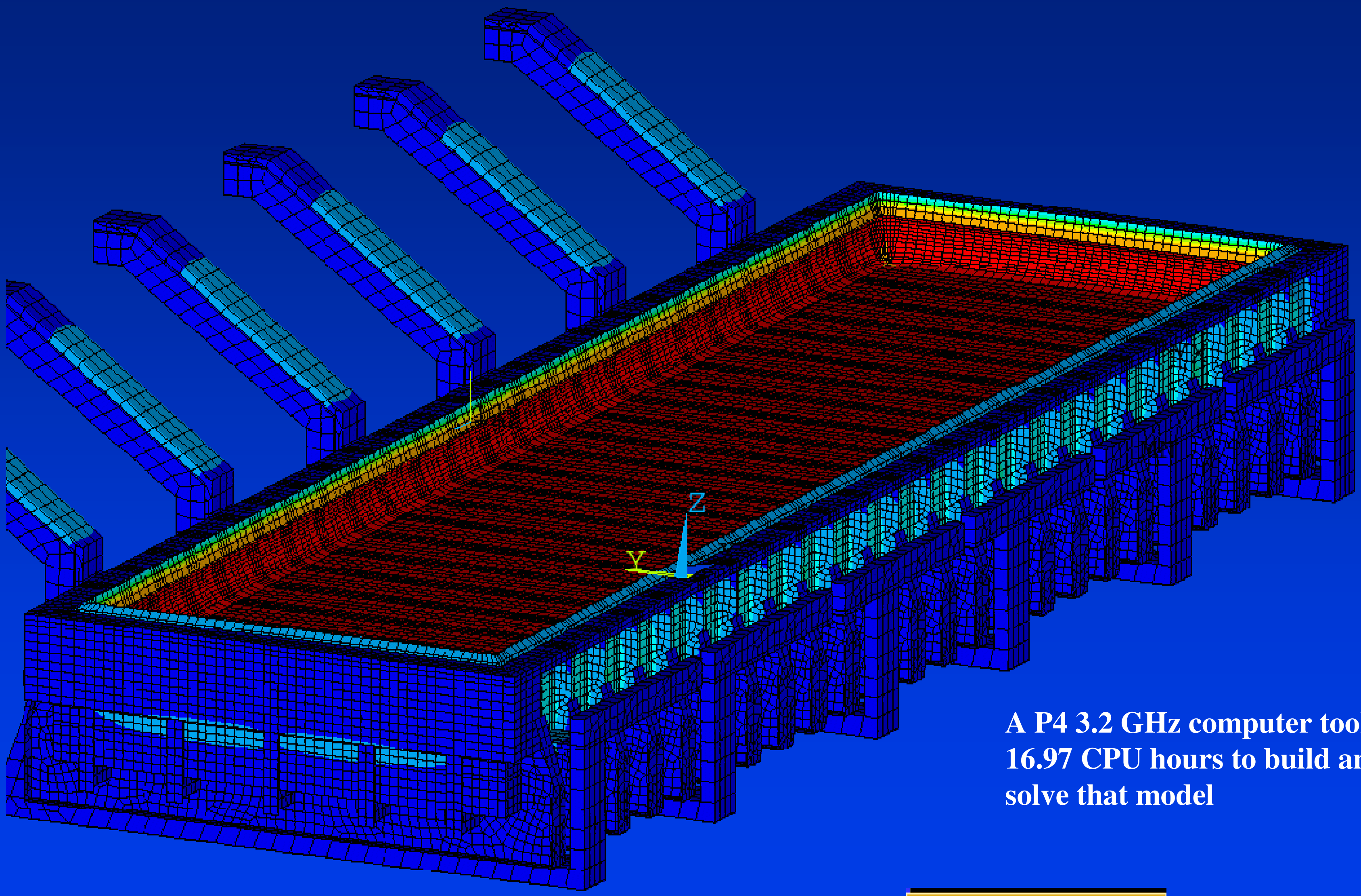

A P4 3.2 GHz computer took 16.97 CPU hours to build and solve that model

GENISIM

2003, 3D thermo-electric full cathode and external busbar model

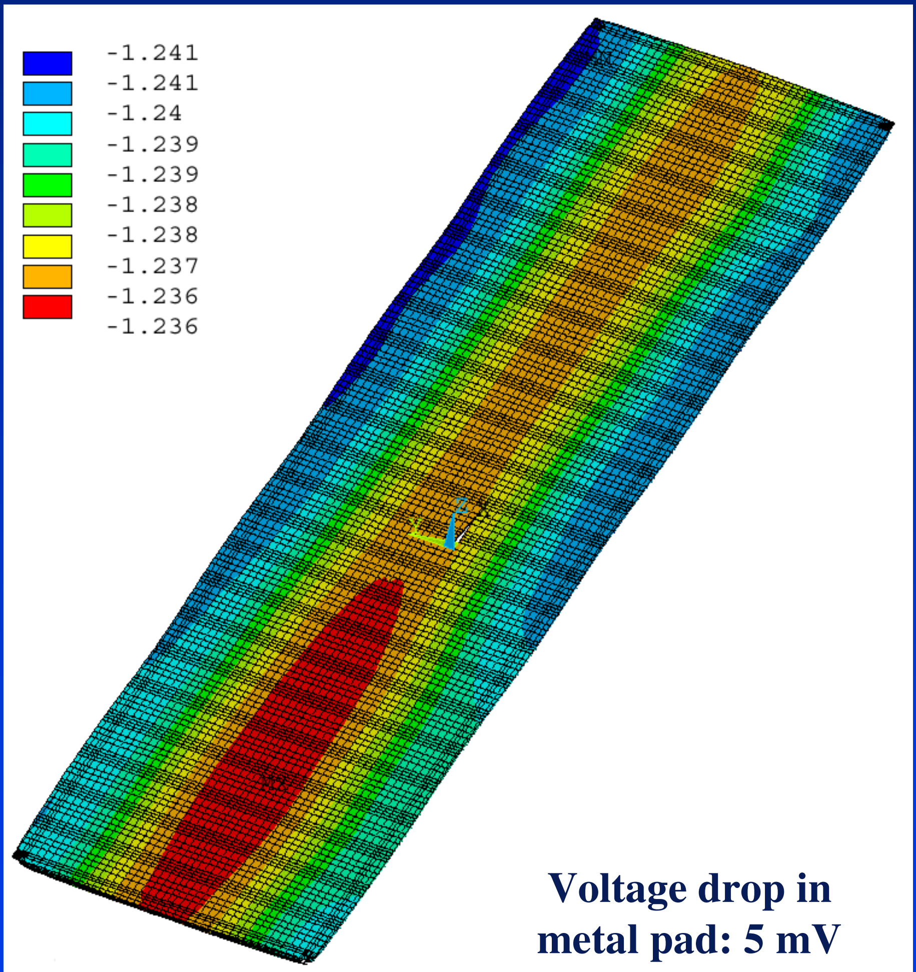

Voltage drop in metal pad: 5 mV

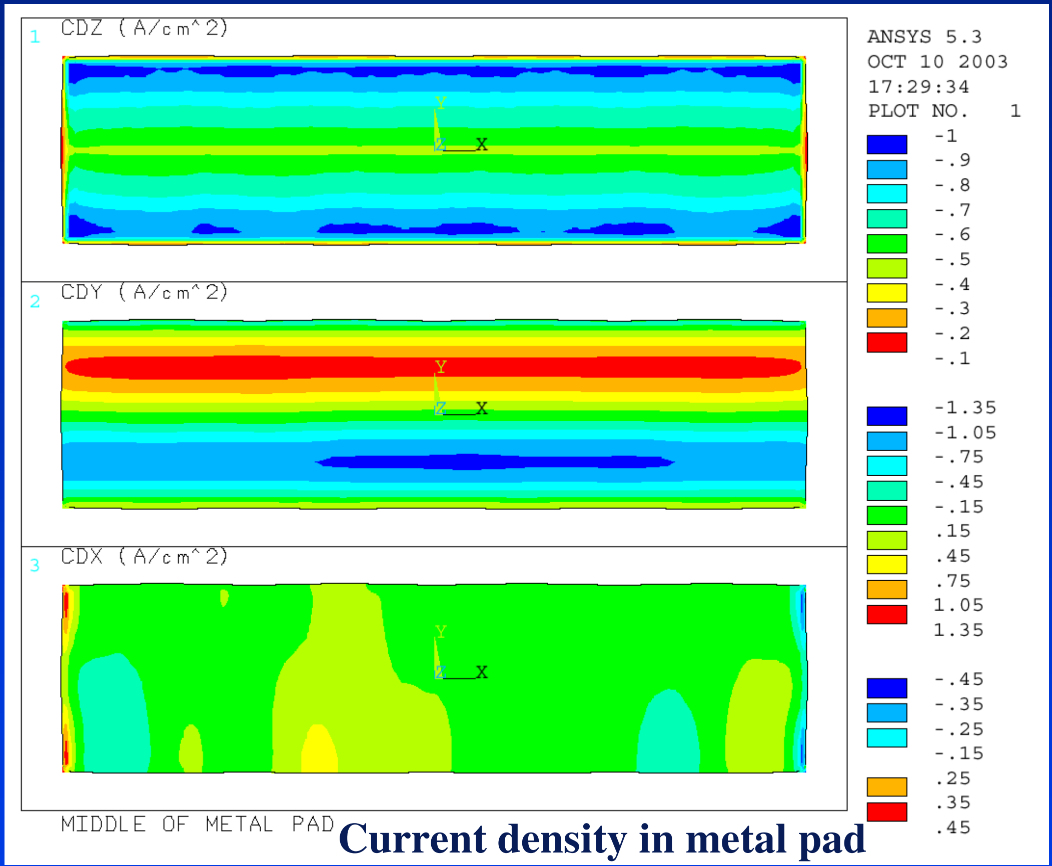

Current density in metal pad

GENISIM

MATHEMATICAL MODELING OF ALUMINUM REDUCTION CELLS IN "RUSSIAN ALUMINUM" COMPANY

COSMOS/M

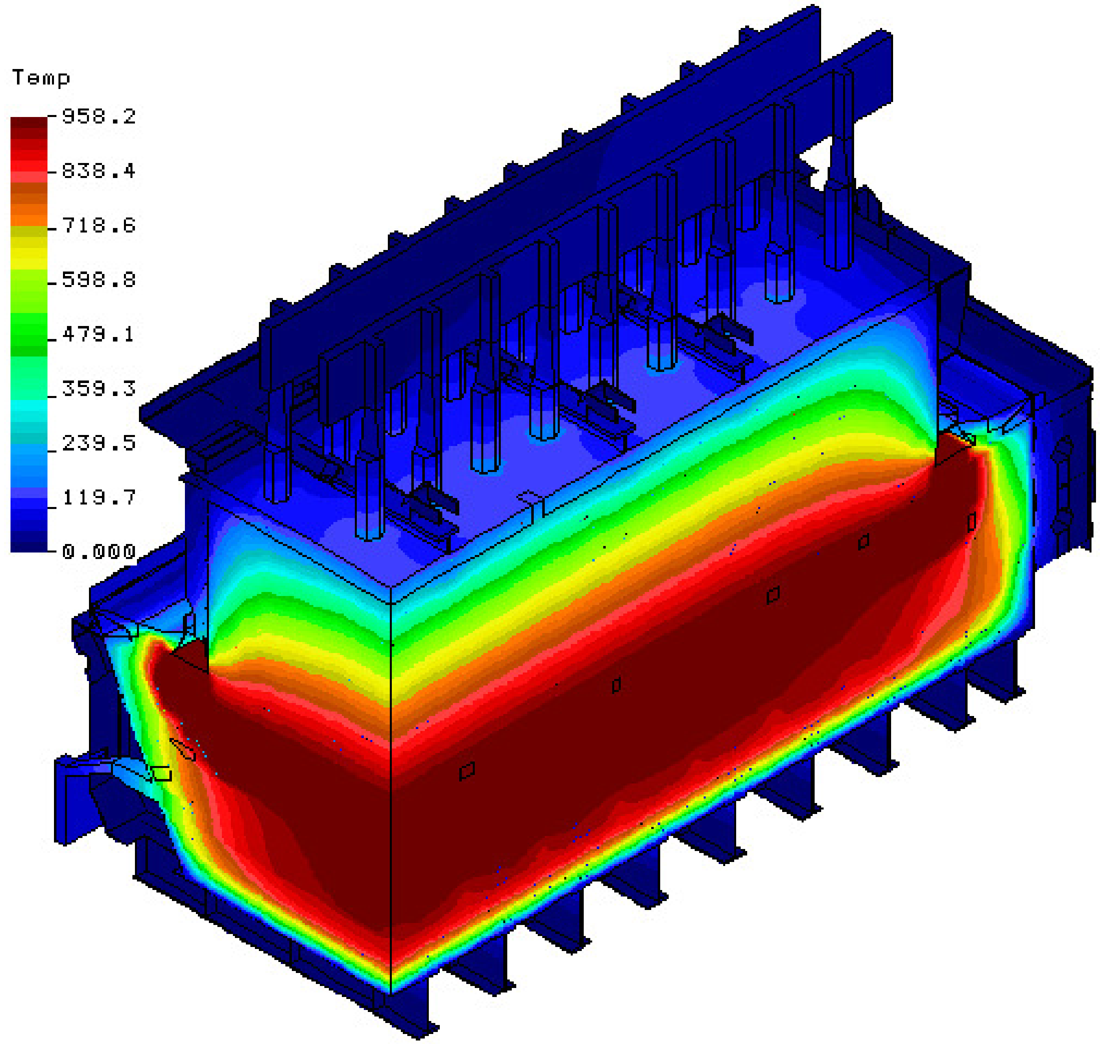

Temperature field of a cell.

MATHEMATICAL MODELING OF ALUMINUM REDUCTION CELLS IN "RUSSIAN ALUMINUM" COMPANY

COSMOS/M

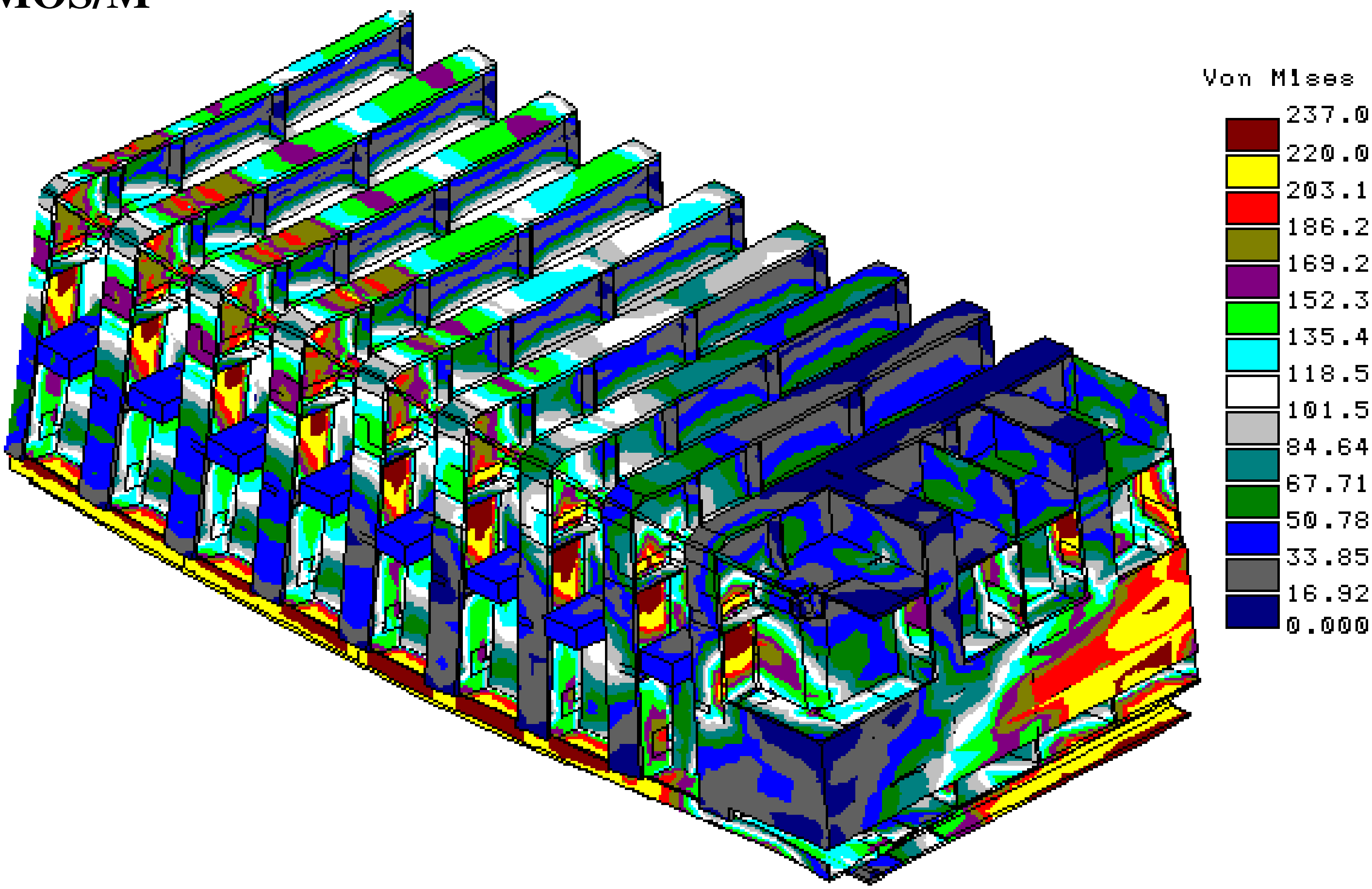

Stress-strain state of the shell and deformation of the cathode structure.

MATHEMATICAL MODELING OF ALUMINUM REDUCTION CELLS IN “RUSSIAN ALUMINUM” COMPANY

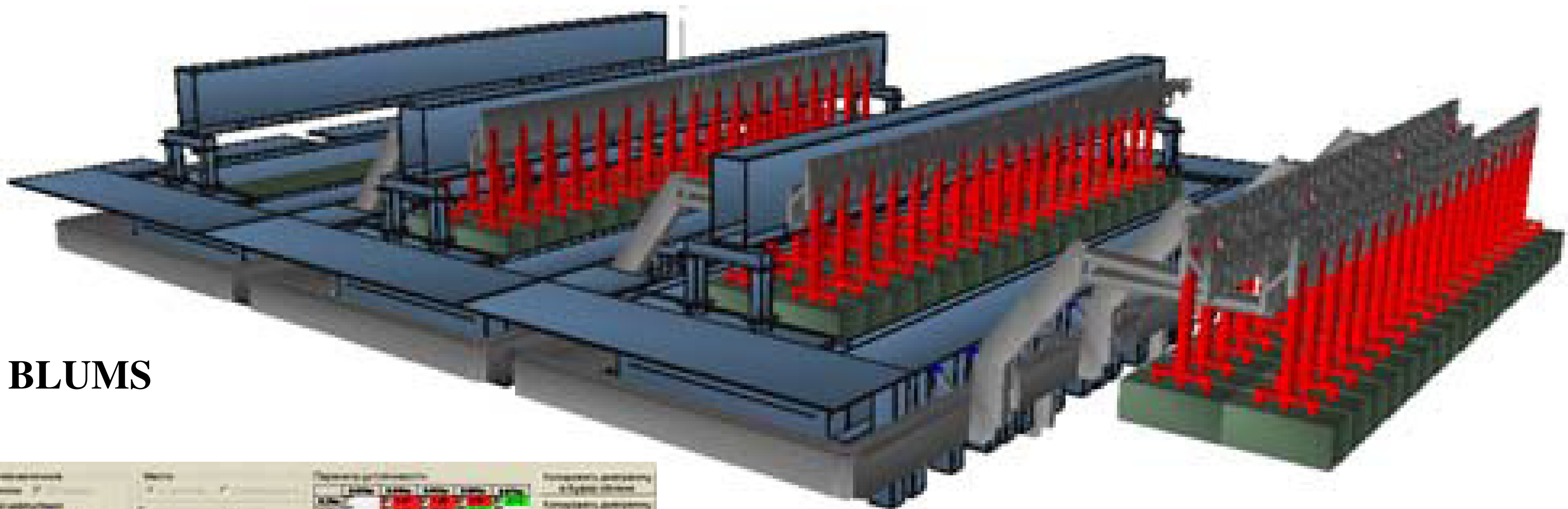

BLUMS

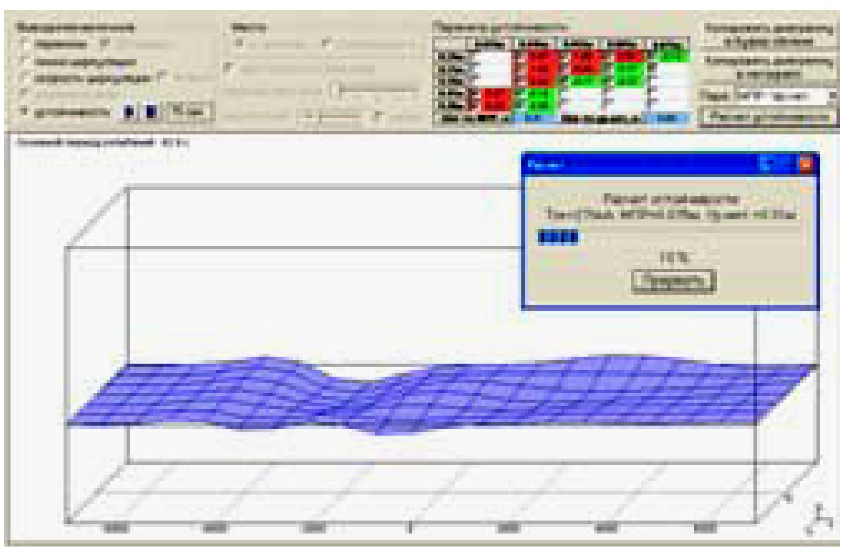

Evaluation of MHD stability in the cell

March 14-18, 2005, Charlotte, NC

MATHEMATICAL MODELING OF ALUMINUM REDUCTION CELLS IN "RUSSIAN ALUMINUM" COMPANY

ANSYS

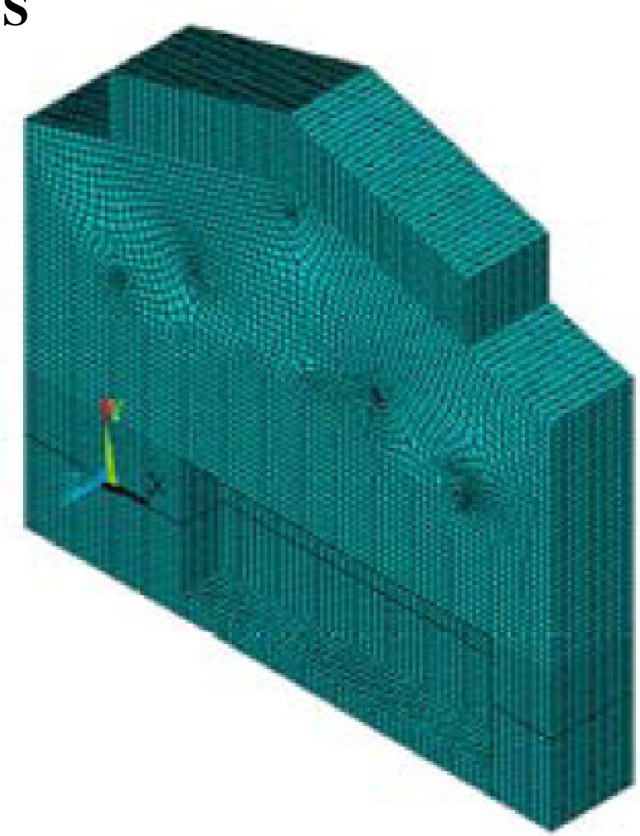

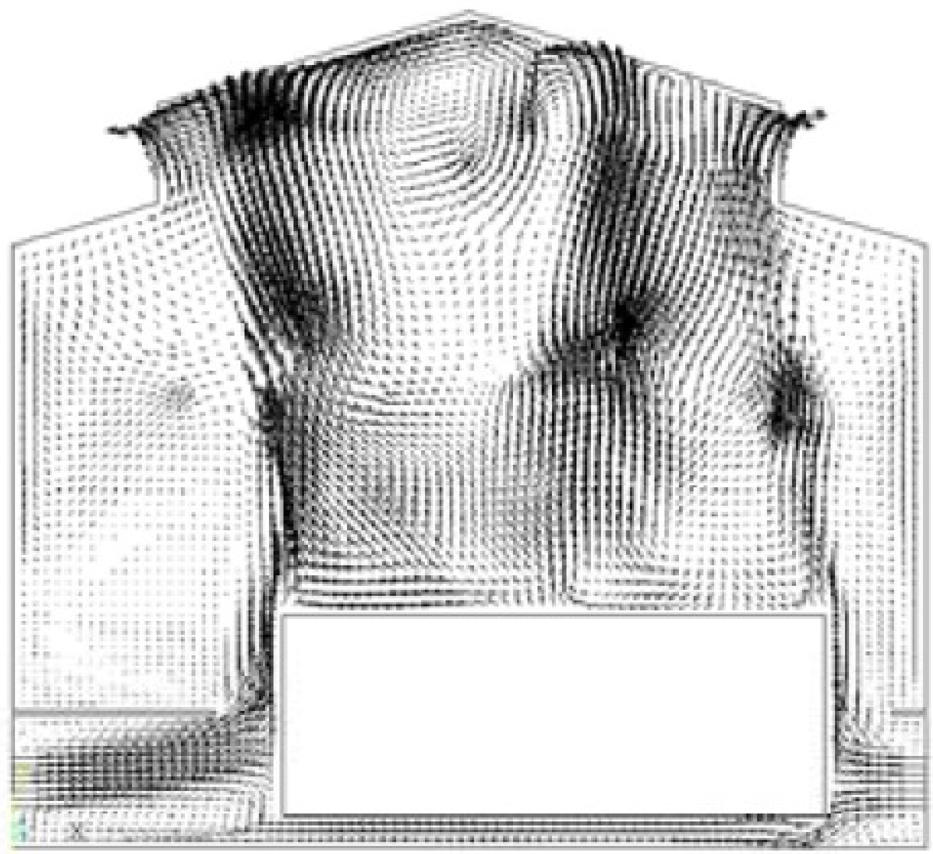

Potroom ventillation: Calculation model and velocity field.

March 14-18, 2005, Charlotte, NC

3-D MODELLING OF THERMAL AND SODIUM EXPANSION IN SODERBERG ALUMINIUM REDUCTION CELLS

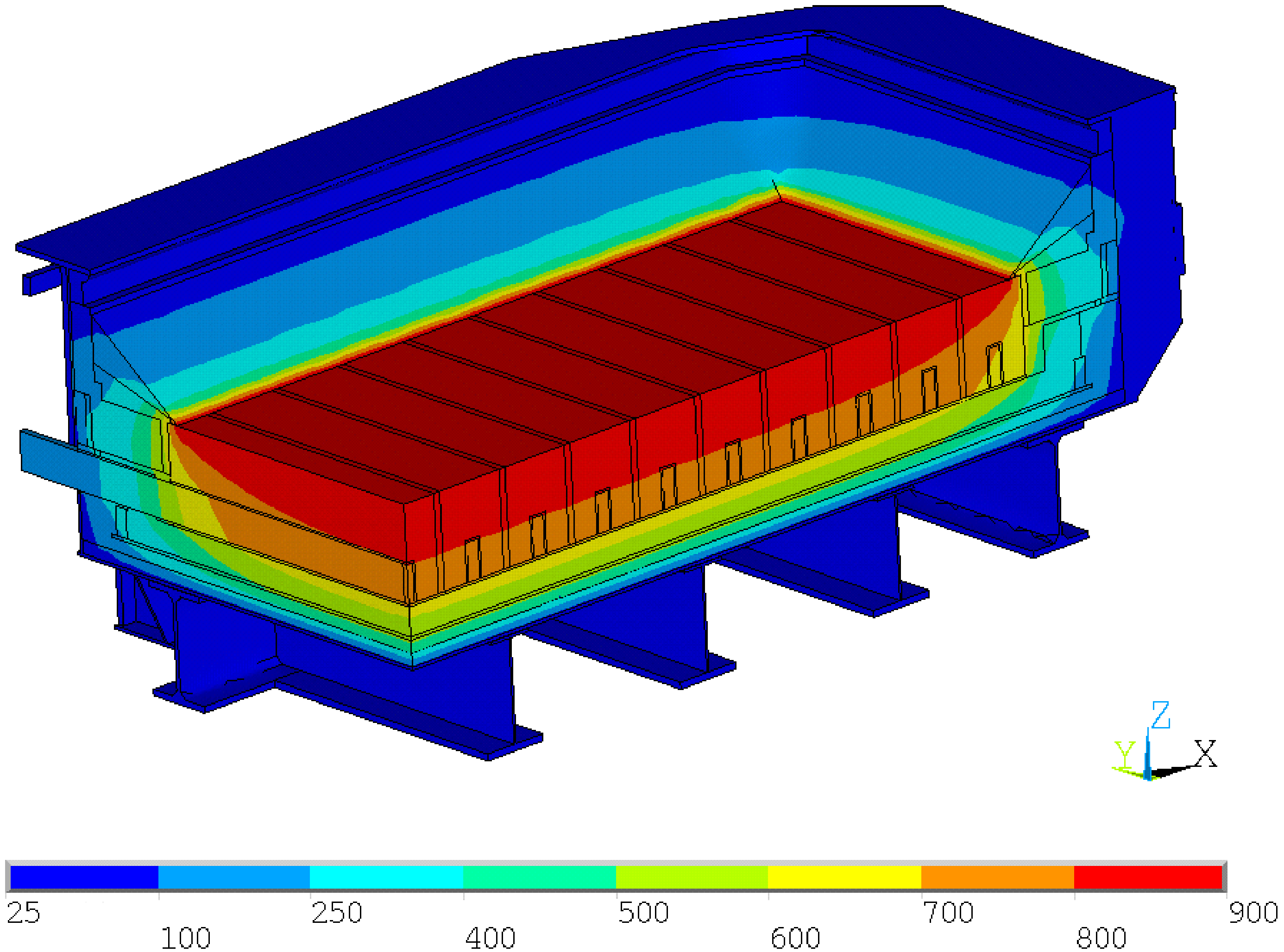

Thermal field distribution after 48 hours preheat

3-D MODELLING OF THERMAL AND SODIUM EXPANSION IN SODERBERG ALUMINIUM REDUCTION CELLS

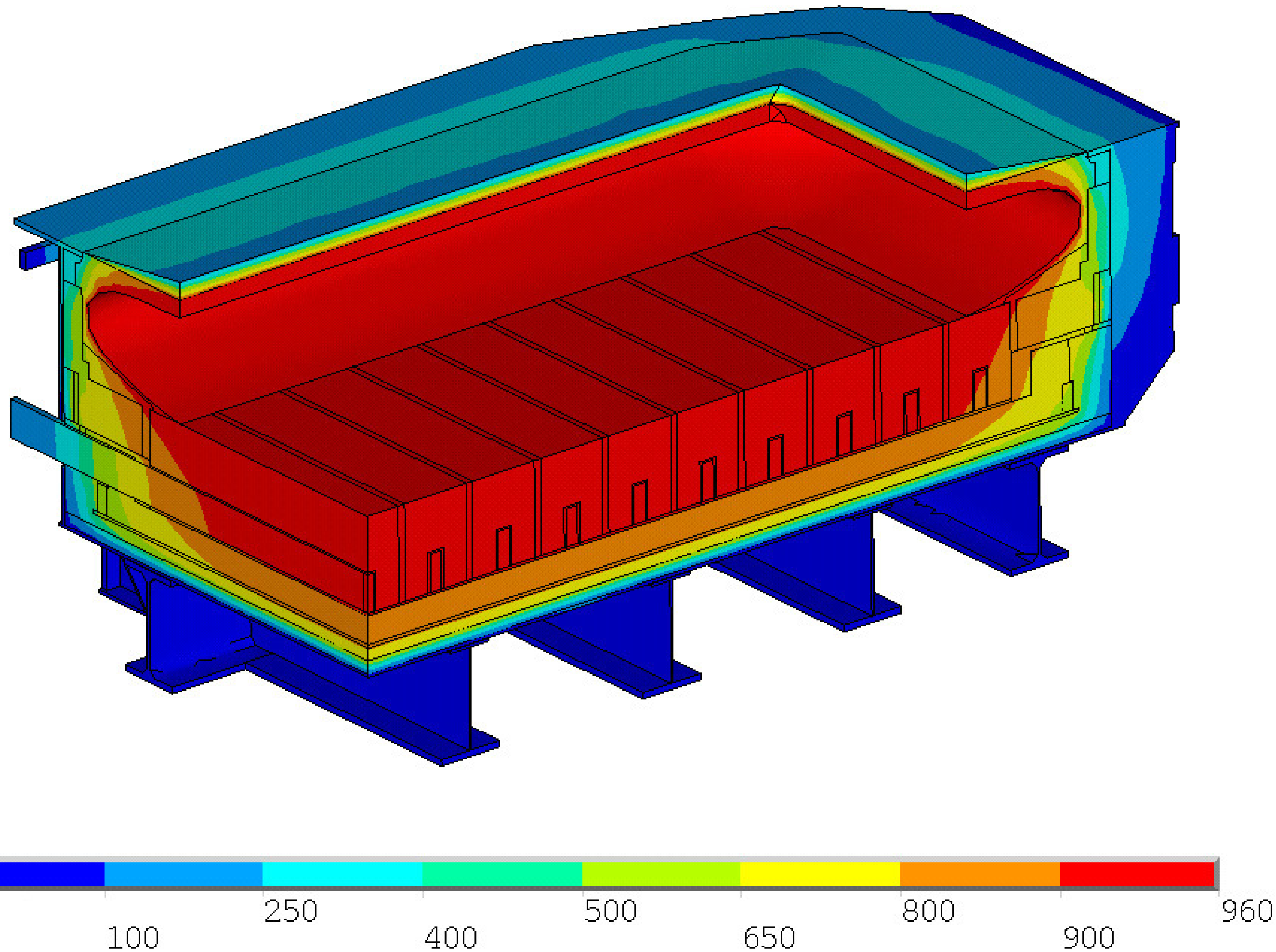

Thermal field distribution, 30 days after start-up (˚C)

March 14-18, 2005, Charlotte, NC

3-D MODELLING OF THERMAL AND SODIUM EXPANSION IN SODERBERG ALUMINIUM REDUCTION CELLS

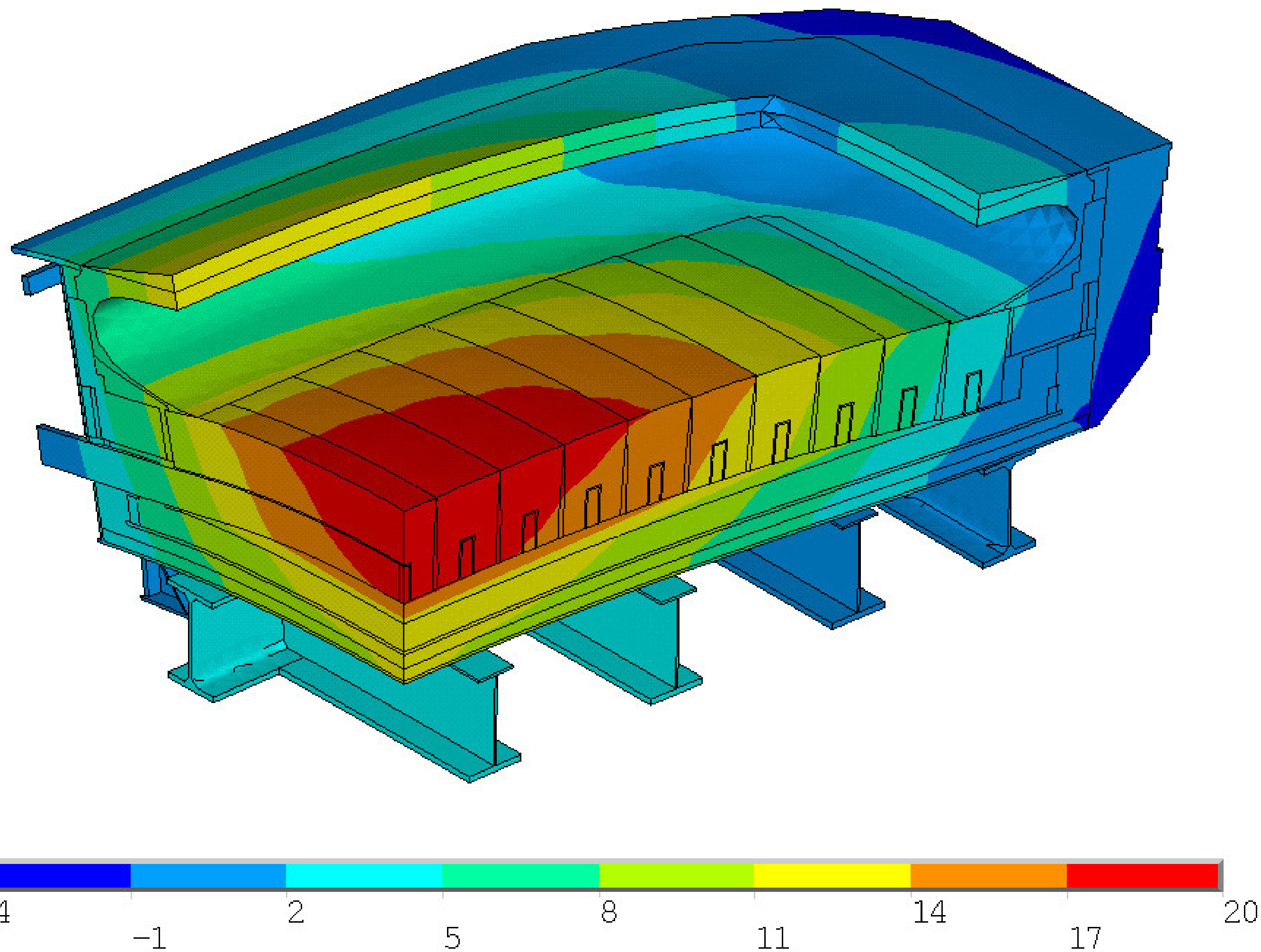

Z-direction displacement with thermal and sodium expansion

March 14-18, 2005, Charlotte, NC

2004, 3D thermo-electric full cell and external busbar model

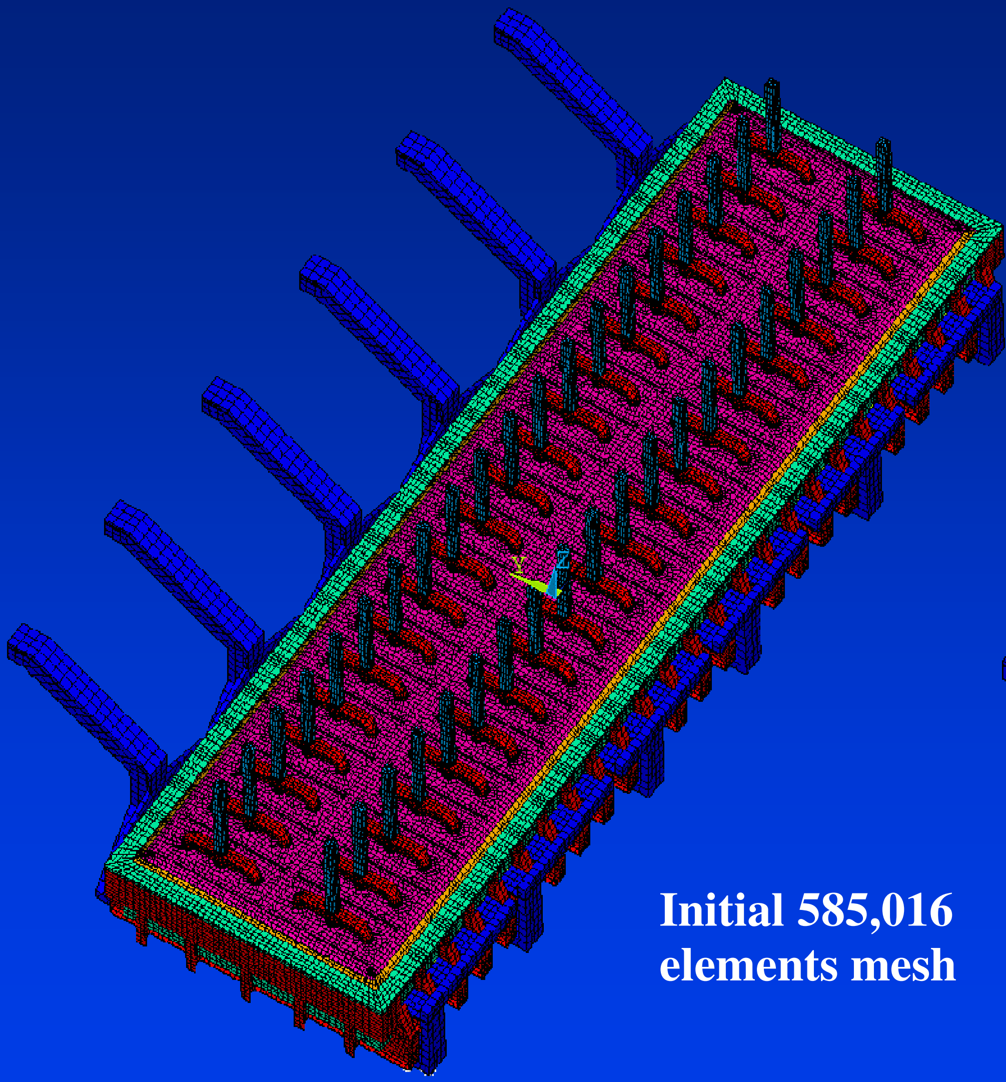

Initial 585,016 elements mesh

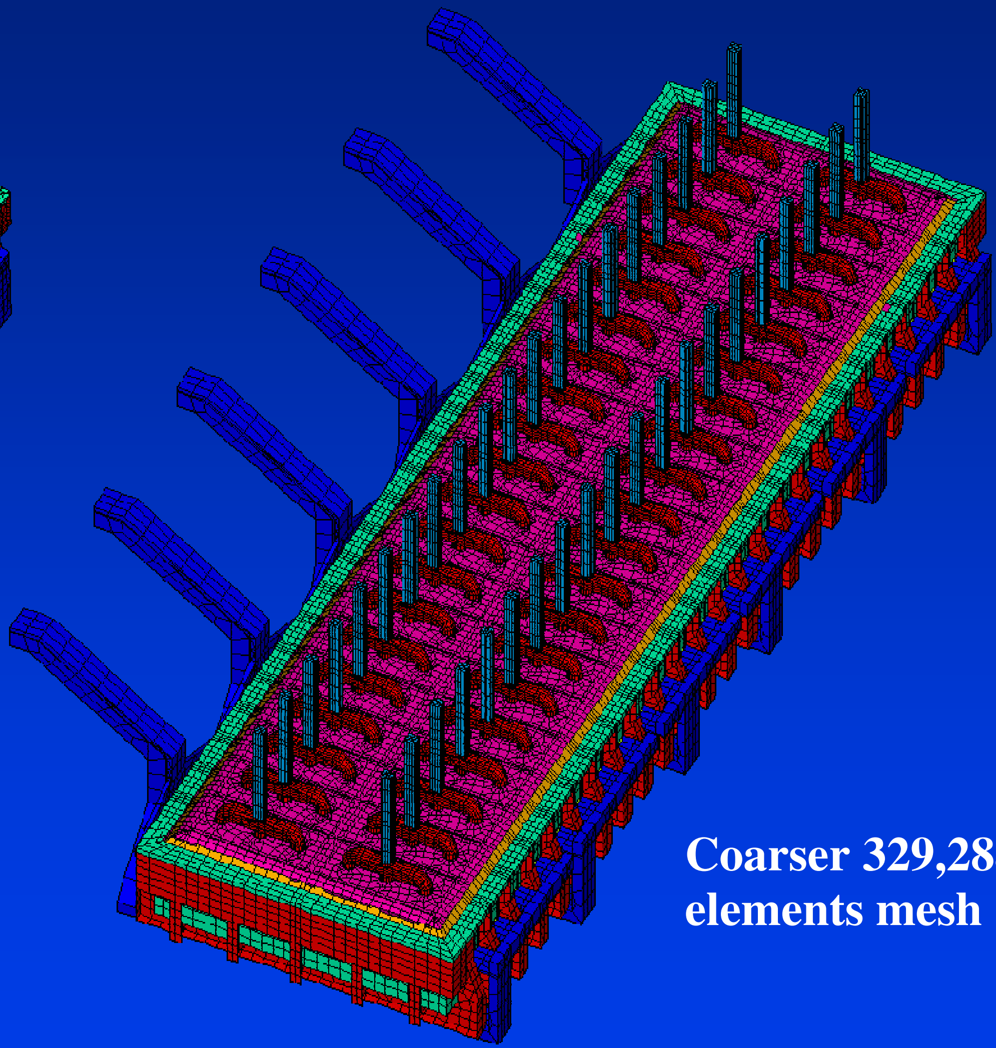

Coarser 329,288 elements mesh

GENISIM

2004, 3D thermo-electric full cell and external busbar model

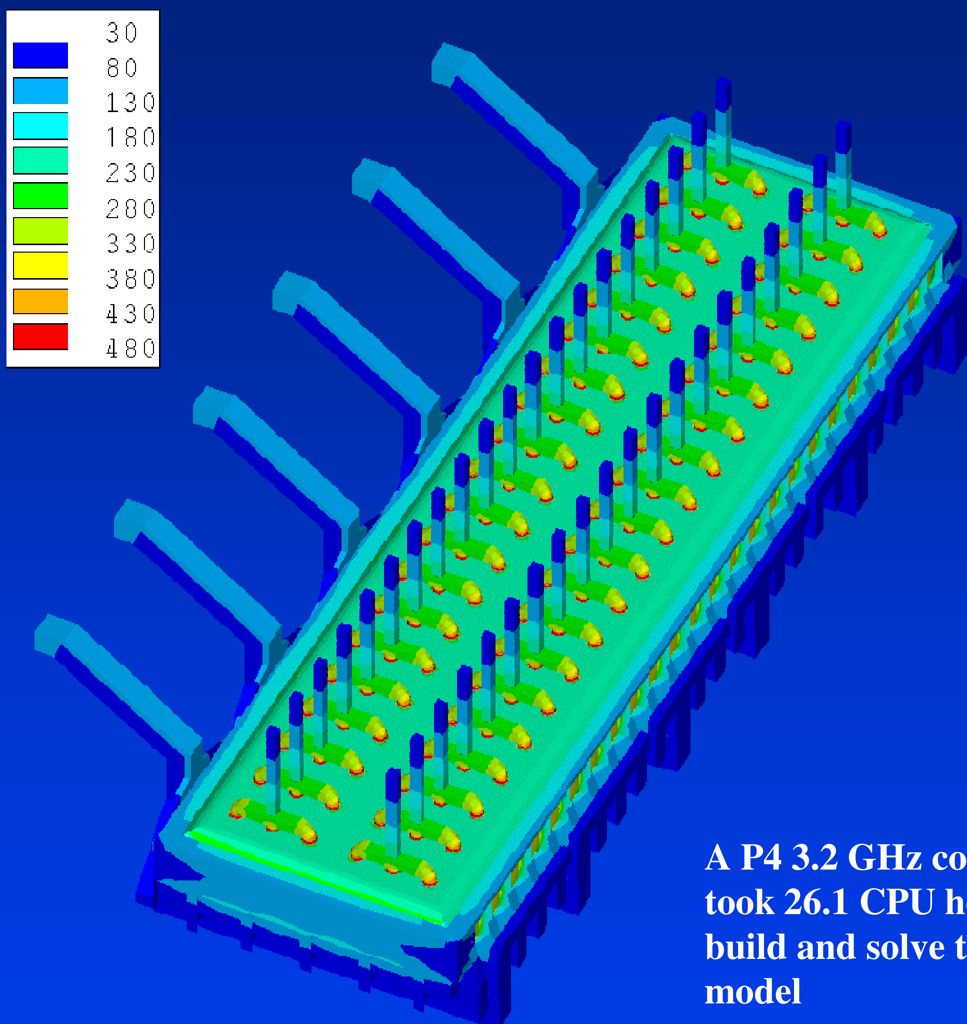

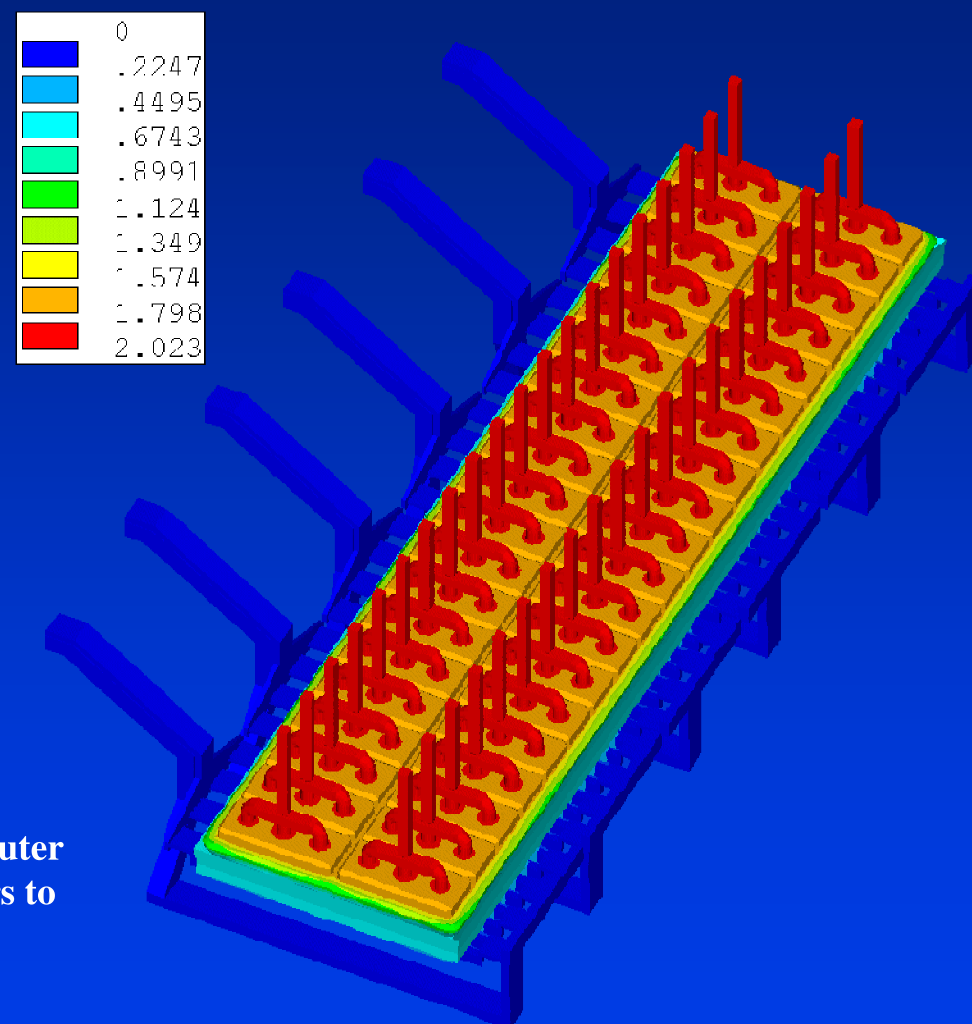

A P4 3.2 GHz computer took 26.1 CPU hours to build and solve that model

Thermo-Electric Design of a 740 kA Cell, Is There a Size Limit?

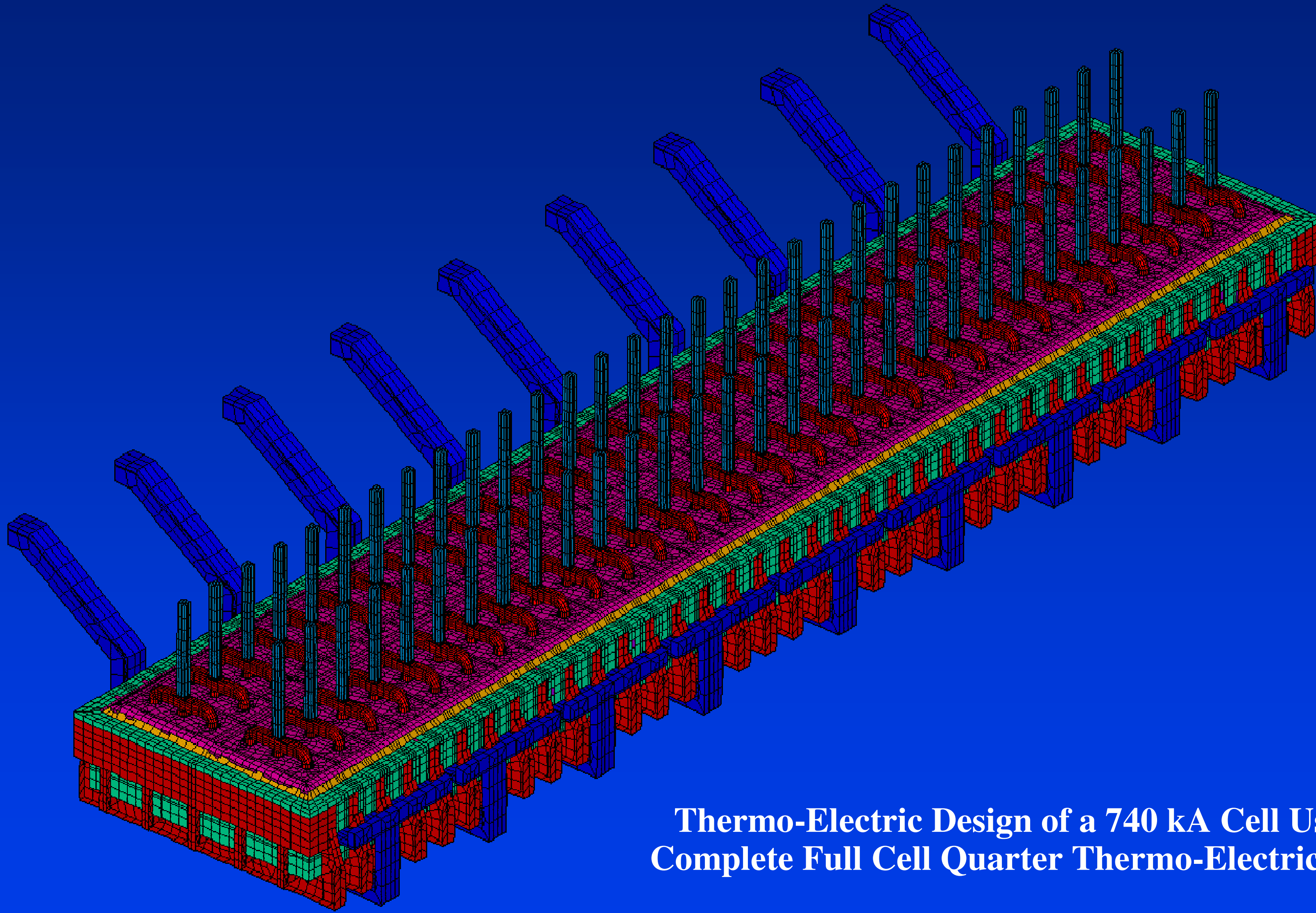

Thermo-Electric Design of a 740 kA Cell Using a Complete Full Cell Quarter Thermo-Electric Model

GENISIM

2004, 3D thermo-electric full cell and external busbar erosion model

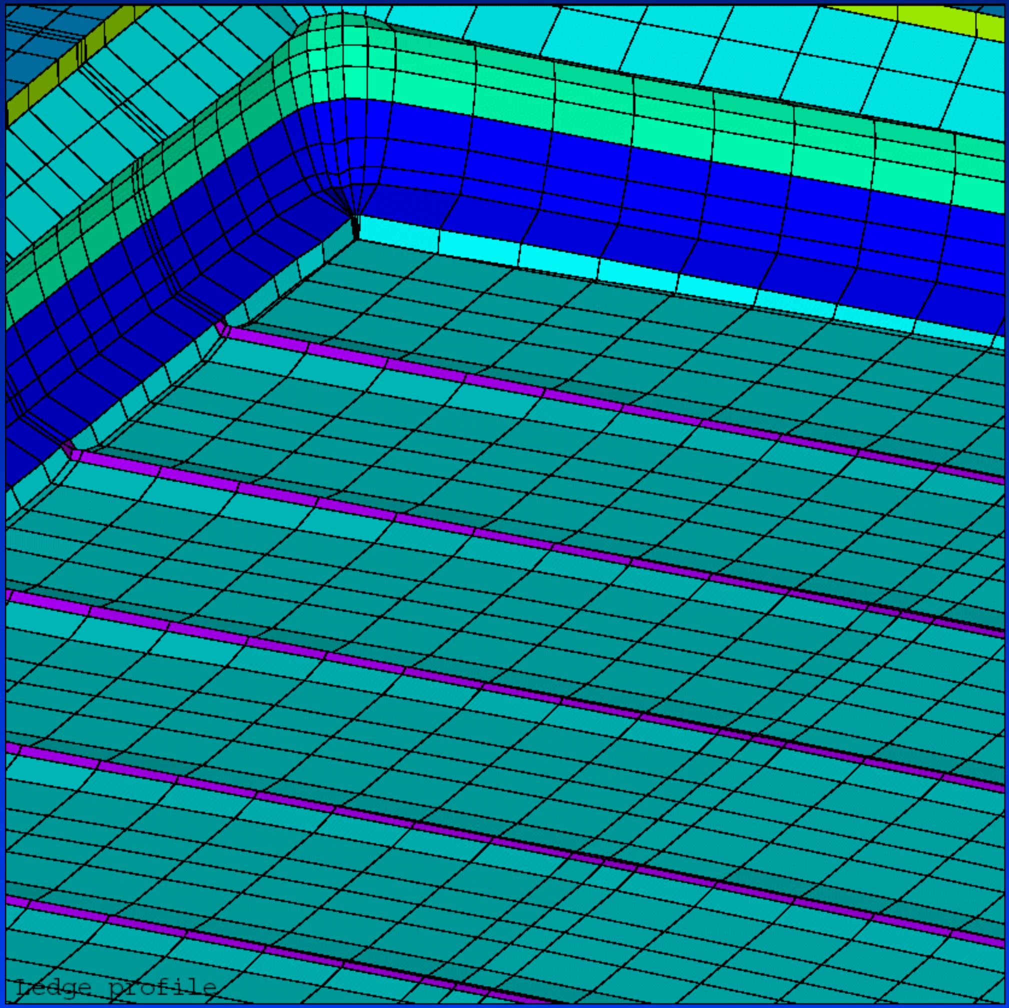

Once the geometry of the ledge is converged, a new iteration loop start, this time to simulate the erosion of the cathode block as function of the surface current density

MHD analysis: application

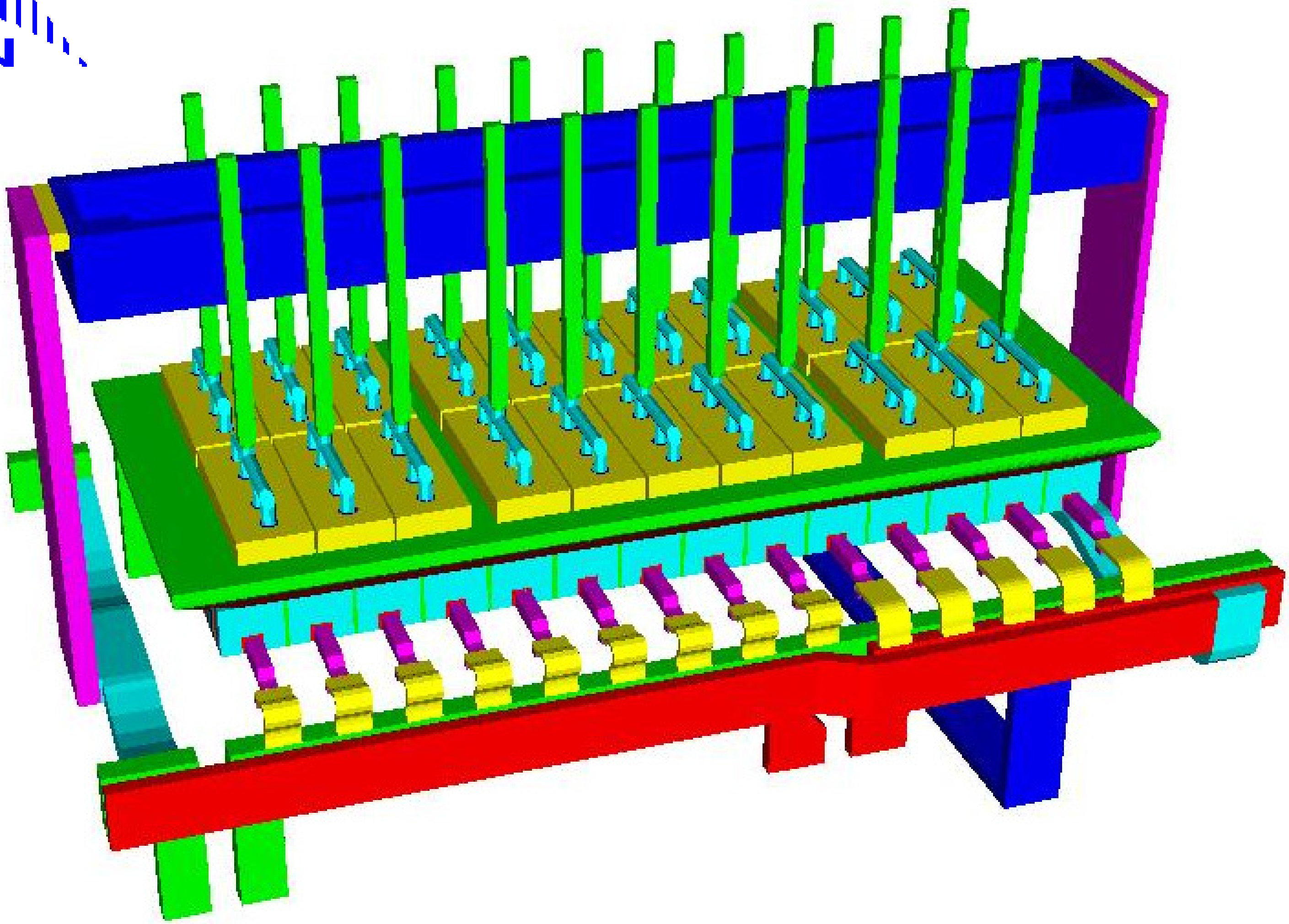

J. Antille, MHD Workshop, Lausanne, 2004

Detailed cell representation

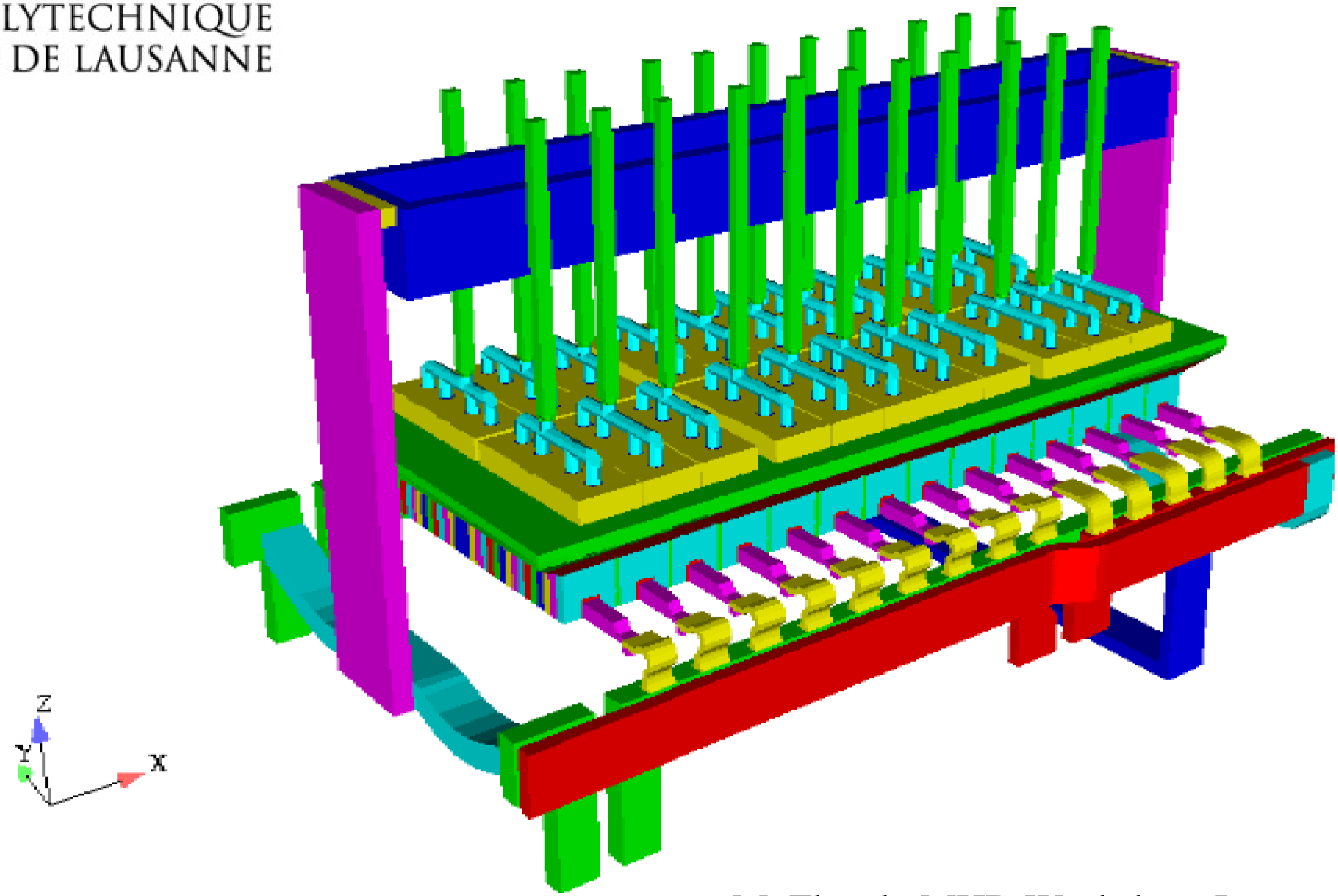

M. Flueck, MHD Workshop, Lausanne, 2004

Tetraedric (500’000) mesh of the cell

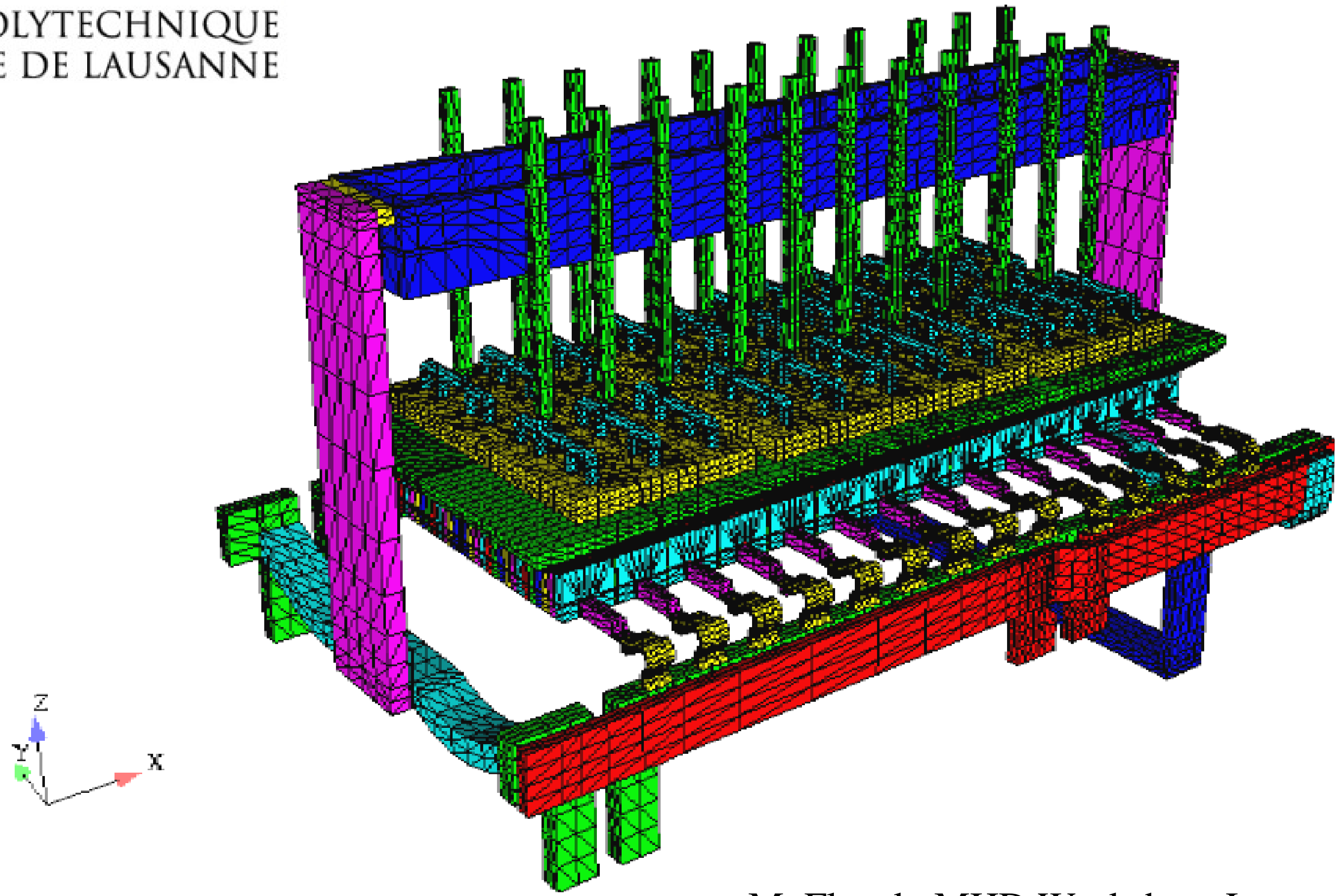

M. Flueck, MHD Workshop, Lausanne, 2004

ÉCOLE POLYTECHNIQUE
FÉDÉRALE DE LAUSANNE

Steady electric potential

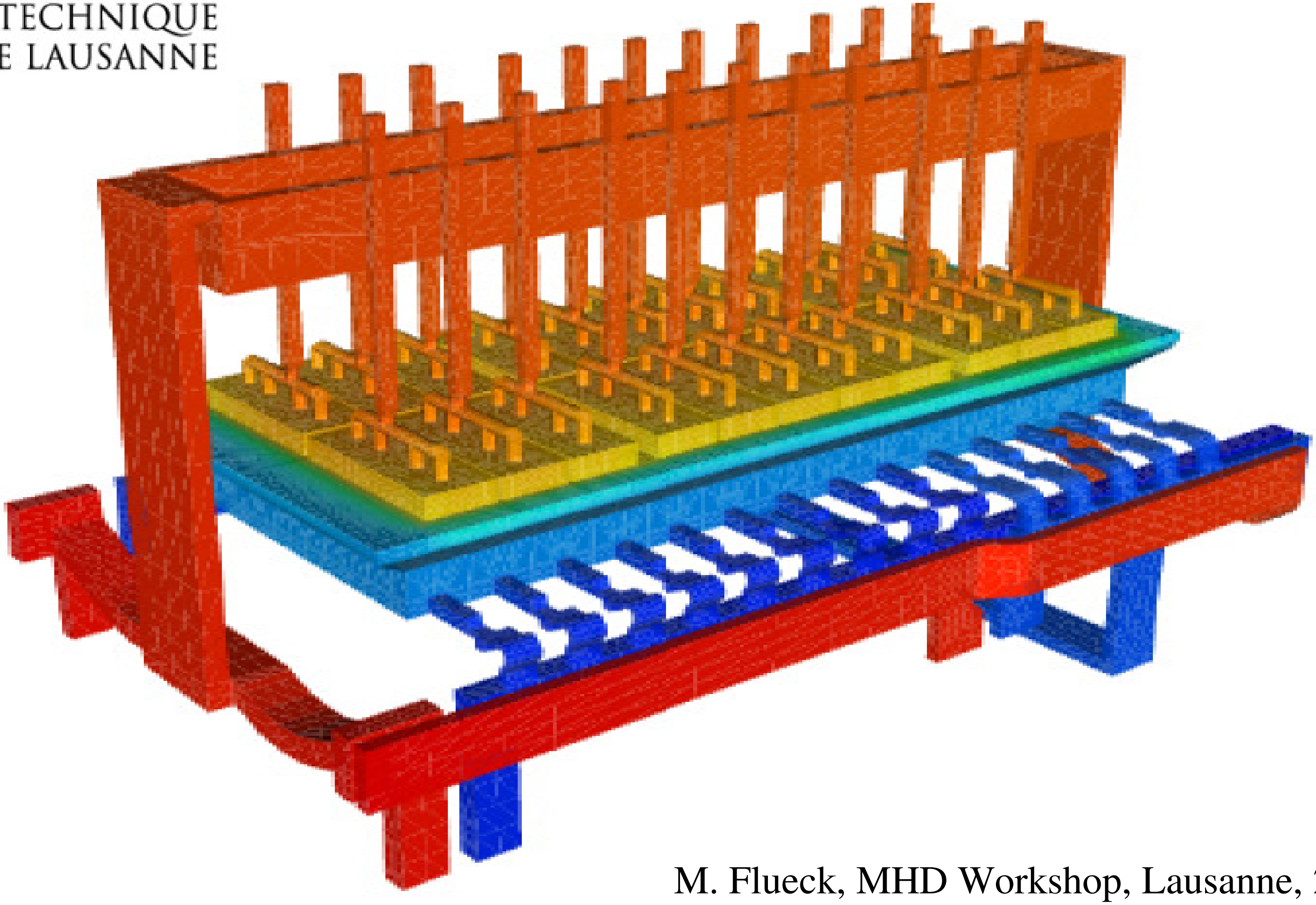

M. Flueck, MHD Workshop, Lausanne, 2004

ÉCOLE POLYTECHNIQUE
FÉDÉRALE DE LAUSANNE

Thermal calculations of reduction cells coupled with magnetohydrodynamic effects

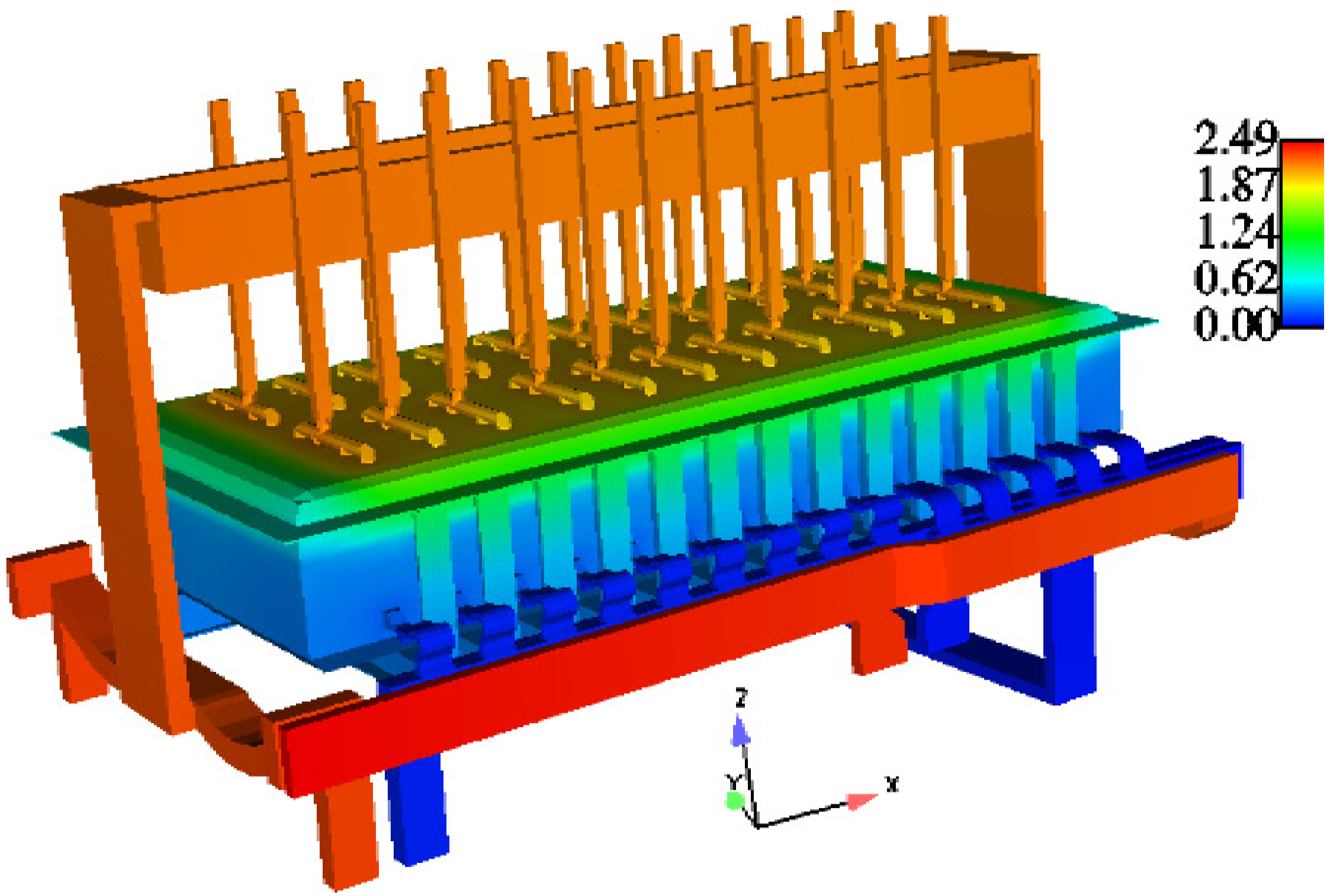

Y. Safa, MHD Workshop, Lausanne, 2004

ÉCOLE POLYTECHNIQUE FÉDÉRALE DE LAUSANNE

Thermal calculations of reduction cells coupled with magnetohydrodynamic effects

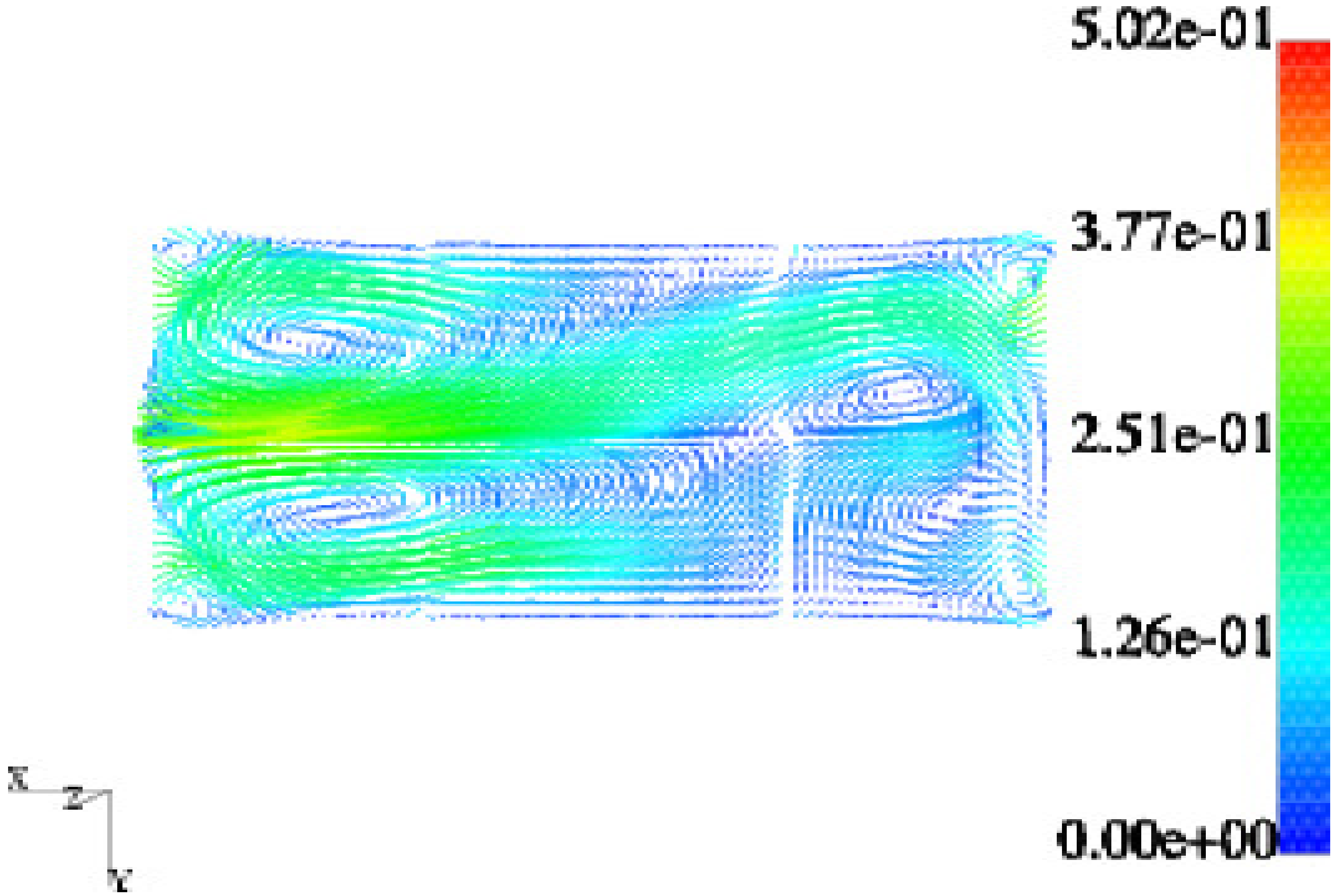

Y. Safa, MHD Workshop, Lausanne, 2004

ÉCOLE POLYTECHNIQUE
FÉDÉRALE DE LAUSANNE

Thermal calculations of reduction cells coupled with magnetohydrodynamic effects

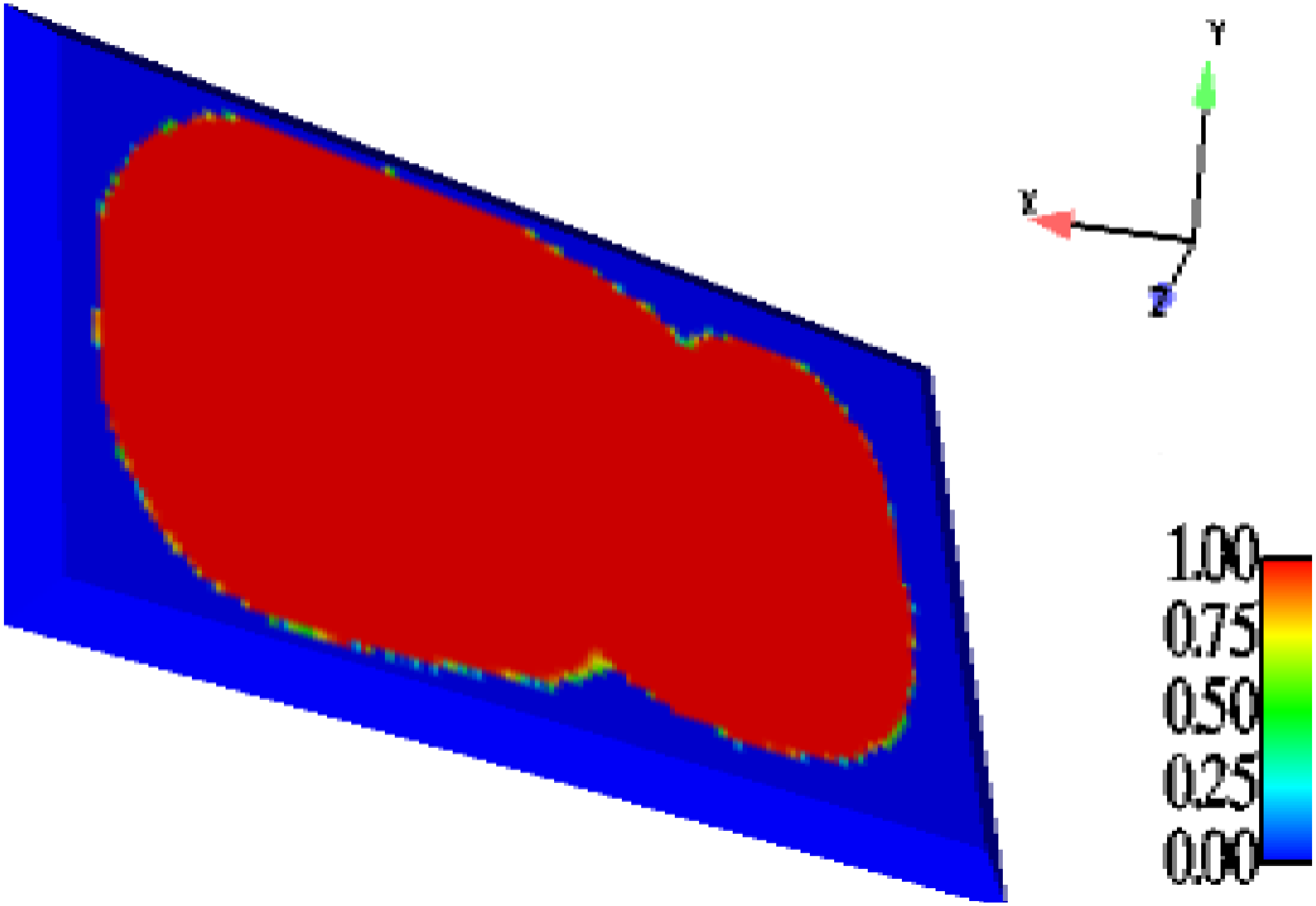

Y. Safa, MHD Workshop, Lausanne, 2004

Application to commercial cells

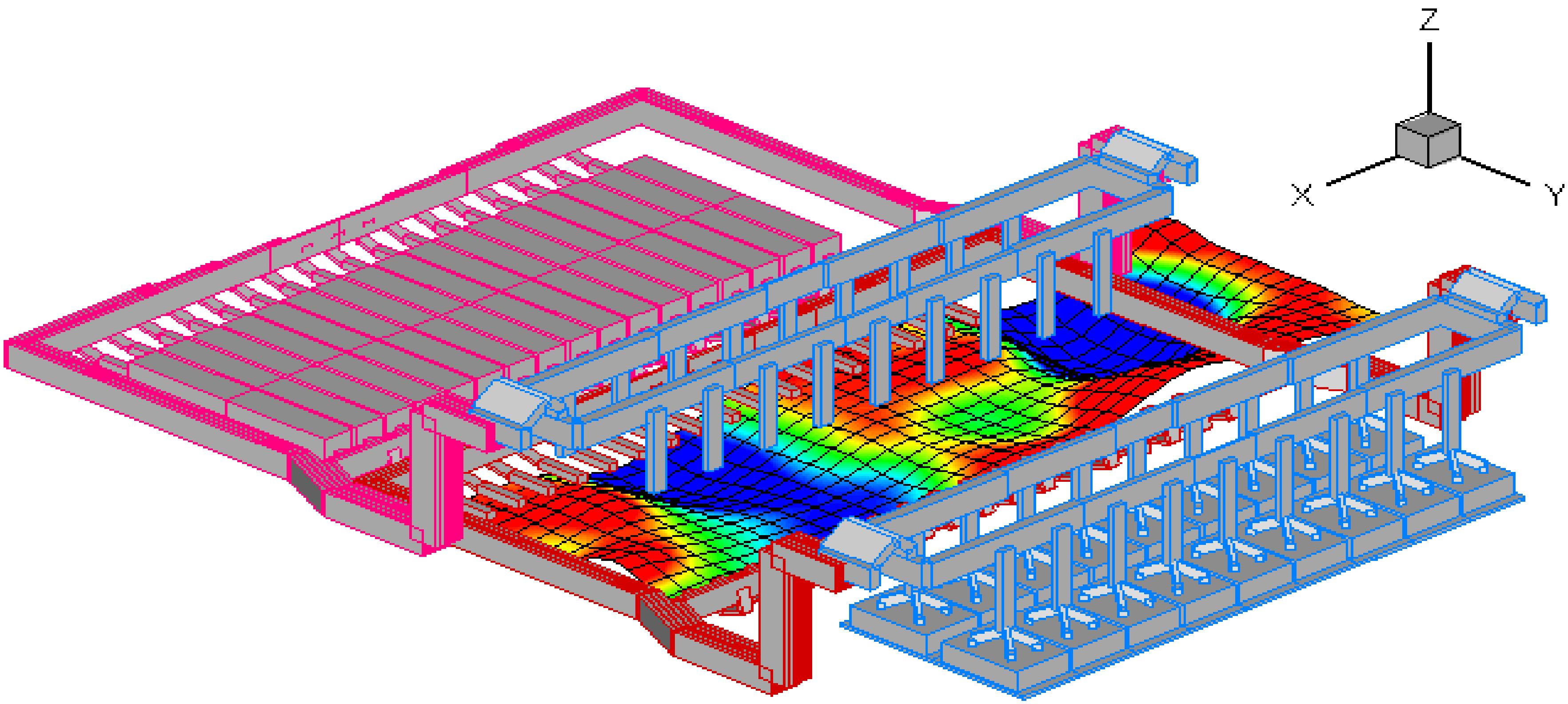

V.Bojarevics, MHD Workshop, Lausanne, 2004

Software Complex to Model Magnetic Fields and MHD Effects in Aluminum Reduction Cells

Gennadiy Arkhipov,
ETC, Russian Aluminum,
Krasnoyarsk

Alexander Kalimov,
State Polytechnic University,
St.-Petersburg

September 2004

Visualization

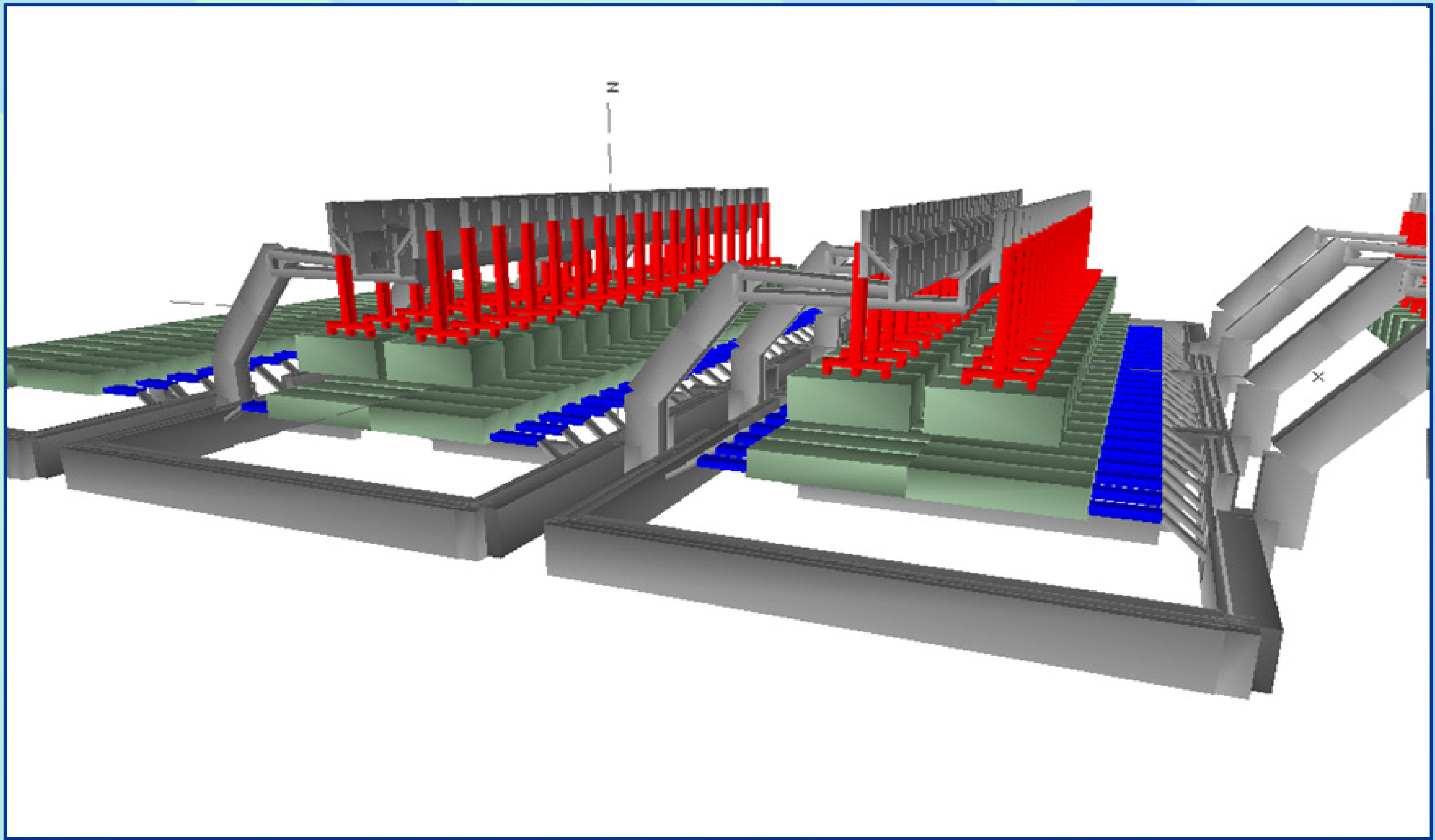

Presentation of output data (currents and magnetic field)

currents in collector bars

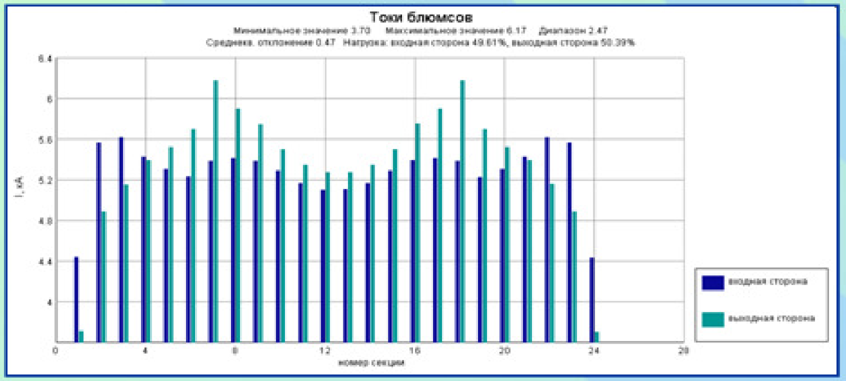

magnetic field

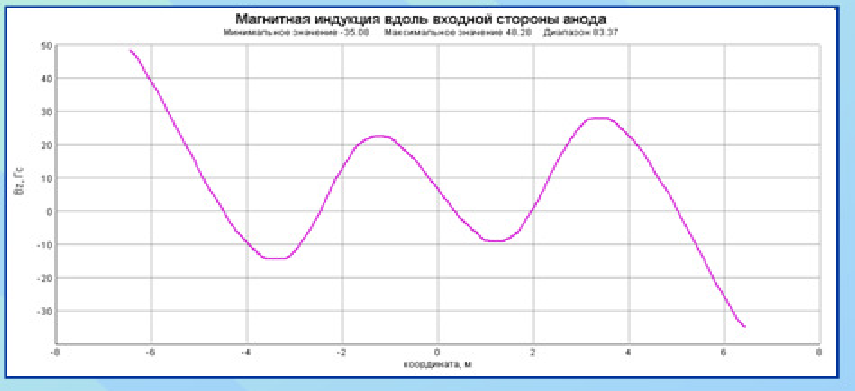

current density in a cathode

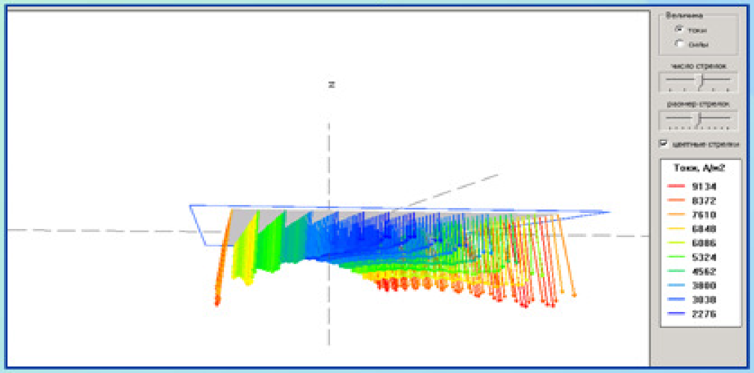

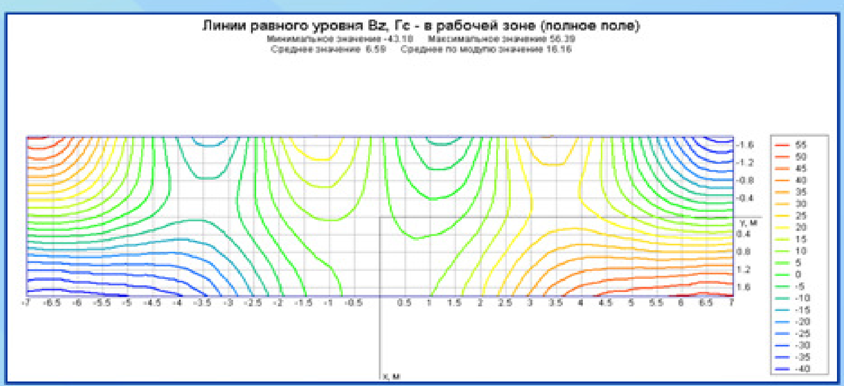

Relations between cell superheats, freeze shape and heat loss

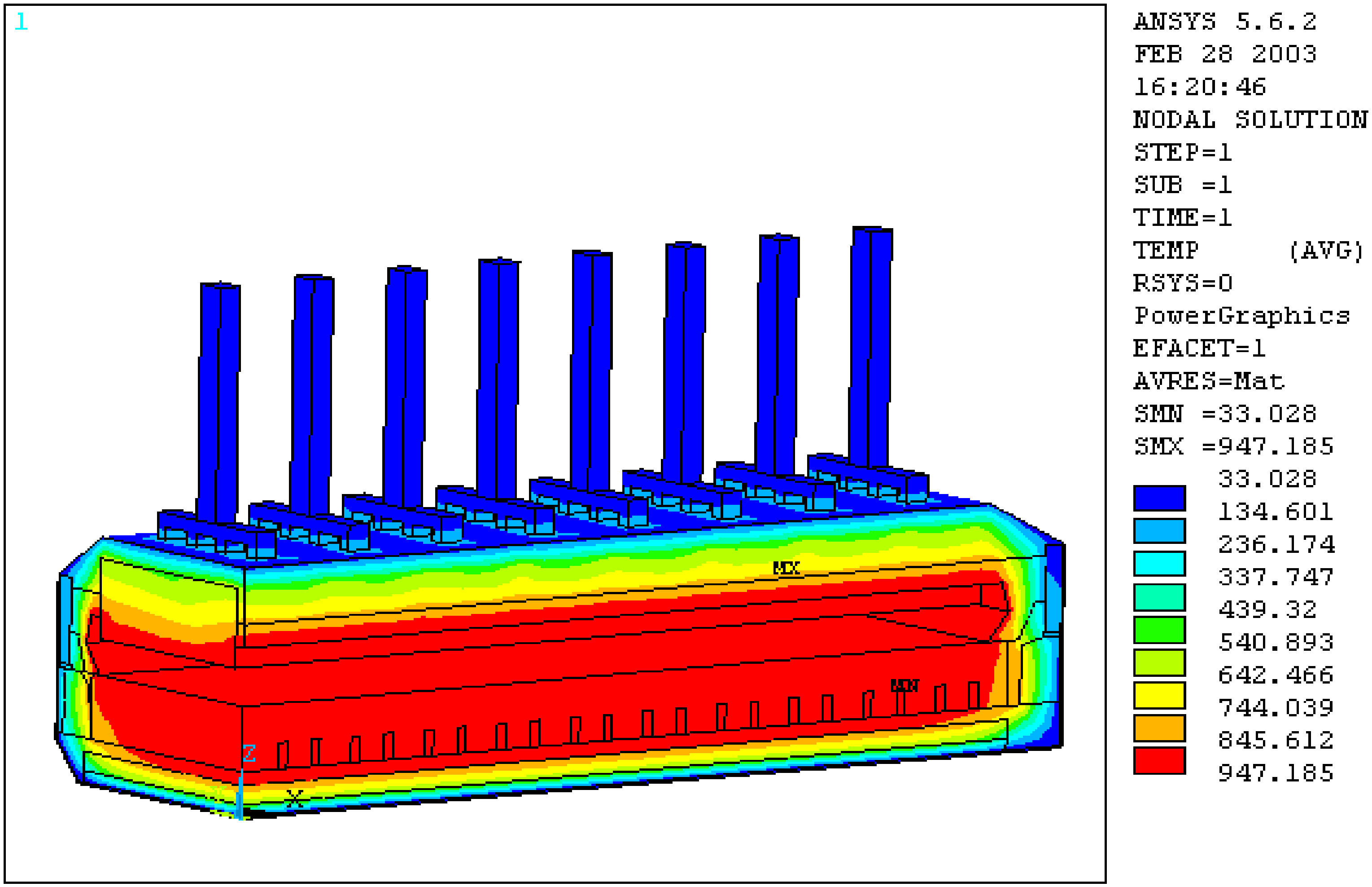

J. Huang, MHD Workshop, Lausanne, 2004

NONLINEAR ELASTO-PLATIC ANALYSIS OF SHELLS OF ALUMINUM REDUCTION CELLS

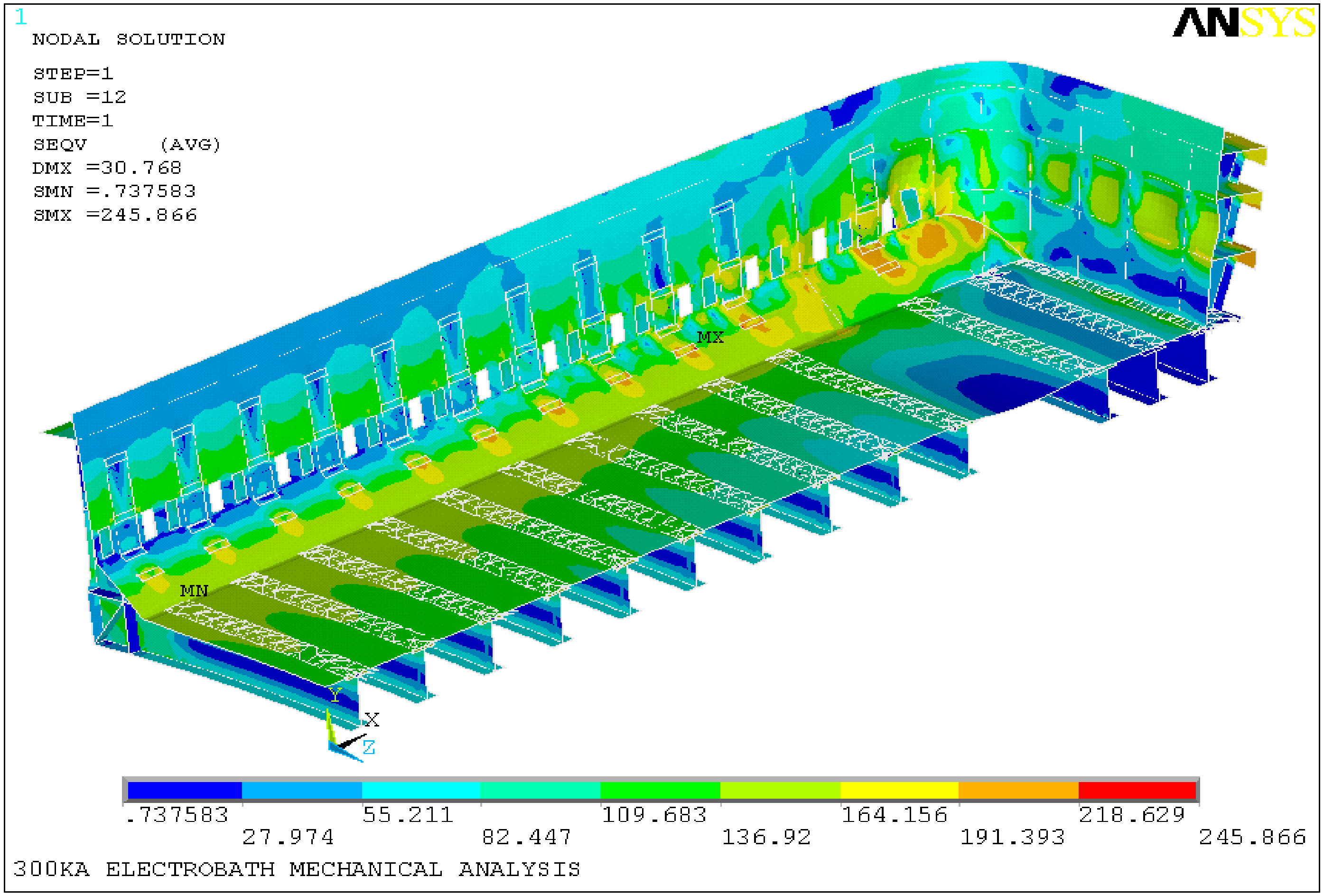

D. Zhou, MHD Workshop, Lausanne, 2004

CFD MODELING OF THE FJARDAAL SMELTER POTROOM VENTILATION

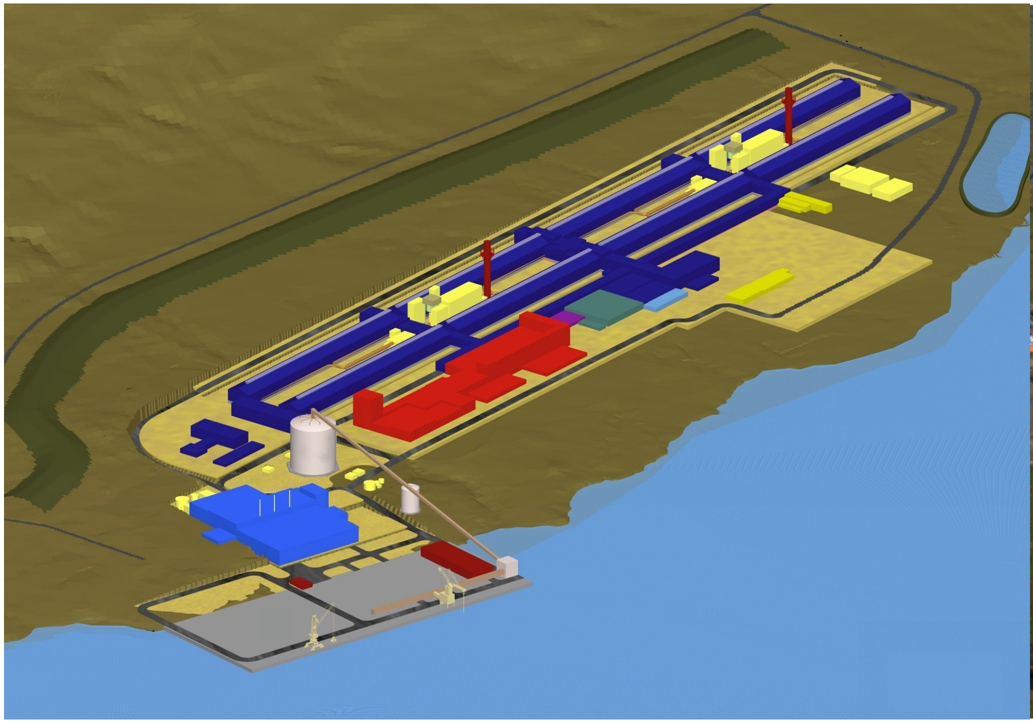

CAD Model of Aluminium Smelter

February 13-17, 2005, San Francisco, CA

CFD MODELING OF THE FJARDAAL SMELTER POTROOM VENTILATION

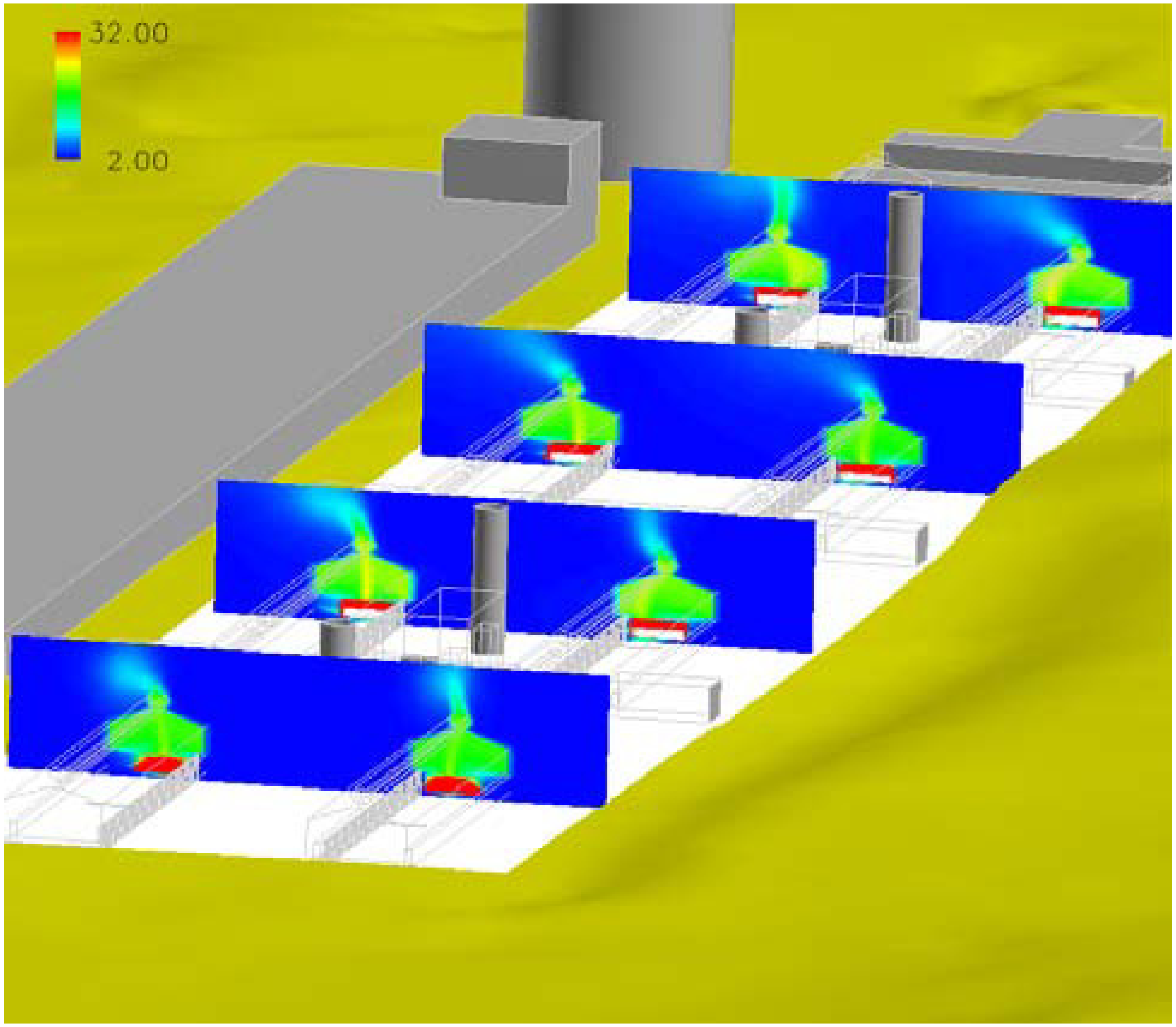

Ambient temperature (°C) through several crosssection of the Potroom generated from full-scale CFD analysis.

ÉCOLE POLYTECHNIQUE FÉDÉRALE DE LAUSANNE

DETERMINATION AND INFLUENCE OF THE LEDGE SHAPE ON ELECTRICAL POTENTIAL AND FLUID MOTION IN A SMELTER

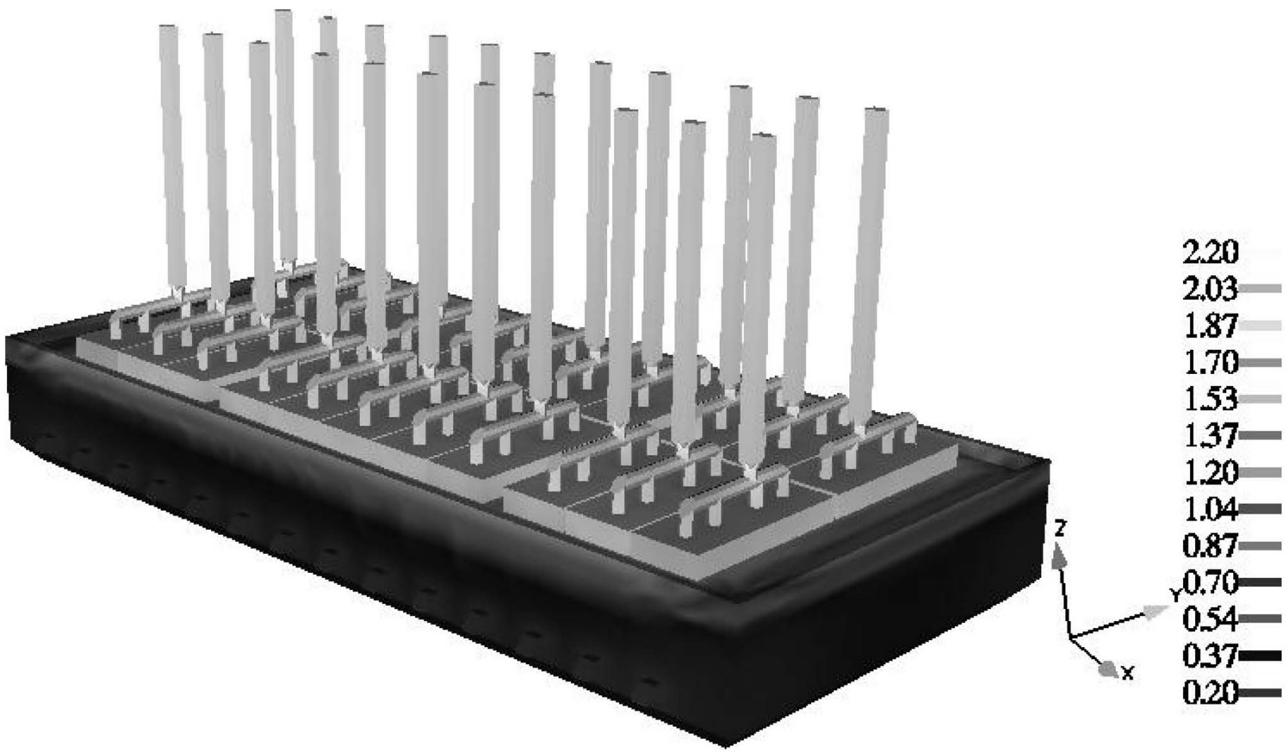

Electric potential results in the cell

ÉCOLE POLYTECHNIQUE
FÉDÉRALE DE LAUSANNE

DETERMINATION AND INFLUENCE OF THE LEDGE SHAPE ON ELECTRICAL POTENTIAL AND FLUID MOTION IN A SMELTER

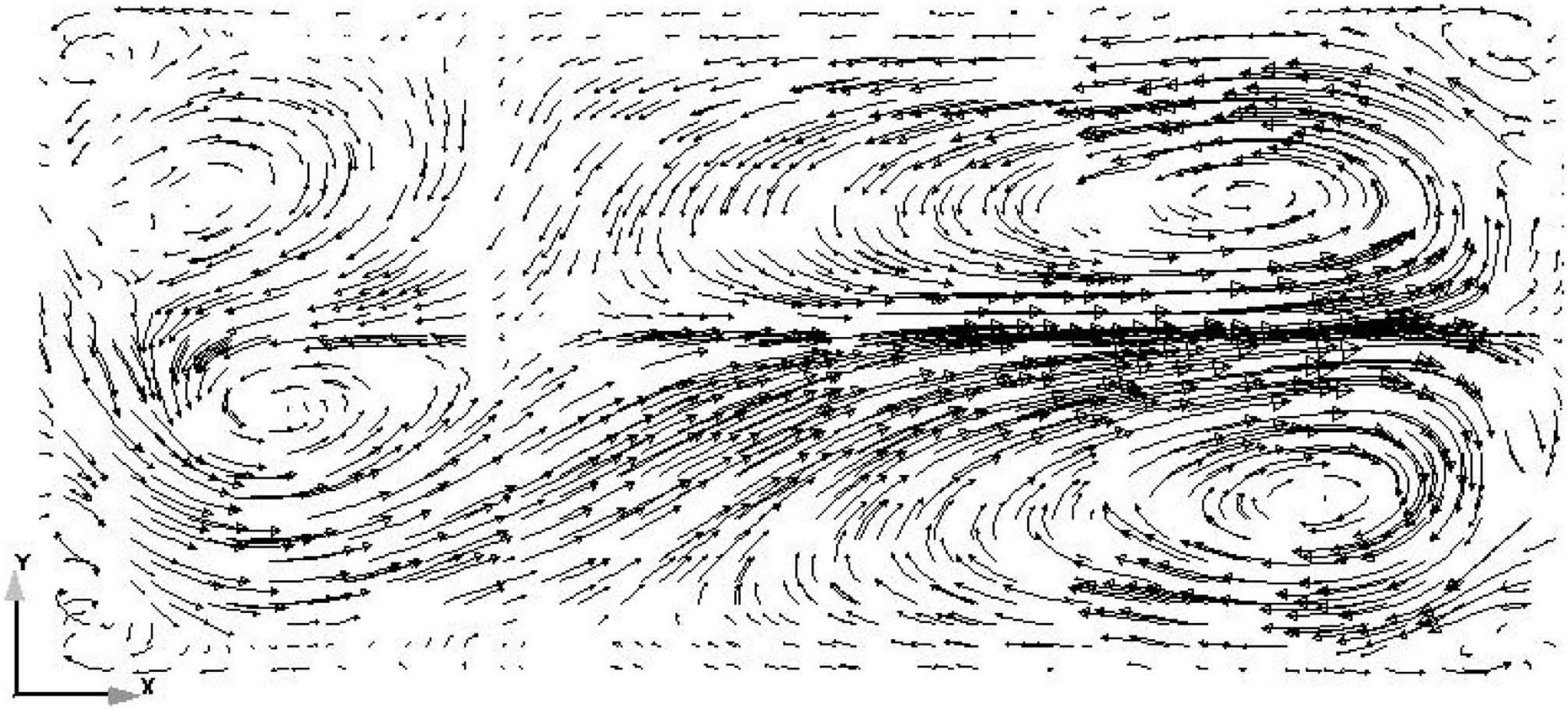

Velocity field at the interface level with maximum value = 0.5 m/s

DETERMINATION AND INFLUENCE OF THE LEDGE SHAPE ON ELECTRICAL POTENTIAL AND FLUID MOTION IN A SMELTER

ÉCOLE POLYTECHNIQUE FÉDÉRALE DE LAUSANNE

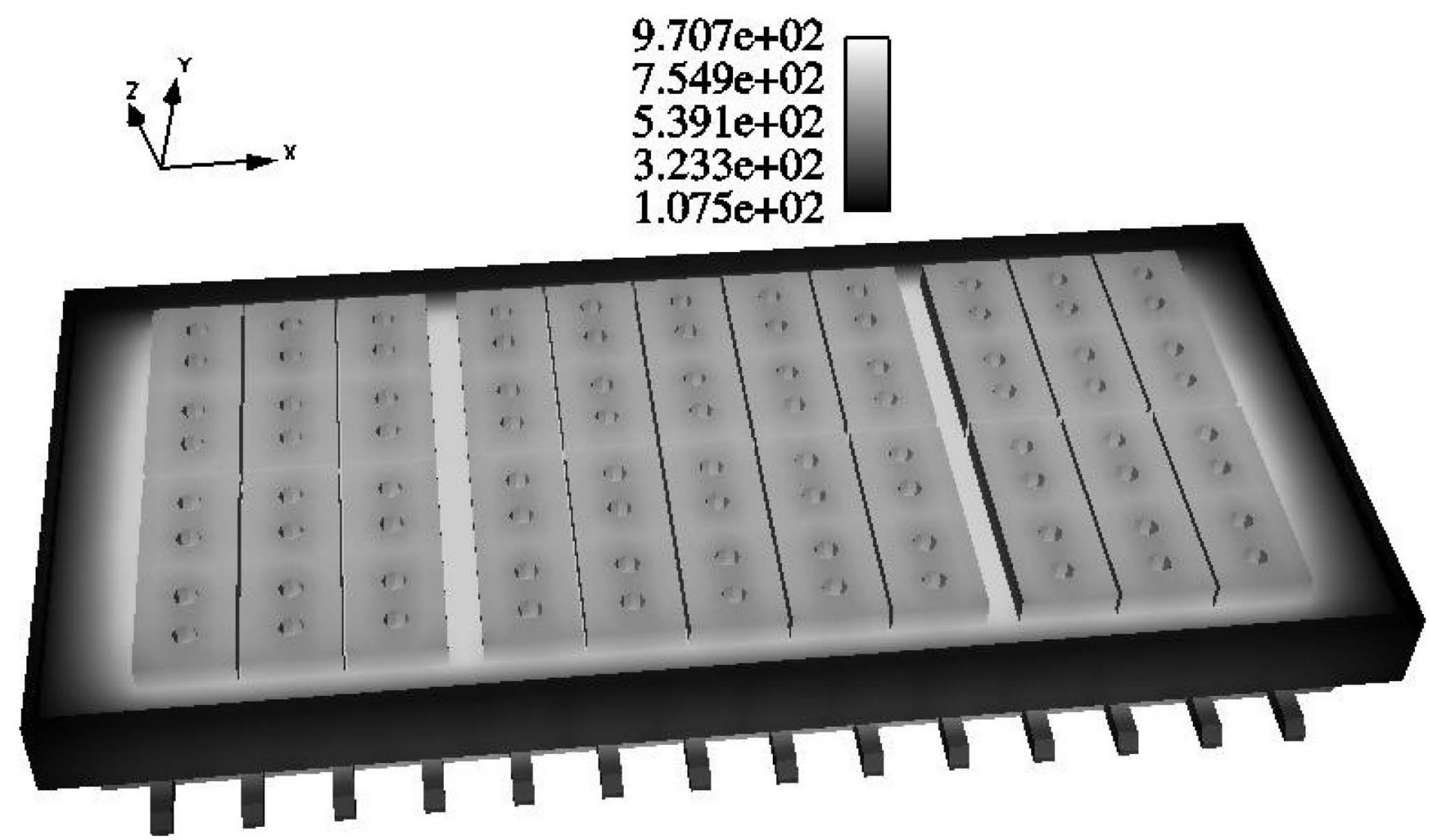

Temperature results in the cell for part of the domain only

MODELING MAGNETOHYDRODYNAMICS OF ALUMINUM ELECTROLYSIS CELLS WITH ANSYS AND CFX

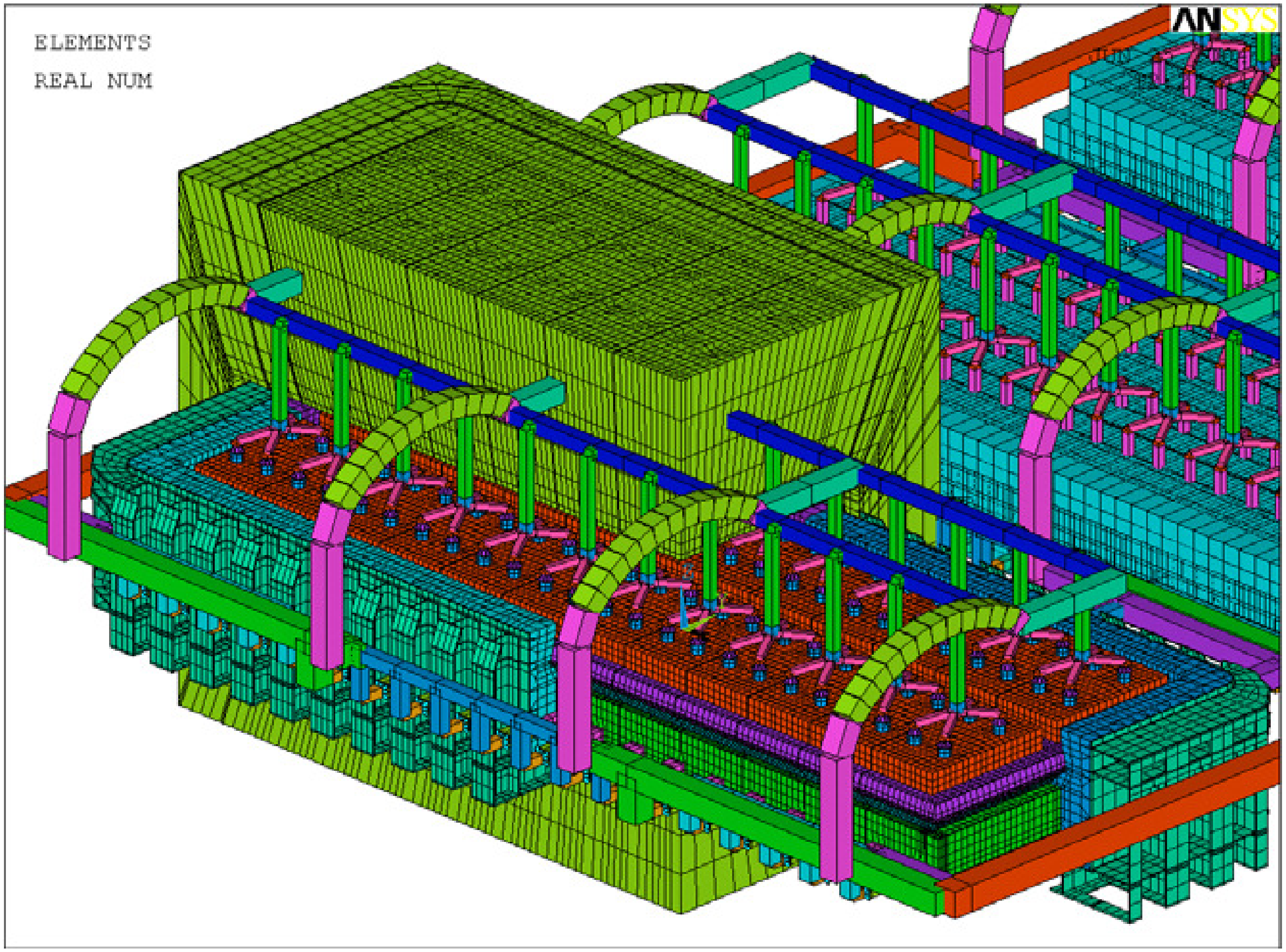

Electromagnetic model mesh.

MODELING MAGNETOHYDRODYNAMICS OF ALUMINUM ELECTROLYSIS CELLS WITH ANSYS AND CFX

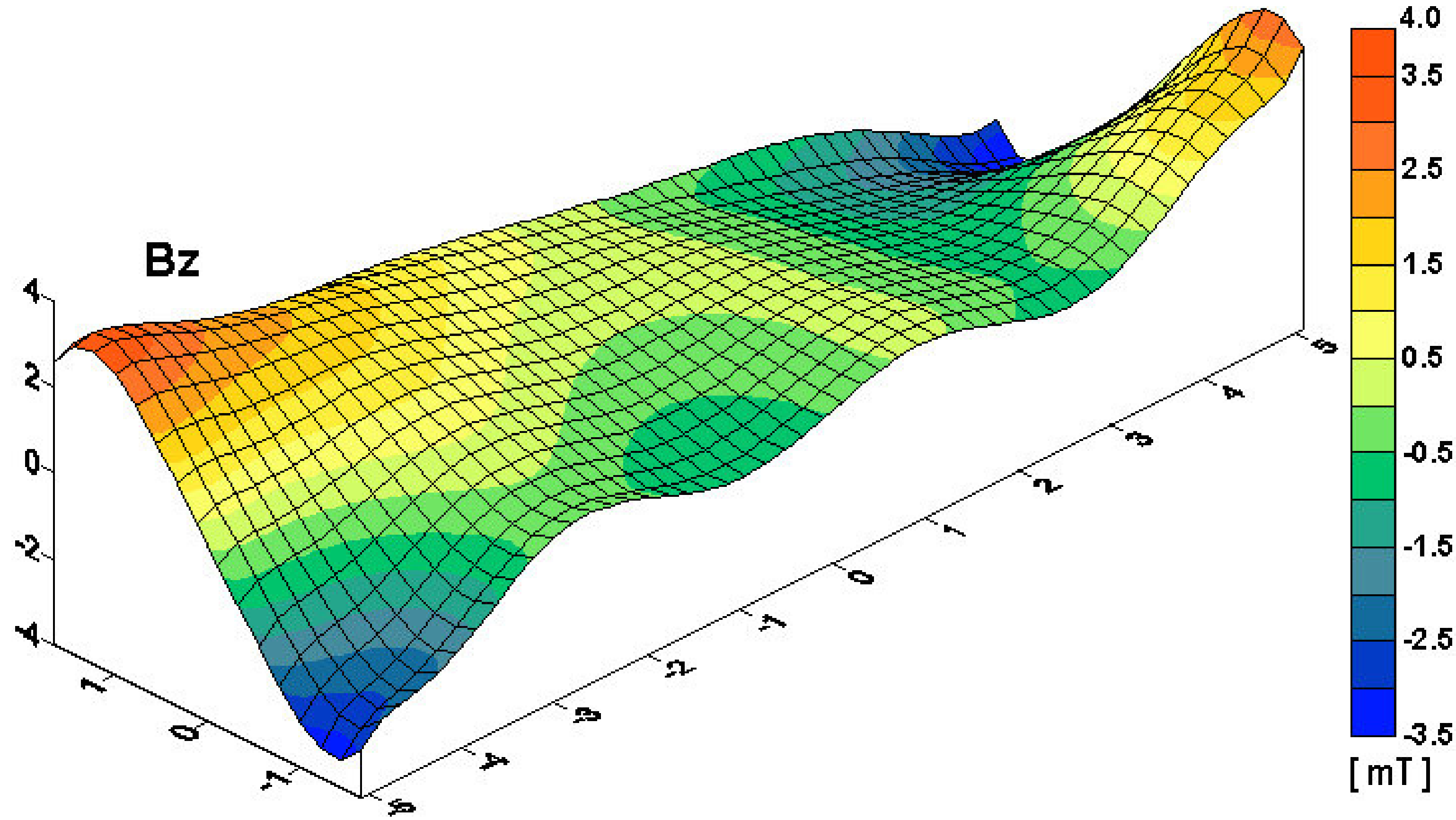

Magnetic field component B_Z , middle of the metal pad.

MODELING MAGNETOHYDRODYNAMICS OF ALUMINUM ELECTROLYSIS CELLS WITH ANSYS AND CFX

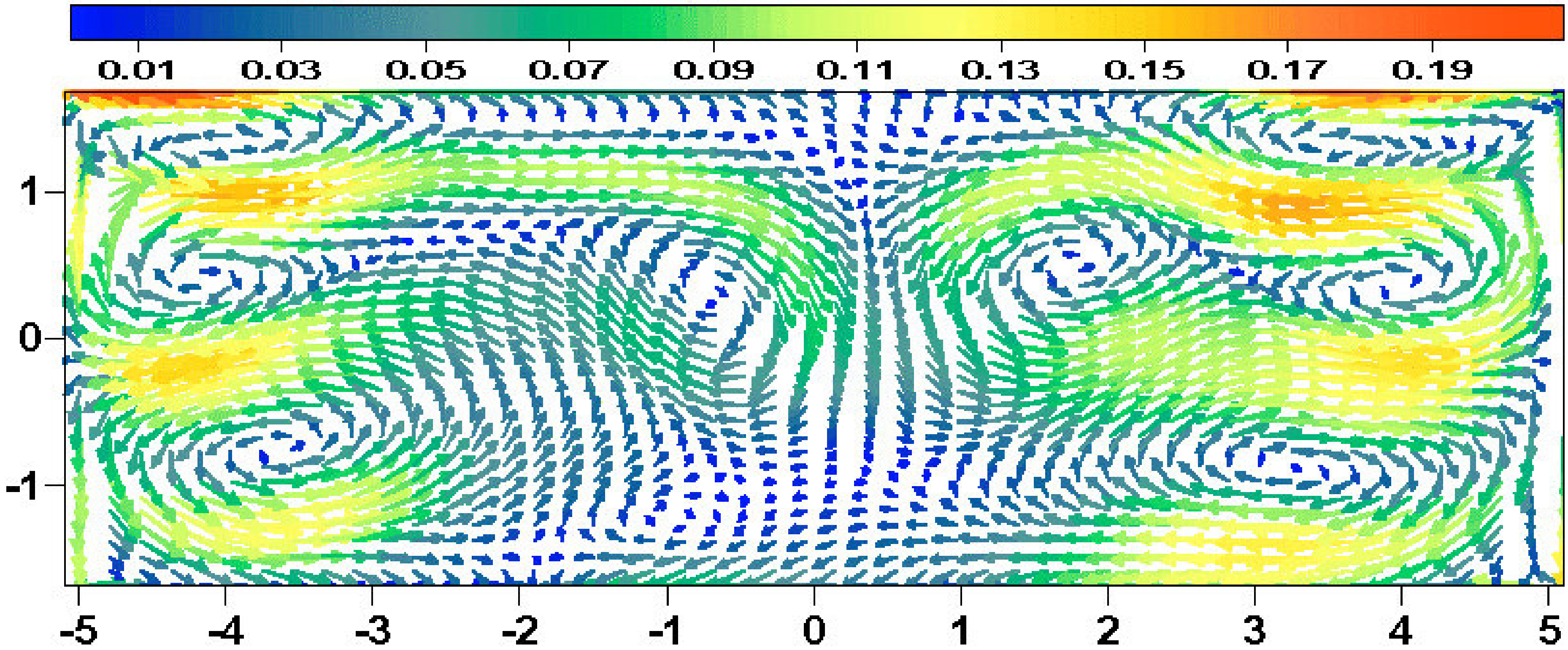

Velocity field in the middle of the metal pad (m/s), primary steady state with k- turbulence model.

February 13-17, 2005, San Francisco, CA

MODELING MAGNETOHYDRODYNAMICS OF ALUMINUM ELECTROLYSIS CELLS WITH ANSYS AND CFX

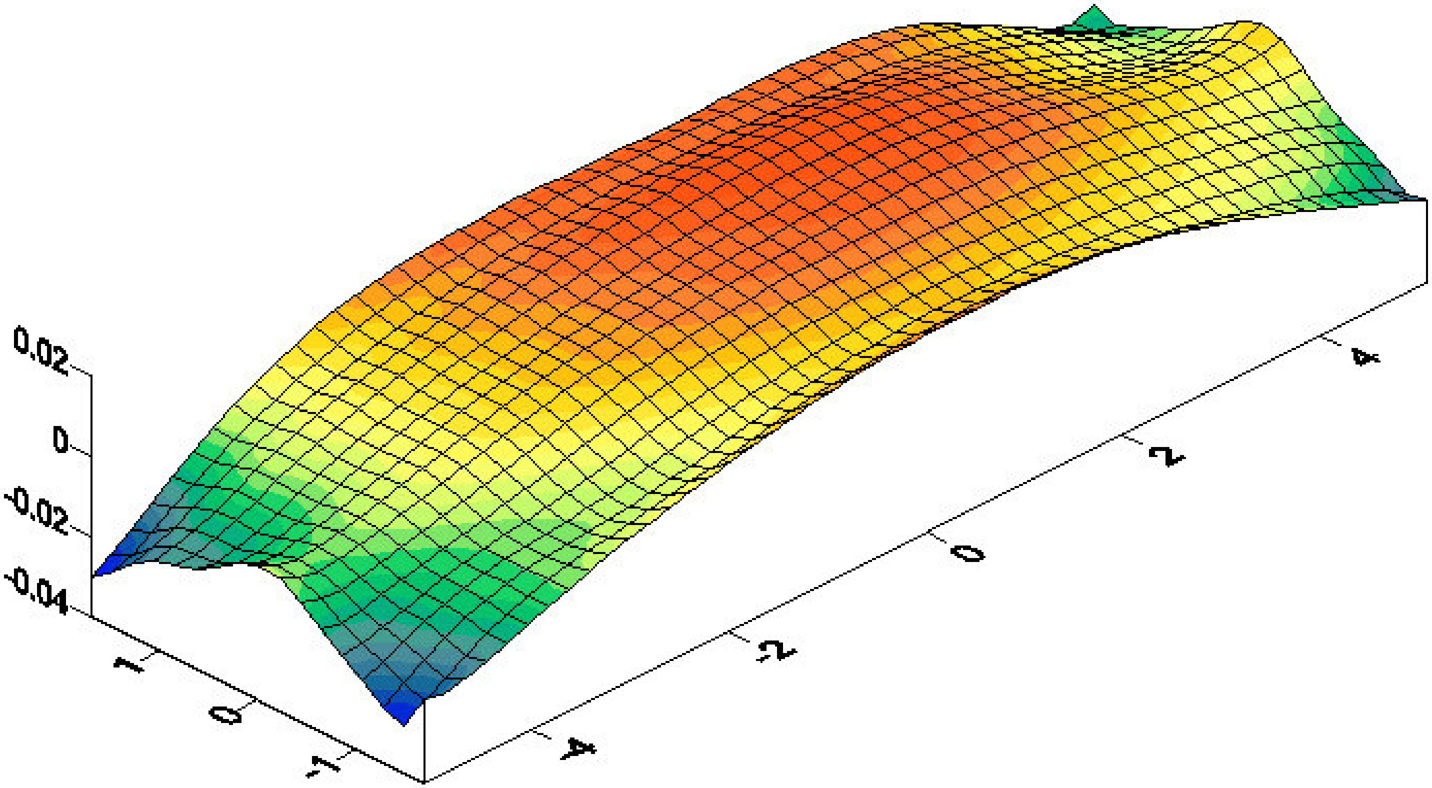

Metal-bath interface shape (m), final steady state, constant viscosity.

The Aluminum Reduction Cell Closed System of 3D Mathematical Models

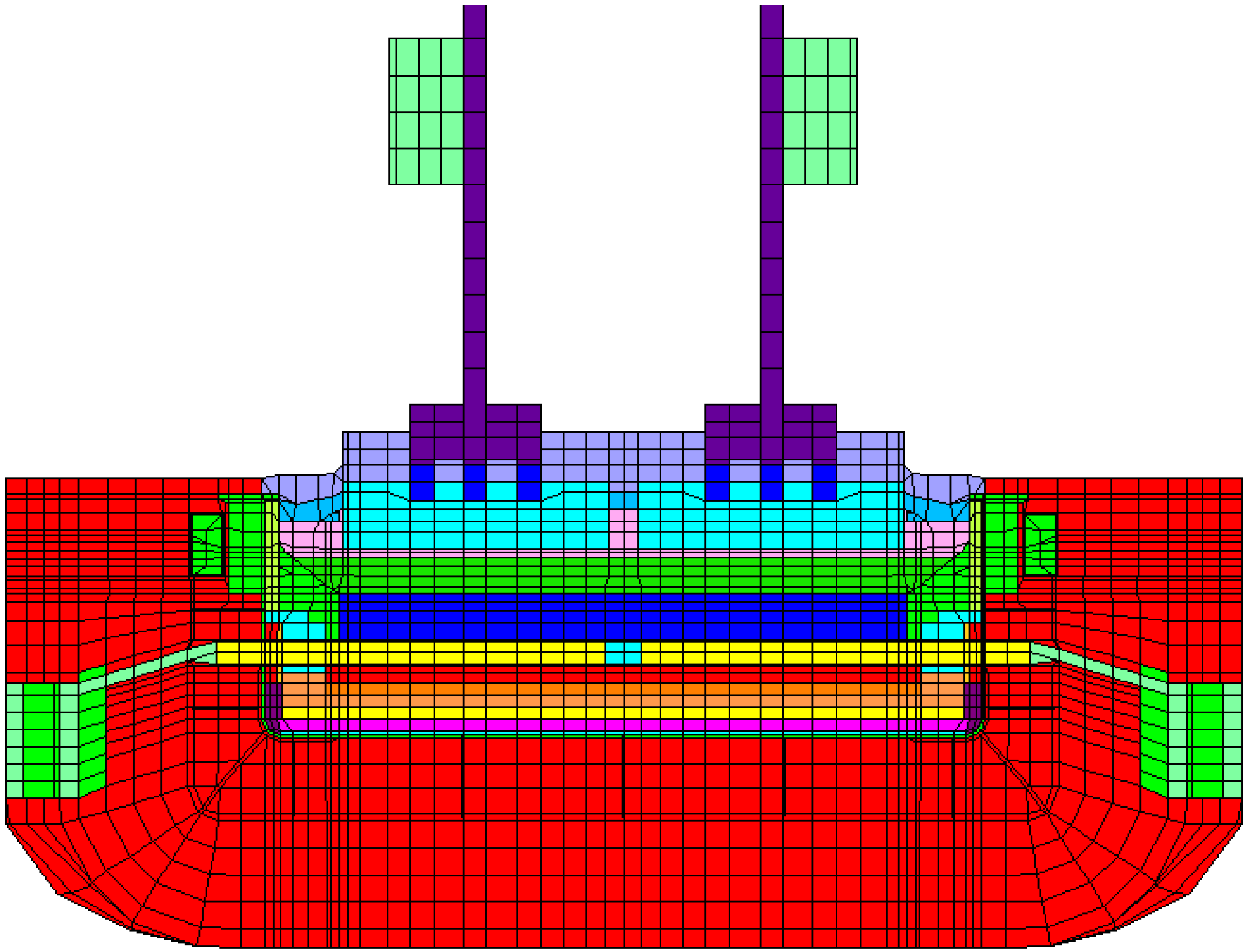

Cross section of the lower part

February 13-17, 2005, San Francisco, CA

The Aluminum Reduction Cell Closed System of 3D Mathematical Models

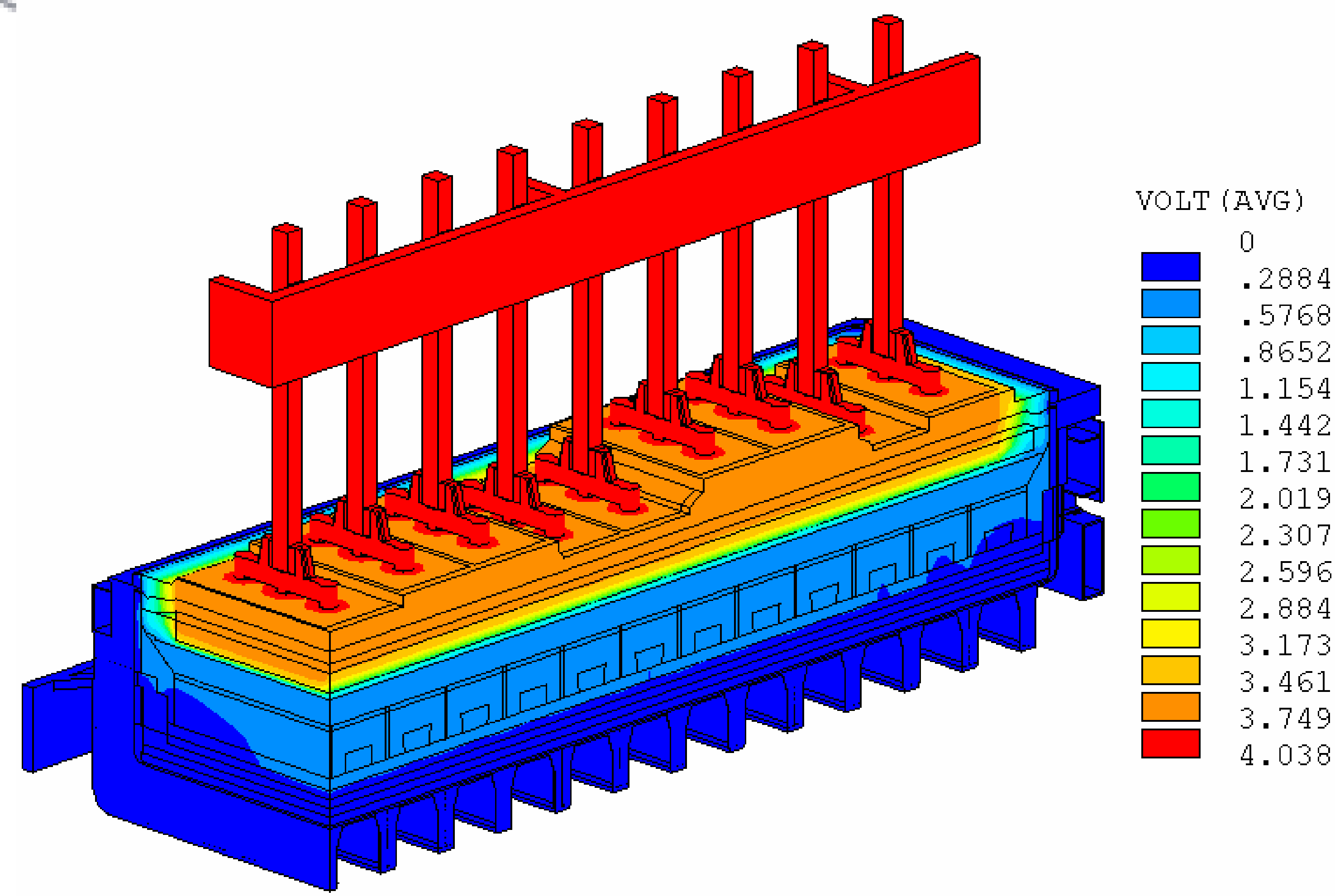

Distribution of electric potential. **ANSYS**

The Aluminum Reduction Cell Closed System of 3D Mathematical Models

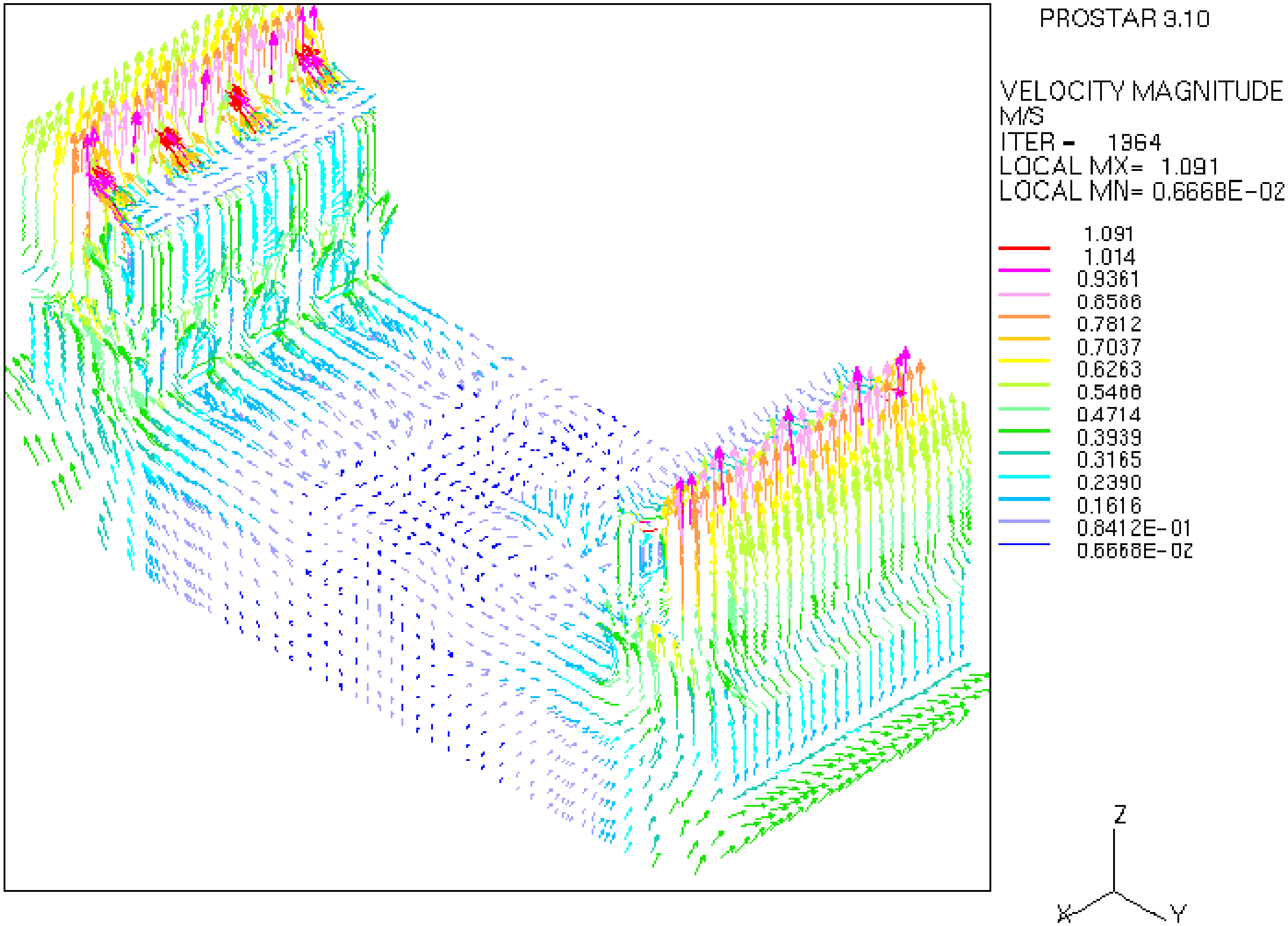

Free convection velocities. Central part. **STAR-CD**

The Aluminum Reduction Cell Closed System of 3D Mathematical Models

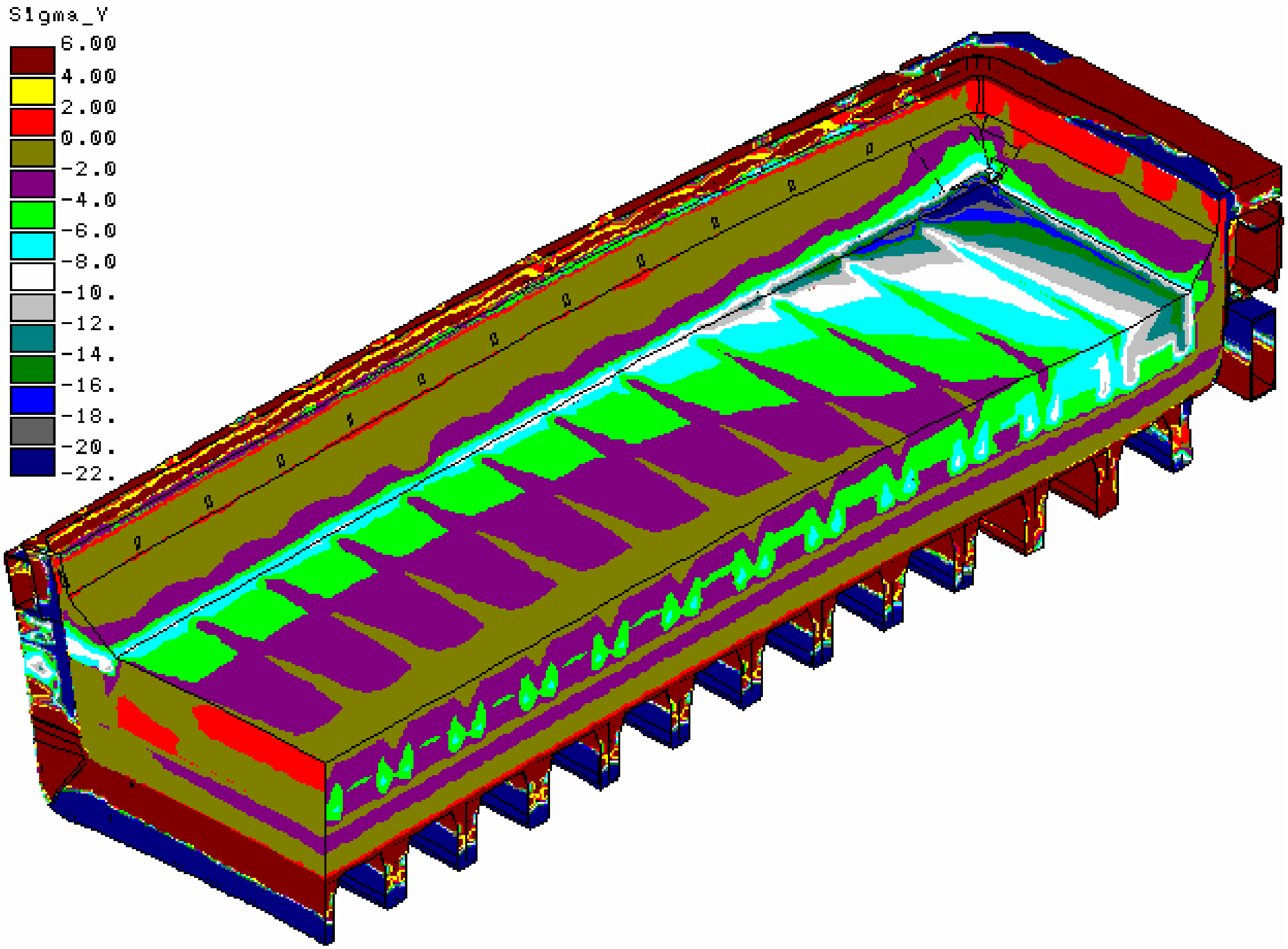

Stress distribution. Crosswise direction. **ANSYS**

INFLUENCE OF THERMO-HYDRAULIC FIELDS ON STRUCTURAL MECHANICS OF REDUCTION CELLS

ÉCOLE POLYTECHNIQUE FÉDÉRALE DE LAUSANNE

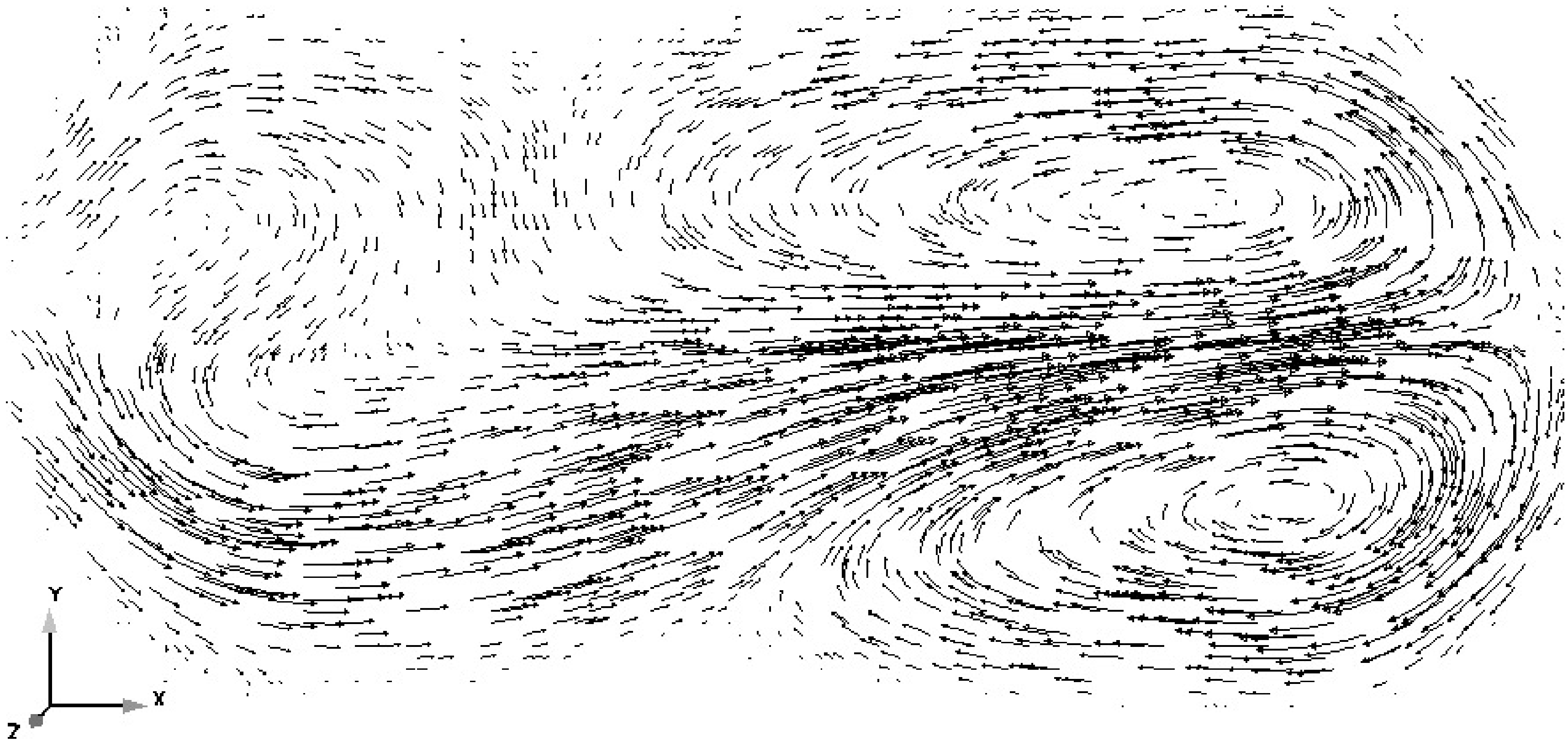

The velocity field at the interface level with a mean value = 8 cm/s

INFLUENCE OF THERMO-HYDRAULIC FIELDS ON STRUCTURAL MECHANICS OF REDUCTION CELLS

ÉCOLE POLYTECHNIQUE FÉDÉRALE DE LAUSANNE

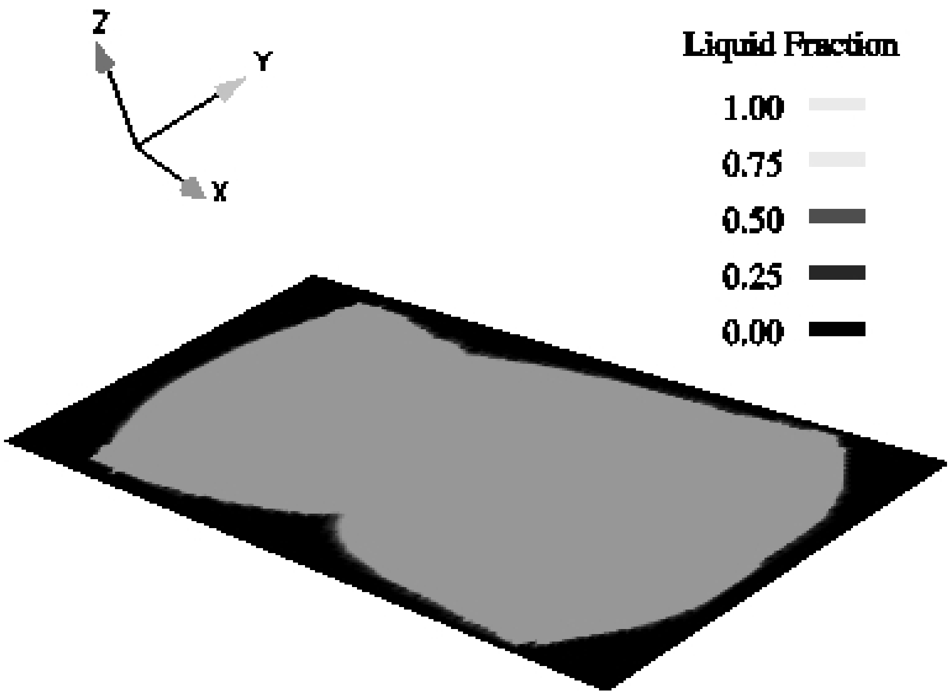

Liquid fraction showing the ledge shape, thermo-magneto-hydrodynamic model

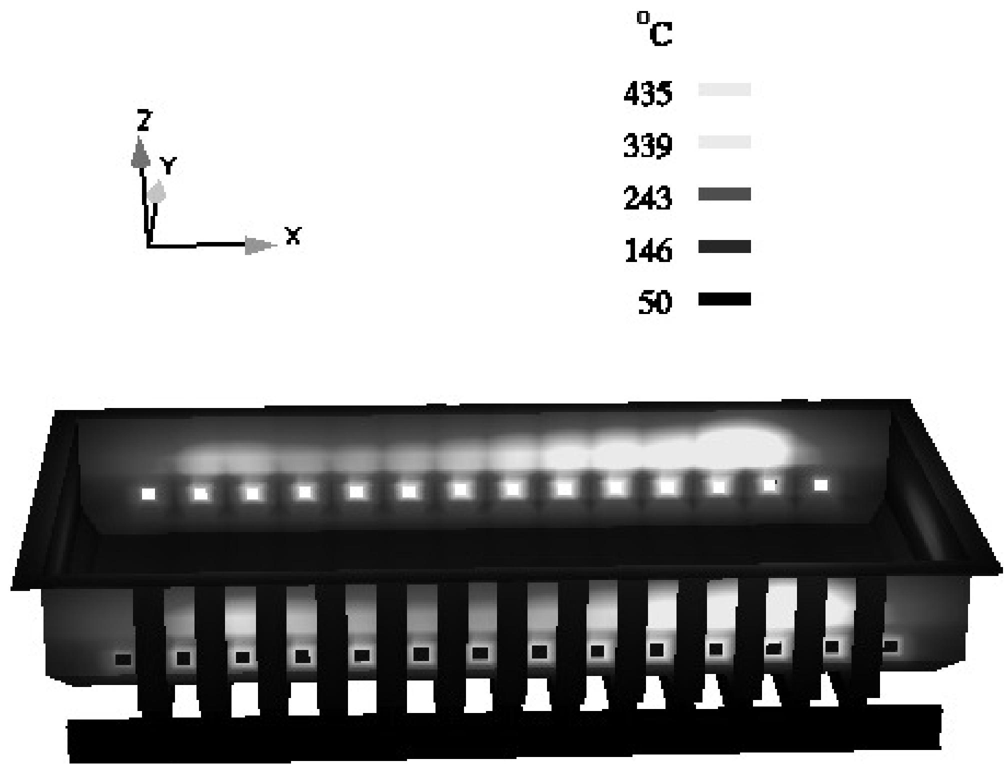

The temperature distribution in the shell, thermo-magneto-hydrodynamic model

MODELING OF A 25 kA de NORA INERT METALLIC ANODE TEST CELL

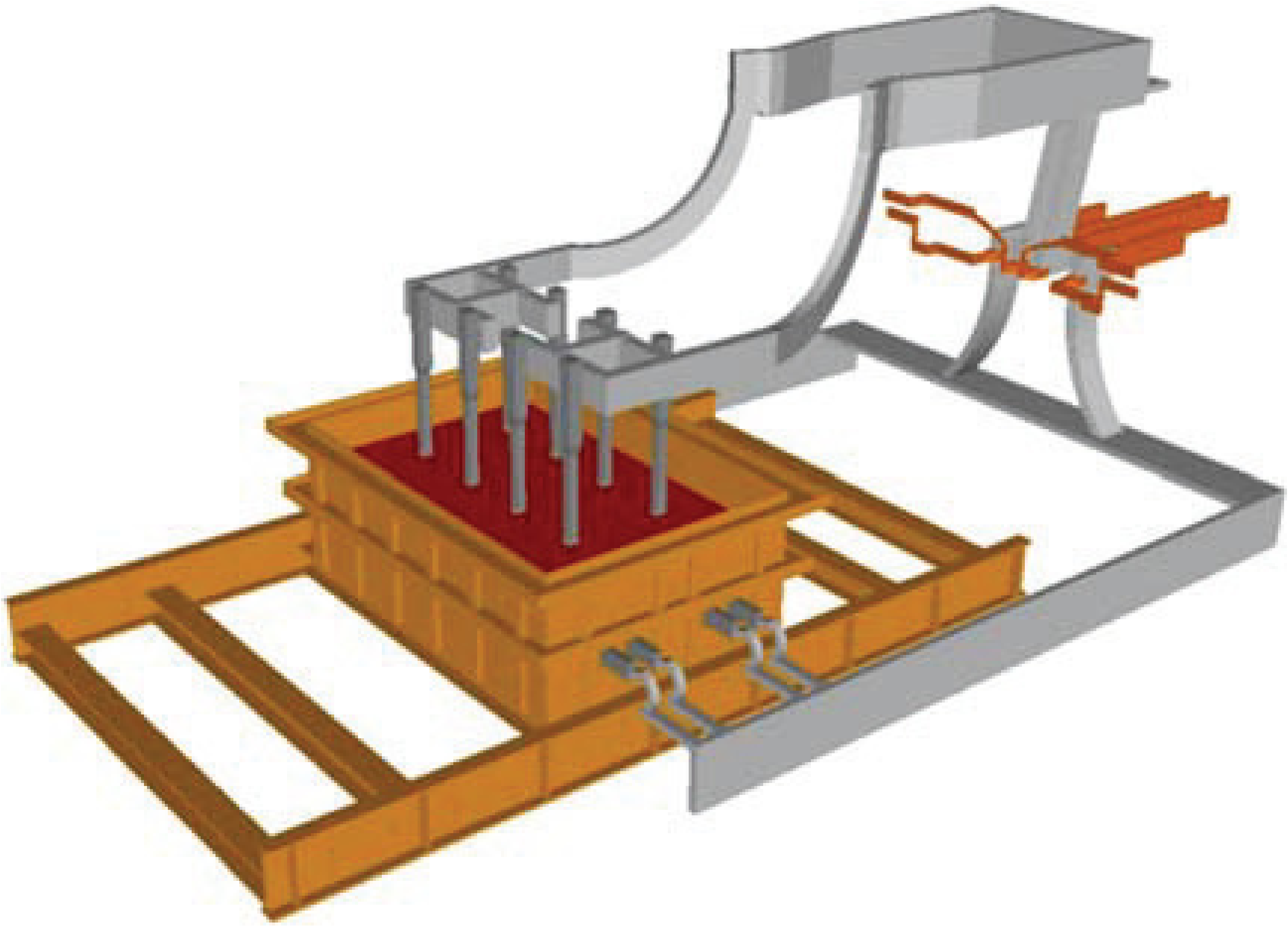

Complete design of the 25 kA industrial metallic anode cell.

MODELING OF A 25 kA de NORA INERT METALLIC ANODE TEST CELL

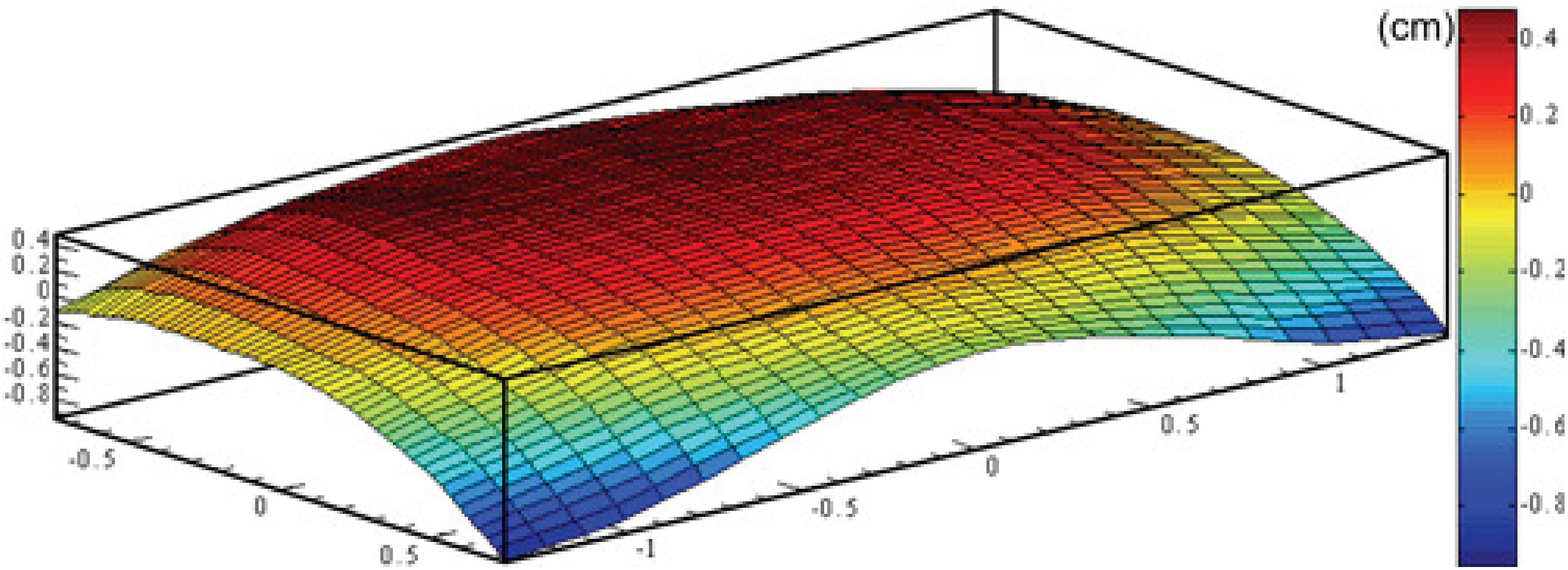

Shape of the metal pad/electrolyte interface.

MODELING OF A 25 kA de NORA INERT METALLIC ANODE TEST CELL

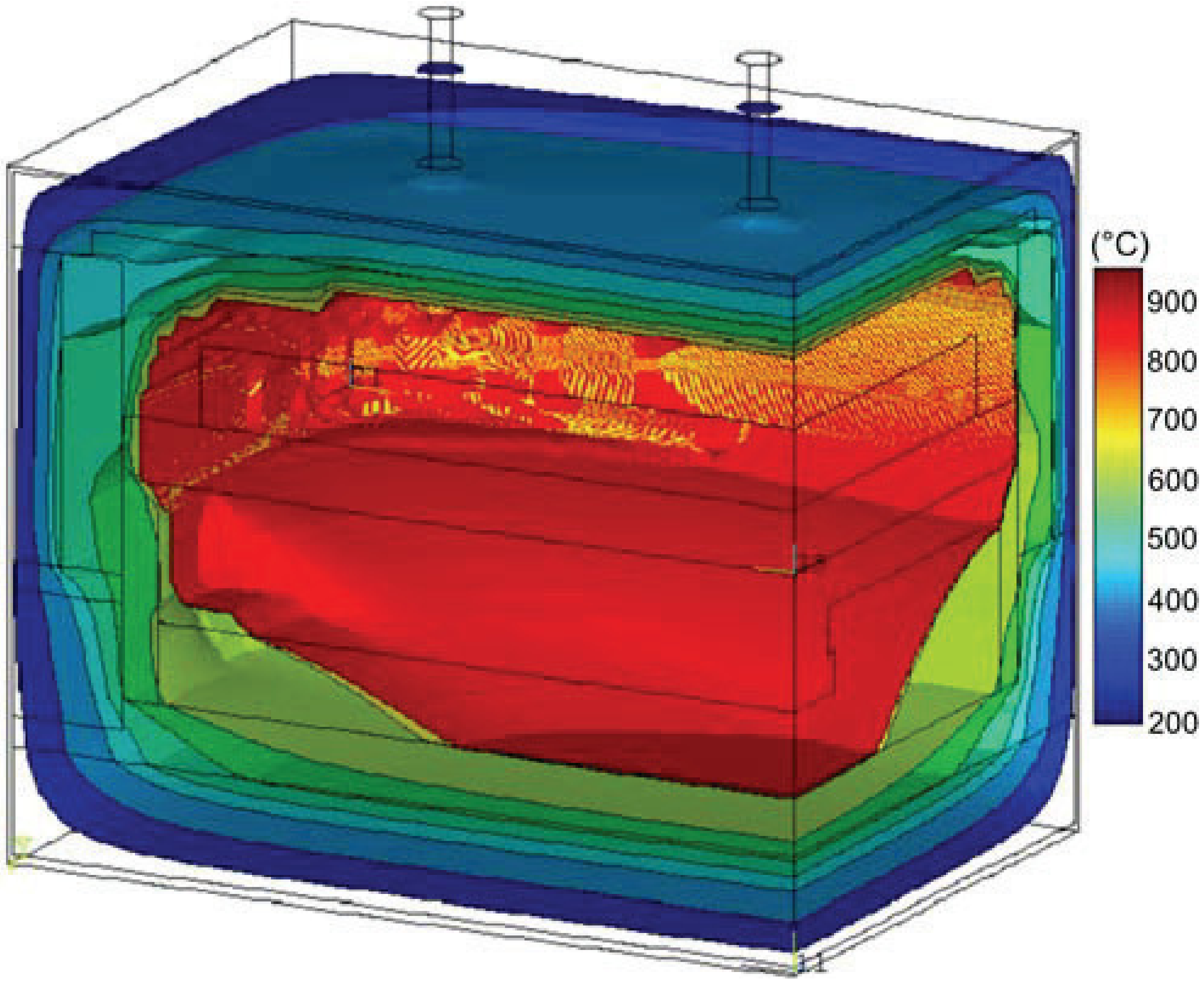

Temperature distribution in the test pot.

MHD-Valdis Stability Analysis

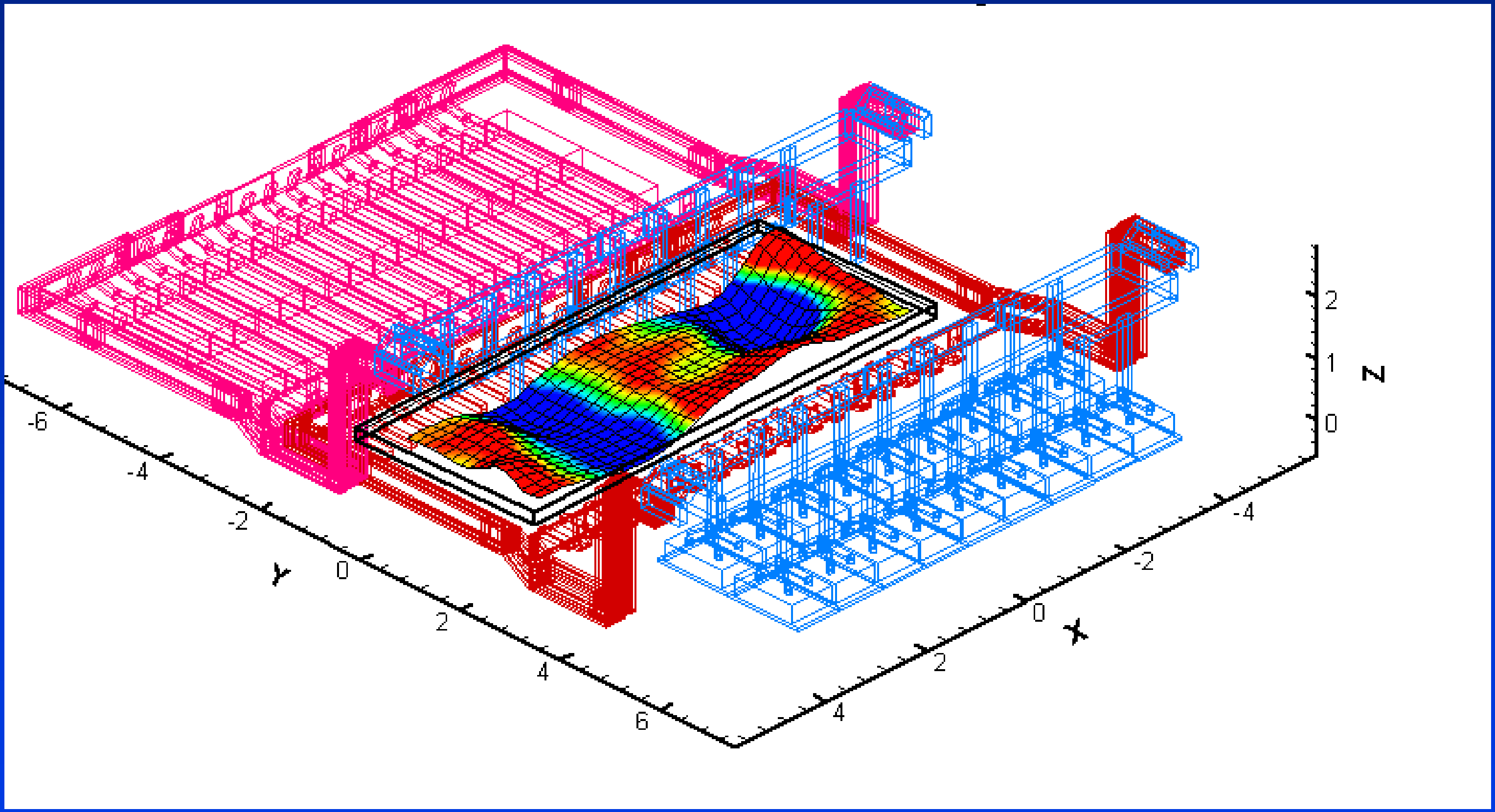

MHD-Valdis Stability Analysis

500 kA cell busbar design inspired from the Pechiney 1987 patent

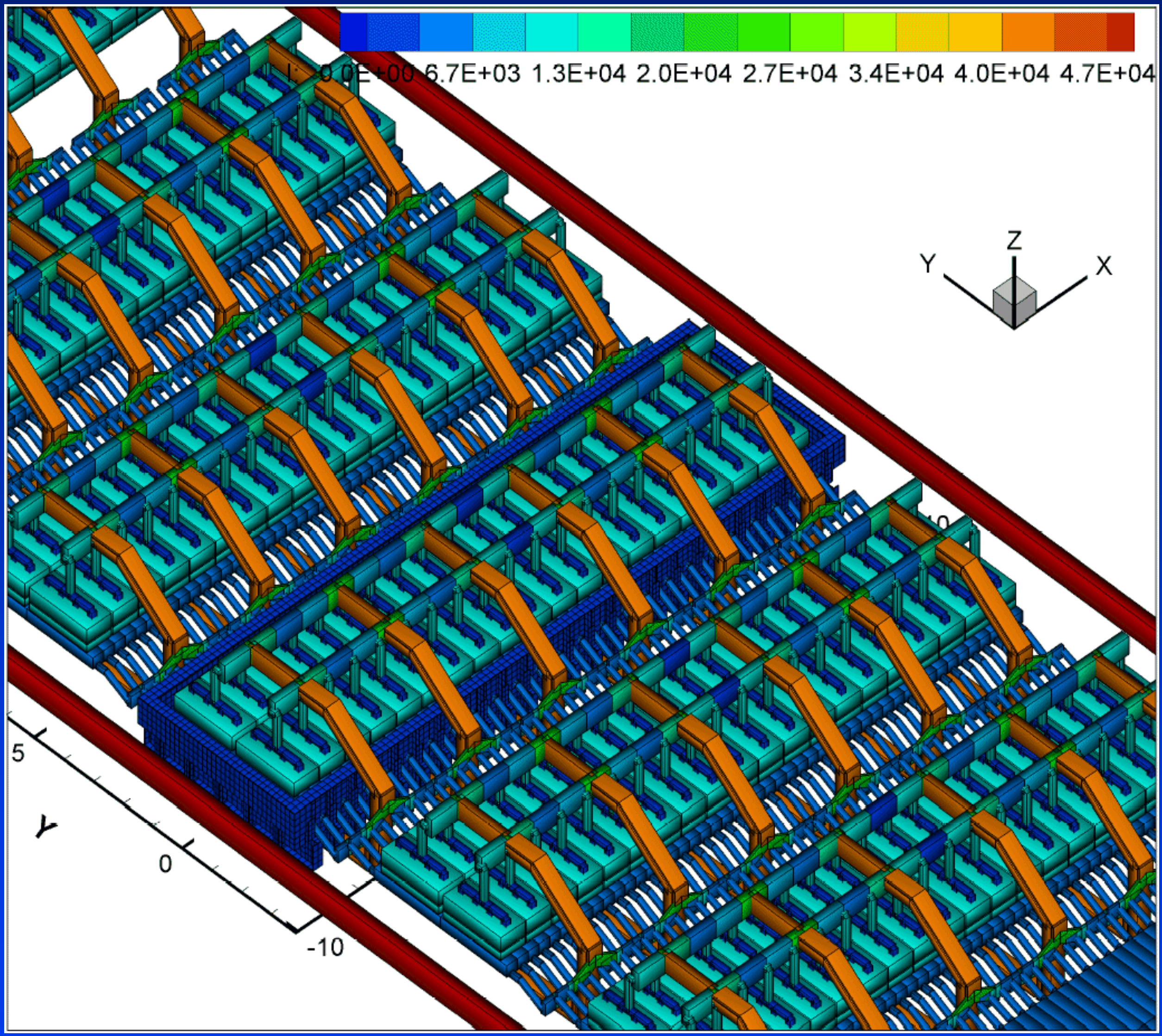

GENISIM

MHD-Valdis Stability Analysis

Current density for base case at 20 cm metal pad thickness and 4 cm ledge thickness.

Maximum horizontal current: 1.21 A/cm²

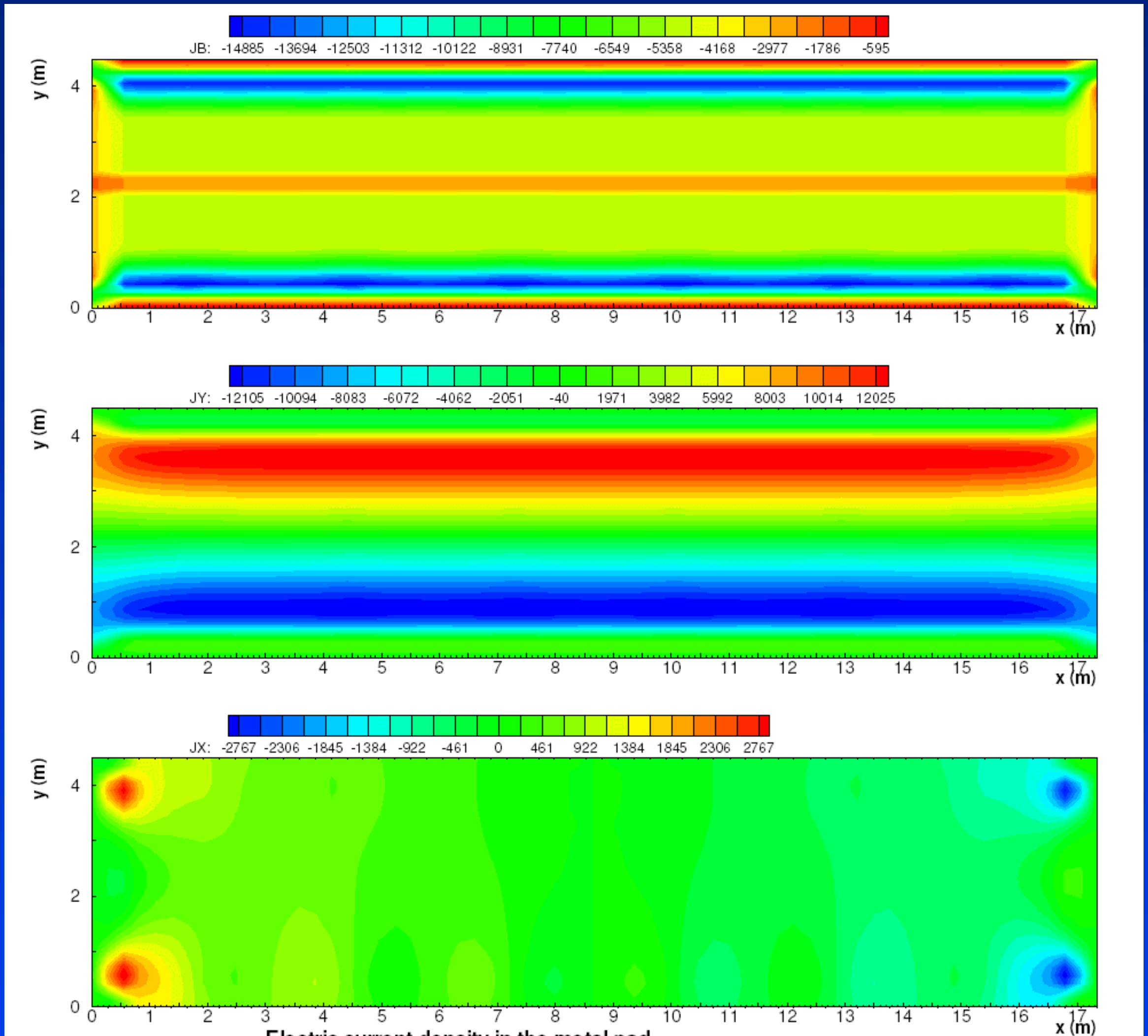

Electric current density in the metal pad

GENISIM

MHD-Valdis Stability Analysis

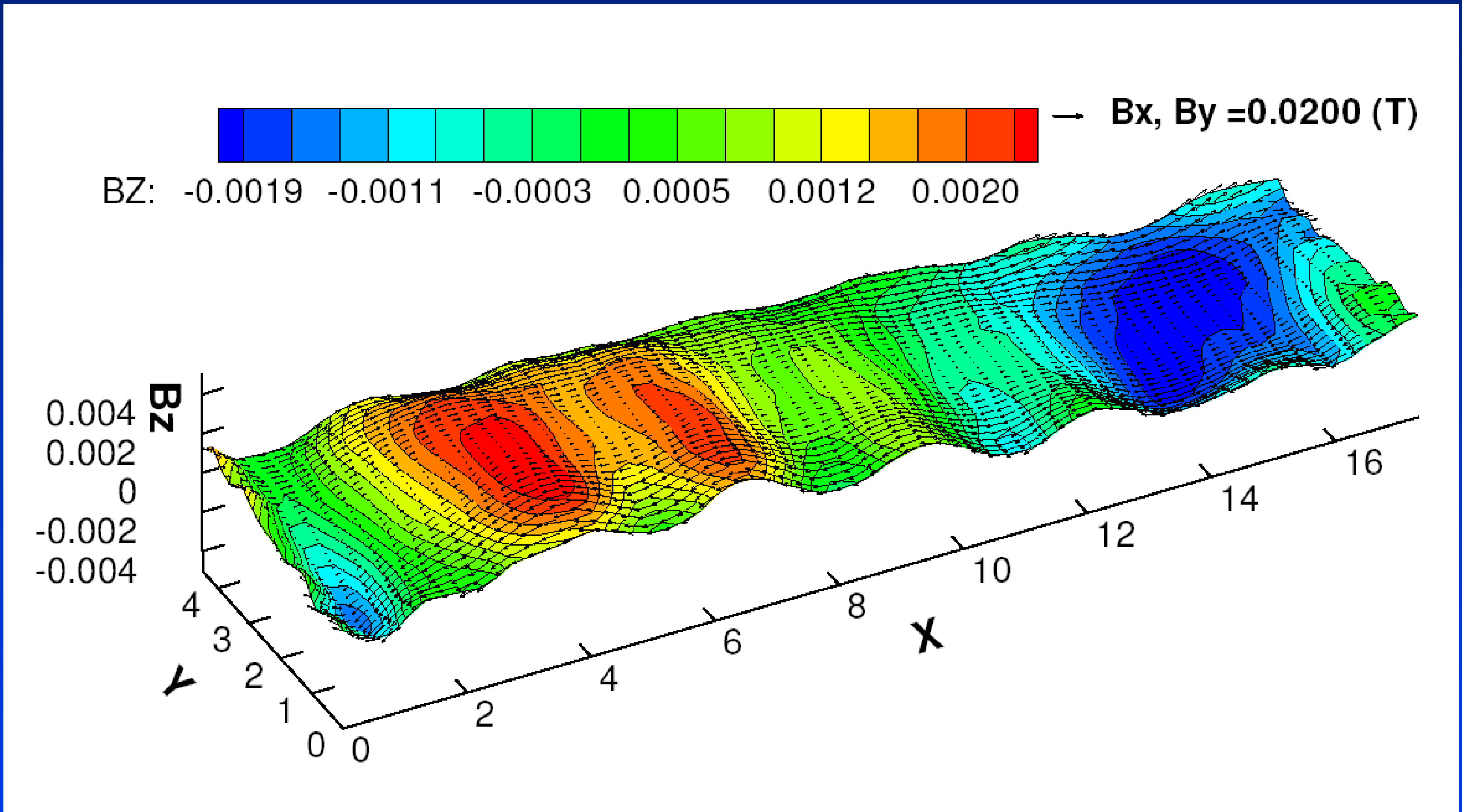

Corresponding Bz magnetic field component

GENISIM

MHD-Valdis Stability Analysis

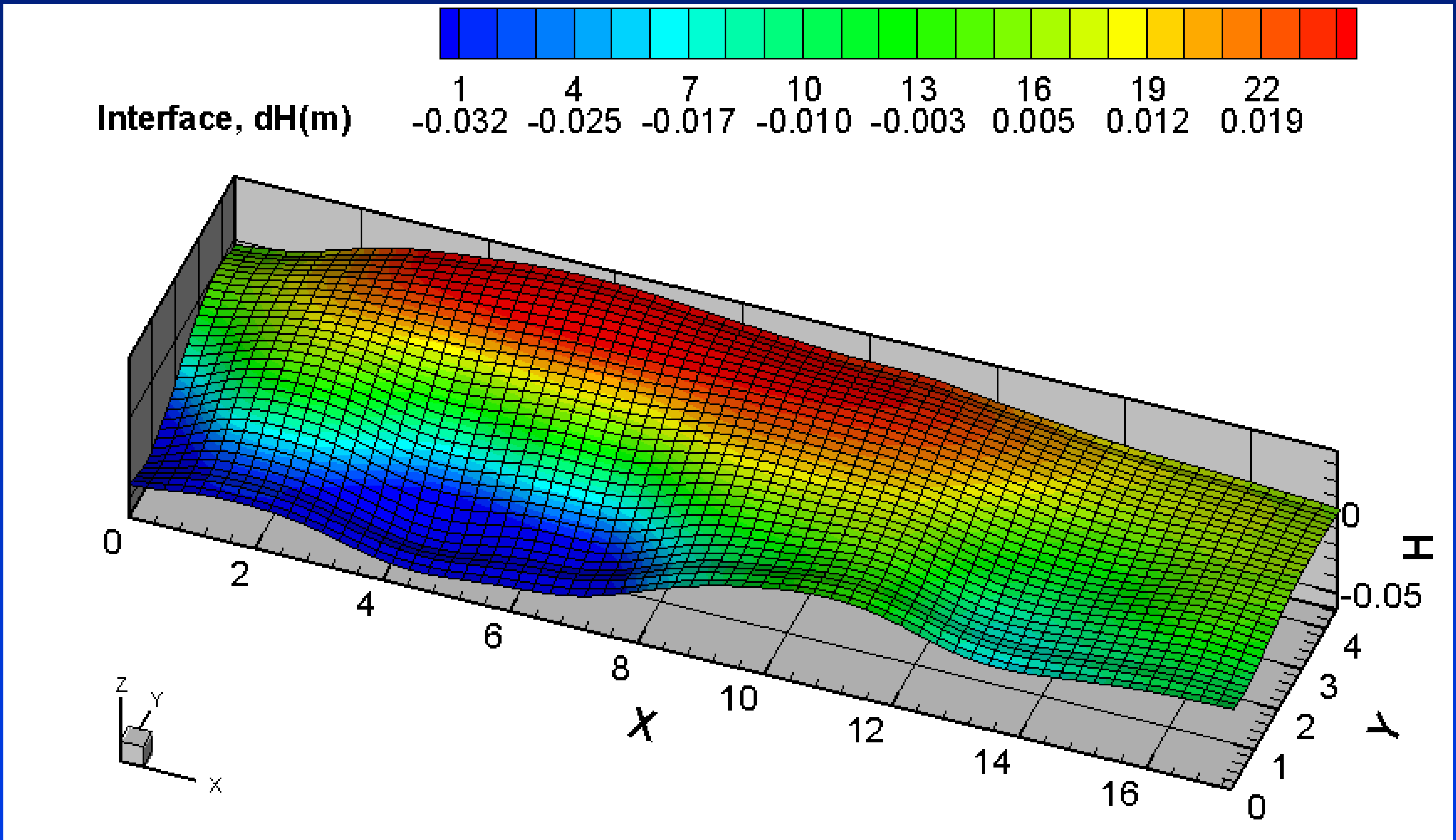

Corresponding bath/metal interface wave

GENISIM

MHD-Valdis Stability Analysis

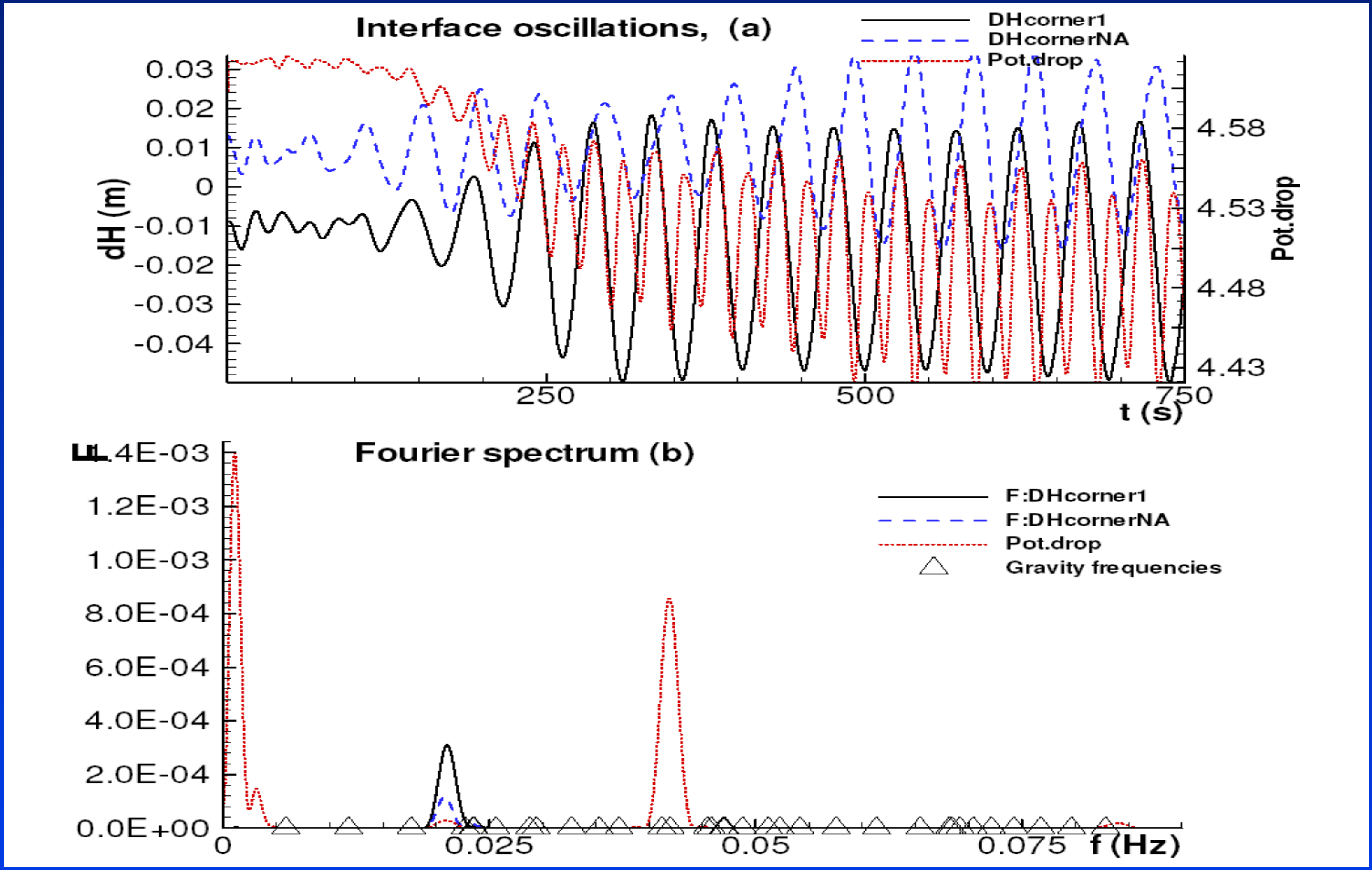

Corresponding interface oscillations Fourier spectrum analysis

2005 Weakly coupled 3D thermo-electric full cell and external busbar and MHD model

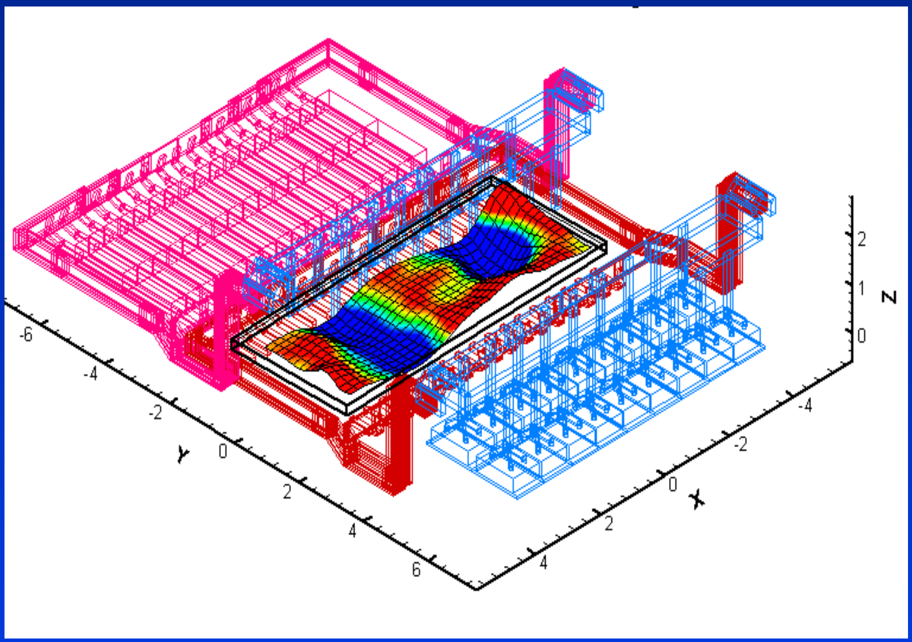

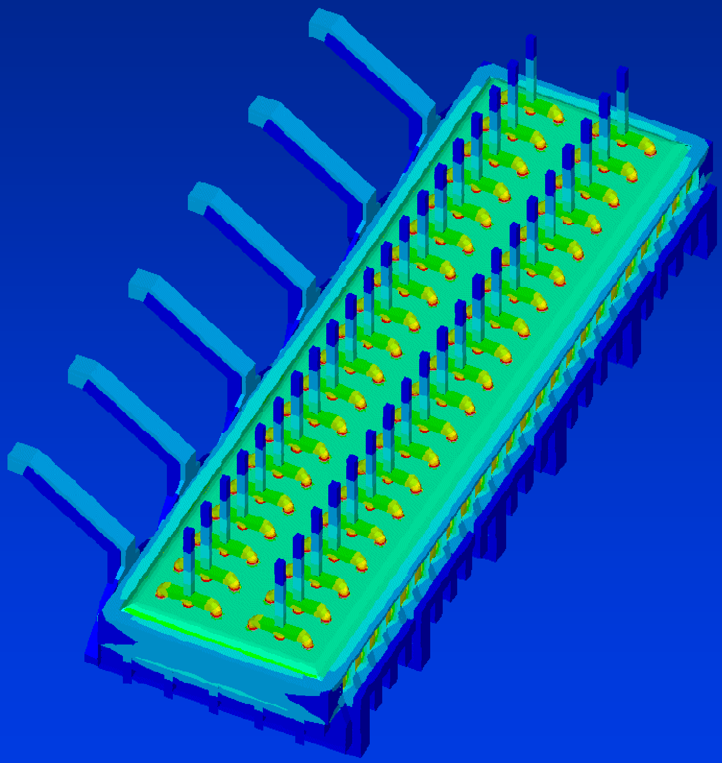

GENISIM

First Weakly Coupled Solution Between Thermo-Electric and MHD Models: 500 kA Cell Design

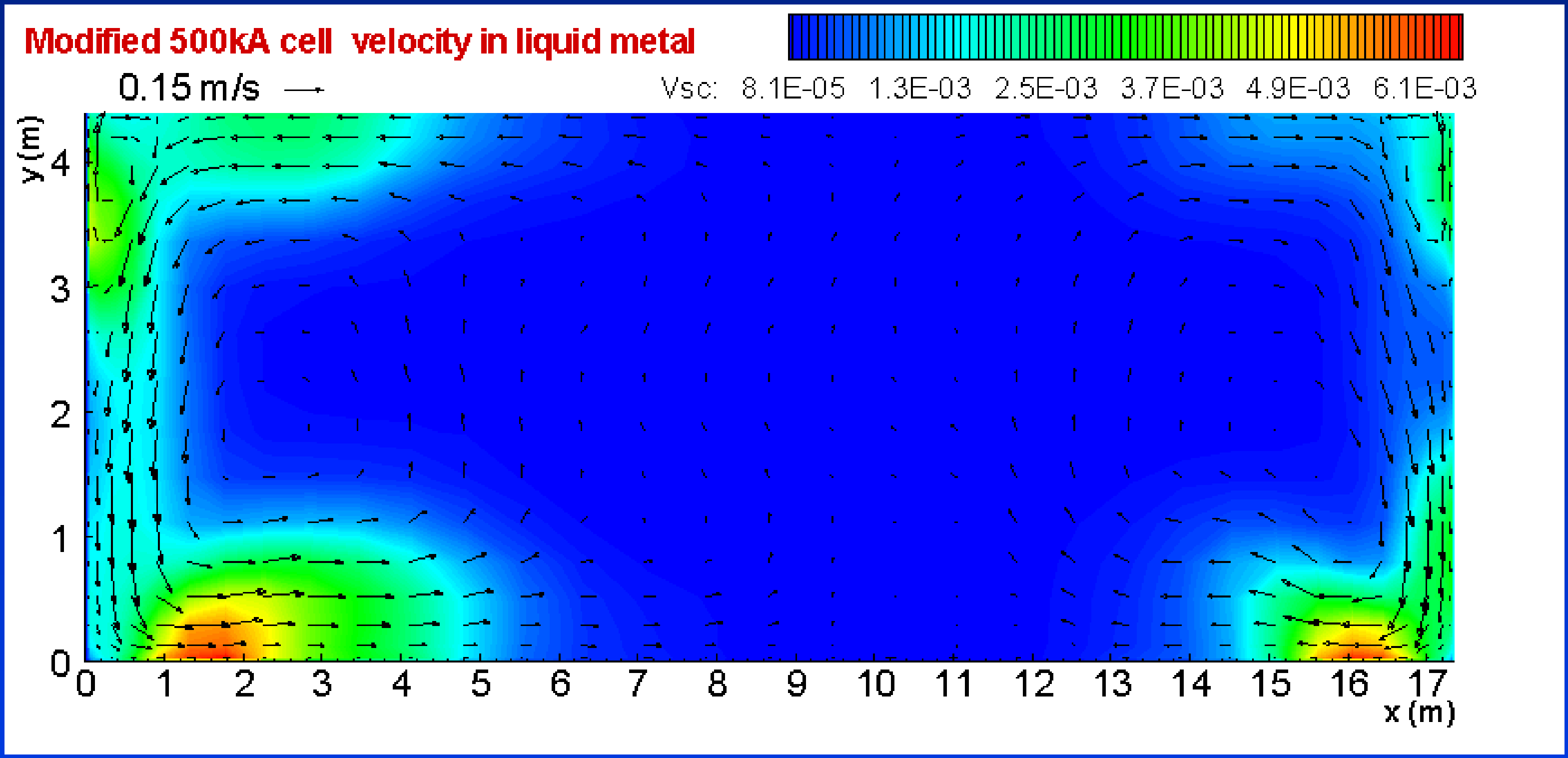

Velocity fields and turbulent effective viscosity distribution in liquid aluminium for the 500 kA cell as predicted by the MHD model

First Weakly Coupled Solution Between Thermo-Electric and MHD Models: 500 kA Cell Design

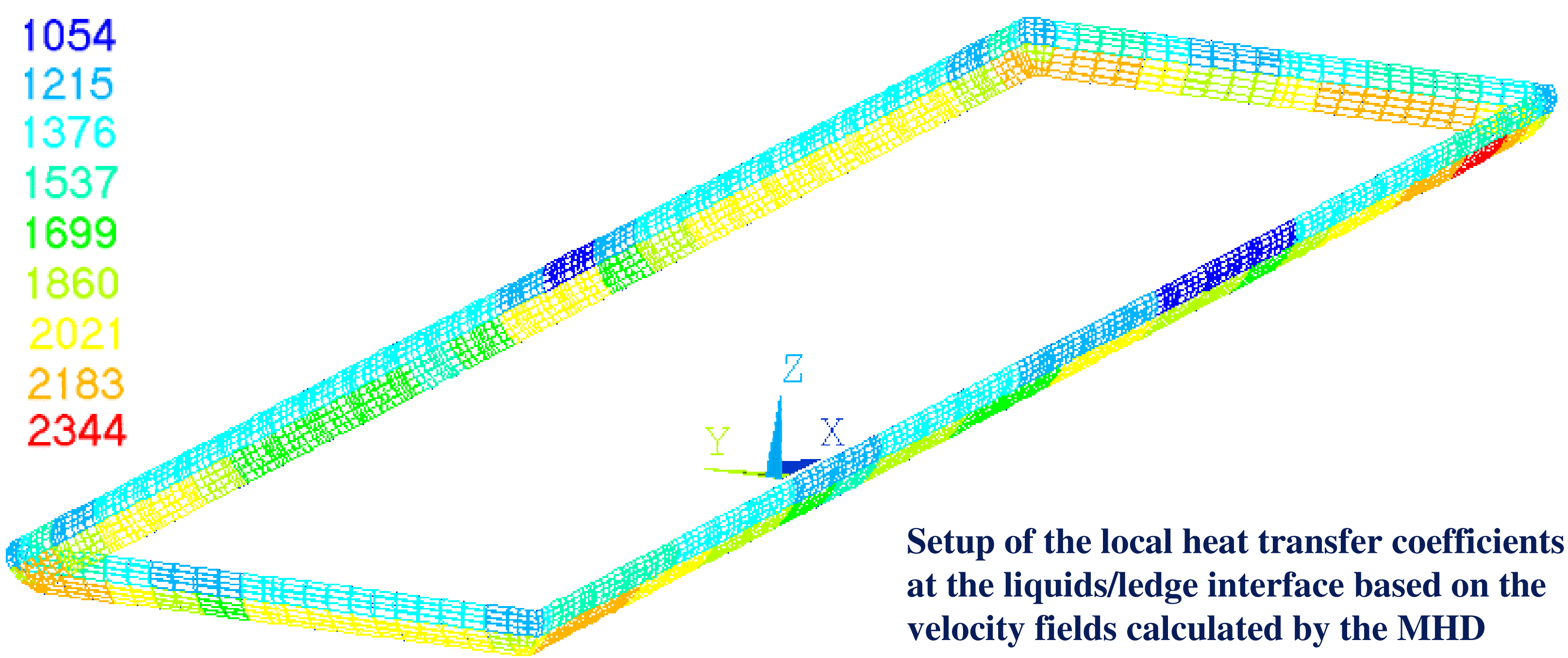

Setup of the local heat transfer coefficients at the liquids/ledge interface based on the velocity fields calculated by the MHD model

$$h_{metal/ledge\ (W/m2K)} = 1684 + 2000\ V^{1/2}_{(m/s)}$$

$$h_{bath/ledge\ (W/m2K)} = 1121 + 2000\ V^{1/2}_{(m/s)}$$

GENISIM

First Weakly Coupled Solution Between Thermo-Electric and MHD Models: 500 kA Cell Design

The obtained ledge profile geometry is transferred to the MHD model and the MHD cell stability analysis is computed again

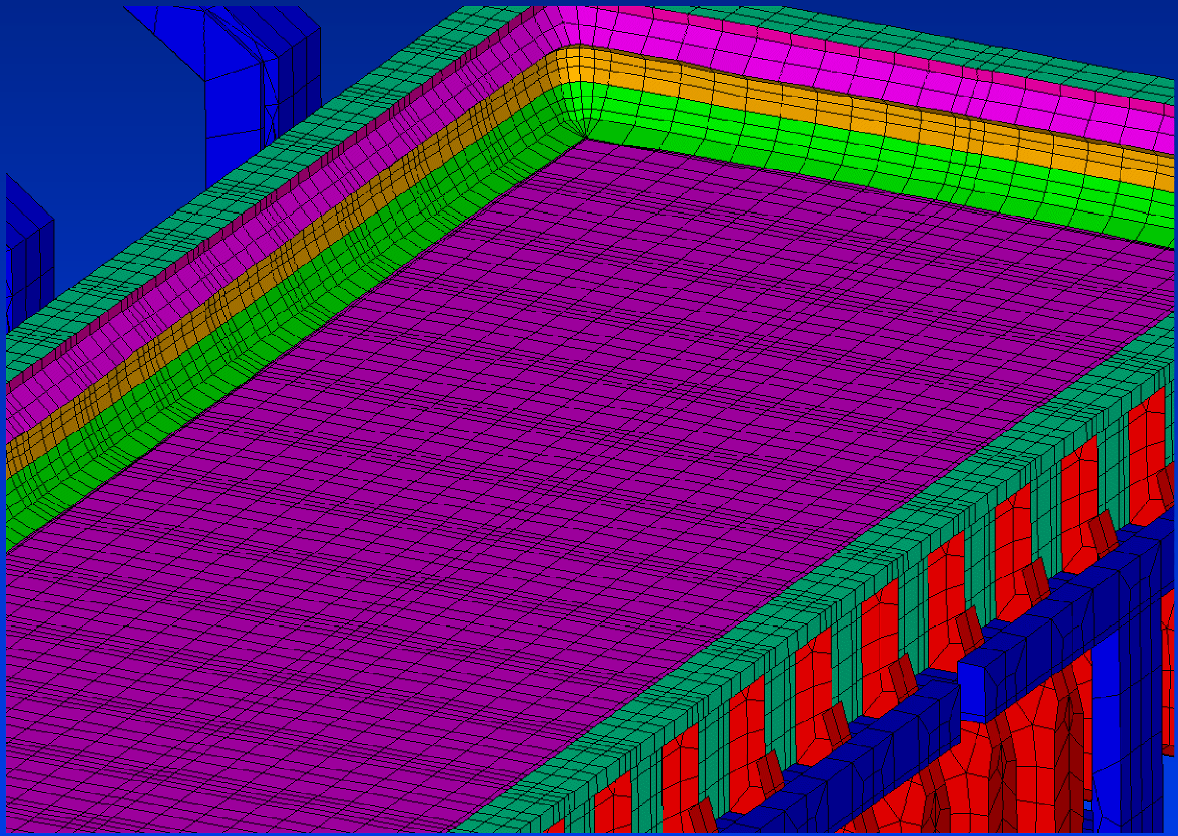

2006 Weakly coupled 3D thermo-electric full cell model and mechanical quarter cell model

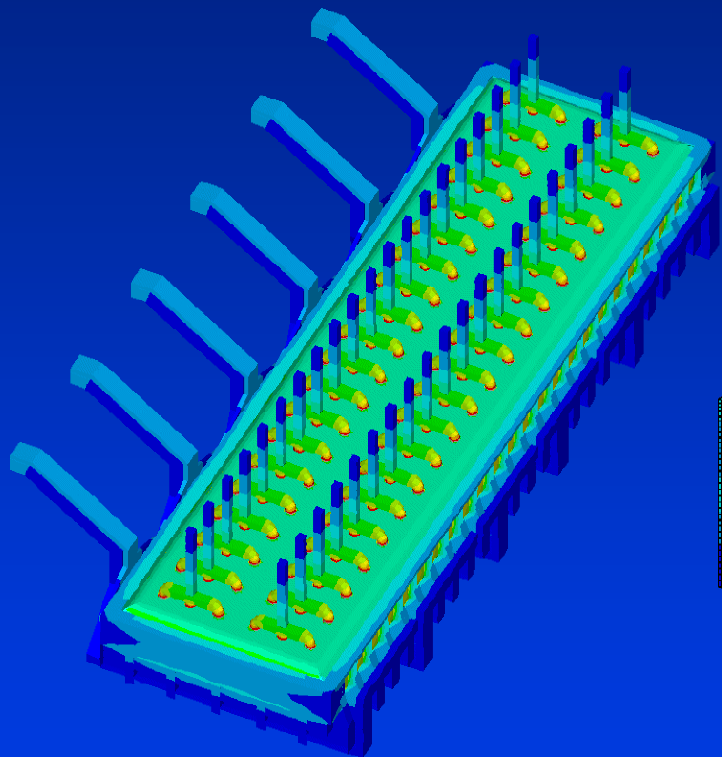

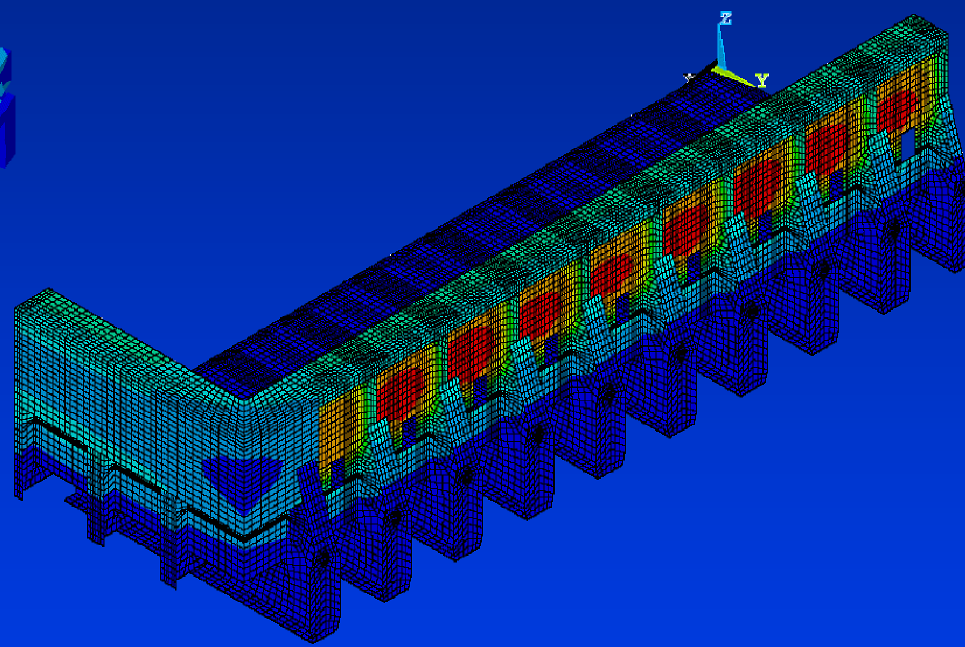

2006 Weakly coupled 3D thermo-electric full cell model and mechanical quarter cell model

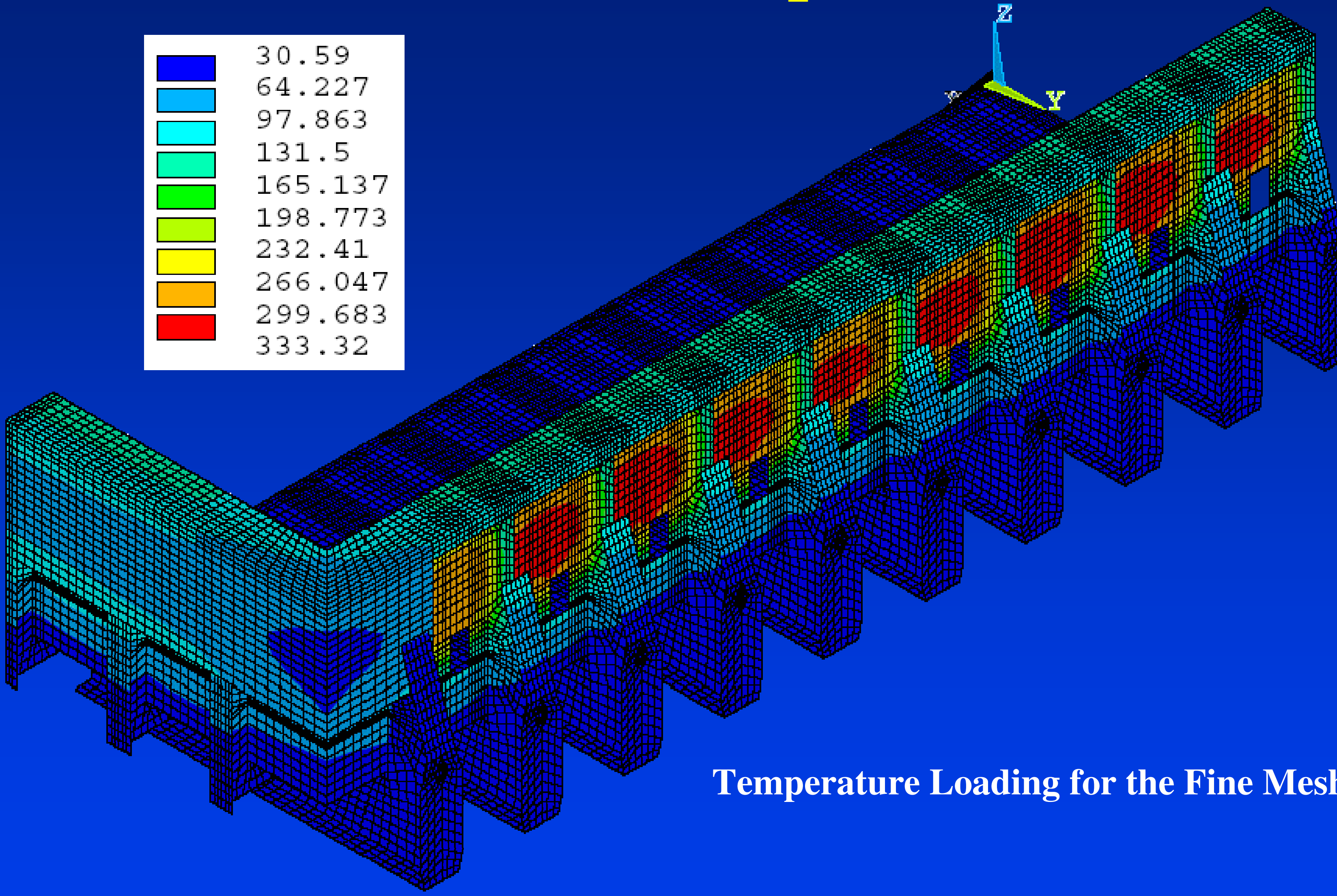

Temperature Loading for the Fine Mesh Model

GENISIM

2006 Weakly coupled 3D thermo-electric full cell model and mechanical quarter cell model

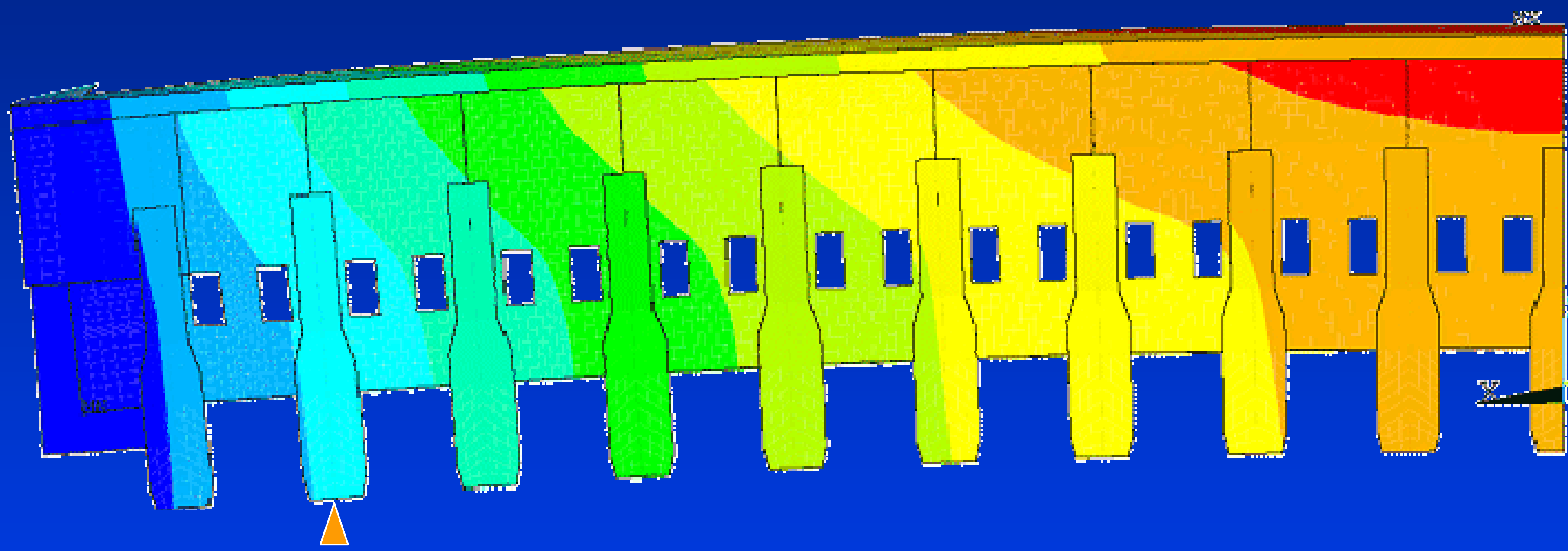

Relative Vertical Displacement for the Fine Mesh Model

500 kA Cell Mechanical Model Results

Base Case.

With Cooling Fins.

With Forced-Air Cooling.

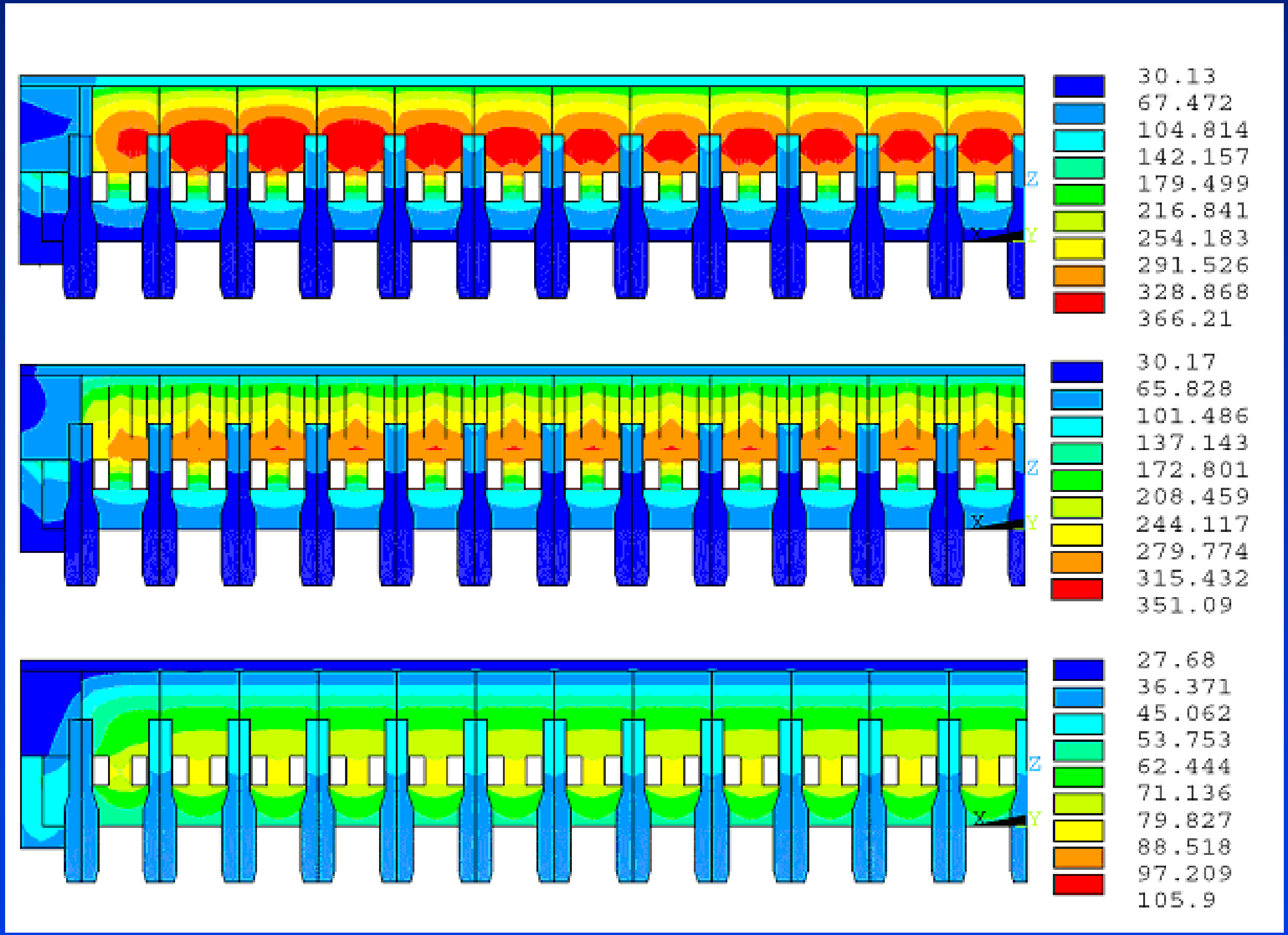

Temperature distribution for the studied 500 kA cell configurations.

500 kA Cell Mechanical Model Results

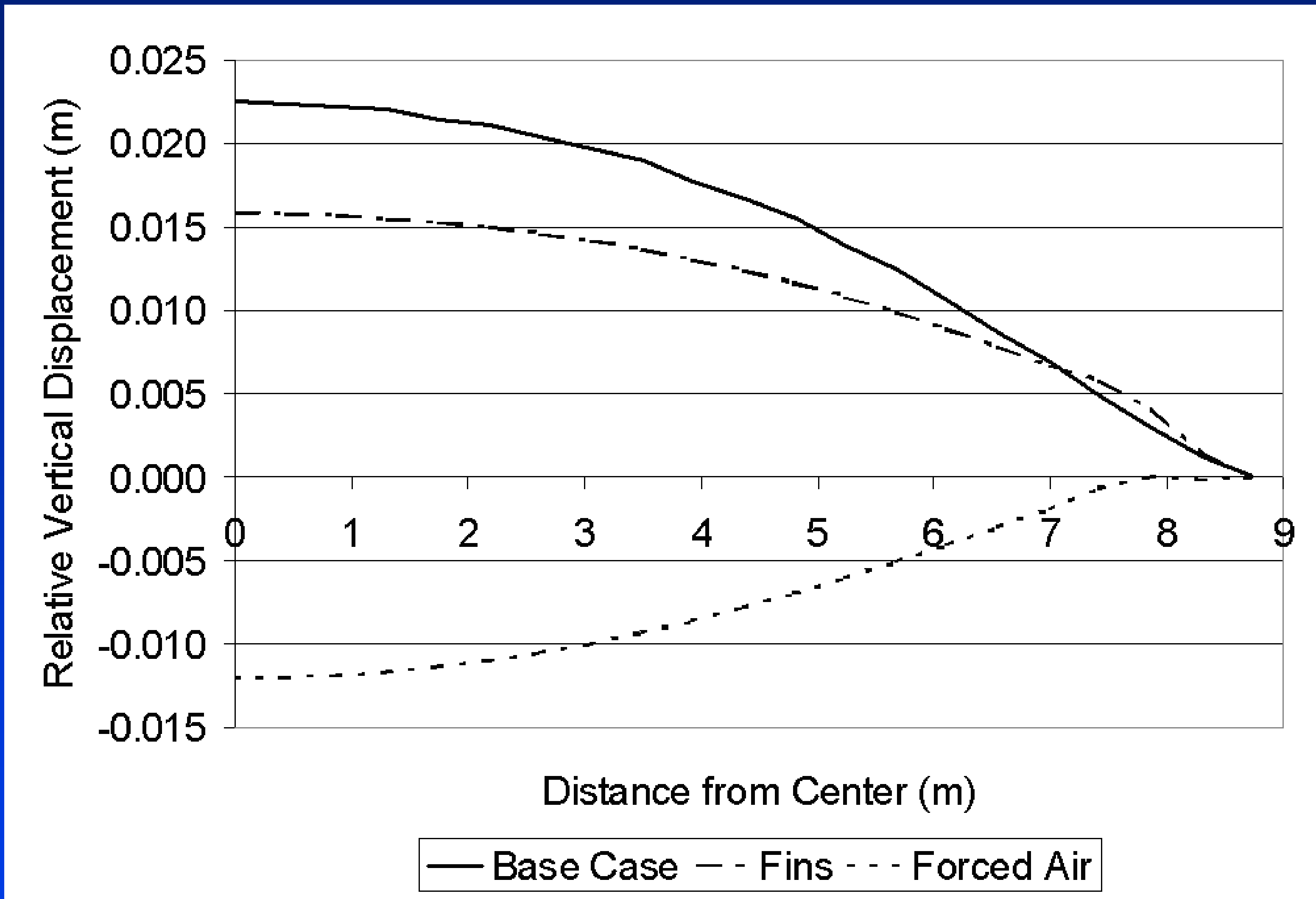

Comparison of the relative vertical displacement on the long axis of the 500 kA cell.

Comportement thermo-chimio-mécanique d'une cuve de Hall-Héroult lors d'un préchauffage au gaz

Jérôme BÉDARD[1], Patrice GOULET[1], Mario FAFARD[1], Daniel RICHARD[2] et Marc DUPUIS[3]

[1]Faculté des sciences et de génie, Québec, Québec, Canada, G1K 7P4
[2]Hatch, 5 Place Ville Marie, Bureau 200 Montréal, Québec, Canada, H3B 2G2
[3]GéniSim Inc., 3111 rue Alger, Jonquière, Québec, Canada, G7S 2M9

Résumé

Une cuve d'électrolyse est certainement un investissement majeur pour une aluminerie. Toutes les mesures sont donc prises en main afin de maximiser la production et la durée de vie de ces cuves. Par exemple, les industries font appel à diverses méthodes de préchauffage afin d'assurer une transition adéquate vers la mise en opération de la cuve. Parmi ces méthodes, Sørlie et Øye notent que le préchauffage au gaz est celle qui donne la distribution de température la plus uniforme dans la cuve.
Afin d'être en mesure de prédire correctement le comportement de la cuve lors du préchauffage, il est nécessaire de développer un modèle thermo-chimio-mécanique représentatif de la réalité. Ce modèle permettra de prévoir et de comprendre les phénomènes présents au démarrage de la cuve afin d'optimiser la longévité et les coûts d'utilisation de la cuve.

Problématique et objectif

Un modèle adéquat des matériaux de la cuve est nécessaire pour détecter les risques d'apparition de fissures dans le bloc cathodique ainsi que le développement d'ouvertures non désirées où le bain d'électrolyse en fusion pourrait s'infiltrer. De plus, la cuisson de la pâte, la nature quasi-fragile des blocs de carbone et les multiples interfaces de contact sont tous des paramètres importants à considérer.
L'objectif est donc de modéliser l'étape de préchauffage au gaz pour un quart de bloc cathodique avec le caisson, le berceau et les matériaux réfractaires correspondant. Une tranche de cuve VAW 300 kA fut donc modélisée à l'aide du logiciel par éléments finis **ANSYS** et plusieurs simulations avec différents scénarios de préchauffage furent lancées à l'aide du code ***FESh++***.

Développement du modèle

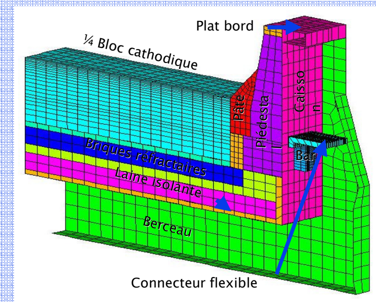

Propriétés des matériaux

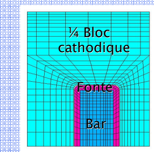

<u>Coque 2D – Thermomécanique</u>
Berceau , Caisson , Plat bord
<u>Brique 3D – Thermique</u>
Connecteur flexible , Briques réfractaires , Laine isolante
<u>Brique 3D – Thermomécanique – Élastique</u>
Bar collectrice , Fonte
<u>Brique 3D – Thermomécanique – Quasi-fragile</u>
Piédestal , Bloc cathodique
<u>Brique 3D – Thermo-chimio-mécanique – Quasi-fragile réactif</u>
Pâte à brasquer

Conditions aux limites

- S1 et S2 : Plans de symétrie pour le bloc cathodique
- P3 : Fondation élastique qui dépend du confinement des matériaux le long de la cuve

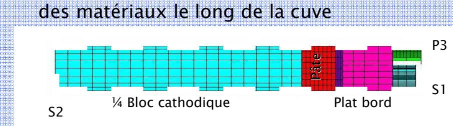

Scénarios de préchauffage

- Coefficient de transfert thermique de 650 W/m^2K
- Température finale de flamme de 955°C
- Rampe constante
- Durée du préchauffage : 12 , 24 , 36 et 72 heures

Résultats des simulations

Thermique

- Les gradients thermiques dans le bloc cathodique diminuent lorsque la durée de préchauffage augmente

Différence de température sur la hauteur du bloc cathodique en fonction du scénario de préchauffage

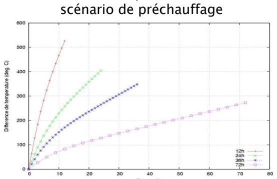

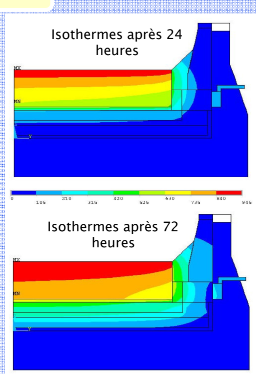

Mécanique

- En admettant P3 comme plan de symétrie, des fissures se développent dans les ailes du bloc. Ces fissures sont absentes si P3 n'est pas considéré.

- L'expansion du bloc ne peut se faire qu'au dépend de la pâte si P3 est considéré comme un plan de symétrie. Des ouvertures se créent alors et l'électrolyte en fusion y est libre de s'infiltrer.

Fissures dans le bloc pour un préchauffage de 24 heures

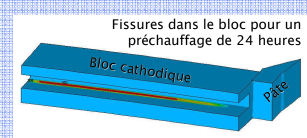

Déformée (x10) pour un préchauffage de 24 heures

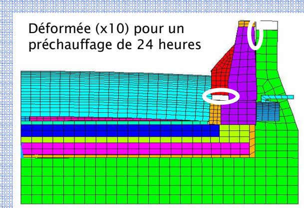

Travaux futurs

<u>Comportement thermo-électro-chimio-mécanique d'une cuve de Hall-Héroult lors d'un préchauffage électrique</u>
- Modélisation de l'anode
- Insertion du lit de coke
- Comparaison des résultats avec ceux d'un préchauffage au gaz

<u>Comportement d'un quart de cuve de Hall-Héroult lors d'un préchauffage électrique ou au gaz</u>
- Modélisation complète du quart de cuve incluant le coin
- Comparaison des résultats avec ceux d'une tranche

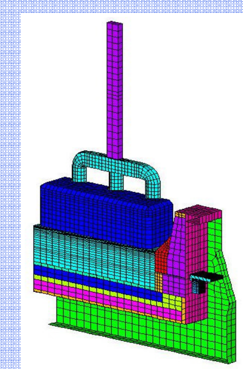

UNIVERSITÉ LAVAL CRSNG NSERC HATCH™ GENISIM

Modeling of the Magnetic Field and MHD Stability in Aluminum Reduction Cells

Alexander Kalimov, Anton Potienko, Sergey Vazhnov

State Polytechnic University,

St.-Petersburg, RUSSIA

October 2006

270 kA cells without ferromagnetic elements

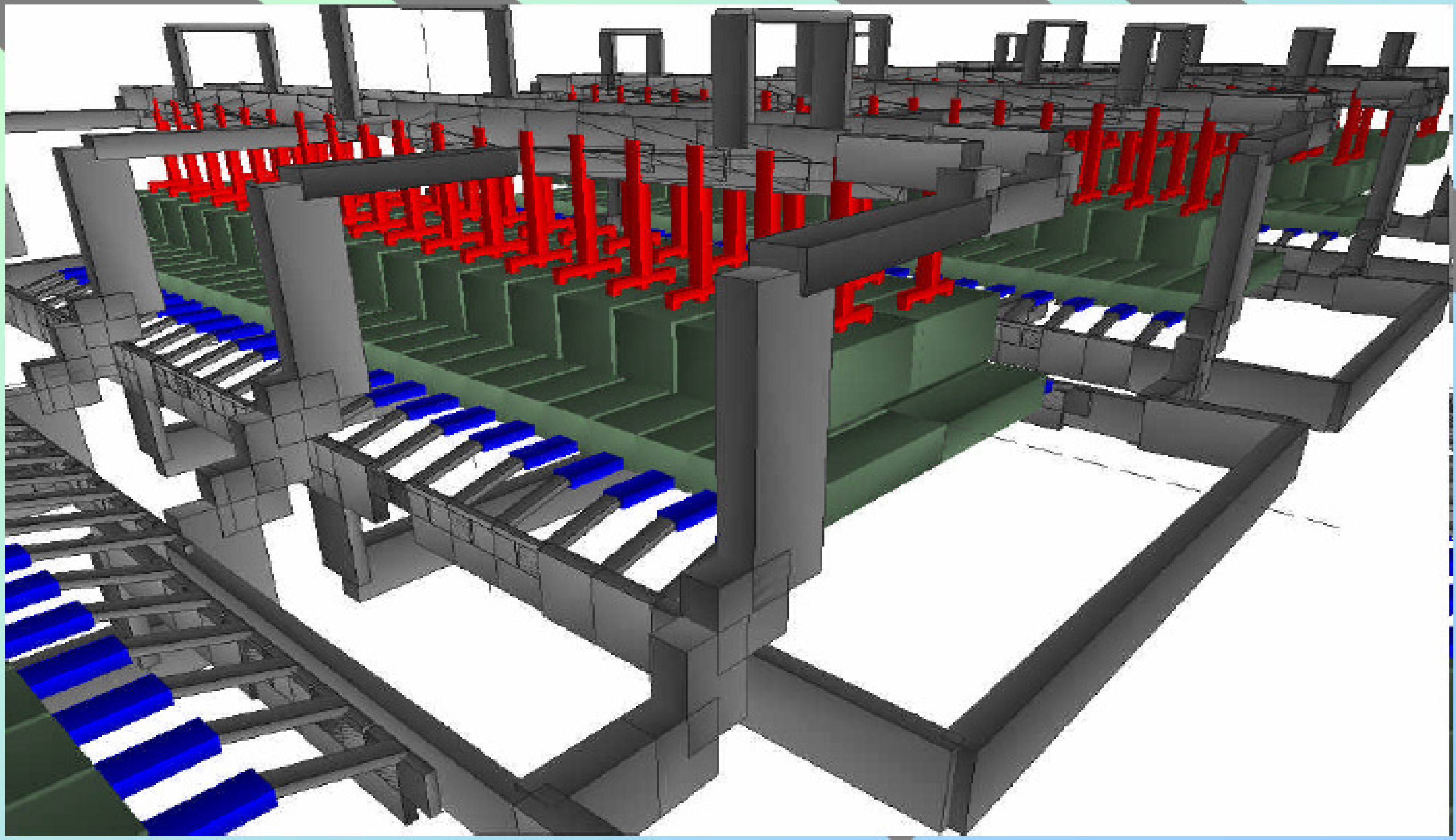

Presentation of output data (MHD)

circulation

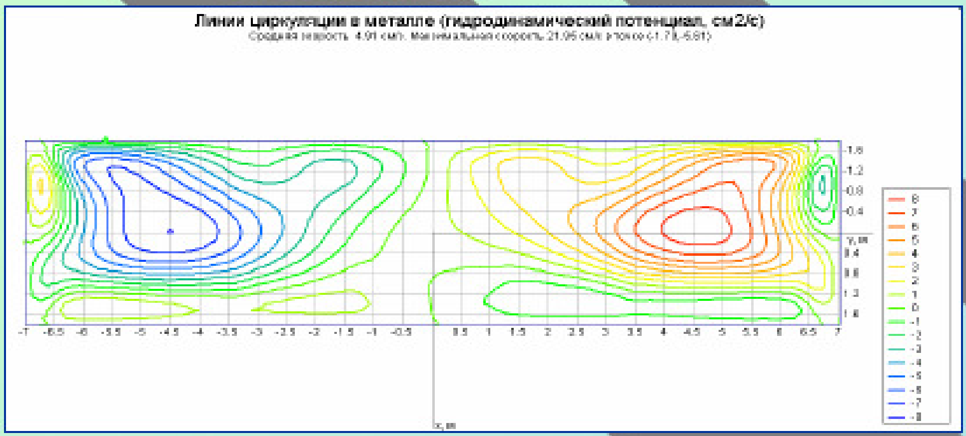

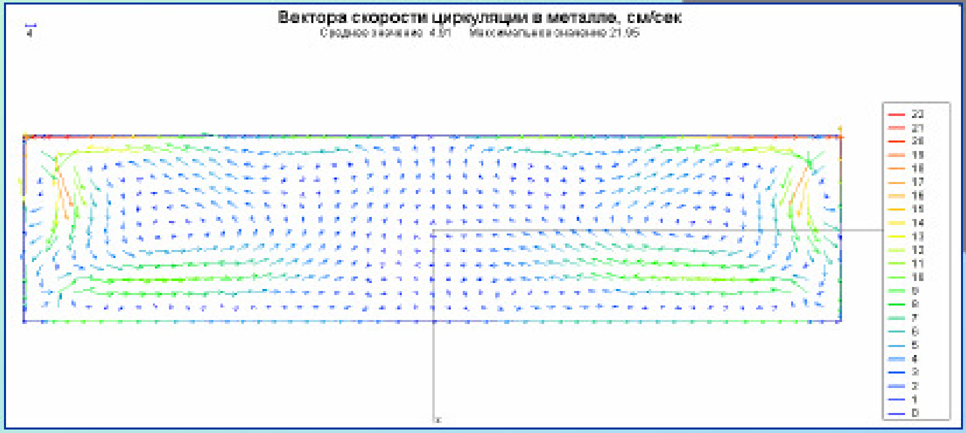

static skew of the interface

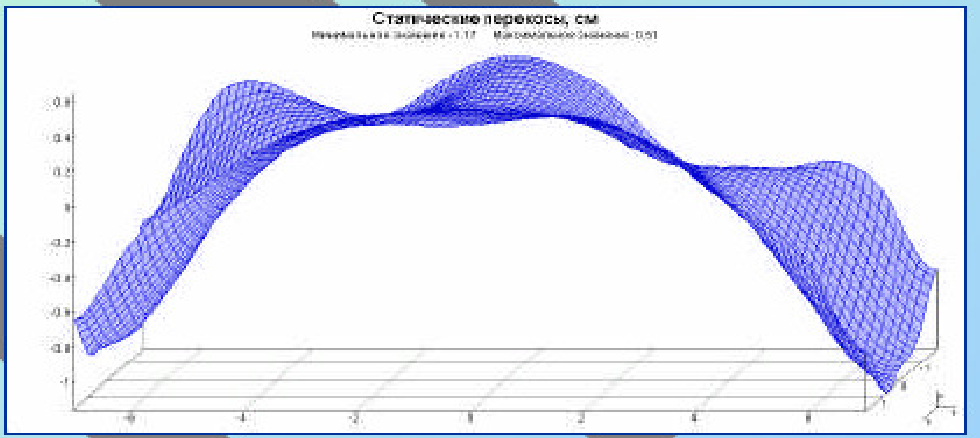

stability map

Interpolar distance, cm (Voltage, V)	Metal level, cm				
	20	22	24	26	28
3 (3.37)	7.974	5.354	3.213	1.371	-0.080
3.5 (3.50)	4.957	2.764	0.891	-0.403	-1.693
4 (3.64)	2.626	0.836	-0.511	-1.885	-3.078
4.5 (3.77)	0.999	-0.491	-1.984	-3.257	-4.491
5 (3.91)	-0.275	-1.807	-3.274	-4.615	-5.713

GLOBAL DELIVERY OF SOLUTIONS TO THE ALUMINIUM INDUSTRY

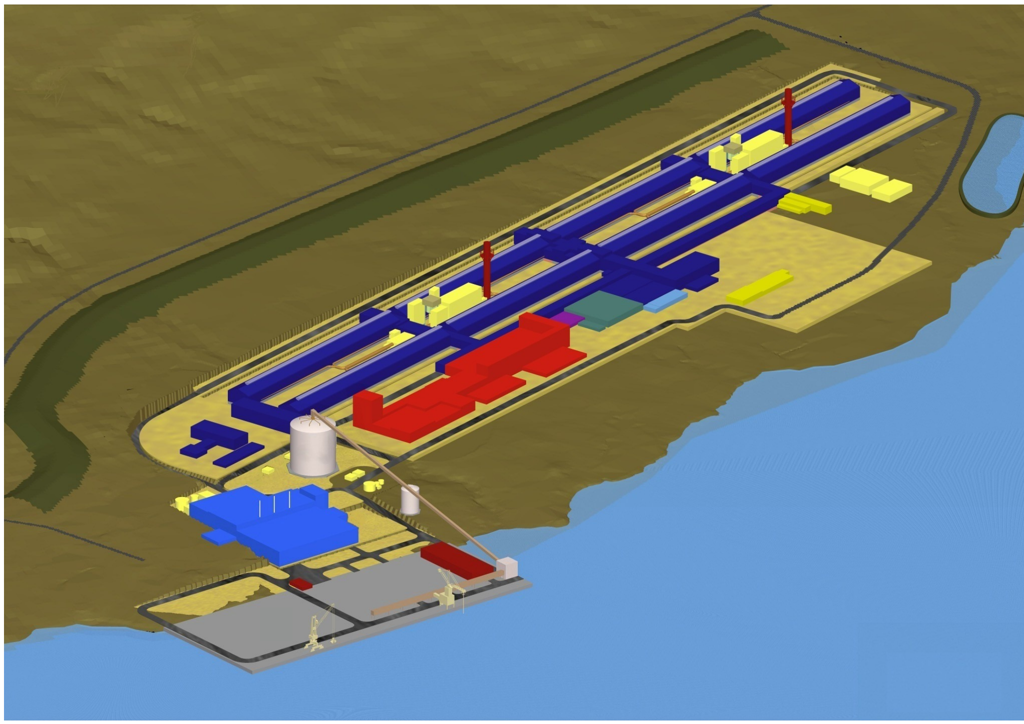


CAD Model of Aluminium Smelter

October 1-4, 2006, Montréal, QC

GLOBAL DELIVERY OF SOLUTIONS TO THE ALUMINIUM INDUSTRY

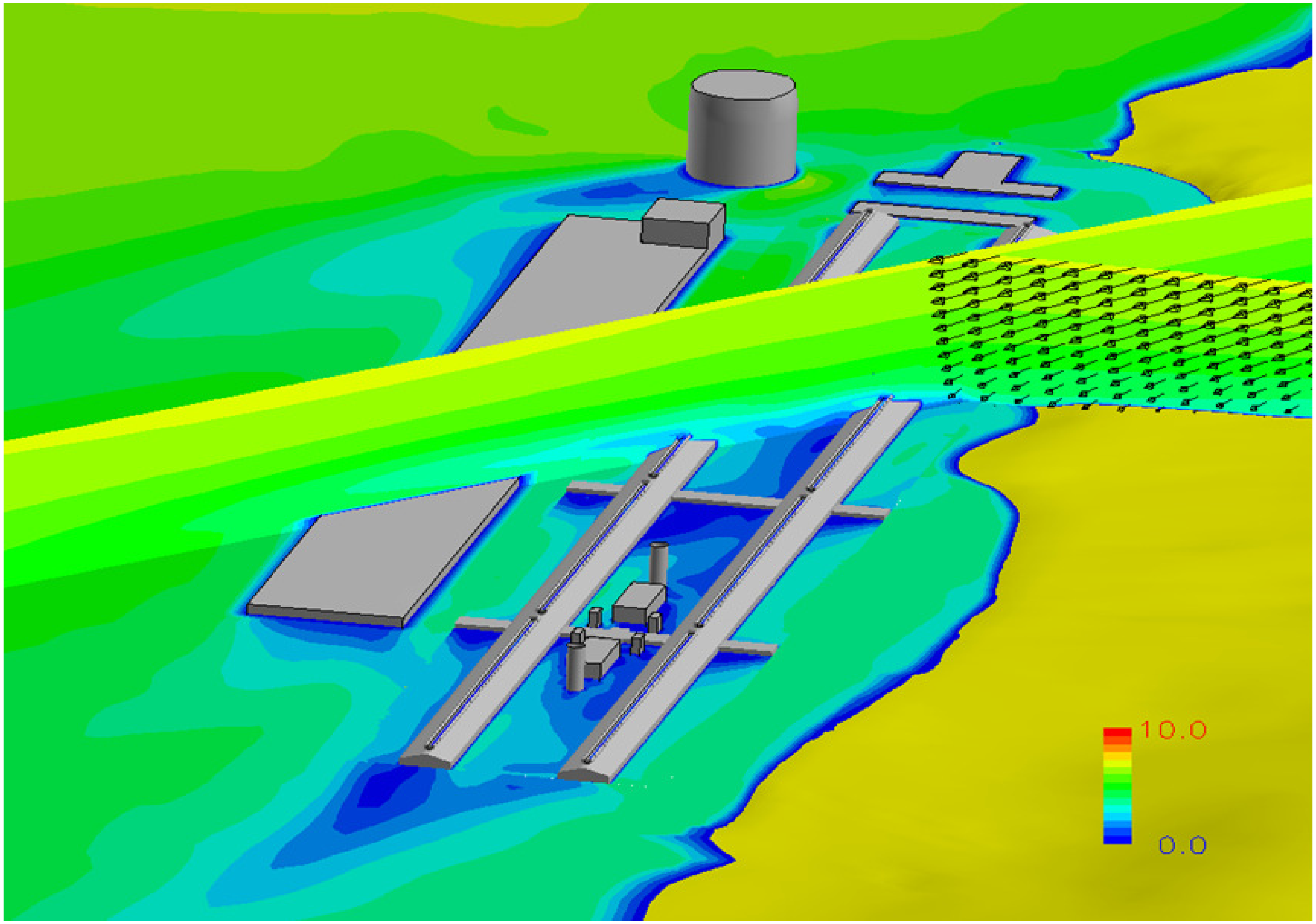

Velocity Contours (m.s-1) at Elevation of 12 m

GLOBAL DELIVERY OF SOLUTIONS TO THE ALUMINIUM INDUSTRY

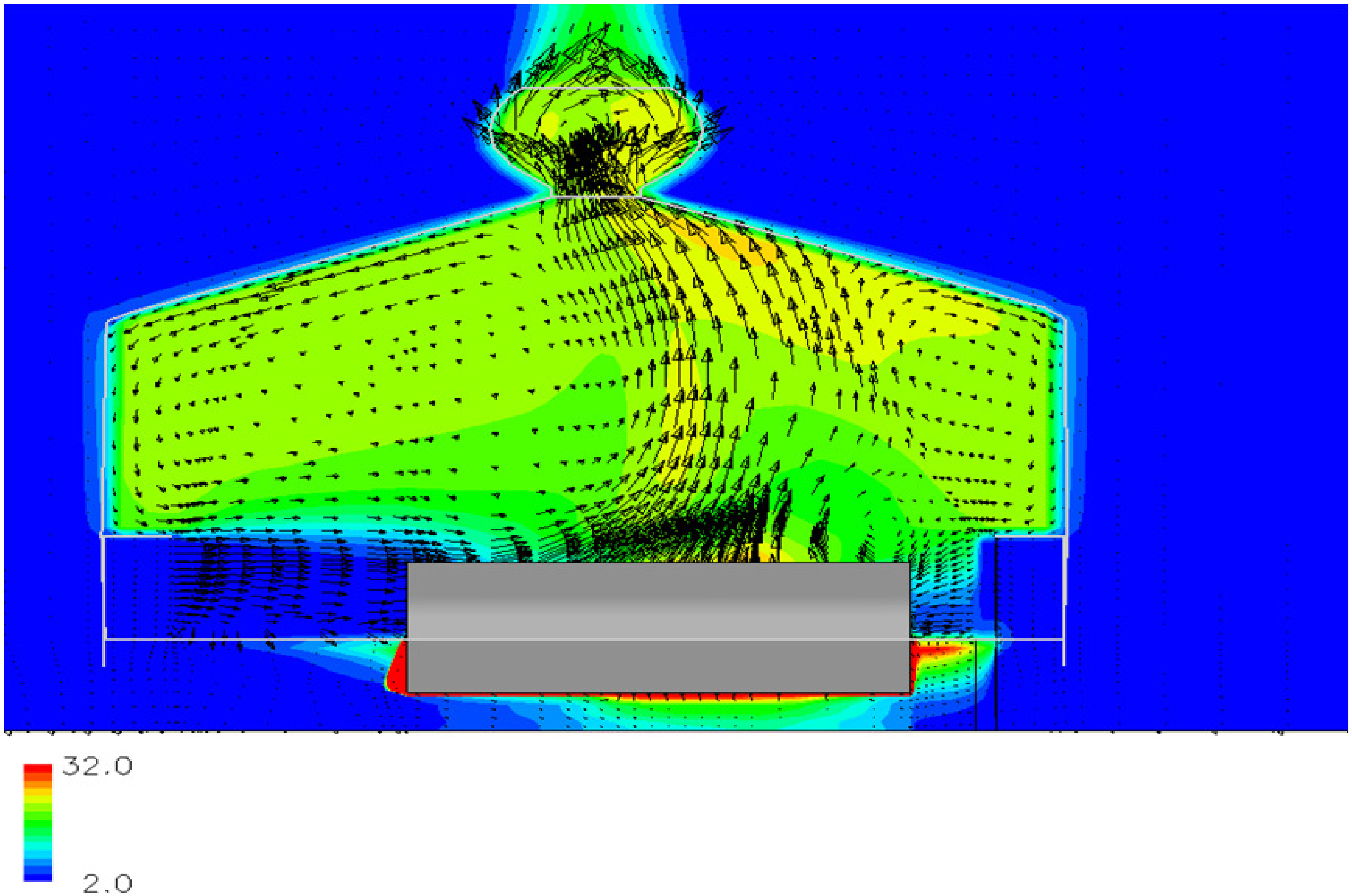

Temperatures (°C) through a Cross-Section of Potroom

DESIGNING VENTILATION SYSTEMS FOR POTROOMS USING COMPUTATIONAL FLUID DYNAMICS MODELING

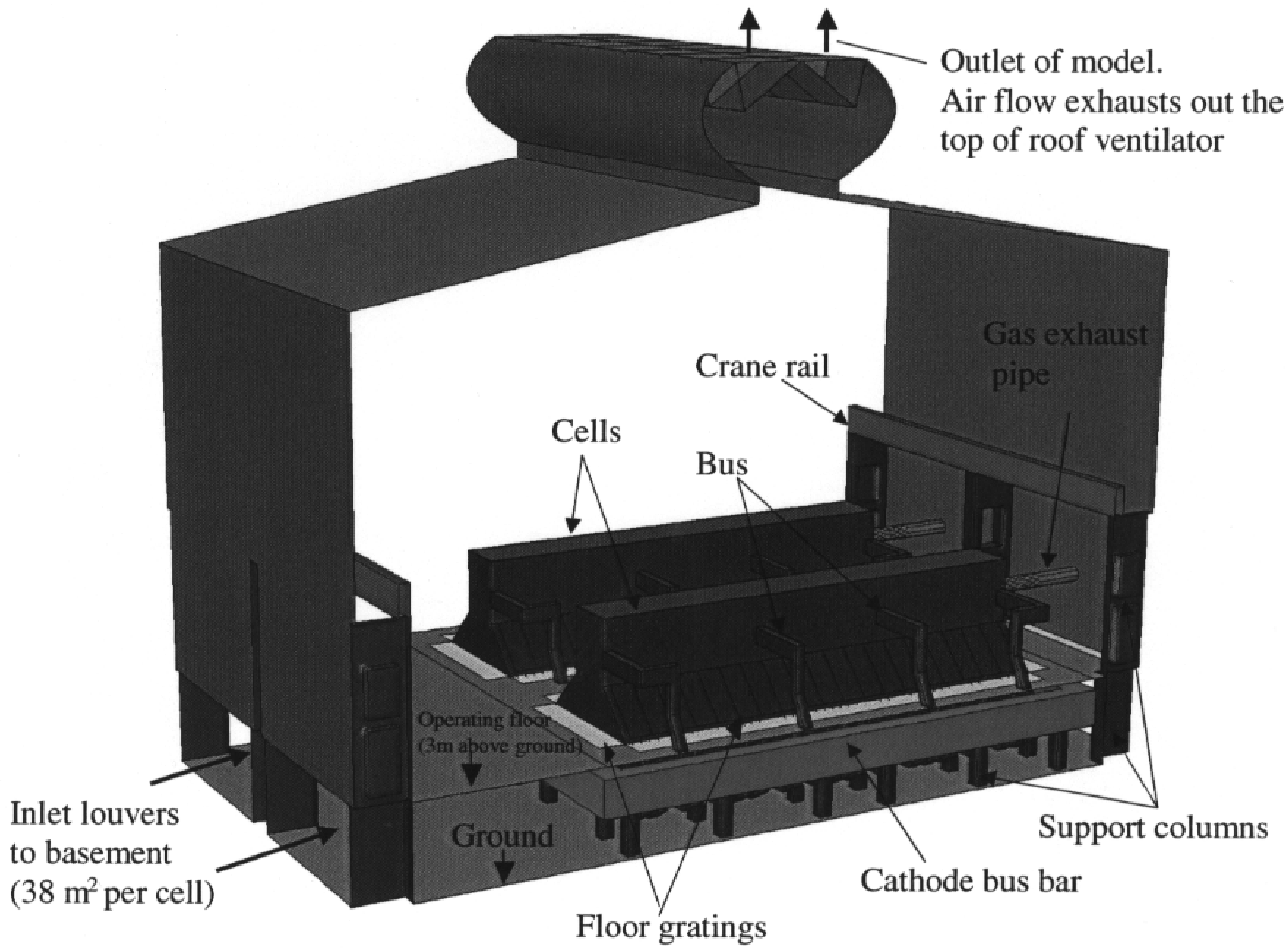

Isometric view of CFD model of potroom

October 1-4, 2006, Montréal, QC

DESIGNING VENTILATION SYSTEMS FOR POTROOMS USING COMPUTATIONAL FLUID DYNAMICS MODELING

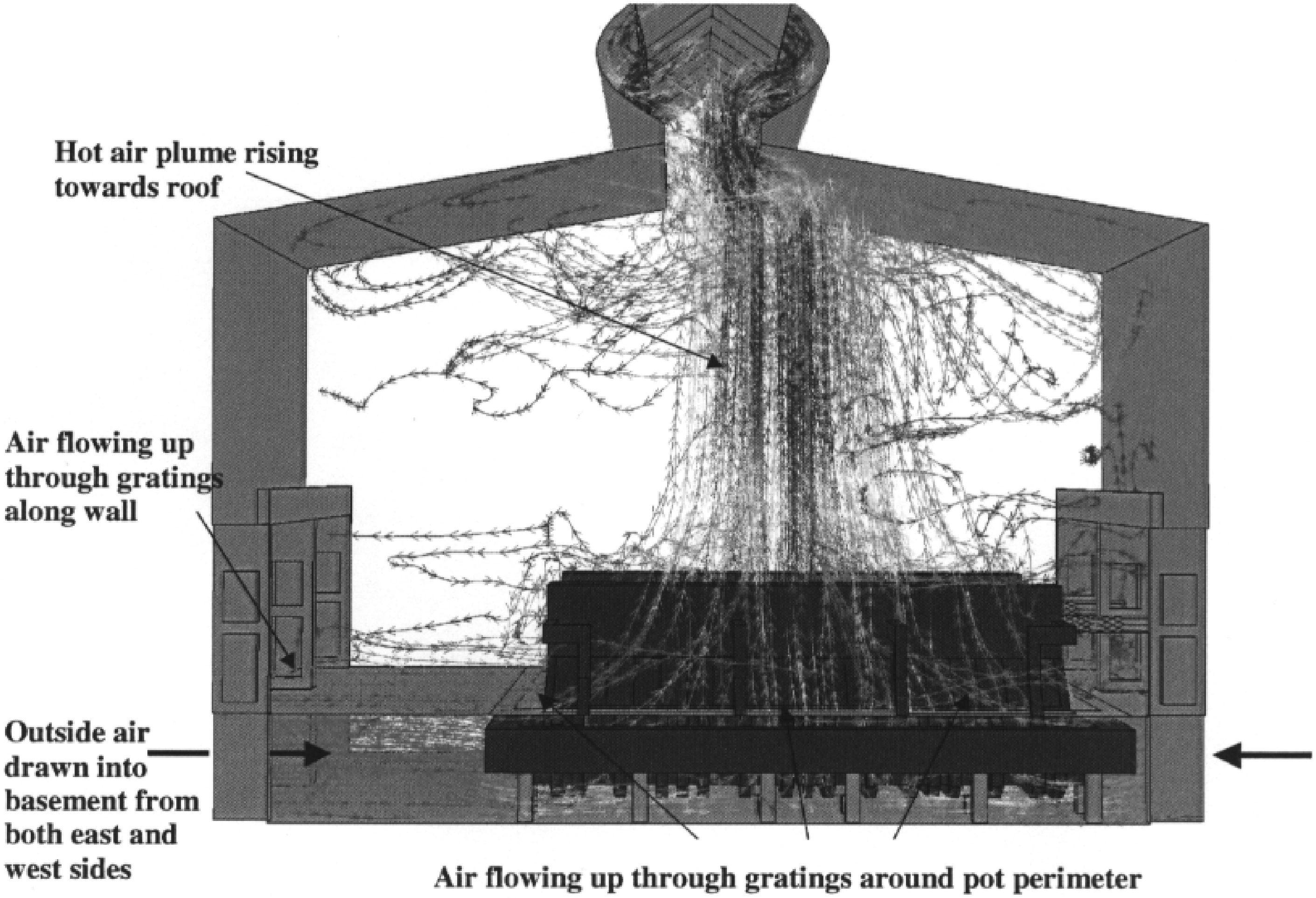

Air flow pattern into potroom during summer

DESIGNING VENTILATION SYSTEMS FOR POTROOMS USING COMPUTATIONAL FLUID DYNAMICS MODELING

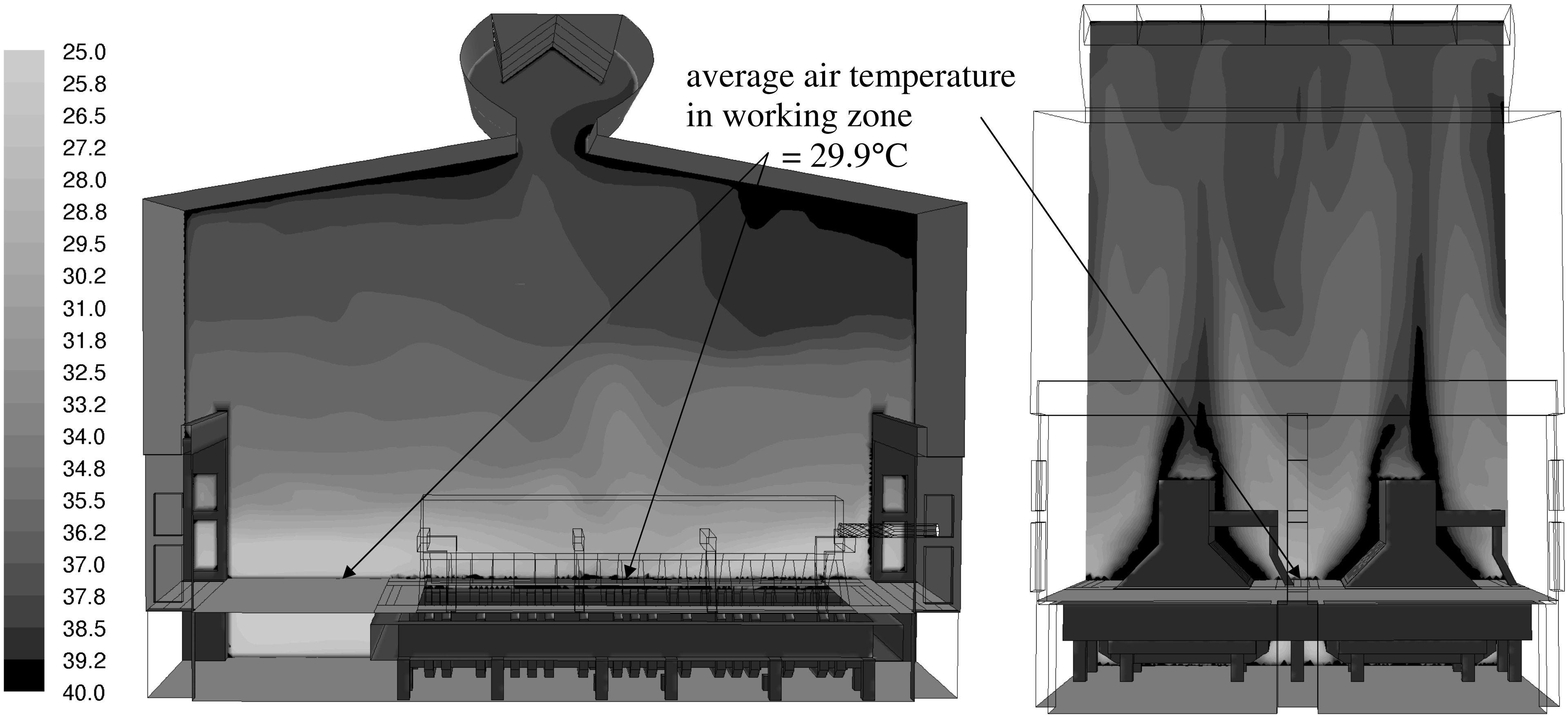

Air temperature (°C) through working zone during summer

THE IMPORTANCE OF ISO TESTING OF MATERIALS USED IN THE PRIMARY ALUMINIUM INDUSTRY

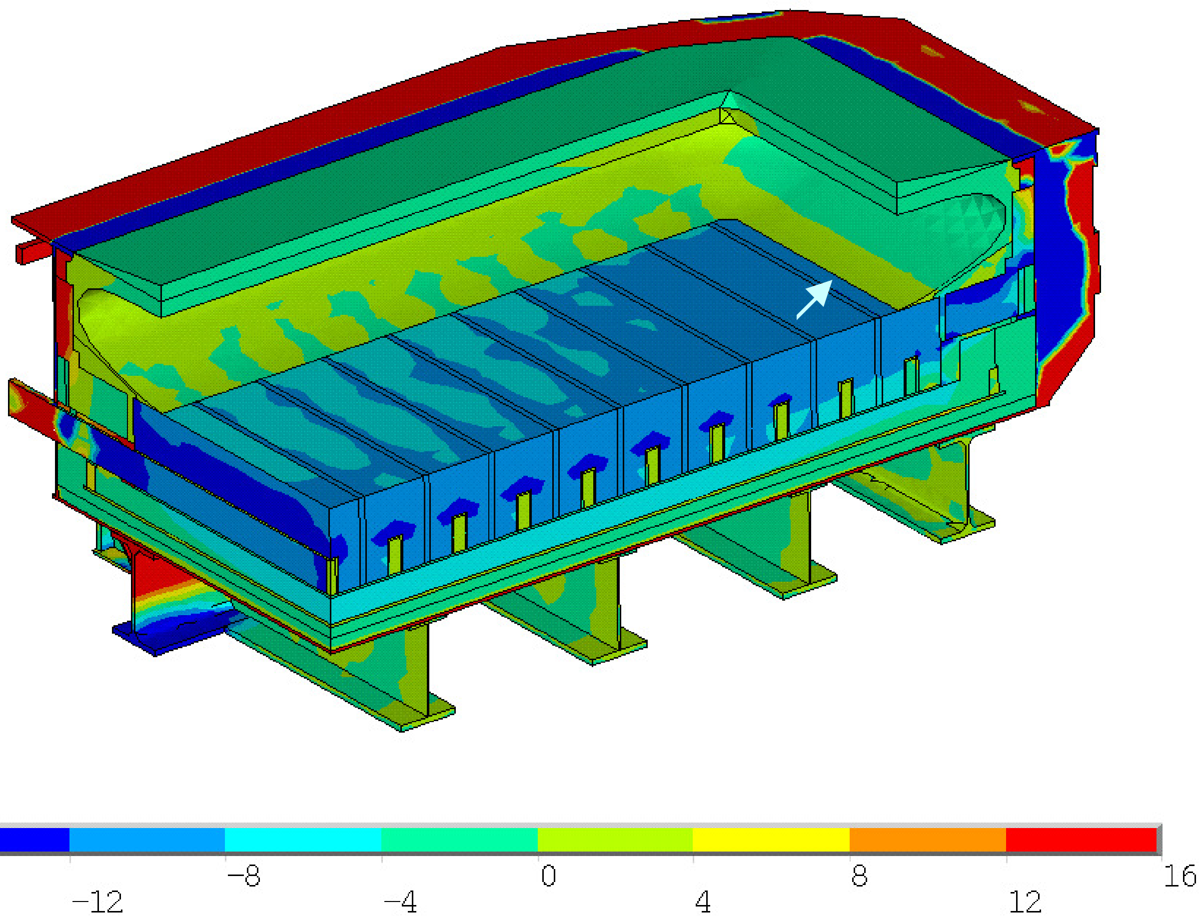

X-direction stress with thermal and sodium expansion, 400 days after start up (MPa)

INTENSIFICATION OF THE PROSSES IN 300 KA PRE-BAKED ANODE CELLS

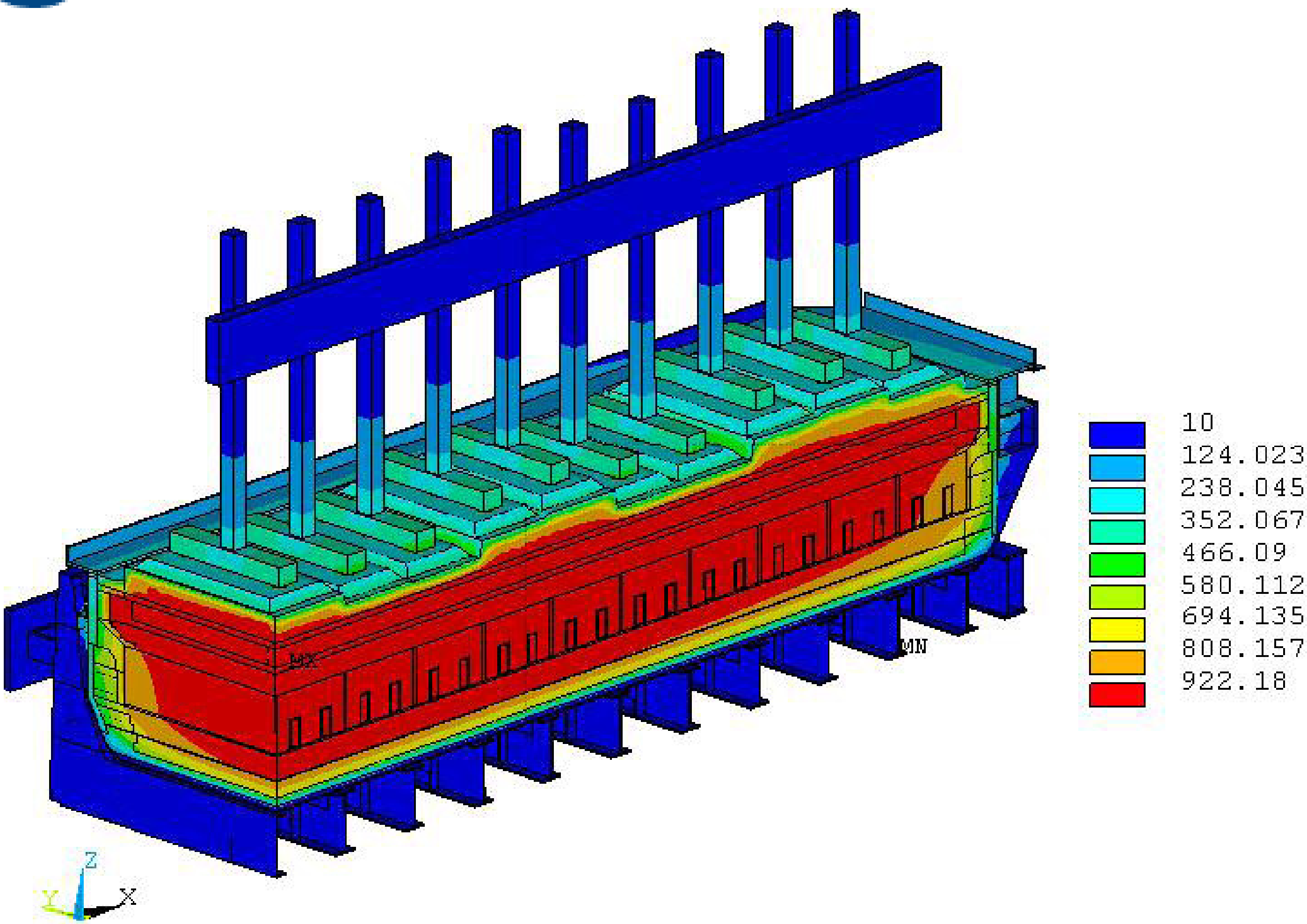

OA-300MI cell temperature field

MODELING THE BUBBLE DRIVEN FLOW IN THE ELECTROLYTE AS A TOOL FOR SLOTTED ANODE DESIGN IMPROVEMENT

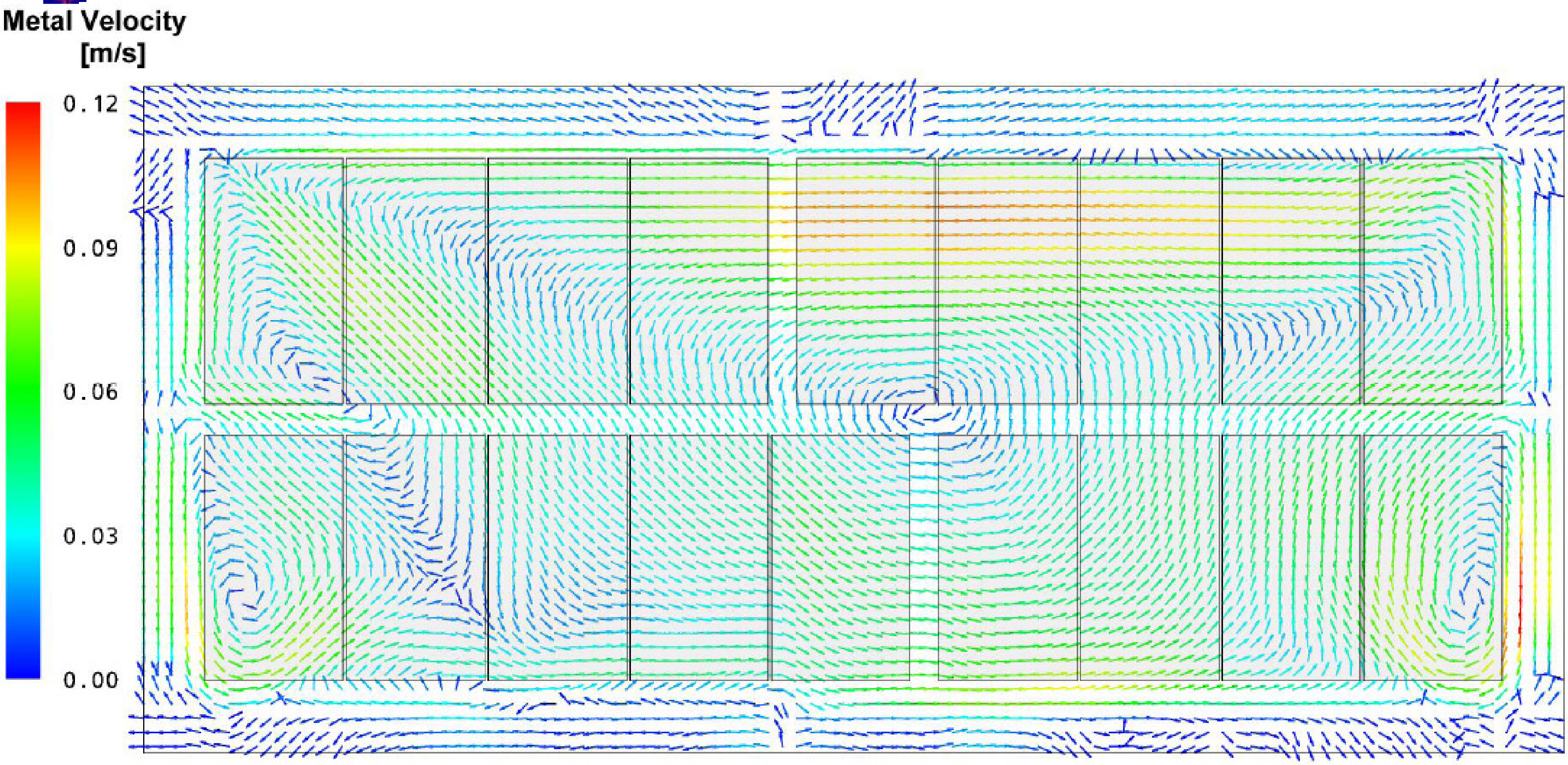

Metal velocity at the bath-metal interface for the fullpot model.

MODELING THE BUBBLE DRIVEN FLOW IN THE ELECTROLYTE AS A TOOL FOR SLOTTED ANODE DESIGN IMPROVEMENT

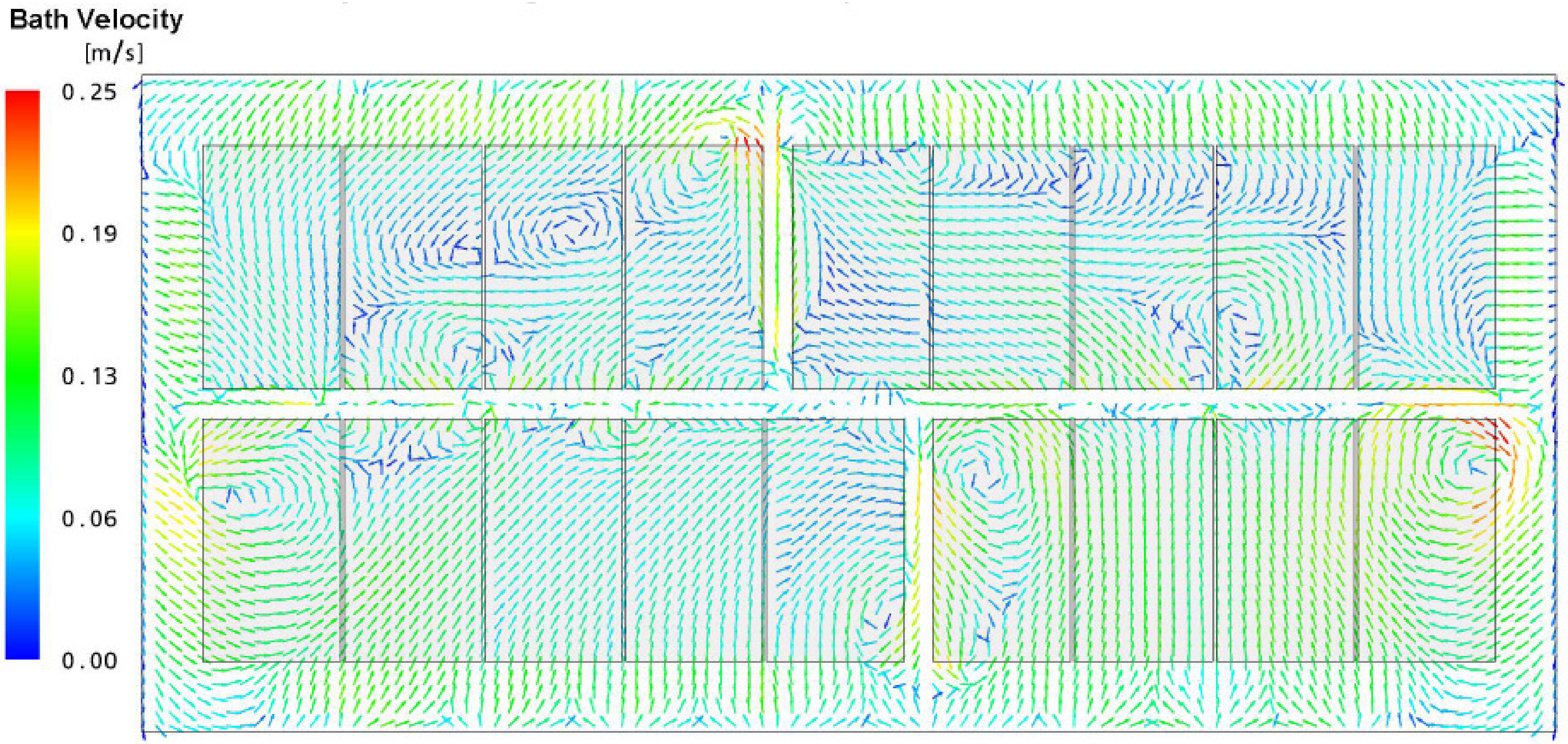

Full pot model bath velocity with MHD without slots

SIMULATION OF CELL THERMOELECTRIC FIELD WITH CONSIDERATION OF ELECTROCHEMICAL PROCESSES

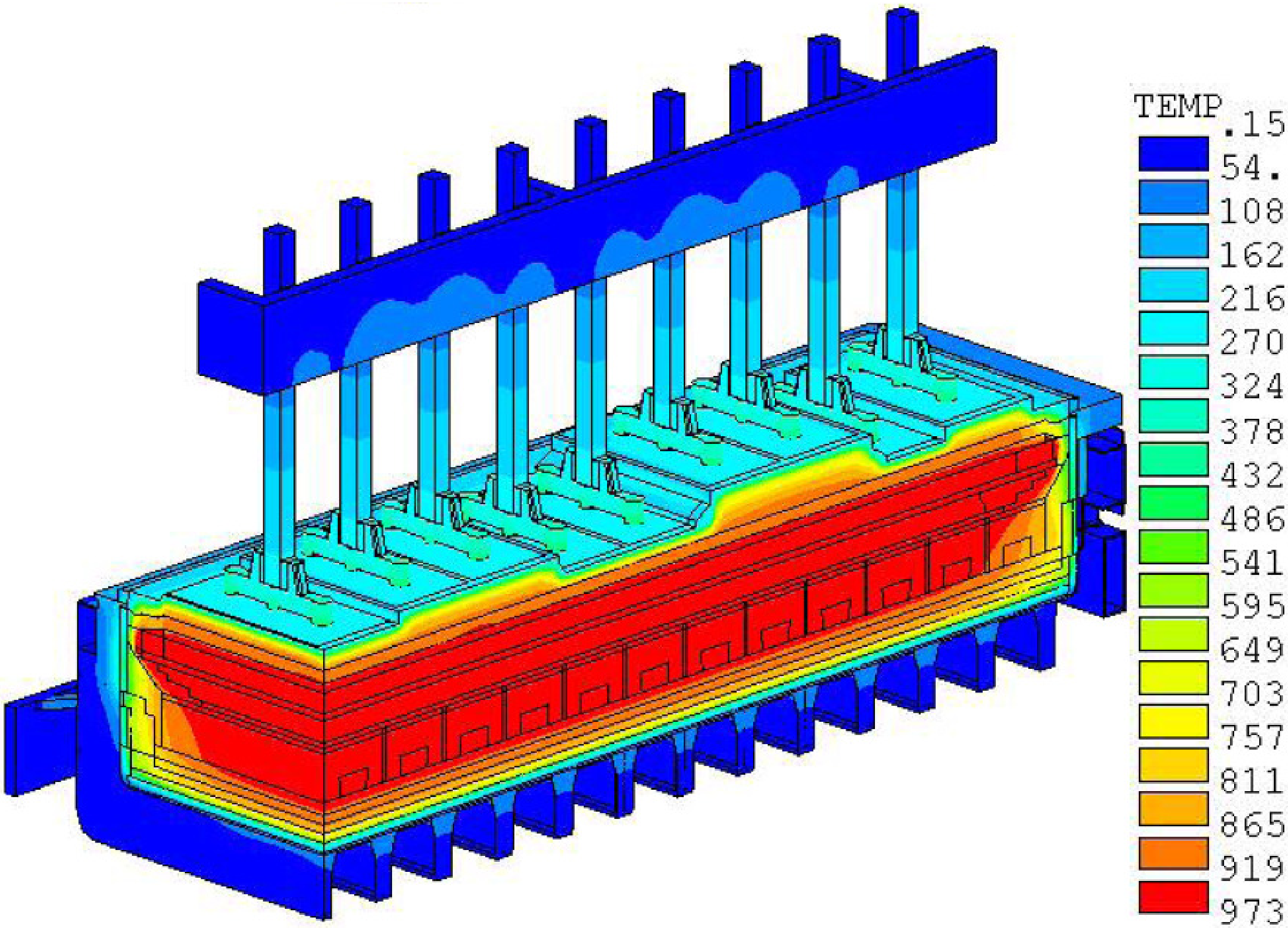

Potential distribution and temperature field of the cell

THE FECRI APPROACH AND THE LATEST DEVELOPMENTS IN THE AP3X TECHNOLOGY

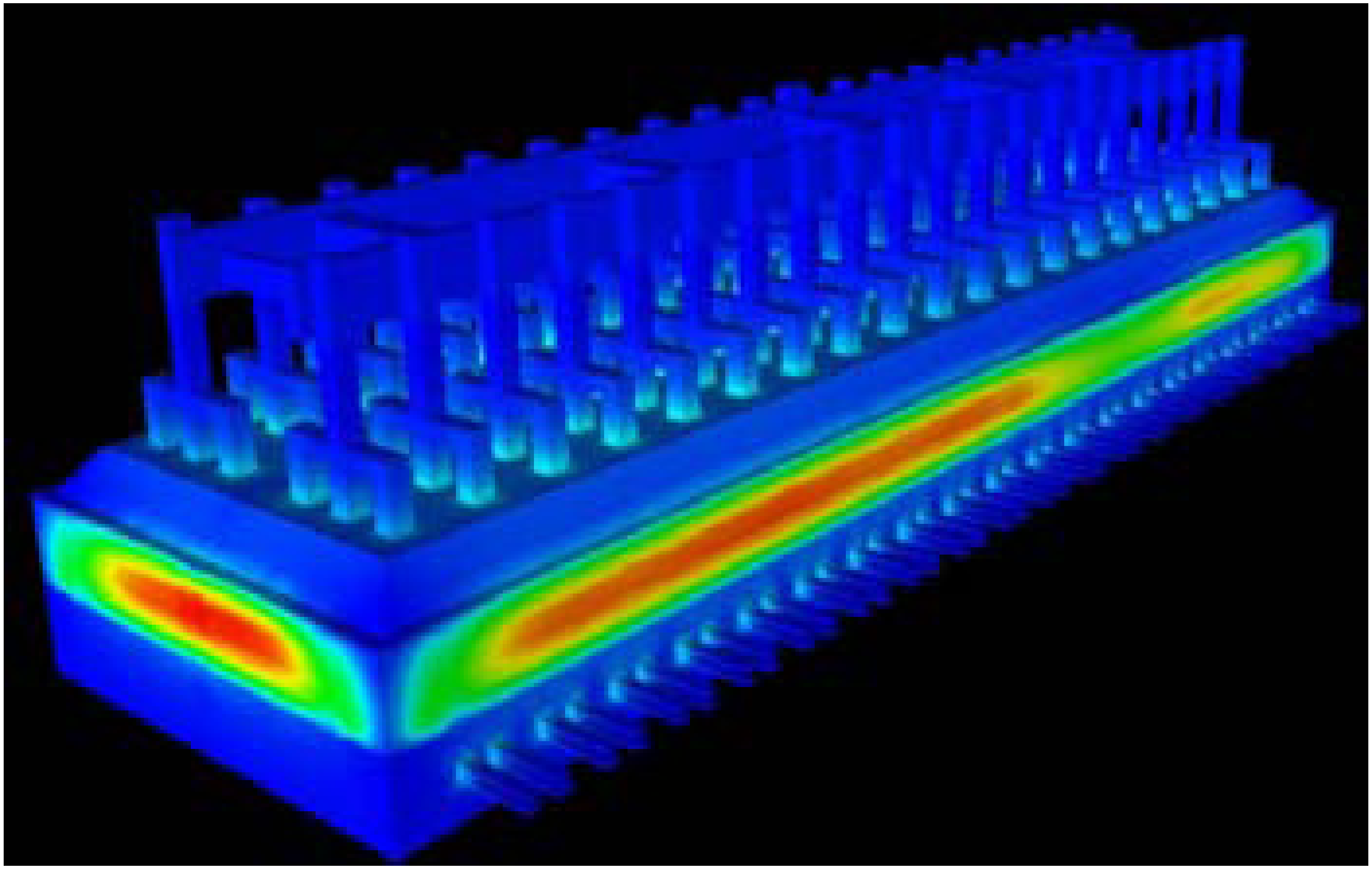

Part of the output of the TE/MHD model, showing the heat flux field

THE FECRI APPROACH AND THE LATEST DEVELOPMENTS IN THE AP3X TECHNOLOGY

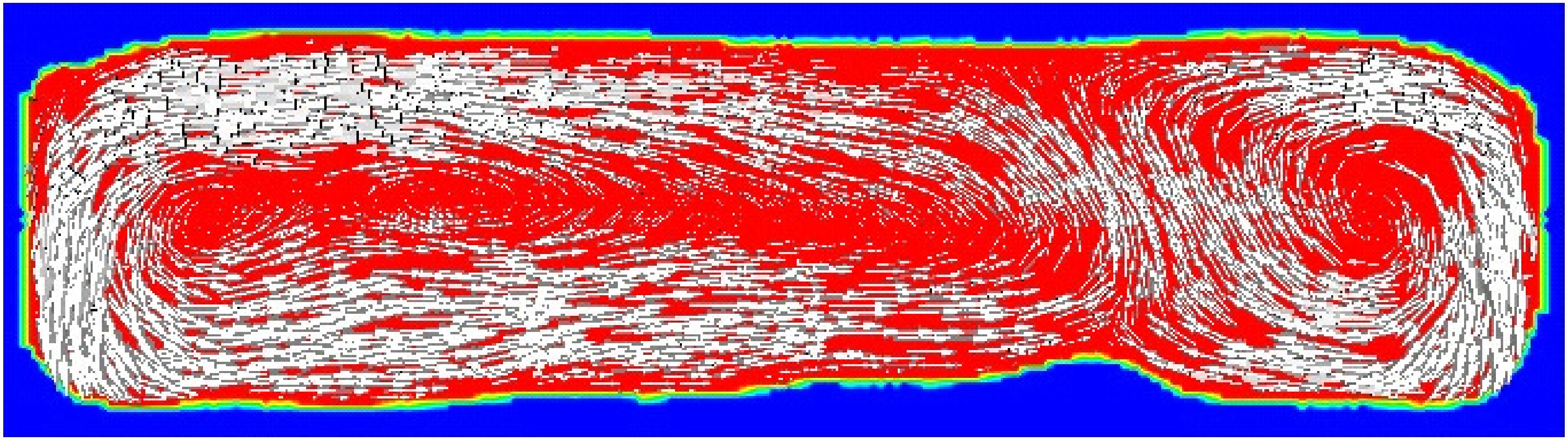

Part of the output of the TE/MHD model, showing the velocity field (in red and grey) with the ledge (in blue).

The Alcan's P155 Smelters now Operating at 195 kA
A Successful Assets Optimization Strategy

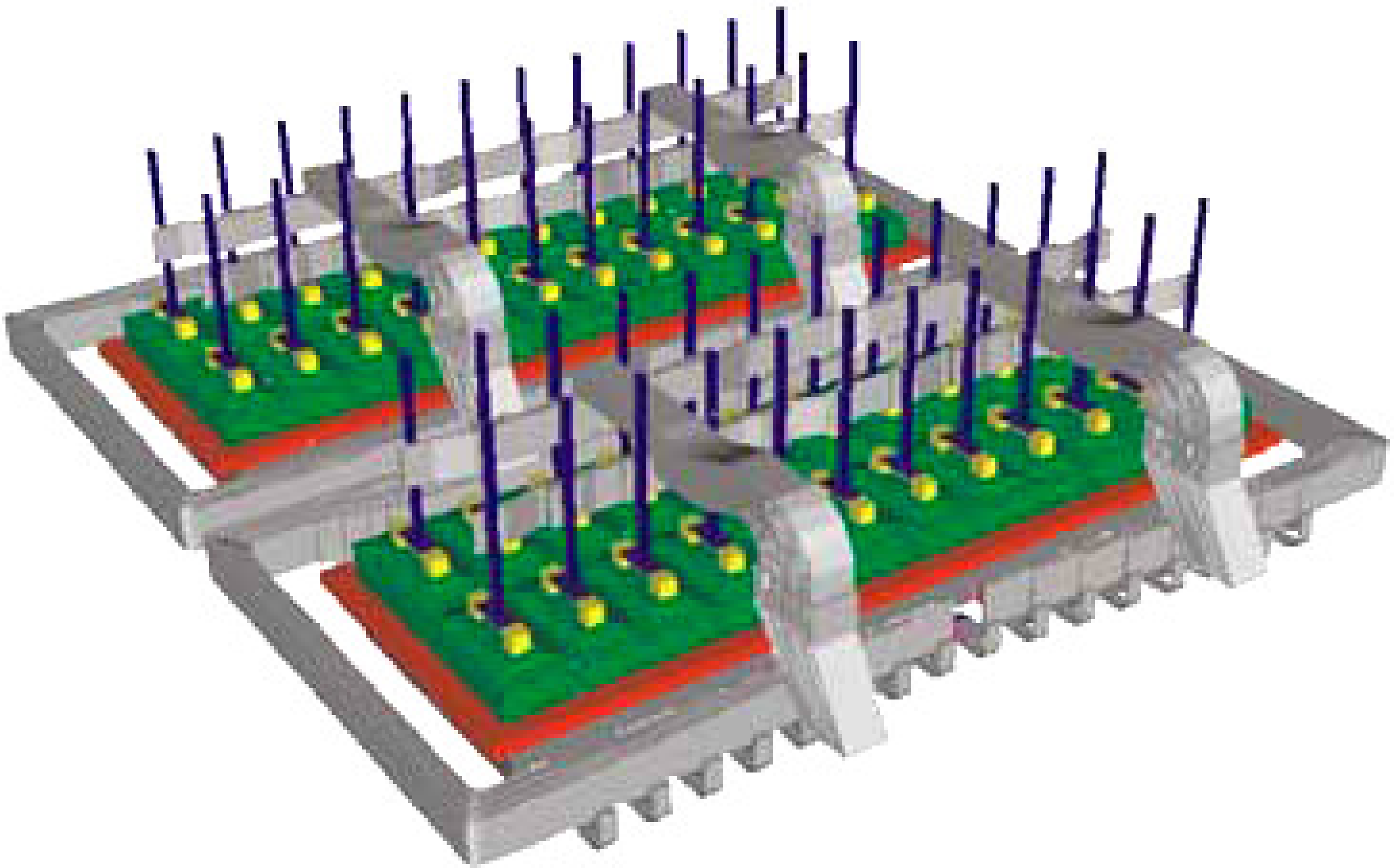

Full MHD cell geometry – P155 technology

March 9-13, 2008, New Orleans, LA

SHENYANG ALUMINUM&MAGNESIUM ENGINEERING&RESEARCH INSTITUTE

THE CONTINUOUS DEVELOPMENT OF SAMI's SY300 TECHNOLOGY

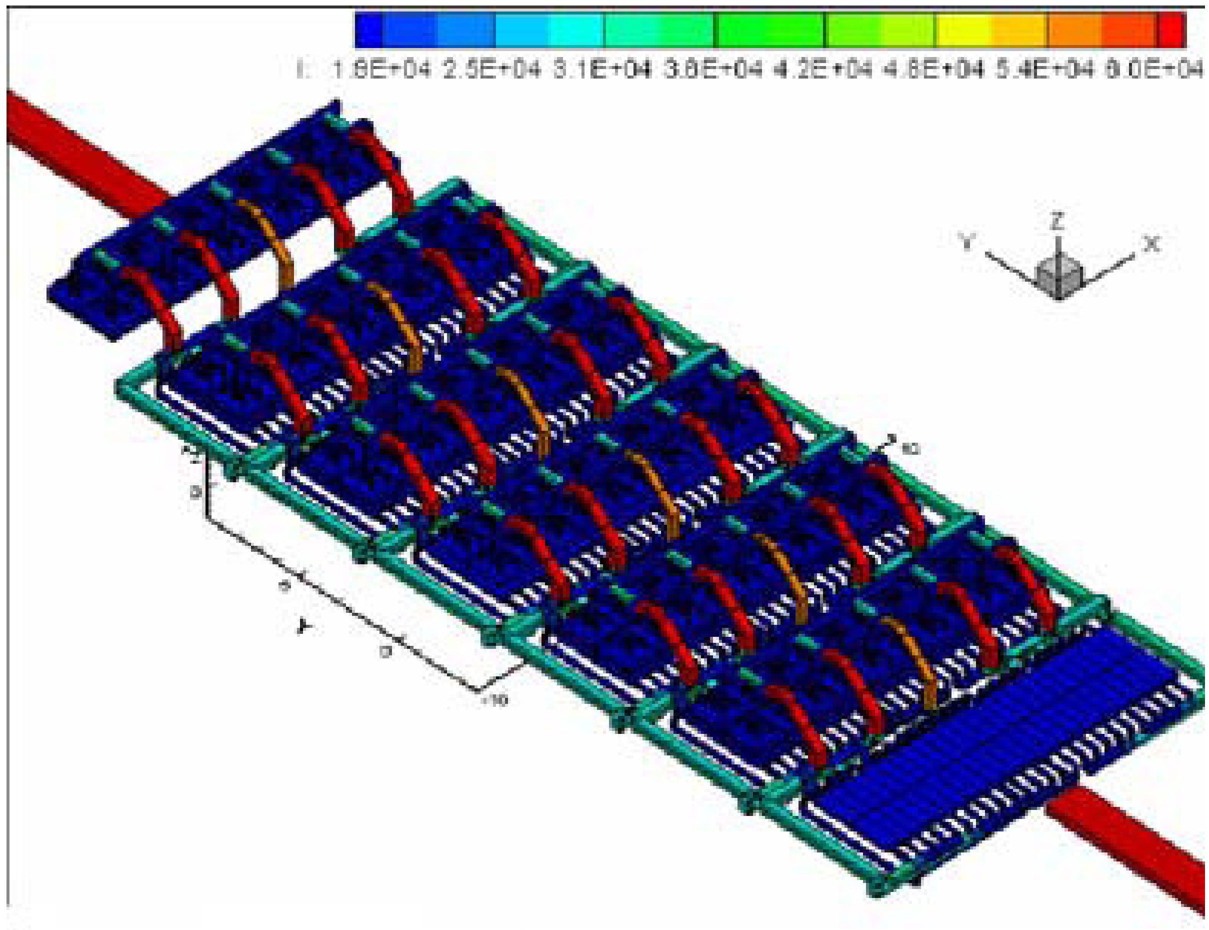

Magneto-Hydrodynamic model

March 9-13, 2008, New Orleans, LA

THE CONTINUOUS DEVELOPMENT OF SAMI's SY300 TECHNOLOGY

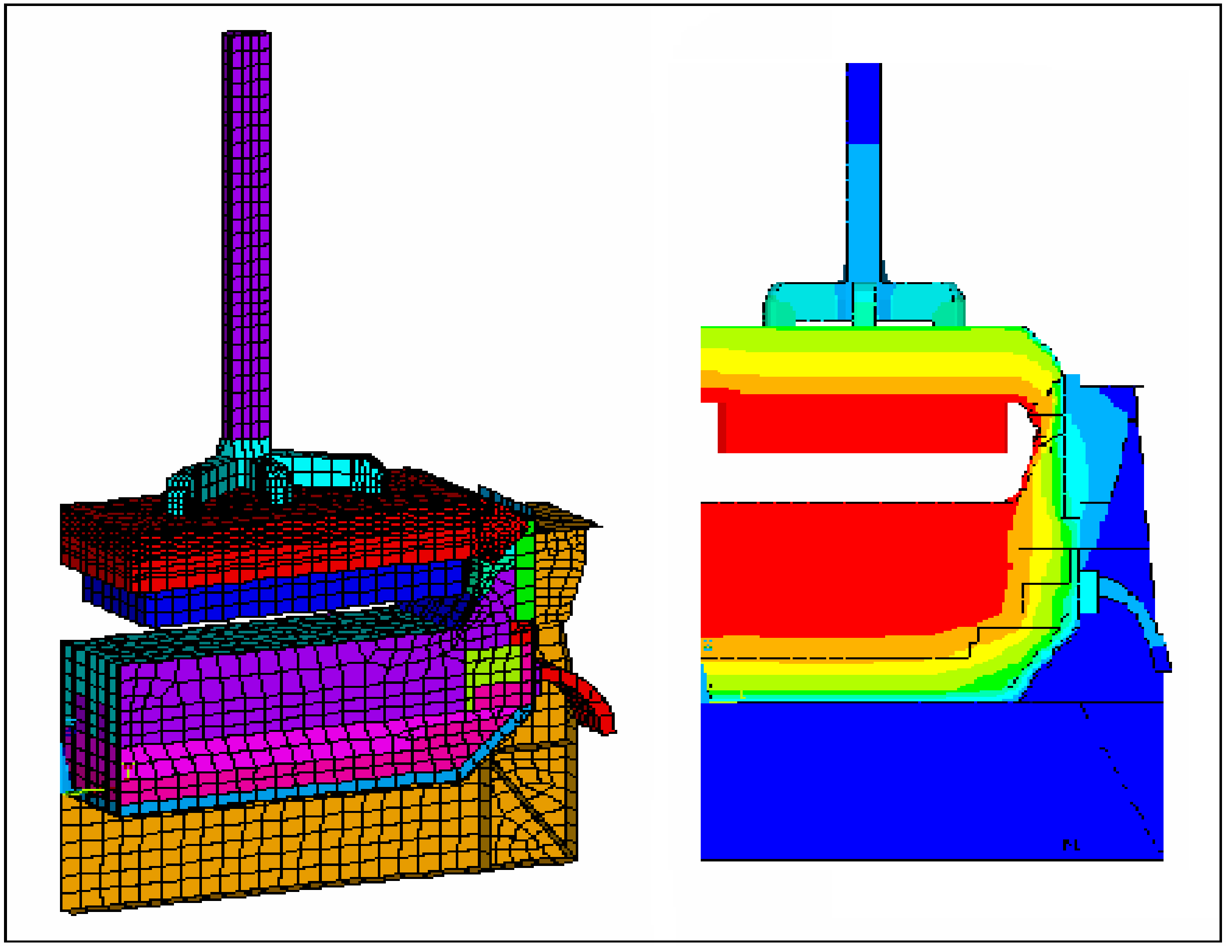

Thermo-Electric model

SHENYANG ALUMINUM&MAGNESIUM ENGINEERING&RESEARCH INSTITUTE

THE CONTINUOUS DEVELOPMENT OF SAMI's SY300 TECHNOLOGY

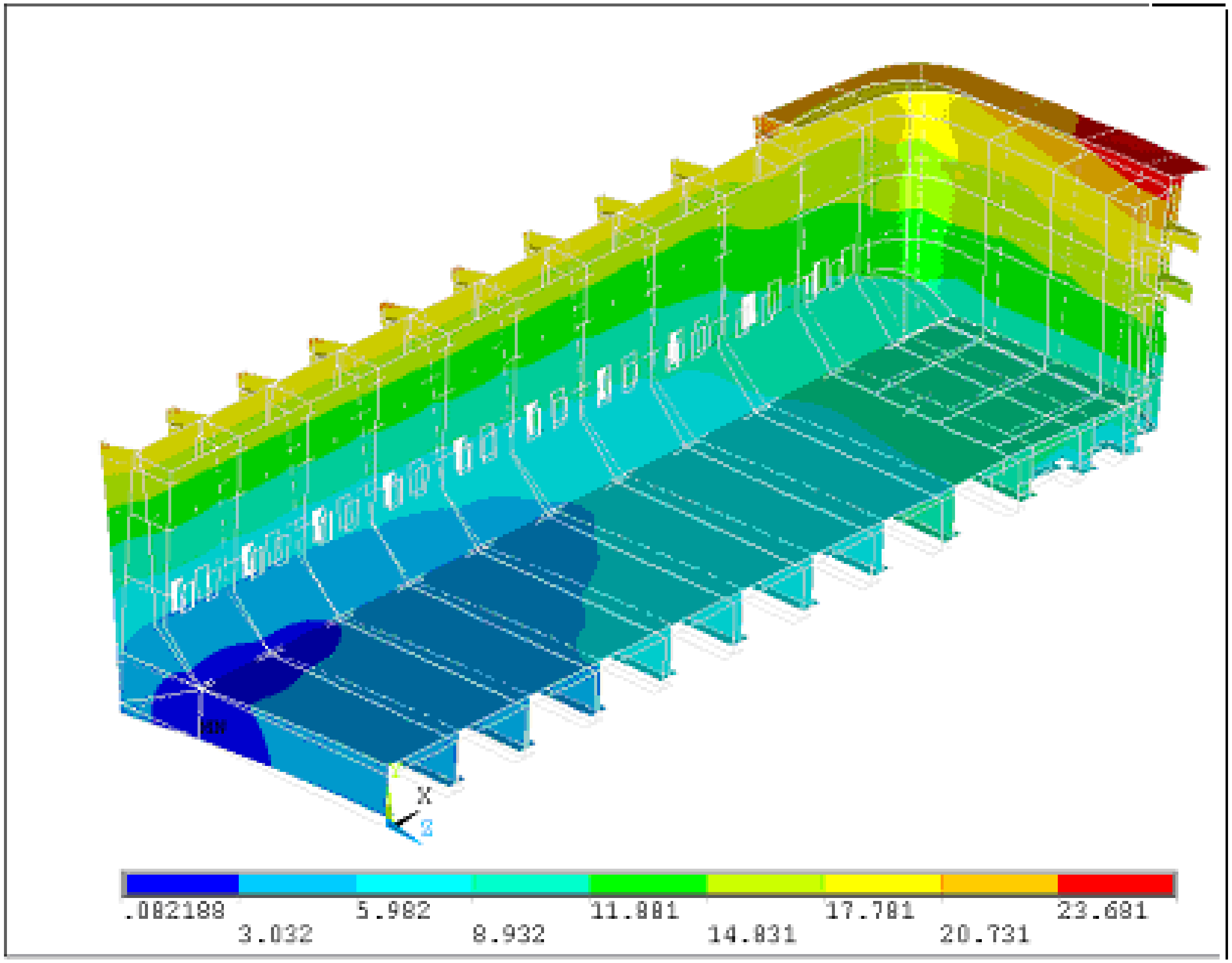

Thermo-Stress model

THE CONTINUOUS DEVELOPMENT OF SAMI's SY300 TECHNOLOGY

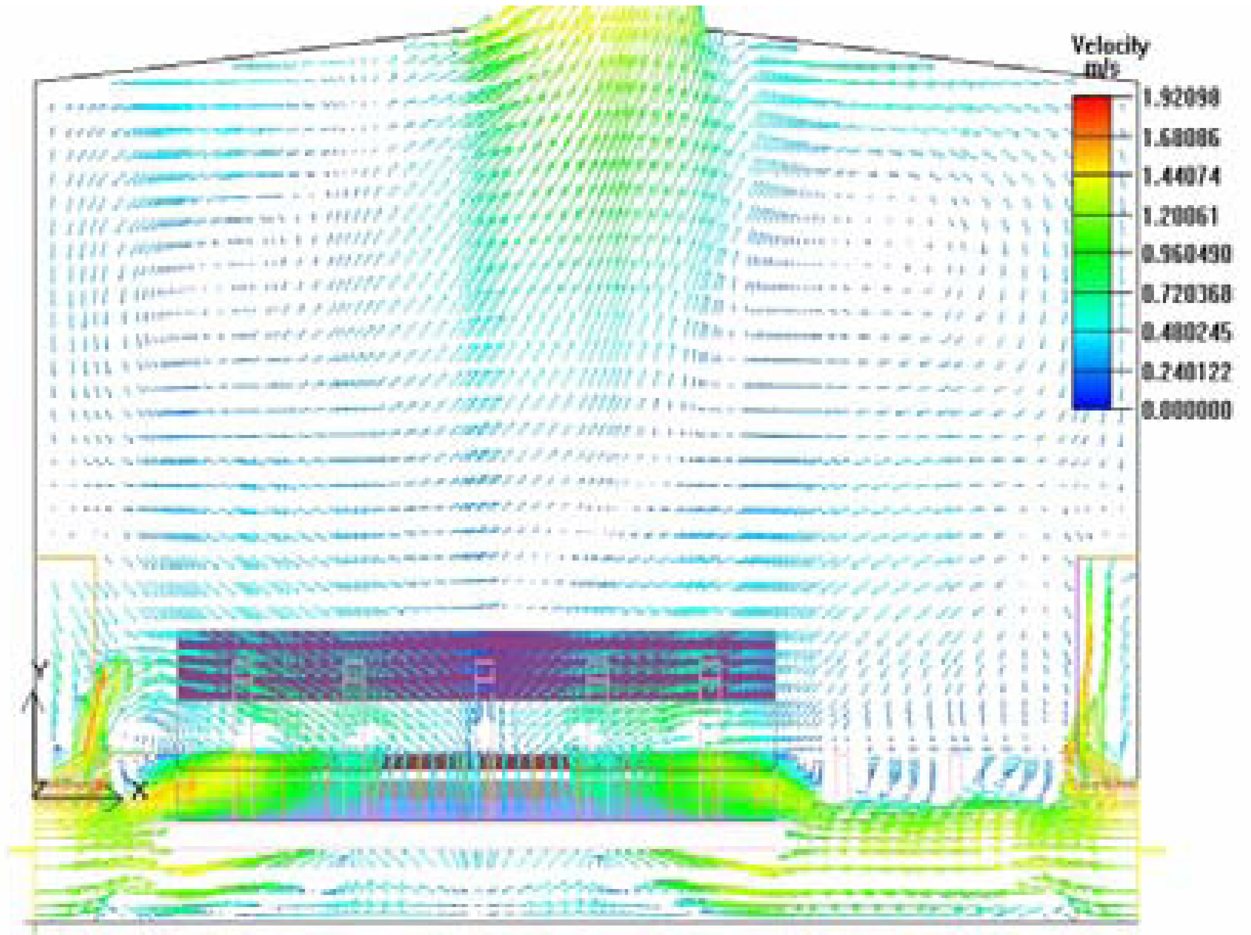

Potroom ventilation model

SHENYANG ALUMINUM&MAGNESIUM ENGINEERING&RESEARCH INSTITUTE

THE CONTINUOUS DEVELOPMENT OF SAMI's SY300 TECHNOLOGY

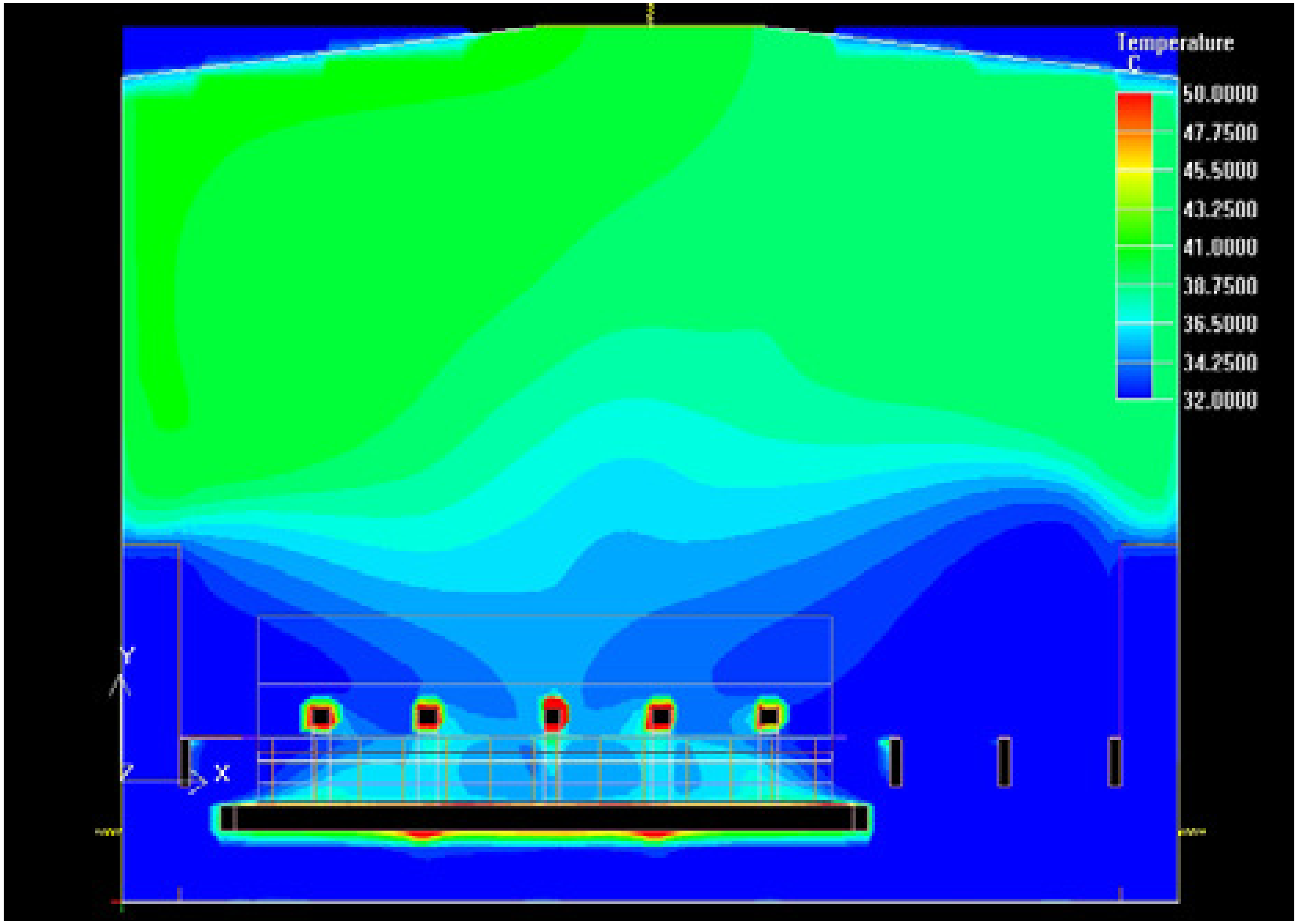

Temperature distribution for a new generation SY300 potroom.

March 9-13, 2008, New Orleans, LA

COMPARISON OF VARIOUS METHODS FOR MODELING THE METAL-BATH INTERFACE

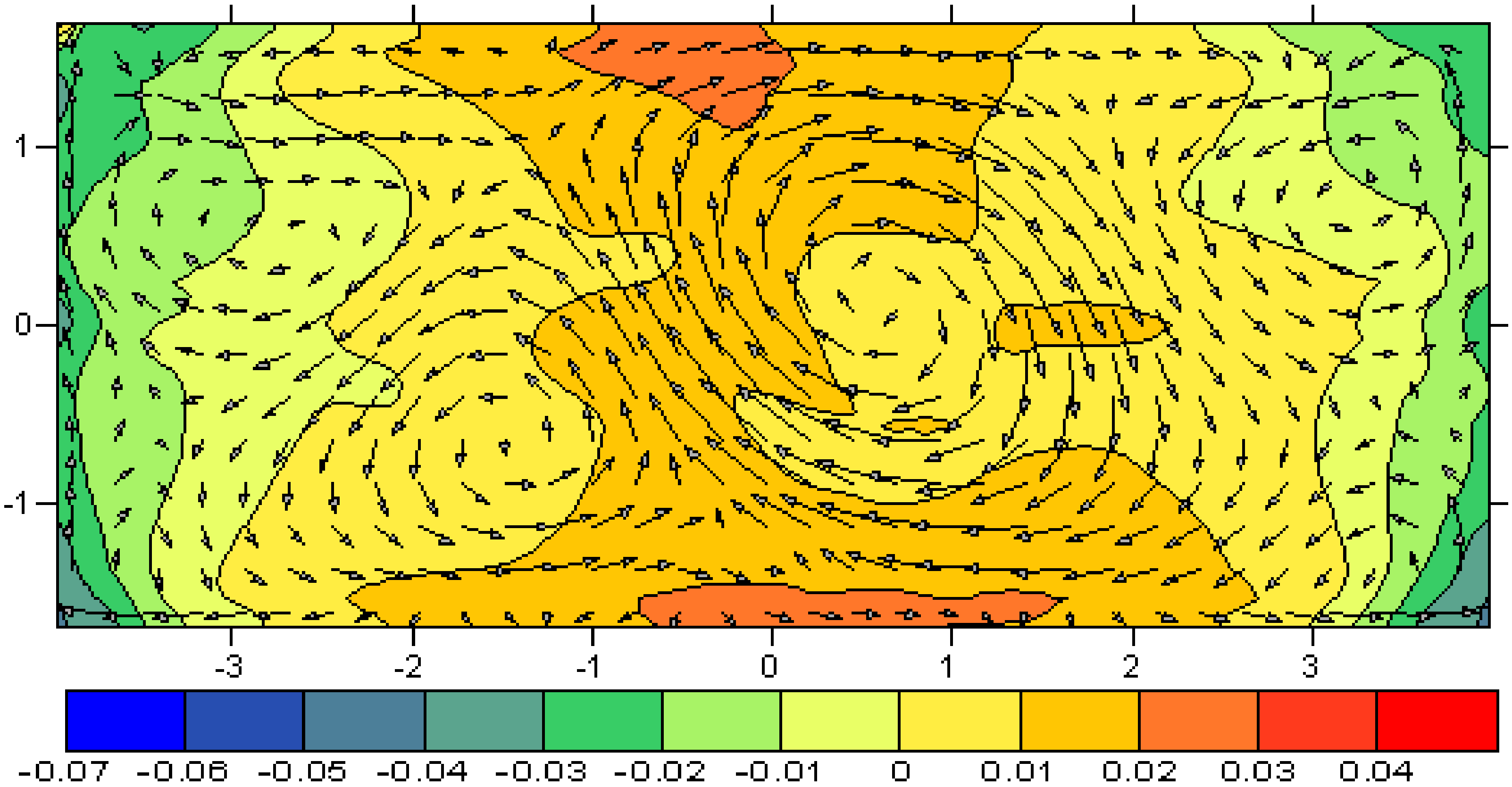

Interface deformation (m) obtained by the 3-phase k-ε turbulence Ansys CFX model

APPLICATION OF MATHEMATICAL METHODS TO OPTIMIZE ALUMINIUM PRODUCTION IN PRE-BAKED ANODE CELLS

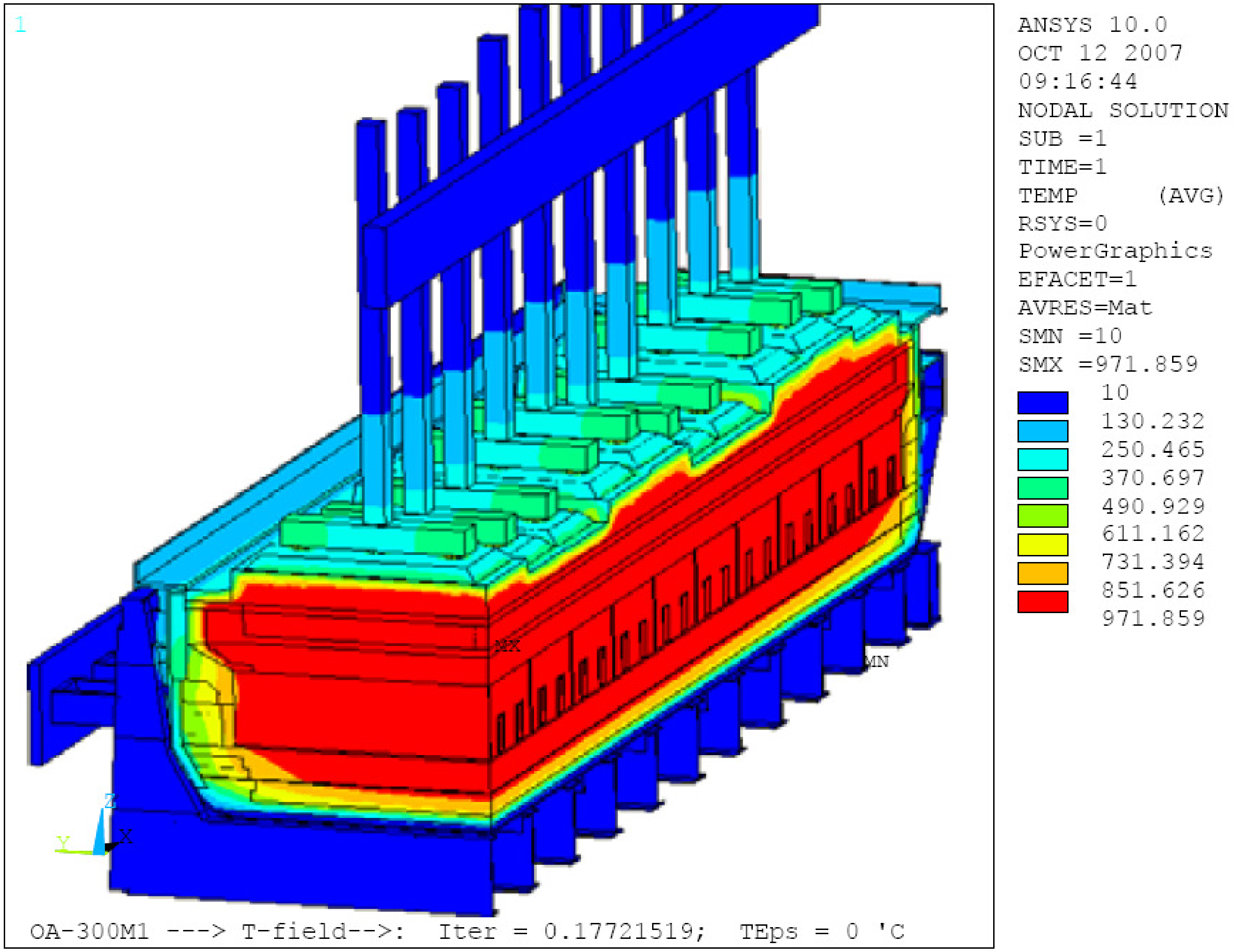

Thermal field of the OA-300M1 cell

March 9-13, 2008, New Orleans, LA

2007 Weakly coupled thermo-electro-mechanical model and magneto-hydro-dynamic full cell and external busbar model

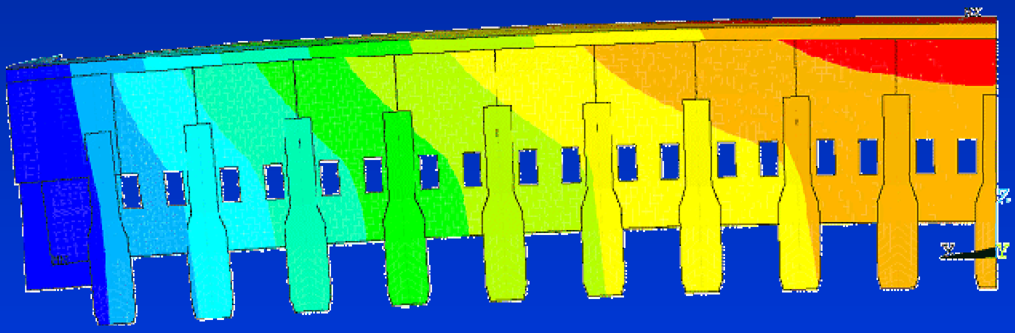

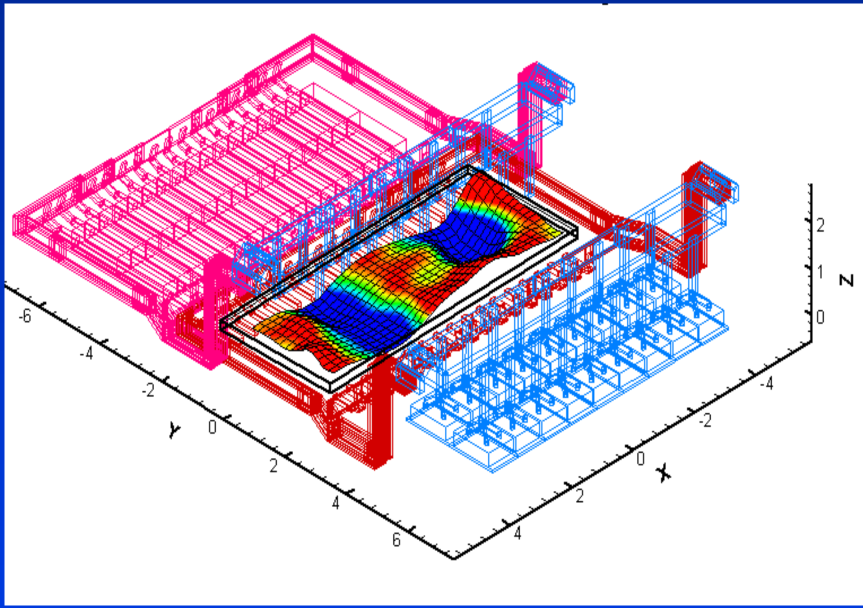

Impact of Vertical Potshell Deformation on MHD Cell Stability

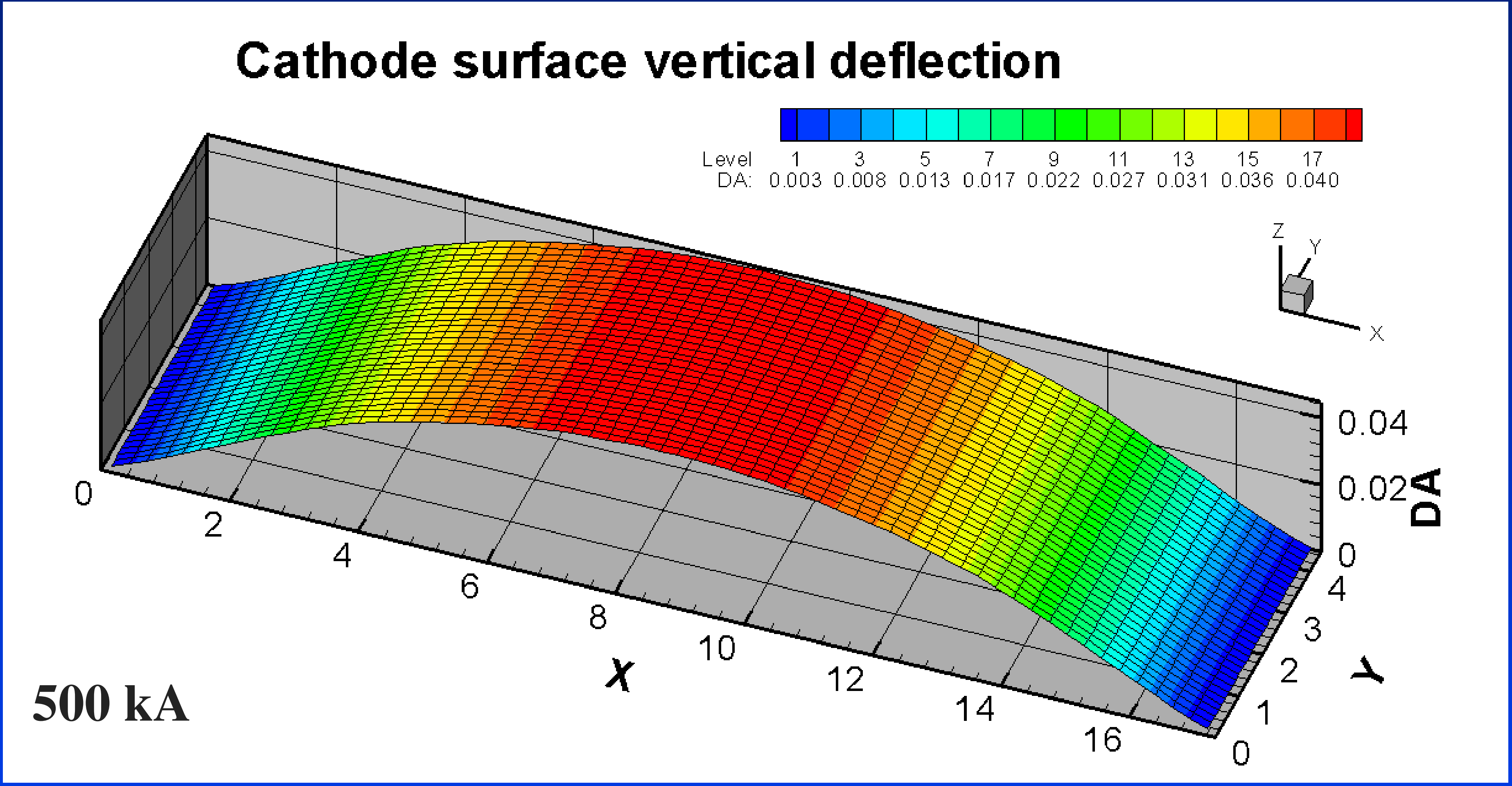

Metal Pad Bottom Profile Input: Case 2

GENISIM

Impact of Vertical Potshell Deformation on MHD Cell Stability

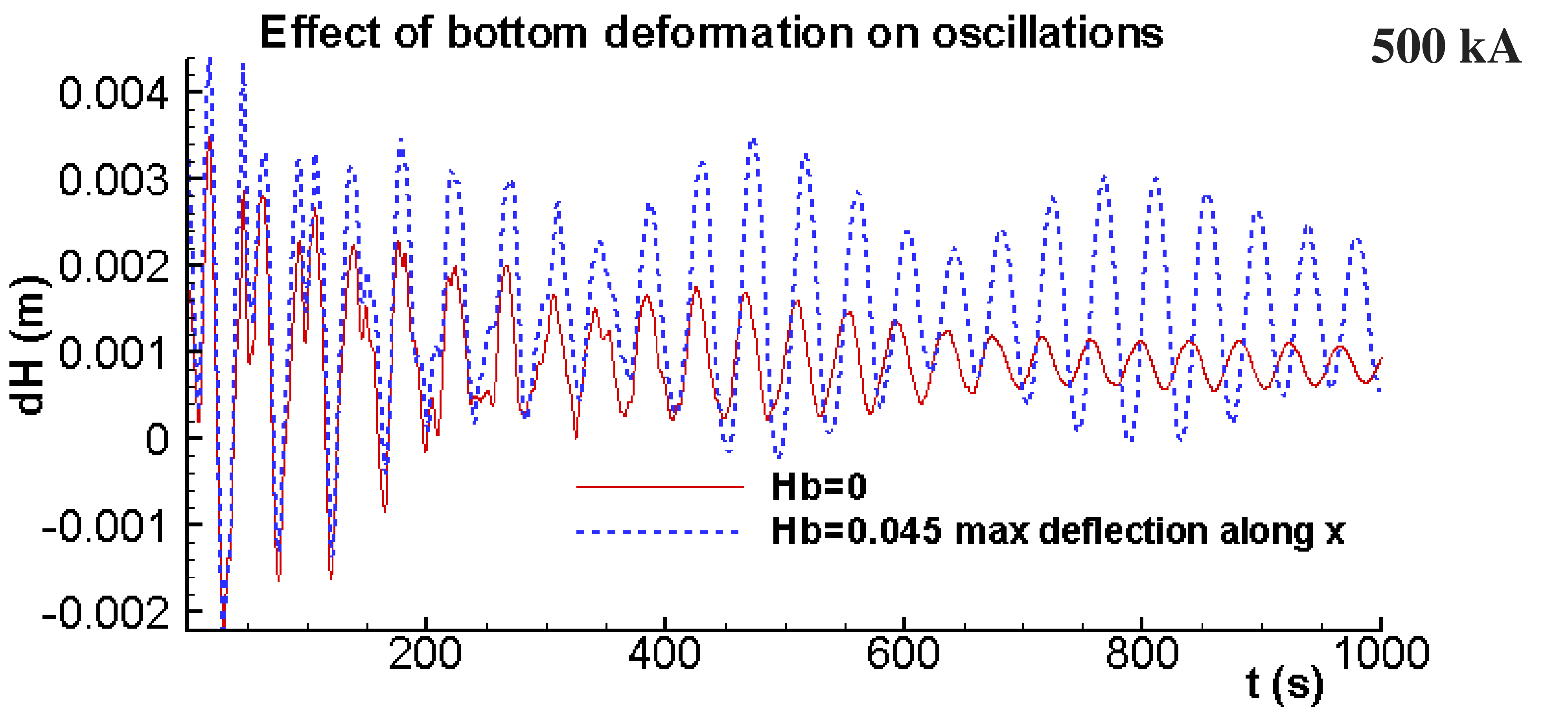

Comparison of the MHD-VALDIS Results With and Without up to 4.5 cm of Vertical Displacement

GENISIM

CHALLENGES IN STUB HOLE OPTIMISATION OF CAST IRON RODDED ANODES

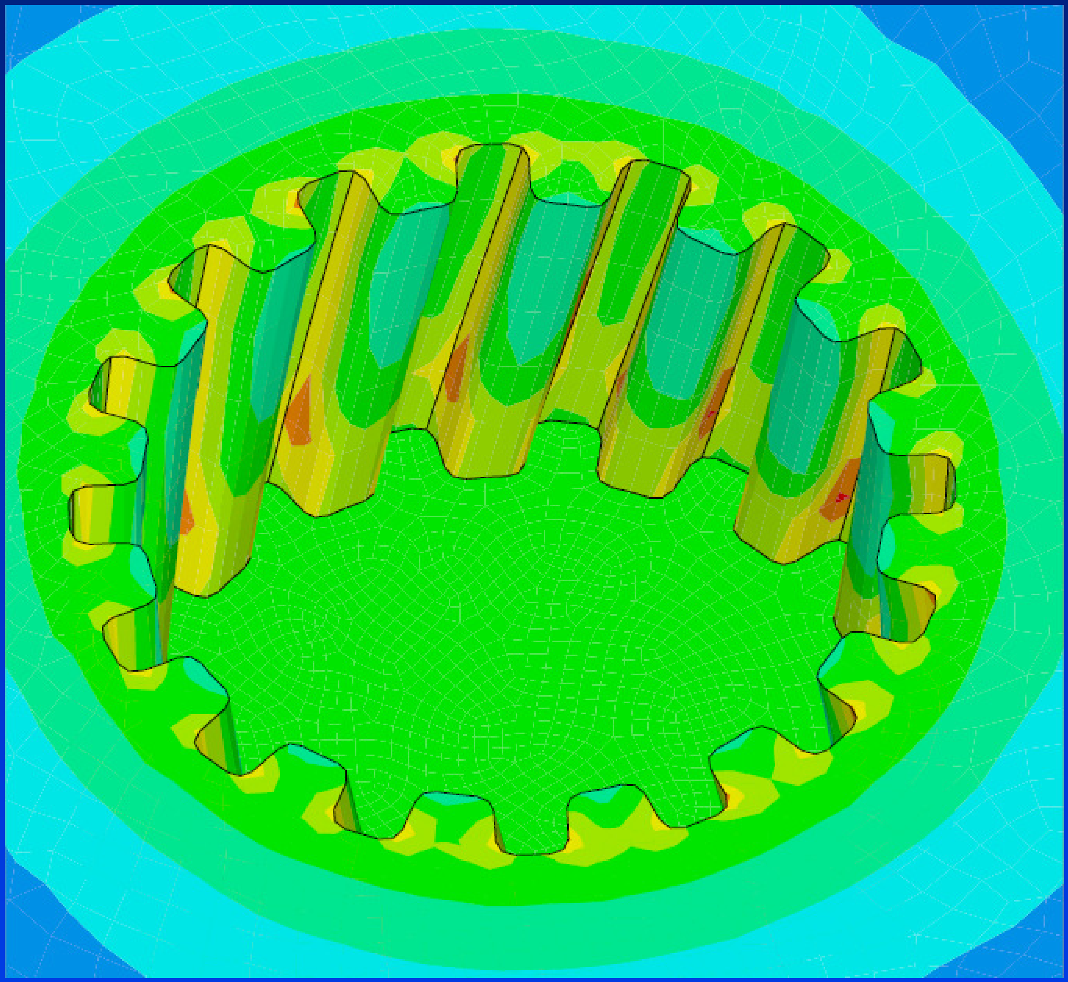

Multiphysics Contact

Surface-to-surface multiphysics contact, including the effects of thermal contact conductance, electrical contact resistance and Joule heat generation at the interface, was developed and implemented by Goulet in the in-house finite element toolbox *FESh*++ using modern Object-Oriented techniques. The use of algebraic equations to specify the material properties allows the direct implementation of the electrical contact resistance equations derived by Richard *et al*.

HEAT TRANSFER CONSIDERATIONS IN DC BUSBAR SIZING

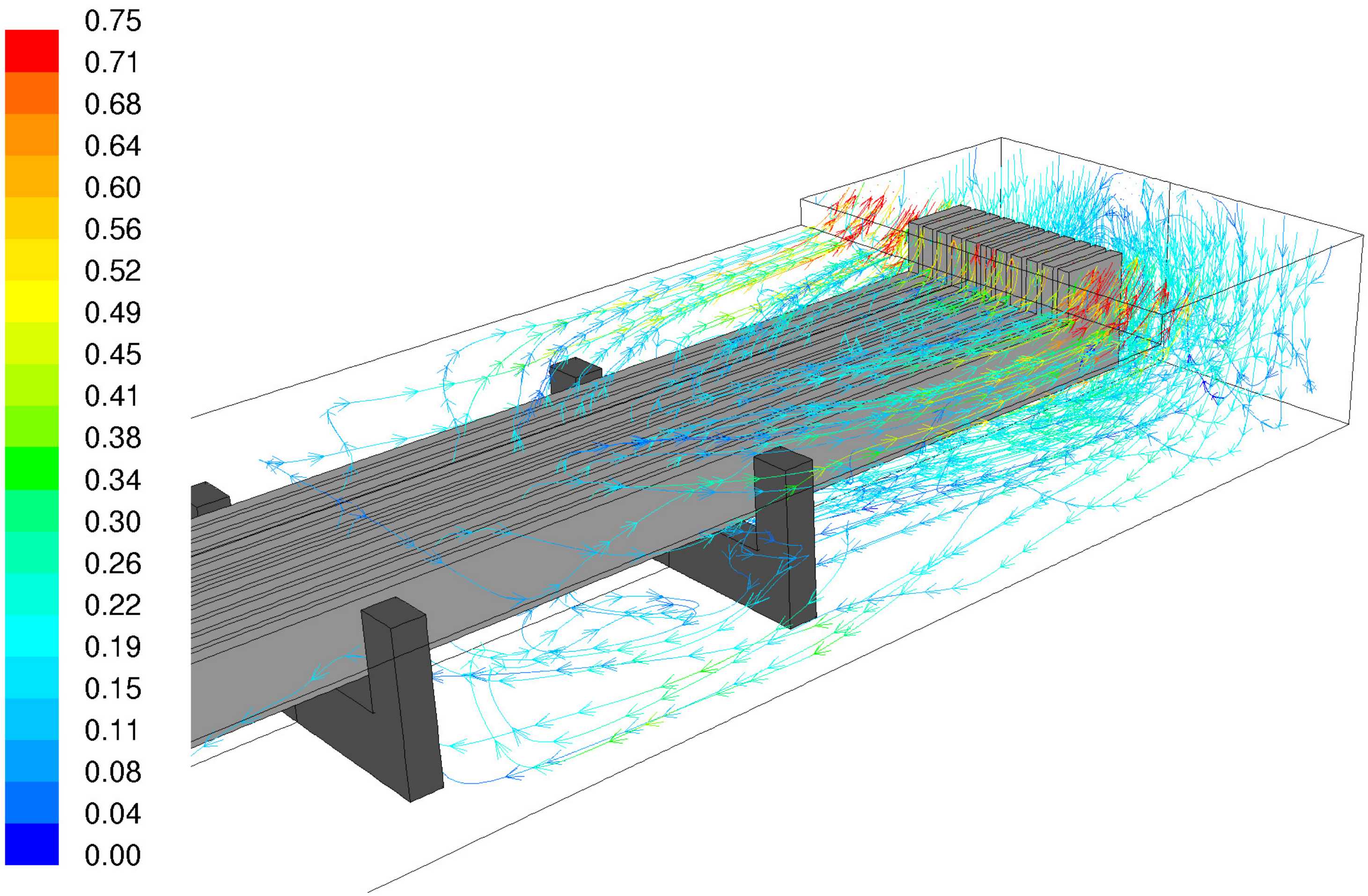

Complex 3D CFD Analysis

February 15-19, 2009, San Francisco, CA

The Impact of Cell Ventilation on the Top Heat Losses and Fugitive Emissions in an Aluminium Smelting Cell

The University of Auckland

Fugitive emissions

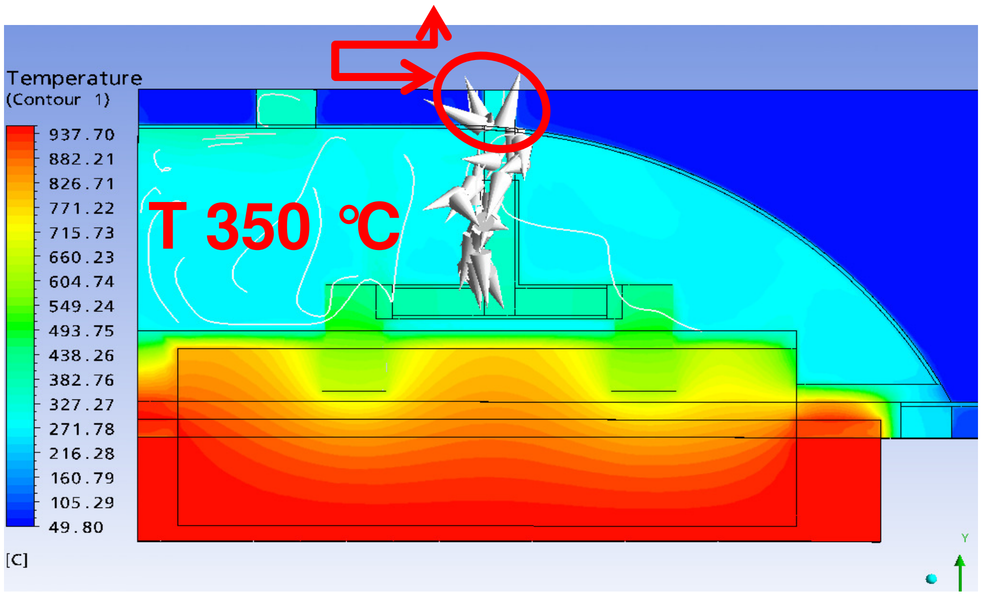

Low draught (150 Nm^3/h)

No fugitive emissions

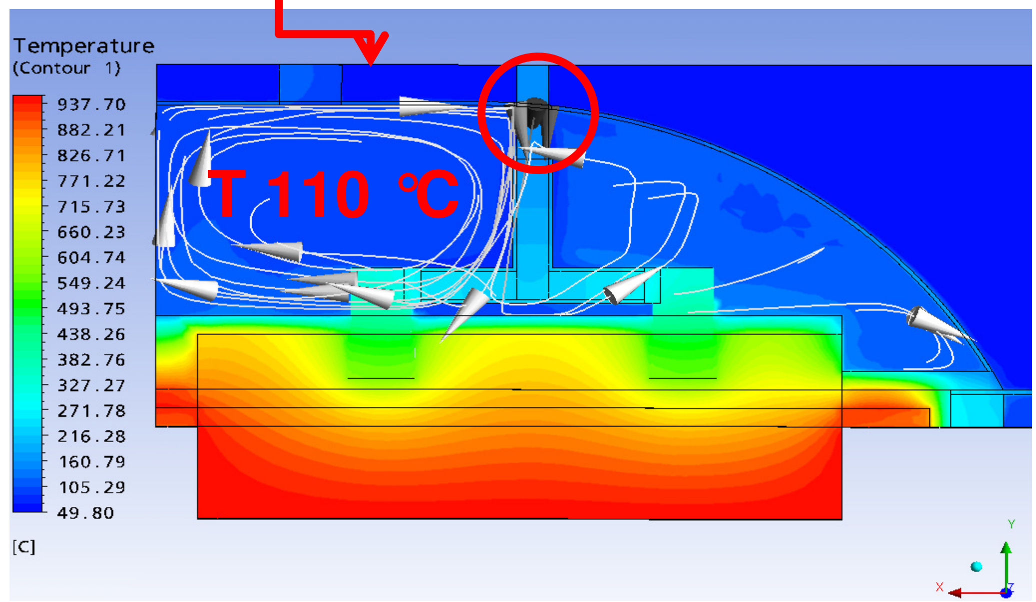

High draught (7690Nm^3/h)

cold air added to reduce T

Draught

February 15-19, 2009, San Francisco, CA

SOLUTIONS FOR THE METAL-BATH INTERFACE IN ALUMINIUM ELECTROLYSIS CELLS

no channels

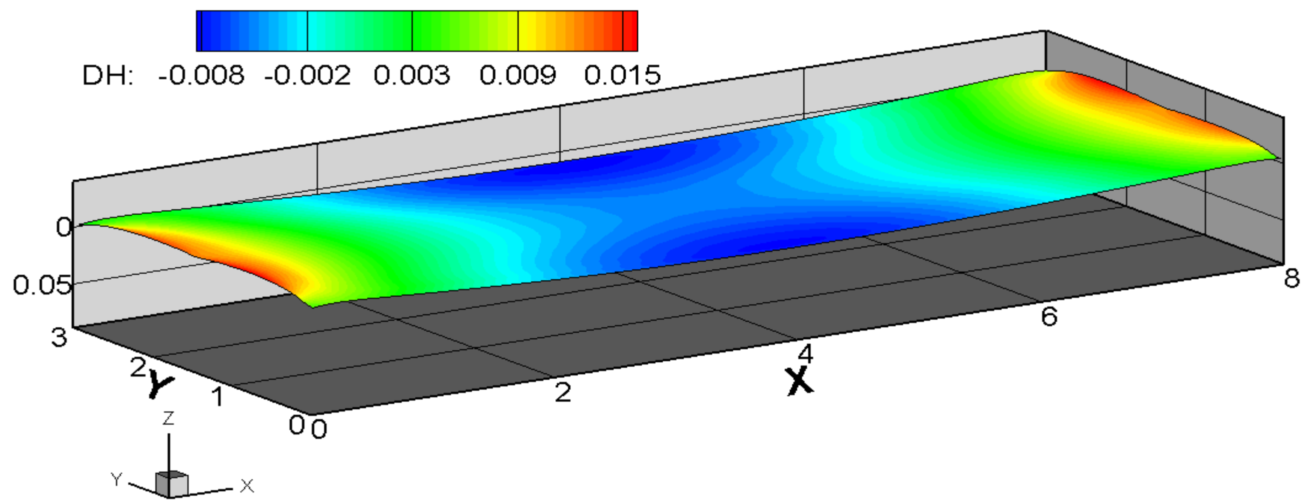

with channels

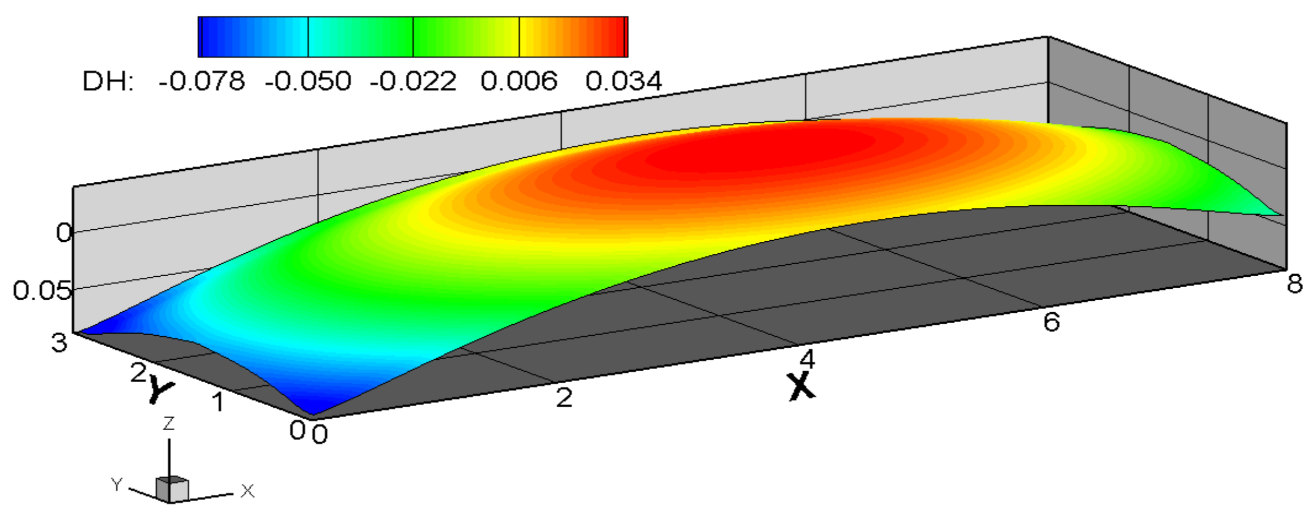

Channel effect on the interface

February 15-19, 2009, San Francisco, CA

Rio Tinto Alcan

AP50 PERFORMANCES AND NEW DEVELOPMENT

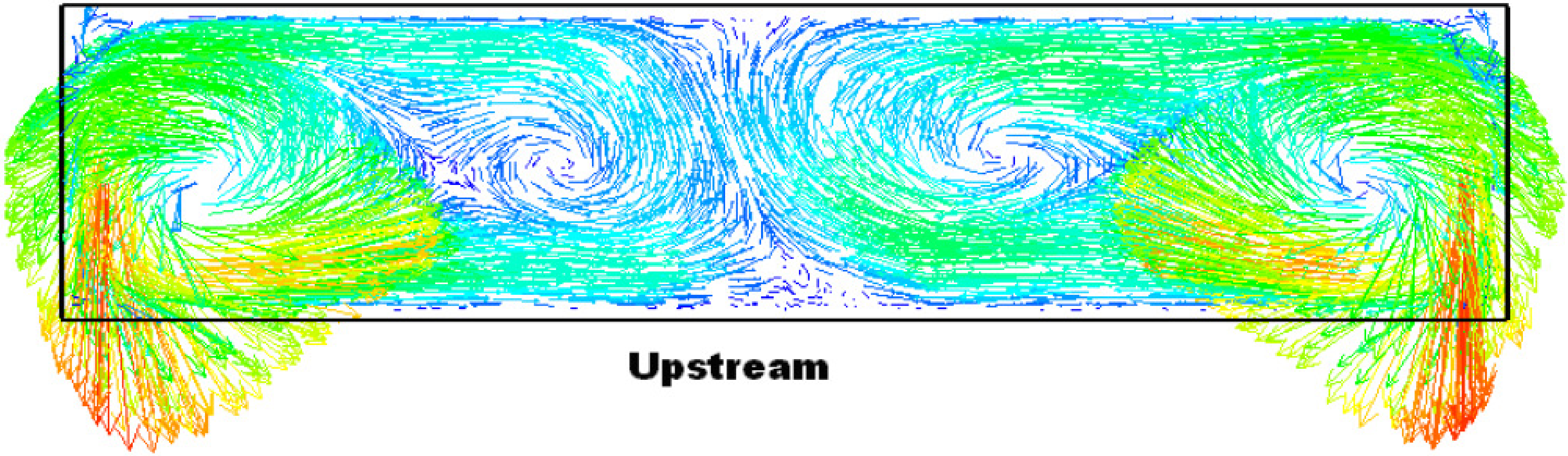

Figure 3: AP50A velocity field with ALUCELL®

AP50 PERFORMANCES AND NEW DEVELOPMENT

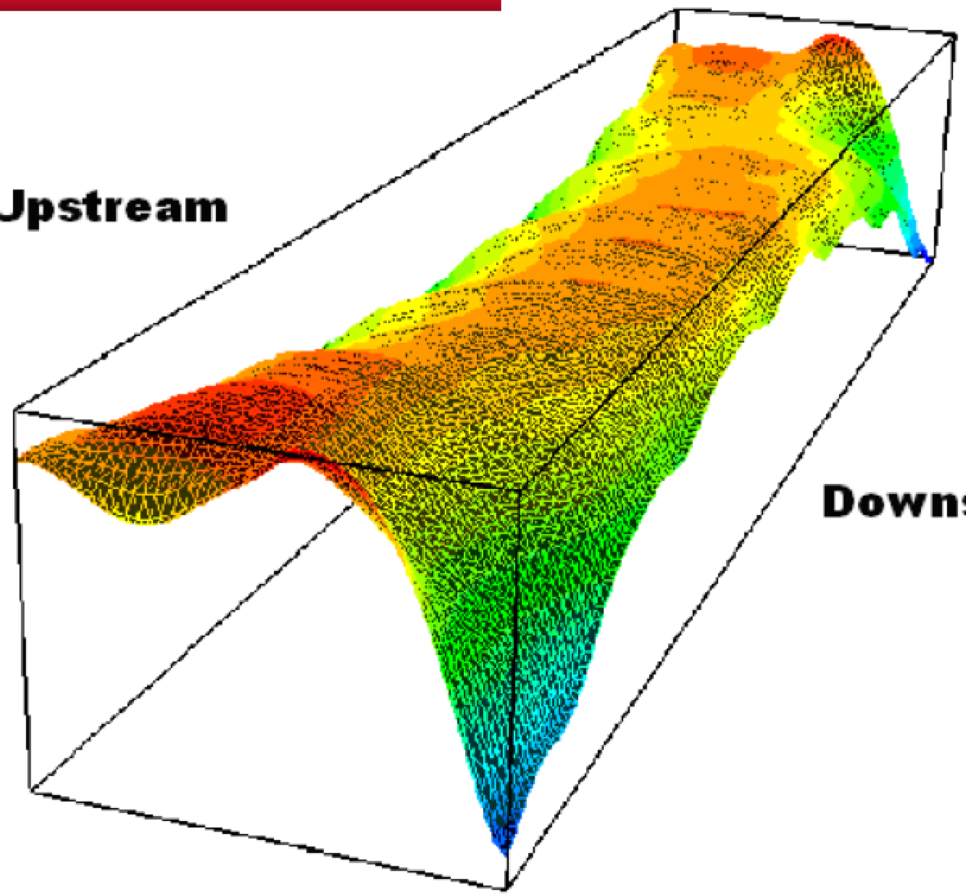

Figure 4: AP50A bath-metal interface deformation with ALUCELL®

A MODELLING APPROACH TO ESTIMATE BATH AND METAL HEAT TRANSFER COEFFICIENTS

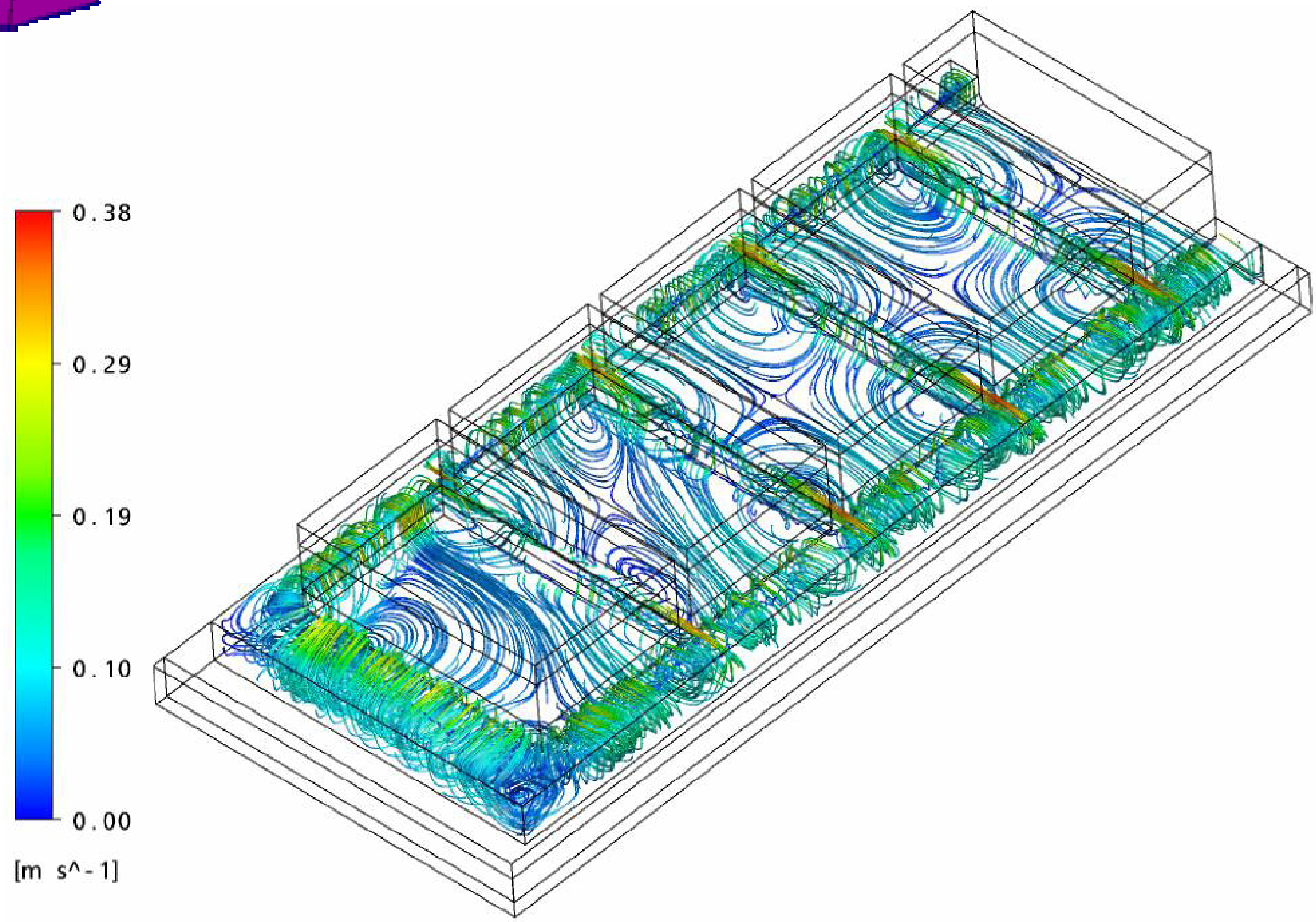

Bath bubble driven flow: general view

A MODELLING APPROACH TO ESTIMATE BATH AND METAL HEAT TRANSFER COEFFICIENTS

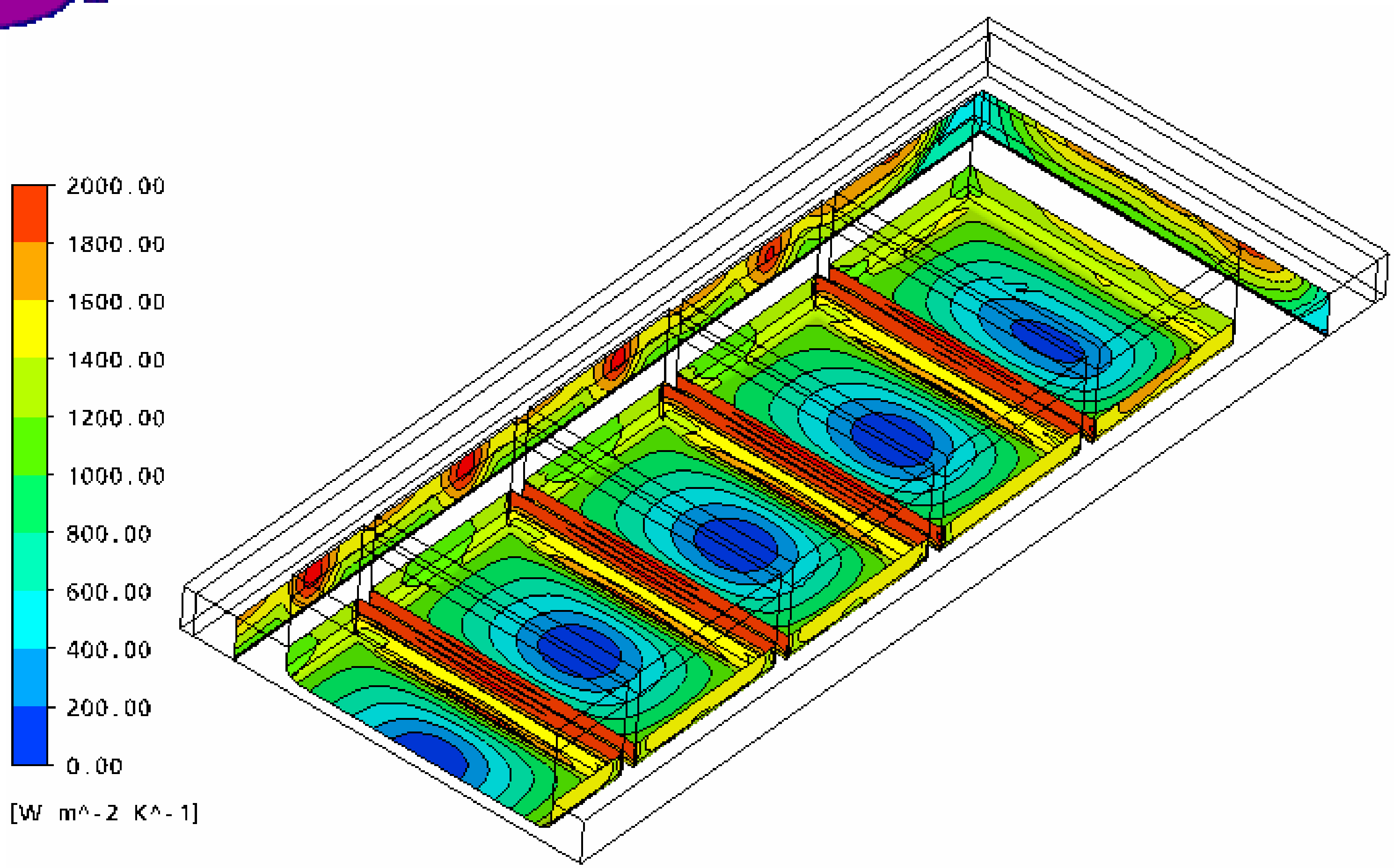

Wall heat transfer coefficient distribution

2009, “Half Empty Shell” Potshell Model

Plastic mode:

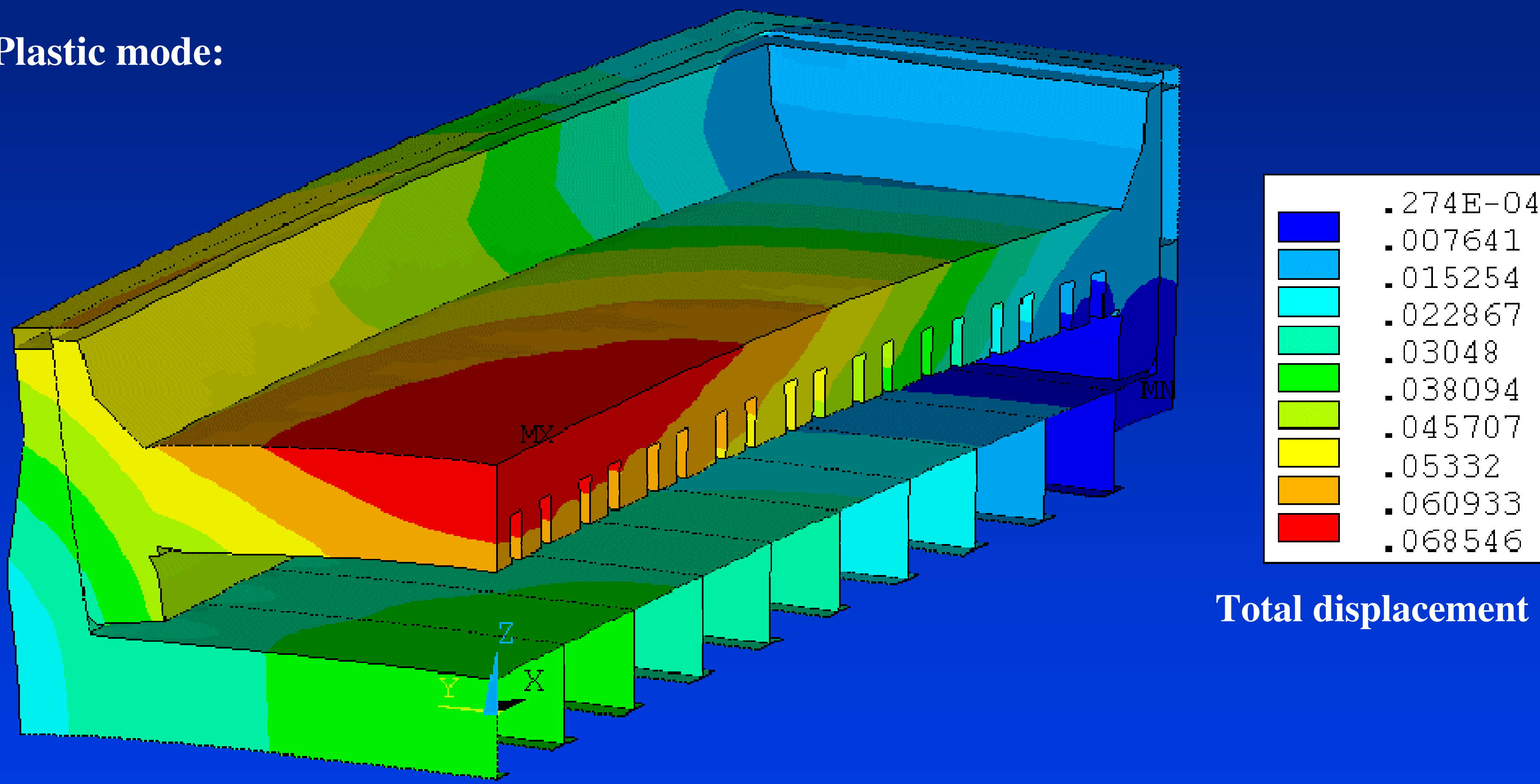

Total displacement (m)

Took 103842 CPU seconds or 1.2 CPU days which is 3.8 times more than what was required to solve the “almost empty shell” potshell model.

GENISIM

2009, " Improved Half Empty Shell" Potshell Model

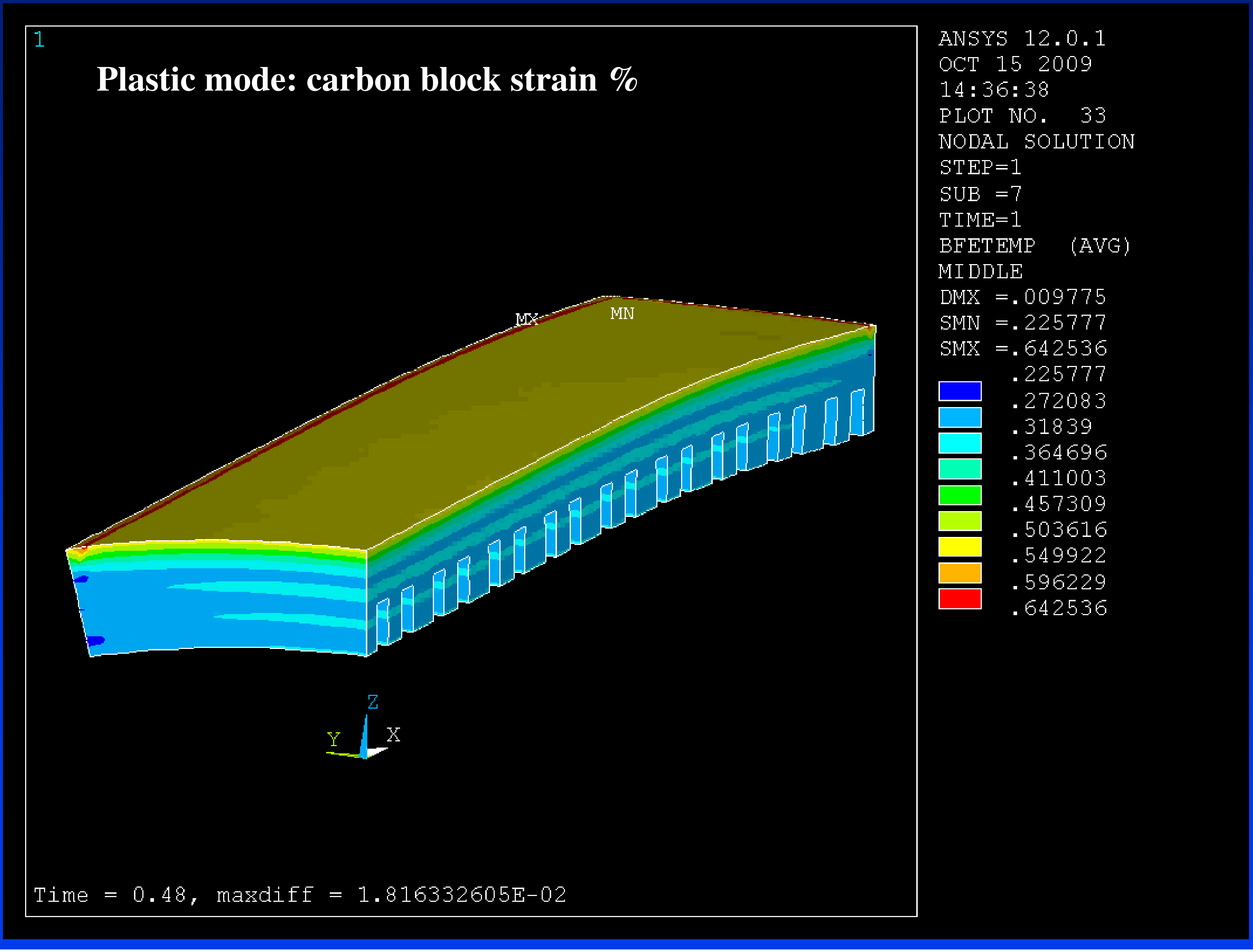

2009, " Improved Half Empty Shell" Potshell Model

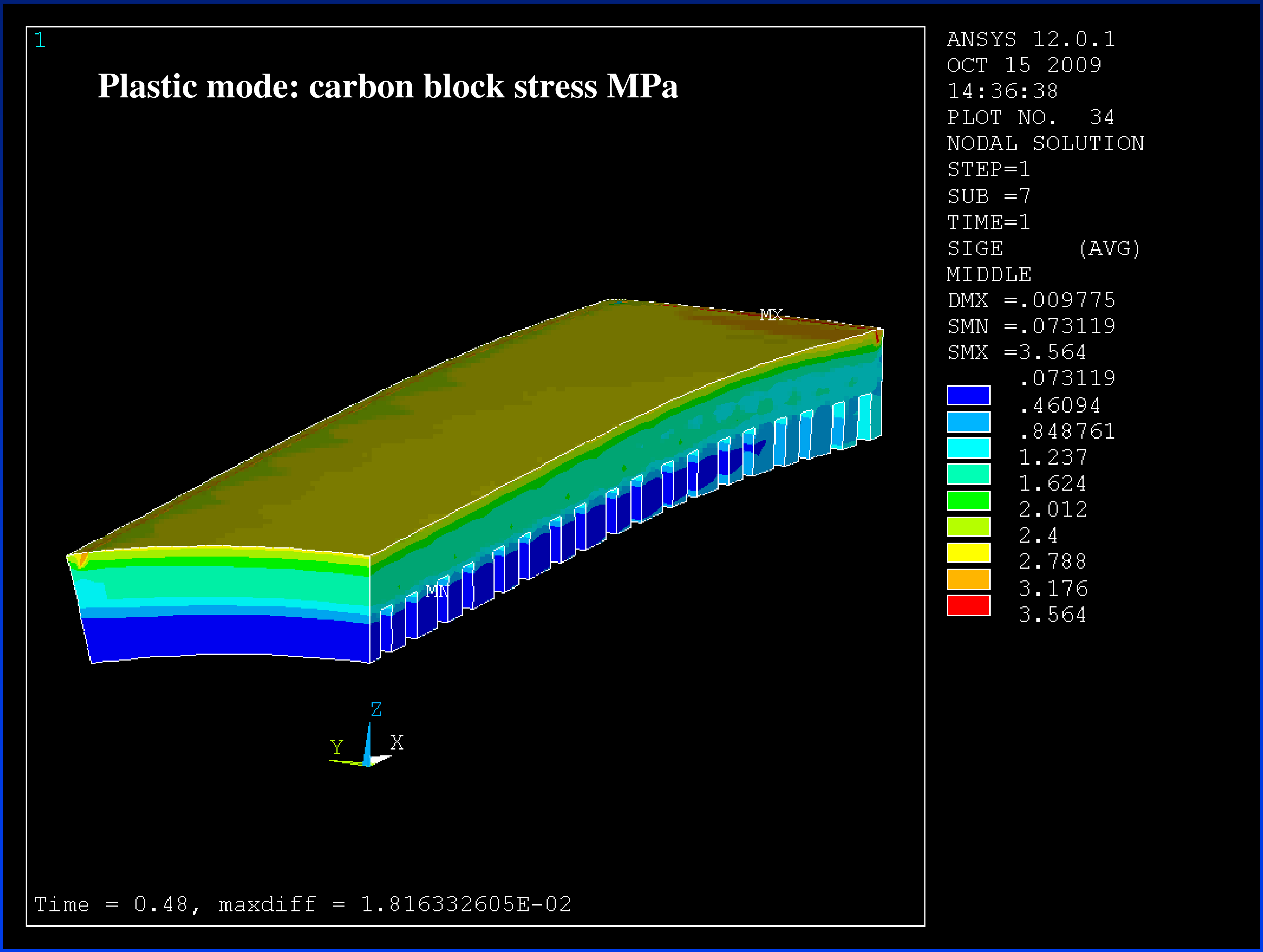

2009, " Improved Half Empty Shell" Potshell Model

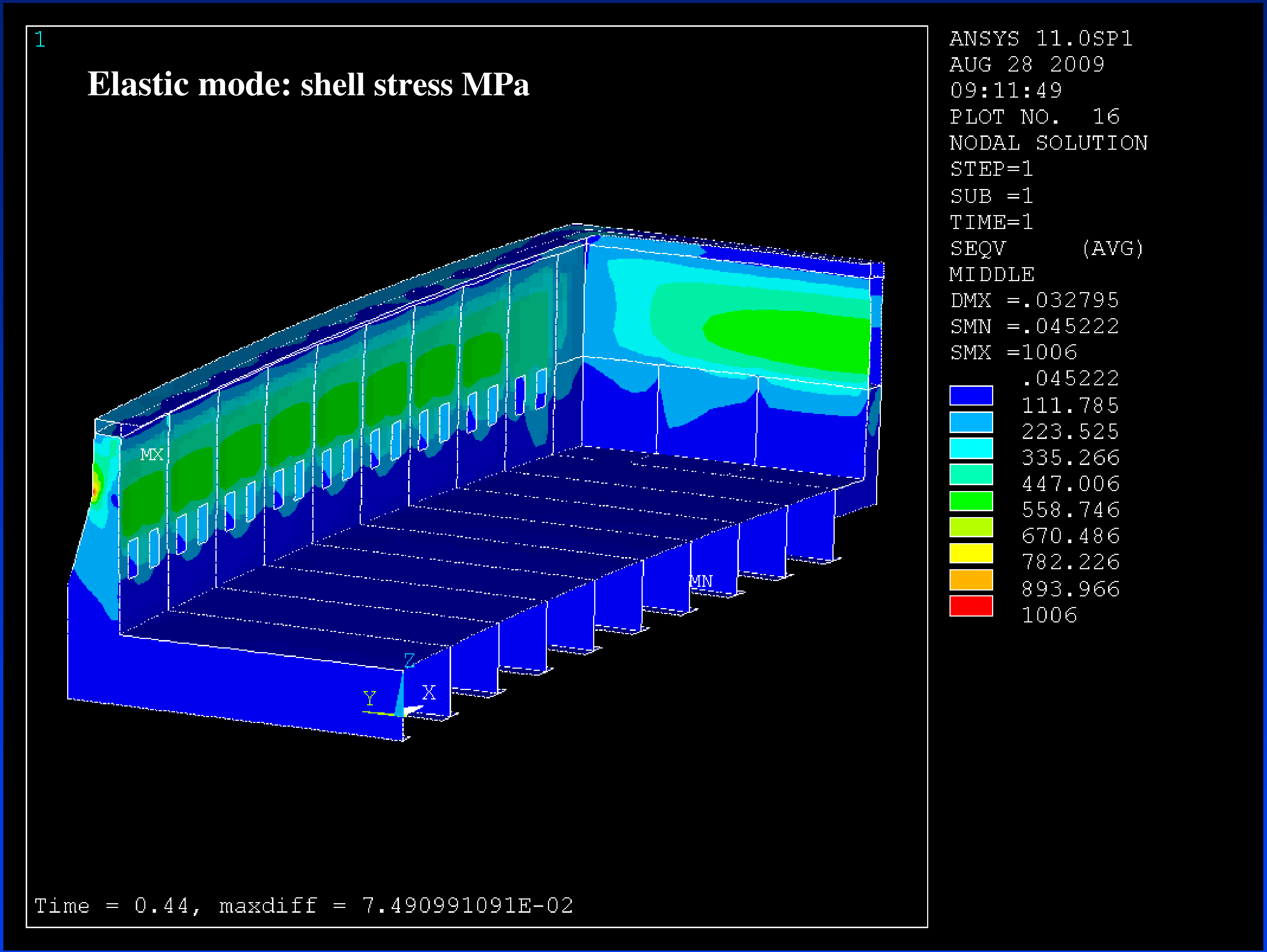

2010, Thermo-Electro-Mechanical Anode Stub Hole Model

Voltage (V)

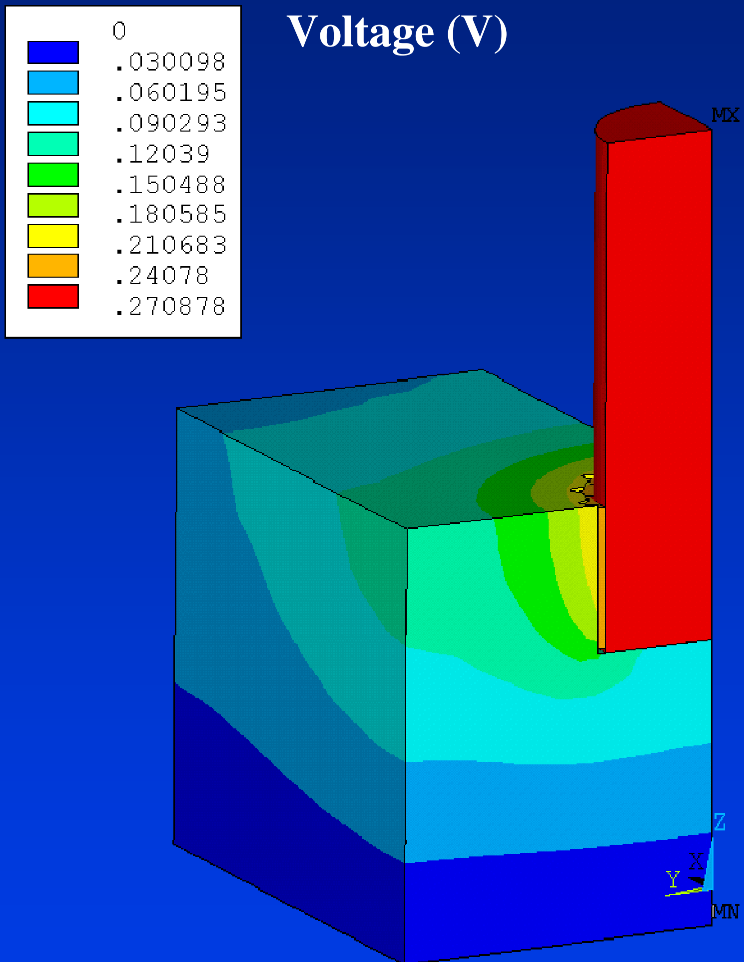

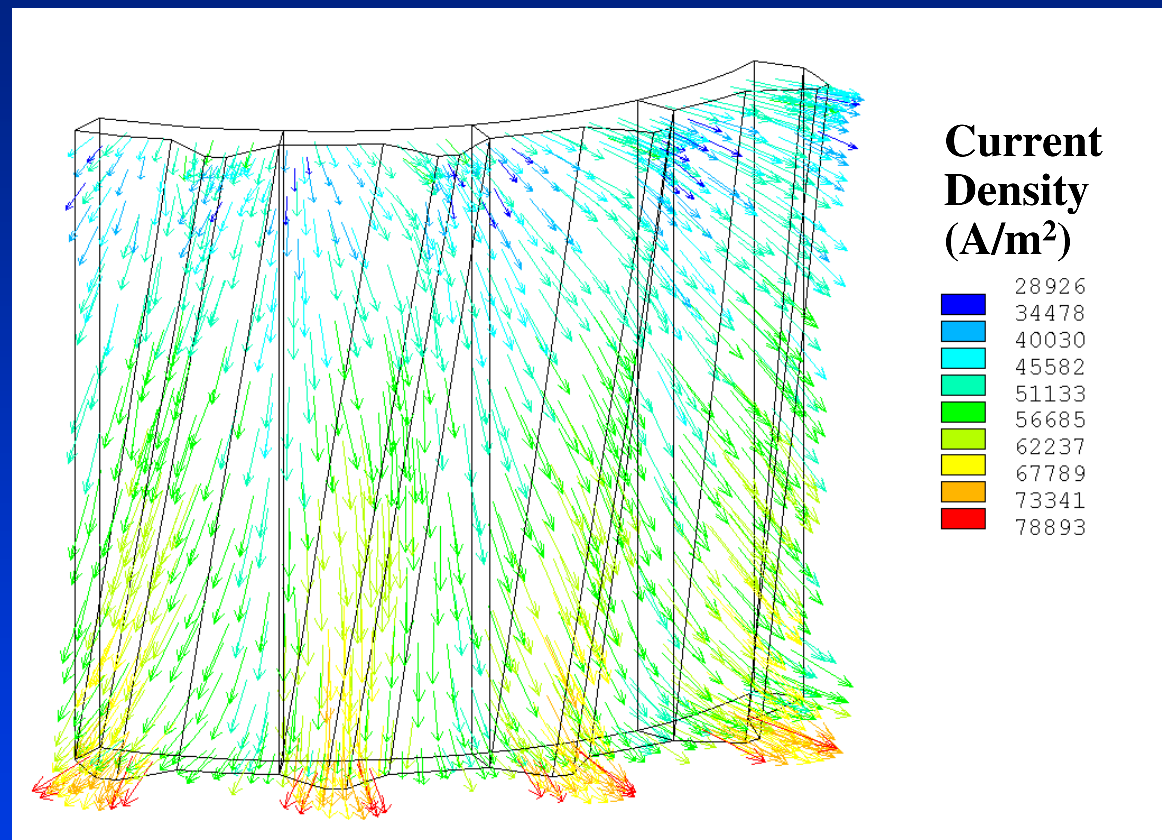

Current Density (A/m^2)

Pressure and temperature dependent contact resistance model results

2010, Thermo-Electro-Mechanical Anode Stub Hole Model

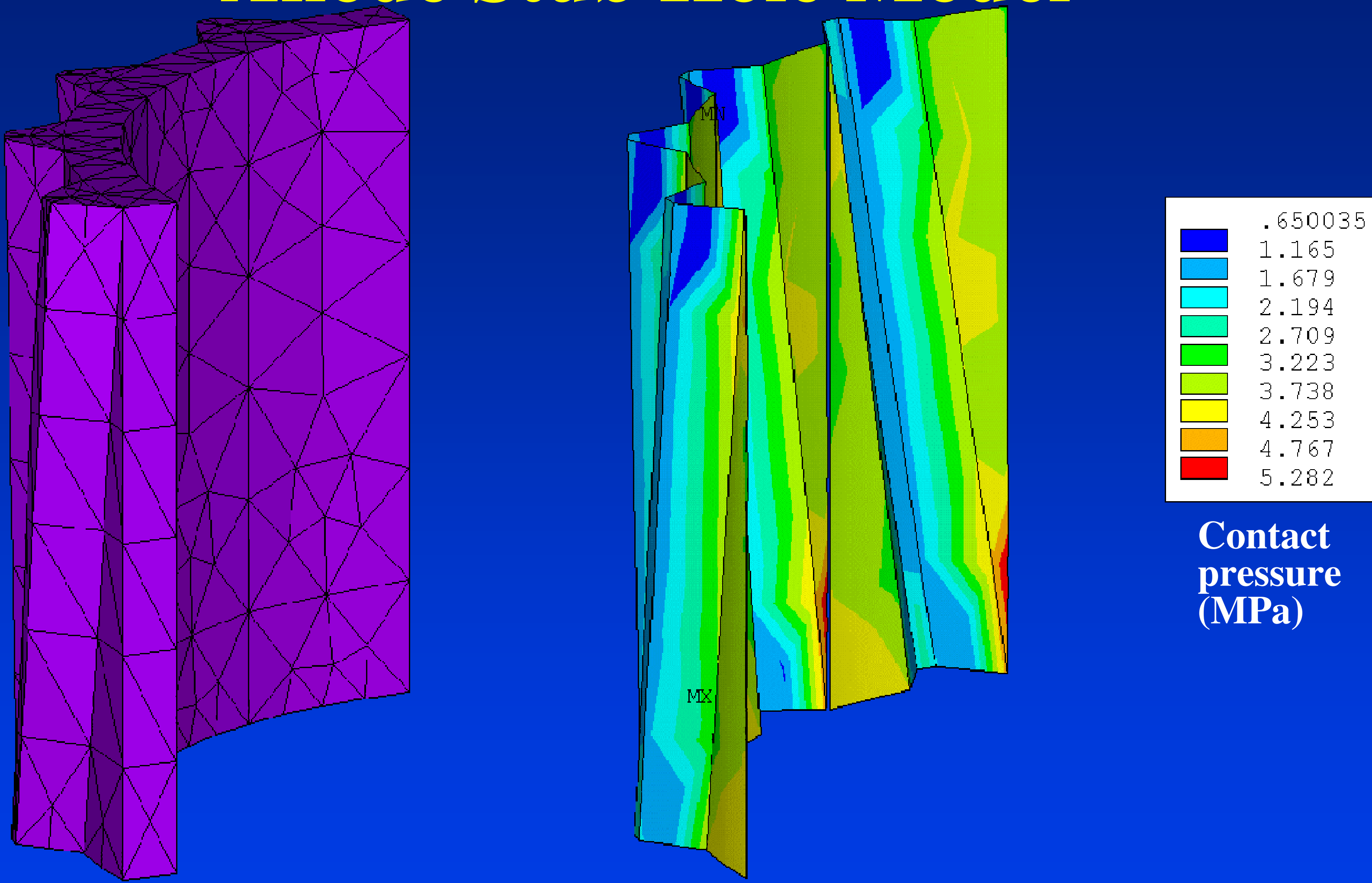

Contact pressure (MPa)

Pressure and temperature dependent contact resistance model results

2010, Thermo-Electro-Mechanical Anode Stub Hole Model

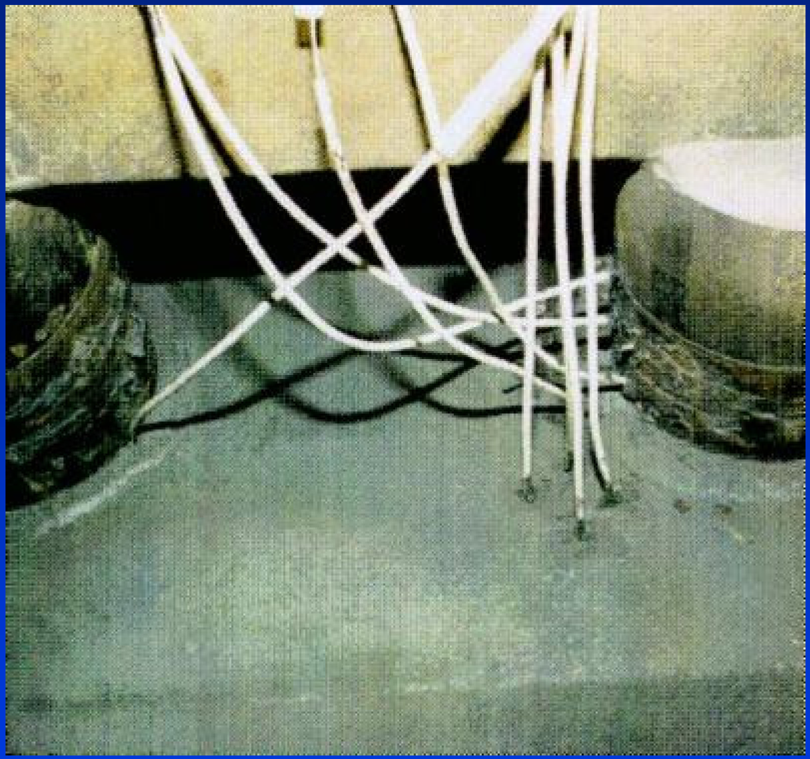

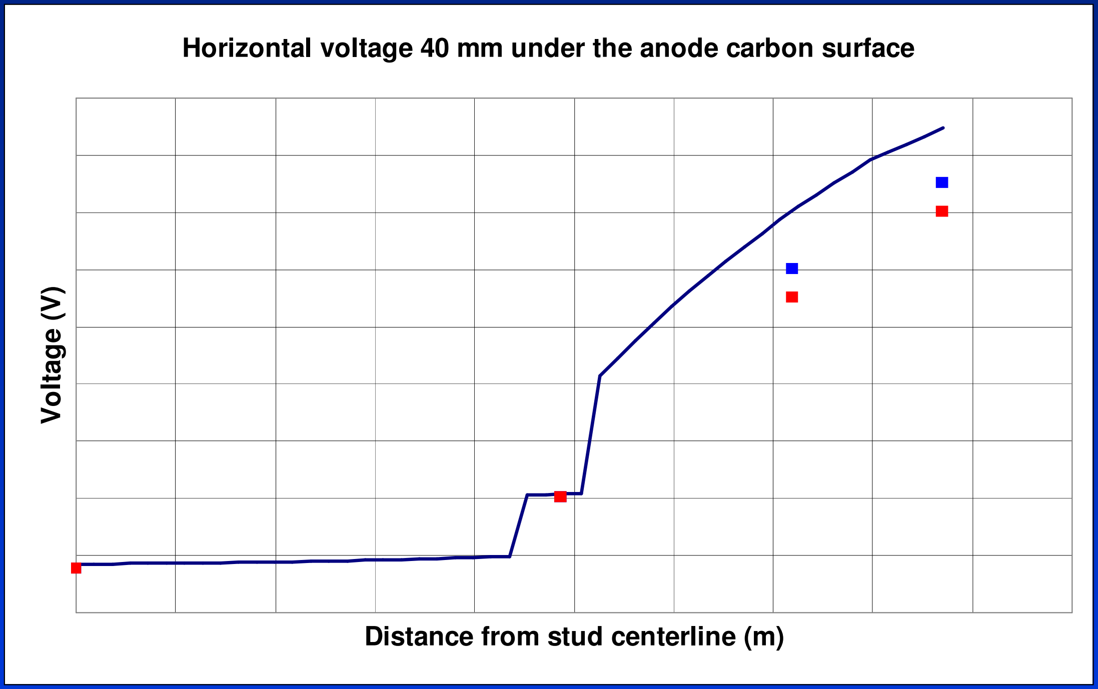

Instrumented Anode:
Anode Stud Voltage Drop Comparison

The use of CFD simulations to optimize potroom ventilation

André van Maarschalkerwaard, Colt Technology

February 14-18, 2010 – Seattle, Washington

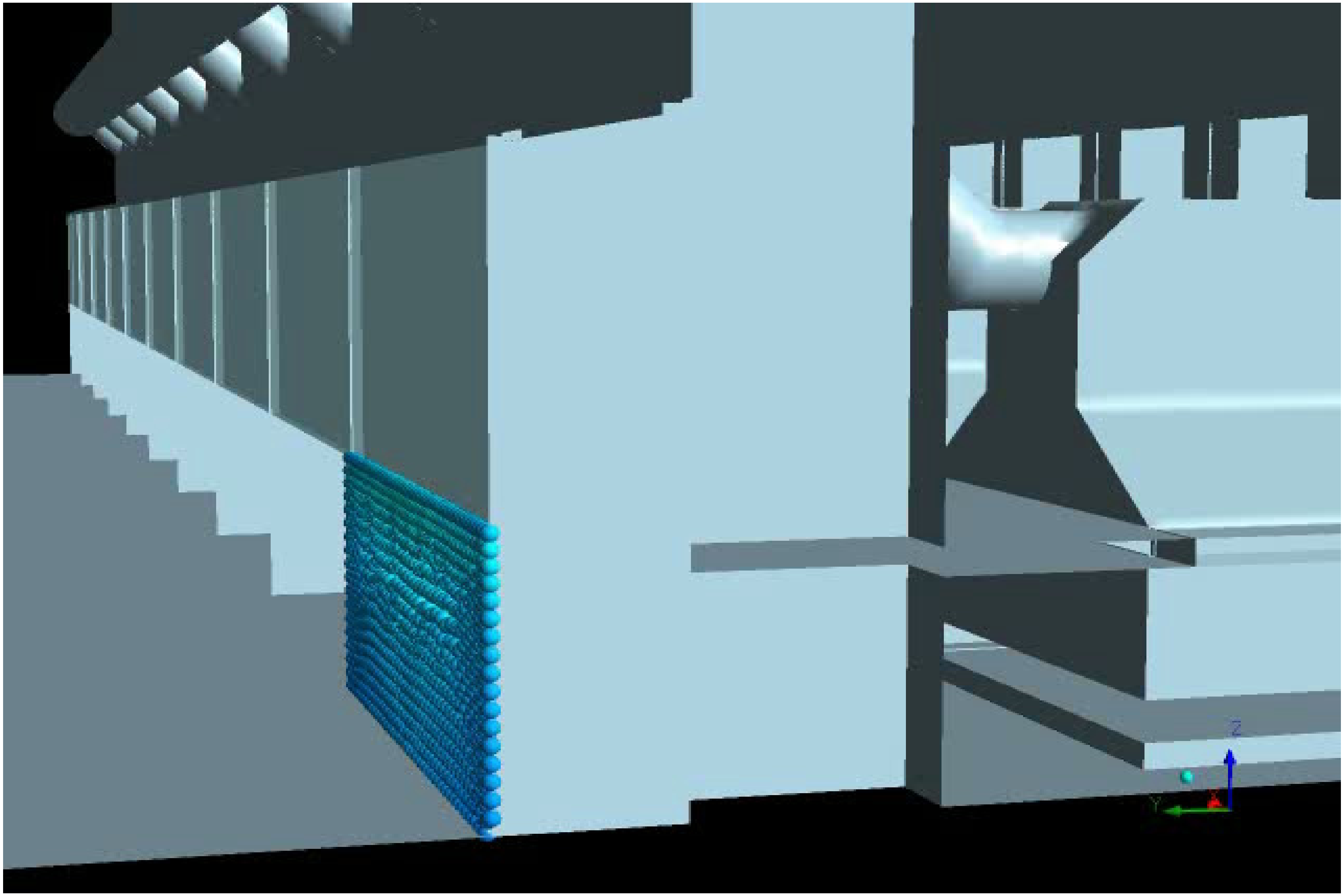
Z
Y
X

National Research
FLAGSHIPS
Light Metals

CSIRO

CFD Modelling of Alumina Mixing in Aluminium Reduction Cells

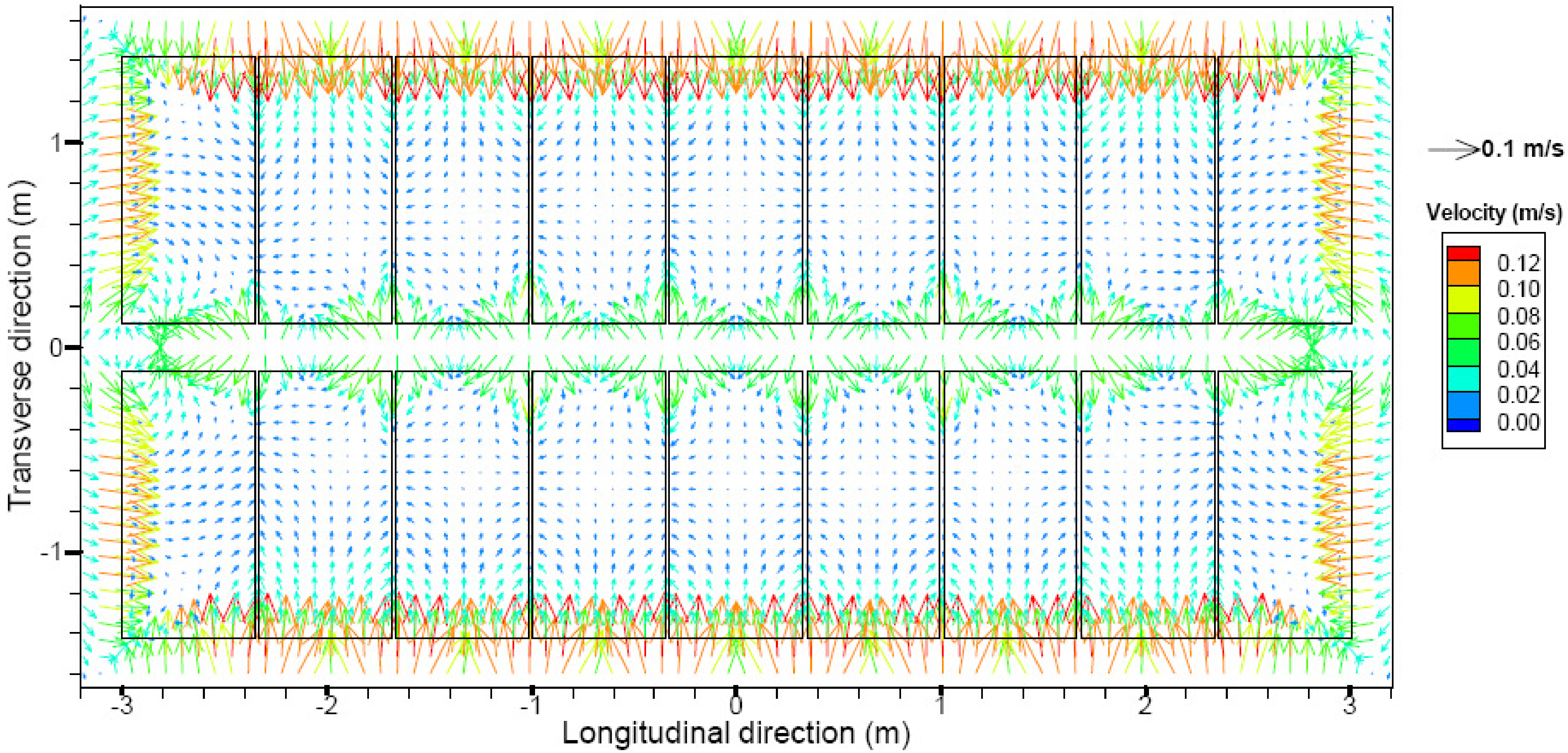

Bath velocity vectors in horizontal mid-plane of ACD

CFD Modelling of Alumina Mixing in Aluminium Reduction Cells

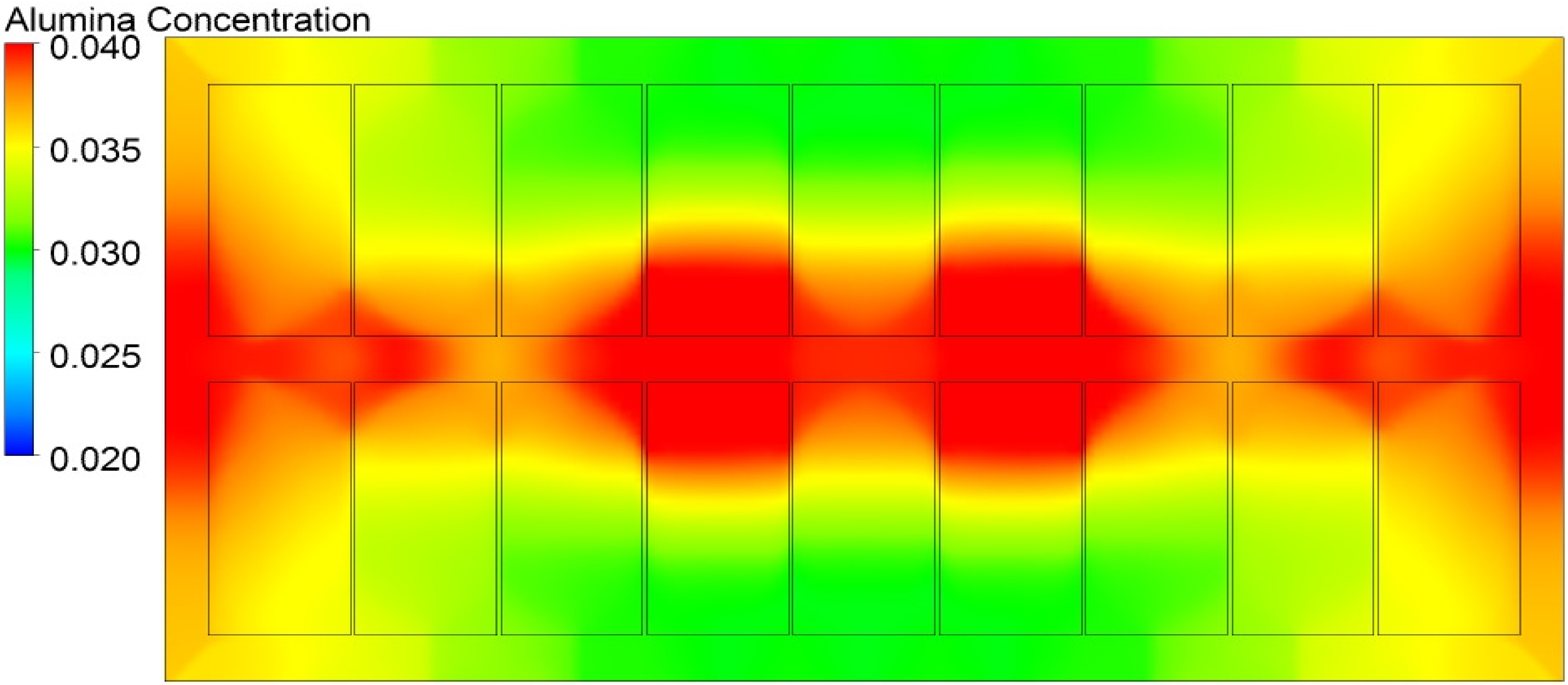

Contour Map

End of Overfeeding

TMS2011, San Diego, USA, 27 Feb – 3 Mar 2011

DX POT TECHNOLOGY POWERS GREEN FIELD EXPANSION

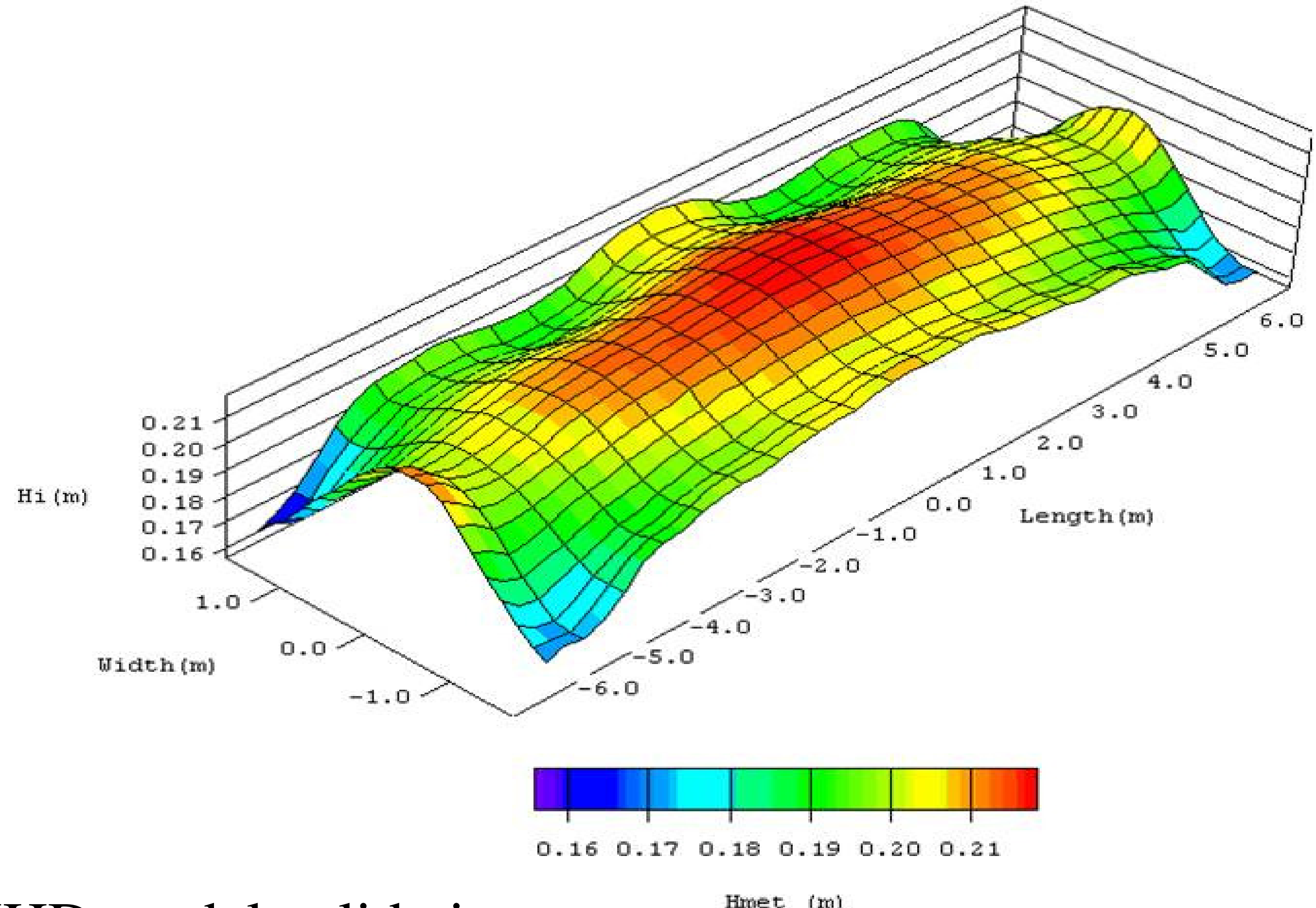

MHD model validation at metal-bath interface

DX POT TECHNOLOGY POWERS GREEN FIELD EXPANSION

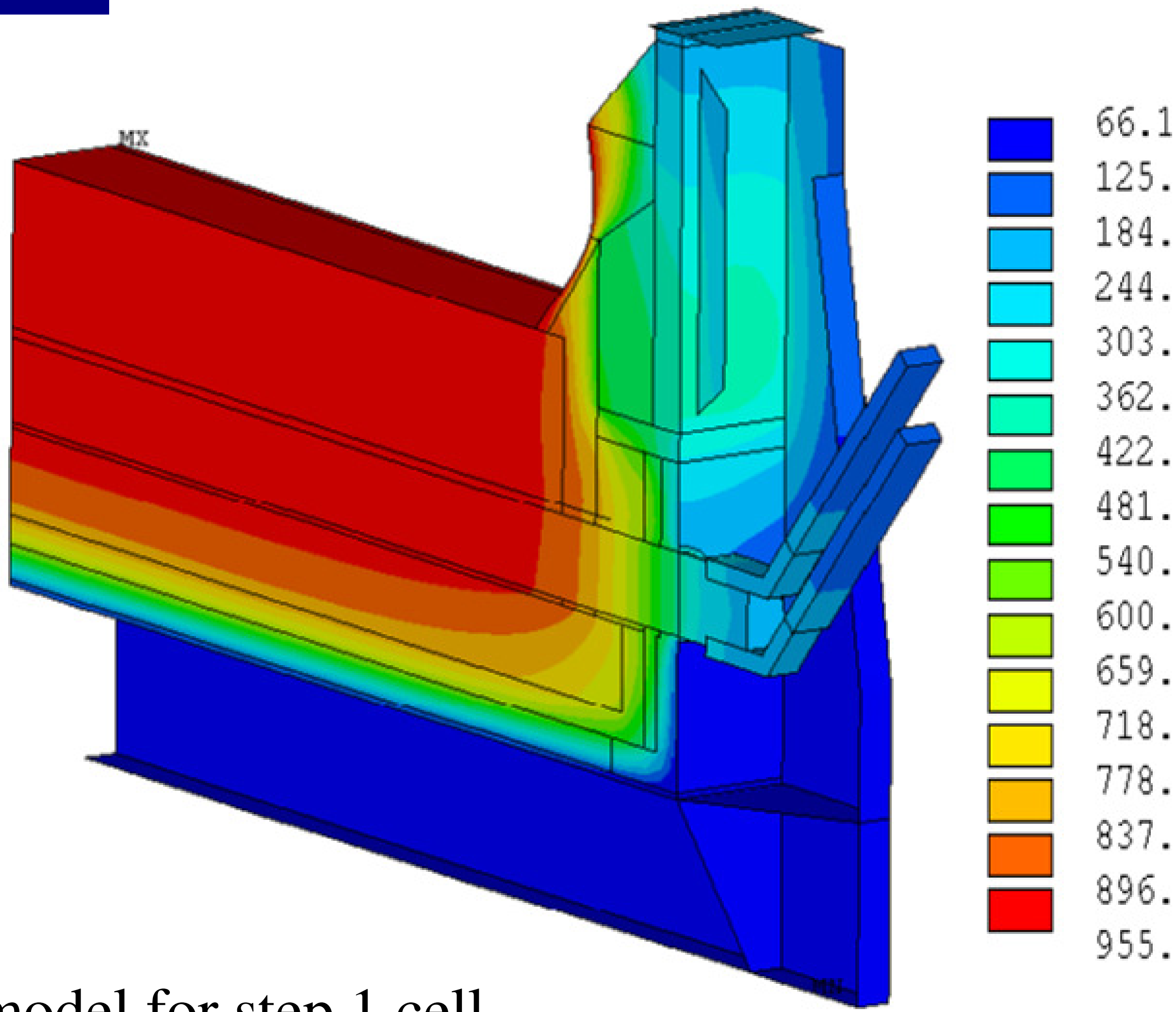

Thermal model for step 1 cell

SHENYANG ALUMINUM&MAGNESIUM
ENGINEERING&RESEARCH INSTITUTE

The Pot Technology Development in China

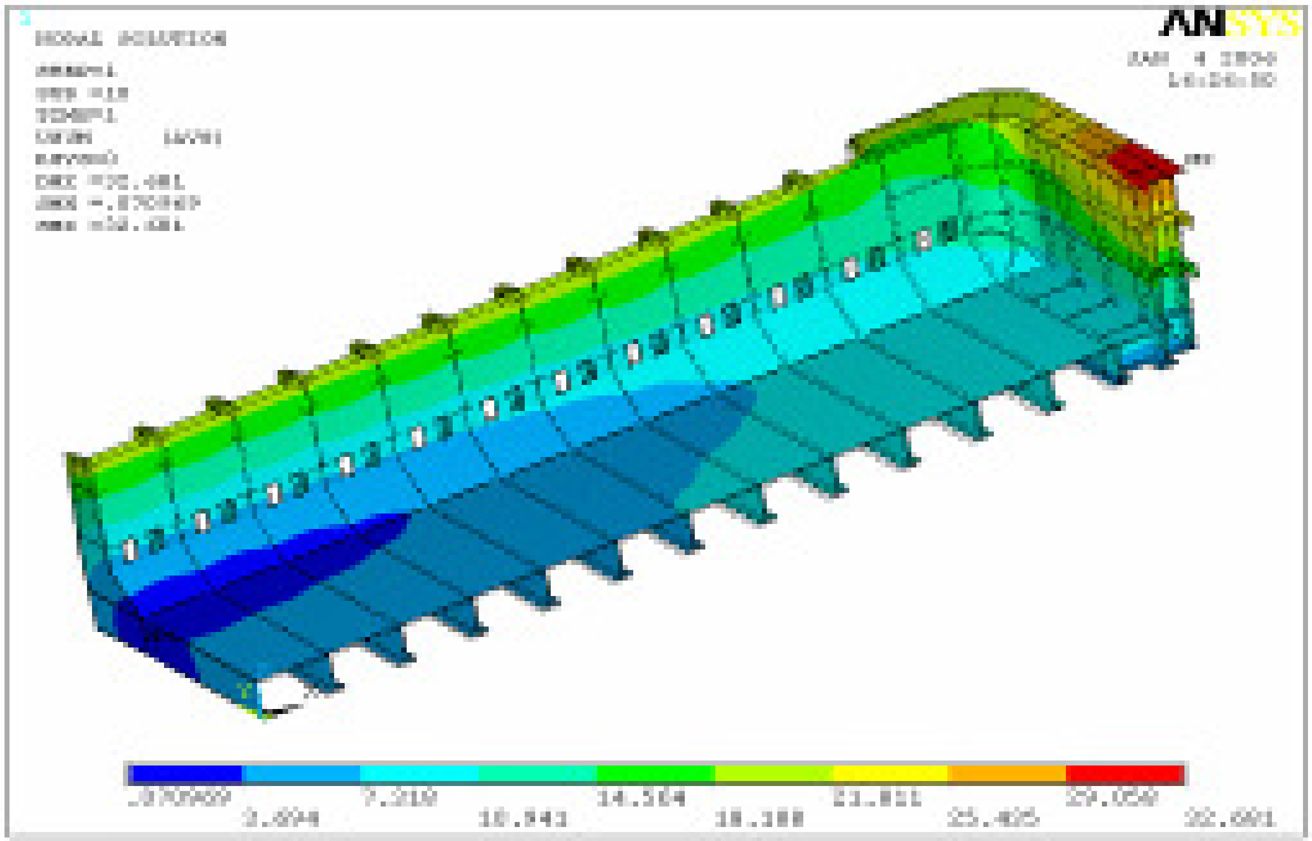

New SY350/400 pot shell

thermo-stress modelling

科技引领时代 人才创造未来

東北大學 设计研究院（有限公司）

Northeastern University Engineering&Research Institute CO.,LTD.

Successful Commercial Operation of NEUI400 Potline

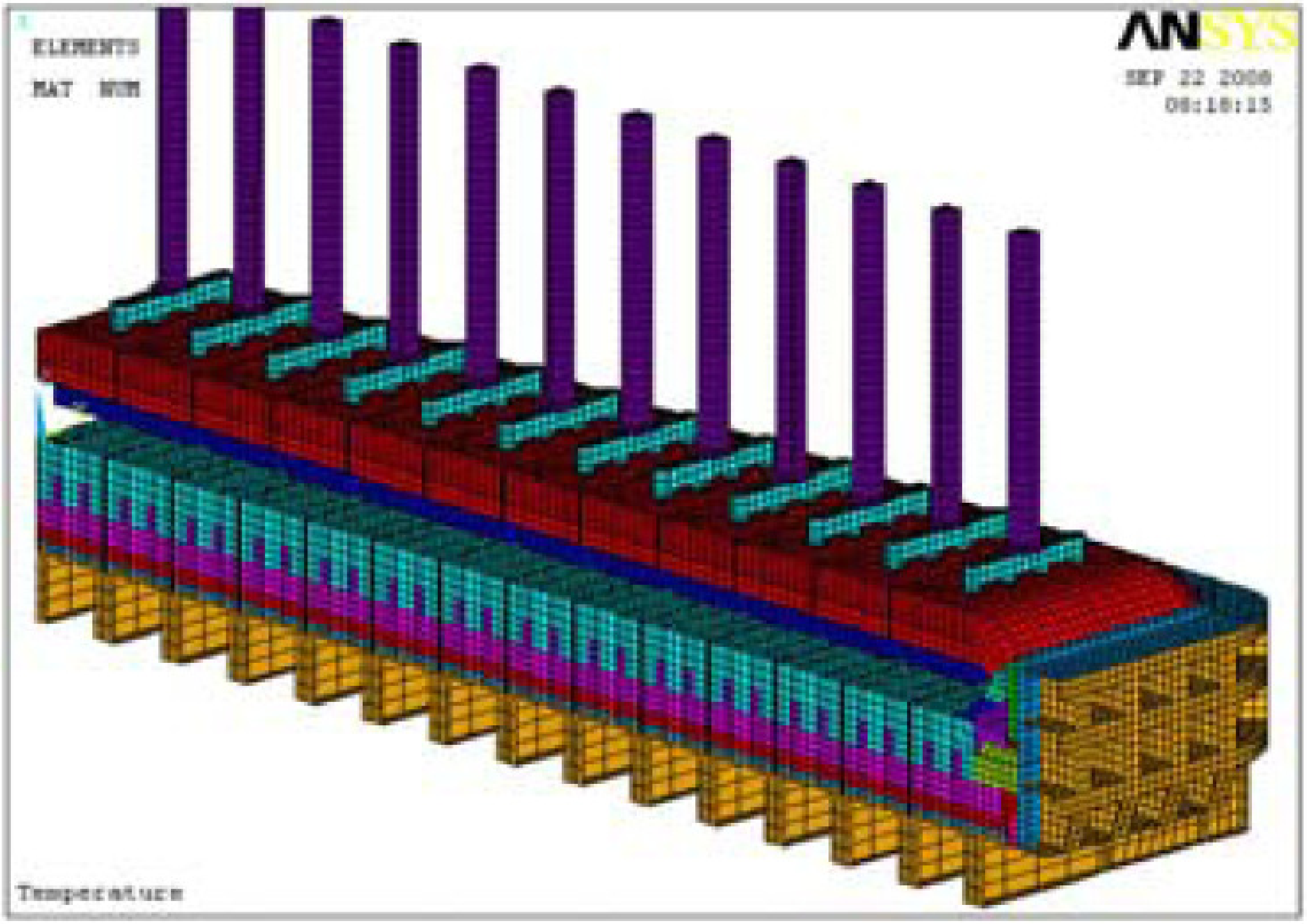

Thermoelectric field model

Successful Commercial Operation of NEUI400 Potline

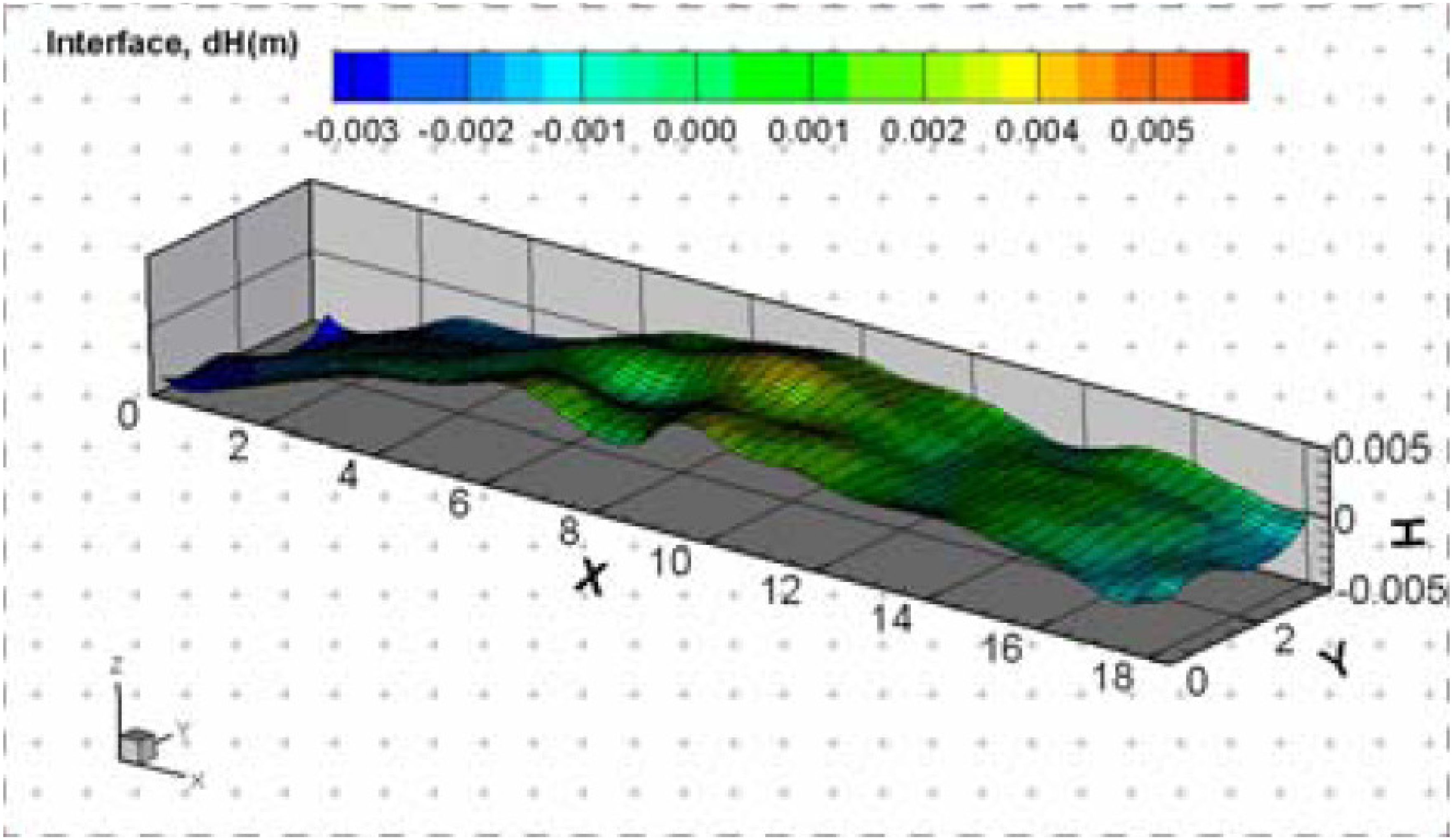

Simulation results of interface deformation

External CFD Model Pressure Profile

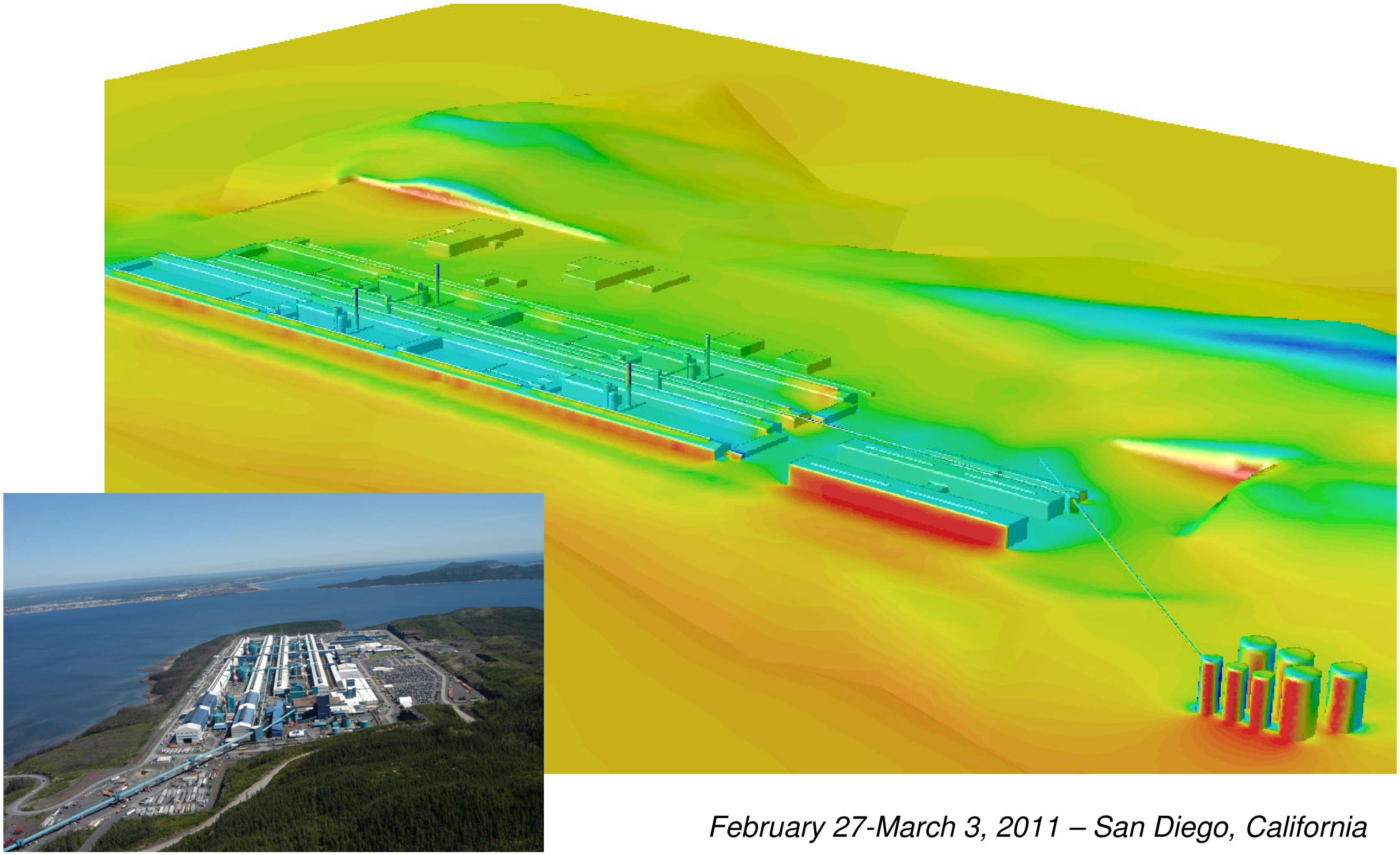

February 27-March 3, 2011 – San Diego, California

Internal Potroom CFD Model Temperature Profile

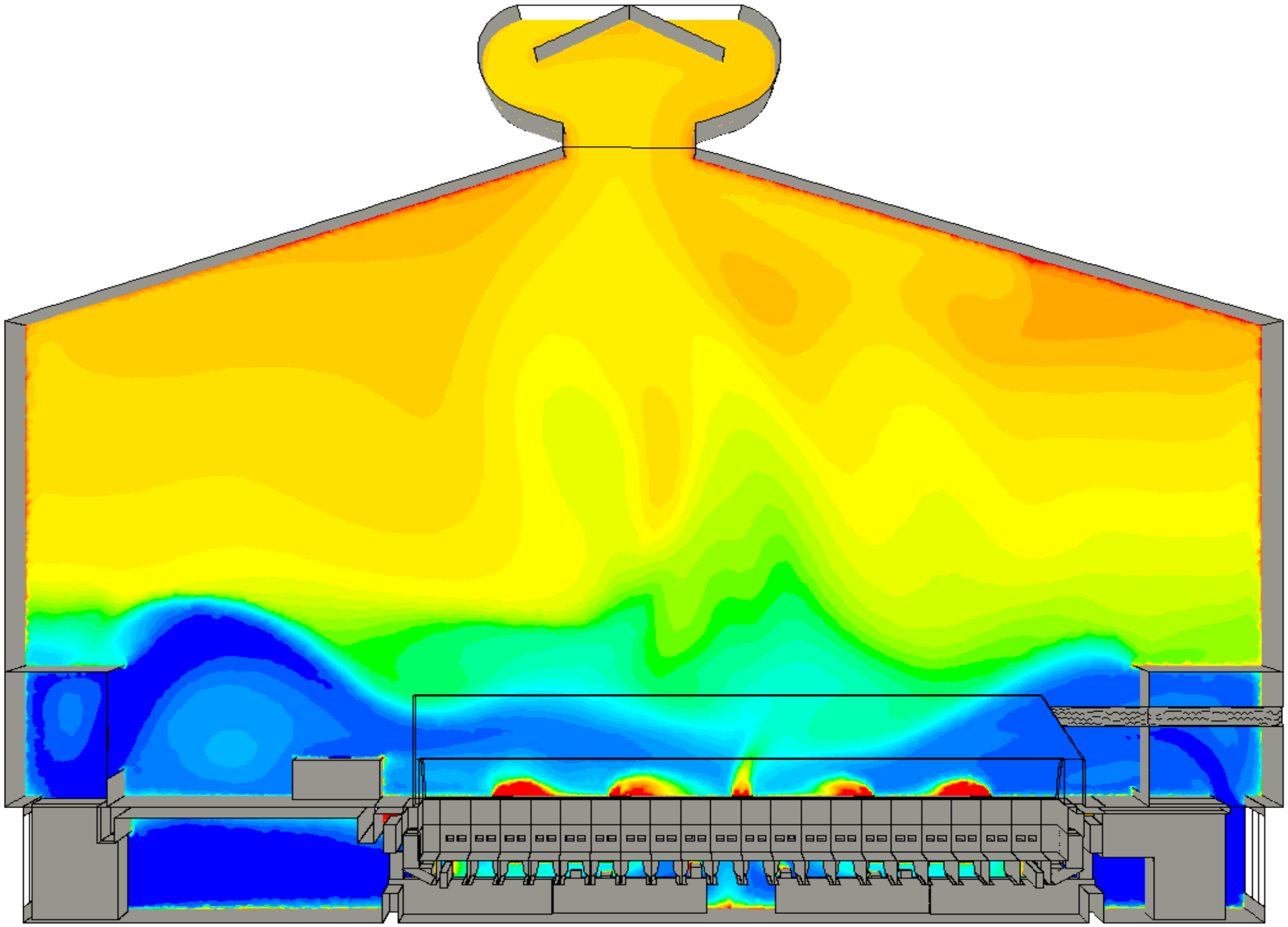

February 27-March 3, 2011 – San Diego, California

MODELING OF ENERGY SAVING BY USING CATHODE DESIGN AND INSERTS

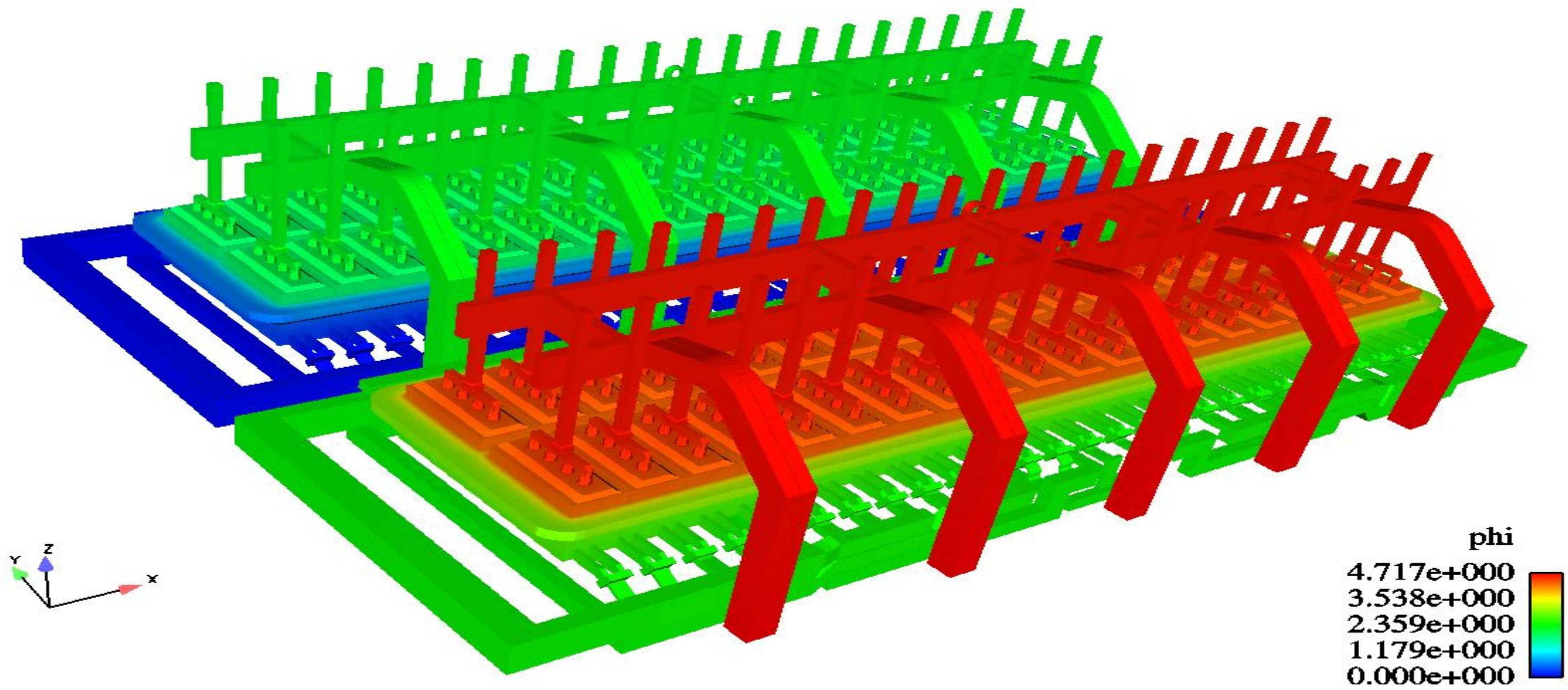

New Cathode Shape and Inserts

Impact on specific energy

New Cell Technology

February 27-March 3, 2011 – San Diego, California

Development of NEUI500 High Energy Efficiency Aluminum Reduction Cell Technology

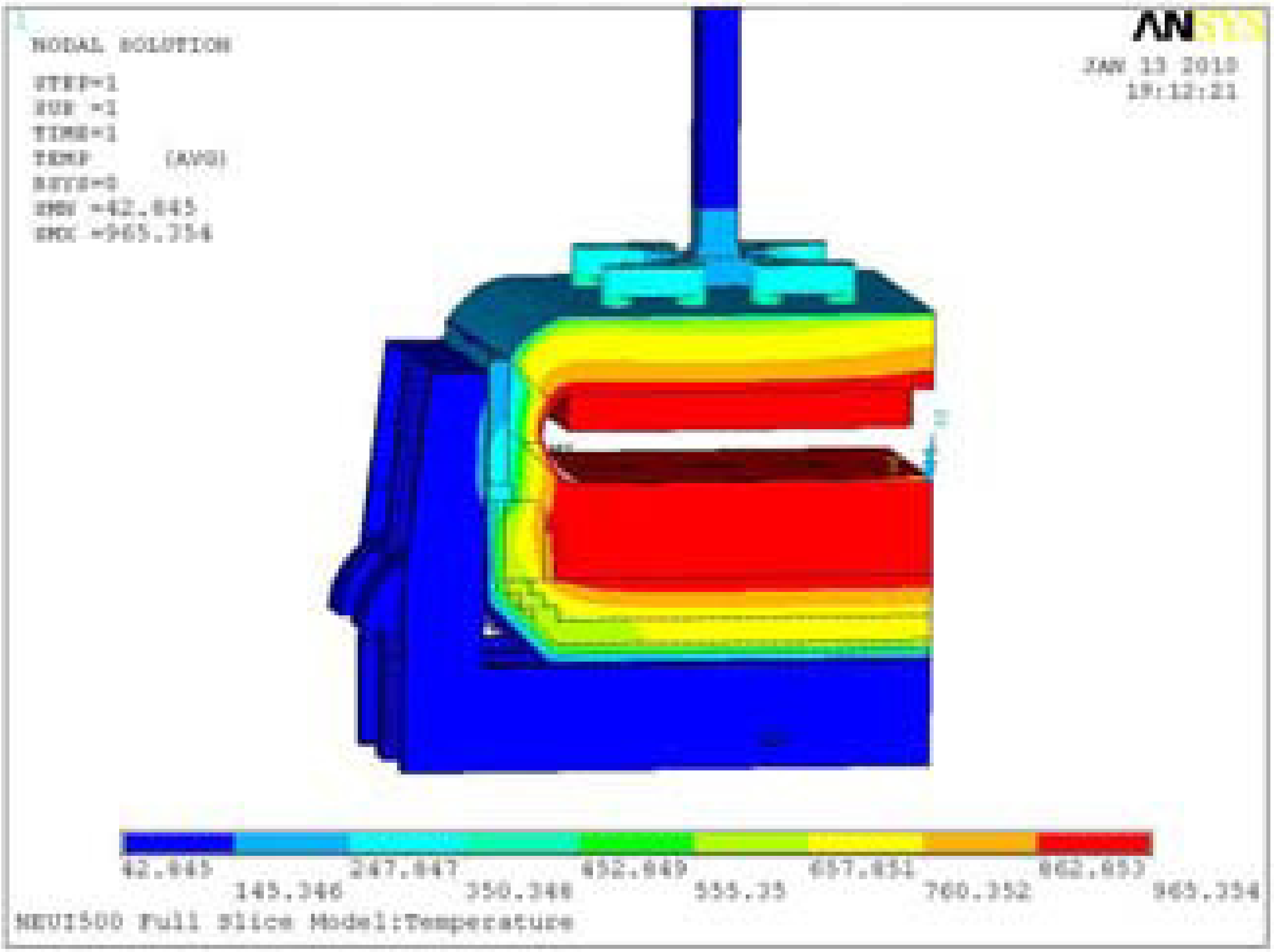

Development of NEUI500 High Energy Efficiency Aluminum Reduction Cell Technology

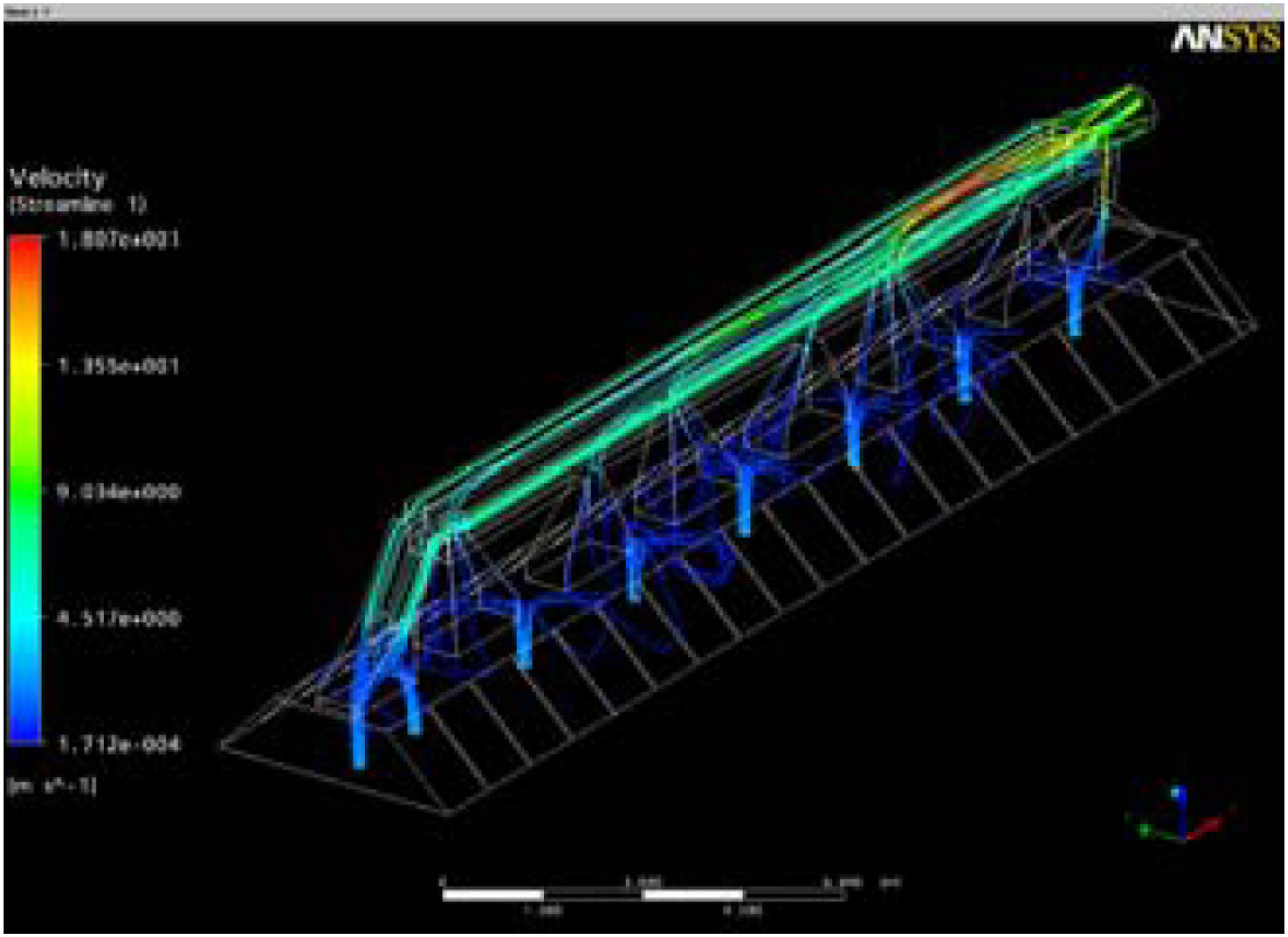

February 27-March 3, 2011 – San Diego, California

Dr. Marc Dupuis has been appointed Technical Consultant of GAMI

Dr. Marc Dupuis has been appointed Technical Consultant of GAMI

LETTER OF APPOINTMENT

Herein to appoint Dr. Marc Dupuis as the technical consultant of Guiyang Aluminum-Magnesium Design & Research Institute

聘　书

兹聘 Dr. Marc Dupuis 为贵阳铝镁设计研究院技术顾问。

贵阳铝镁设计研究院

President of Guiyang Aluminum-Magnesium Design & Research Institute

At the New Year Celebration in Guiyang

中铝国际贵阳分公司 / 贵阳铝镁设计研究院

CHALIECO

GENISIM

Heat dissipation distribution calculation and actual measurement comparison between conventional lining and new thermal insulation lining in 350 kA pot

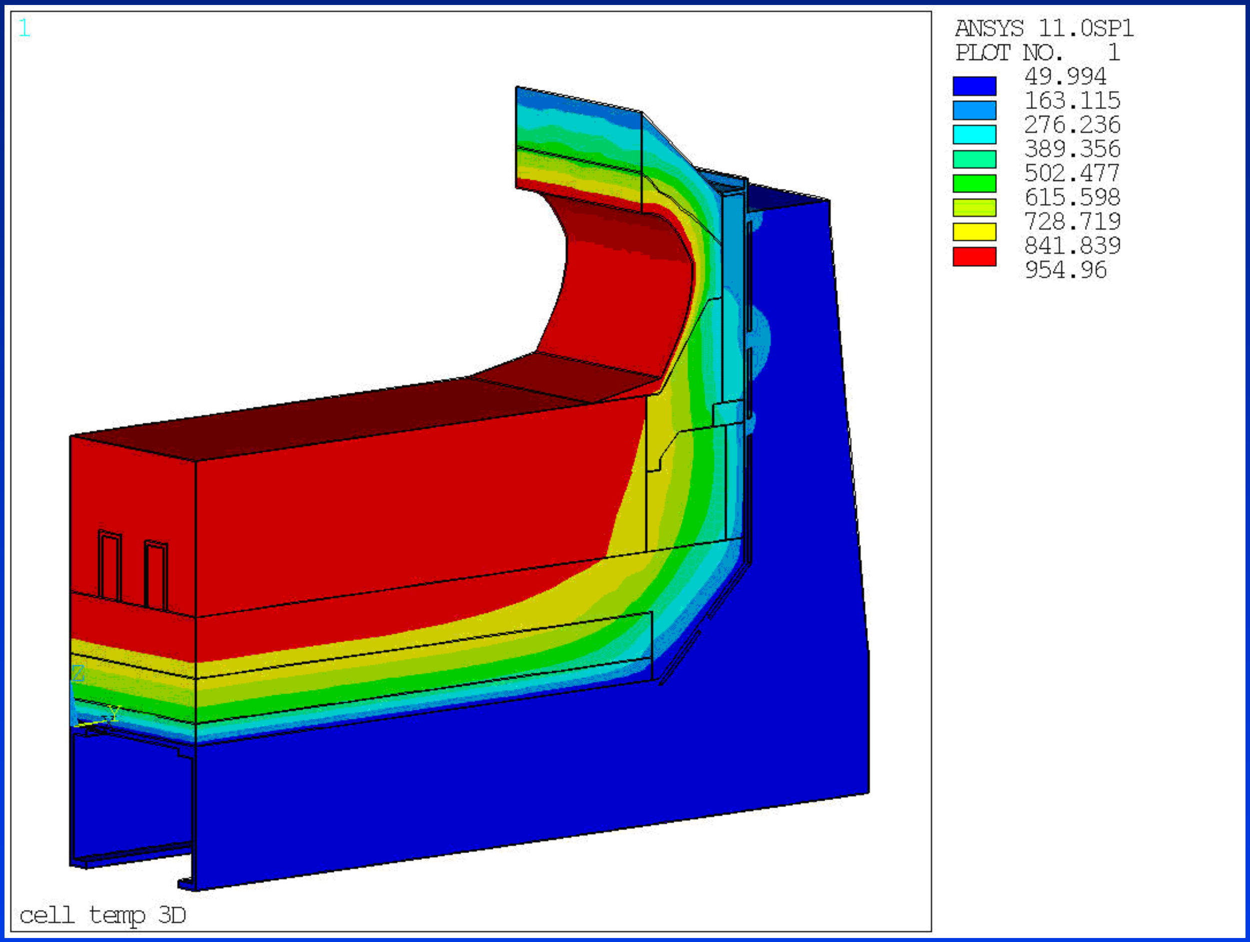

Conventional lining structure, pot side temperature

2012: Cathode Cooling Model

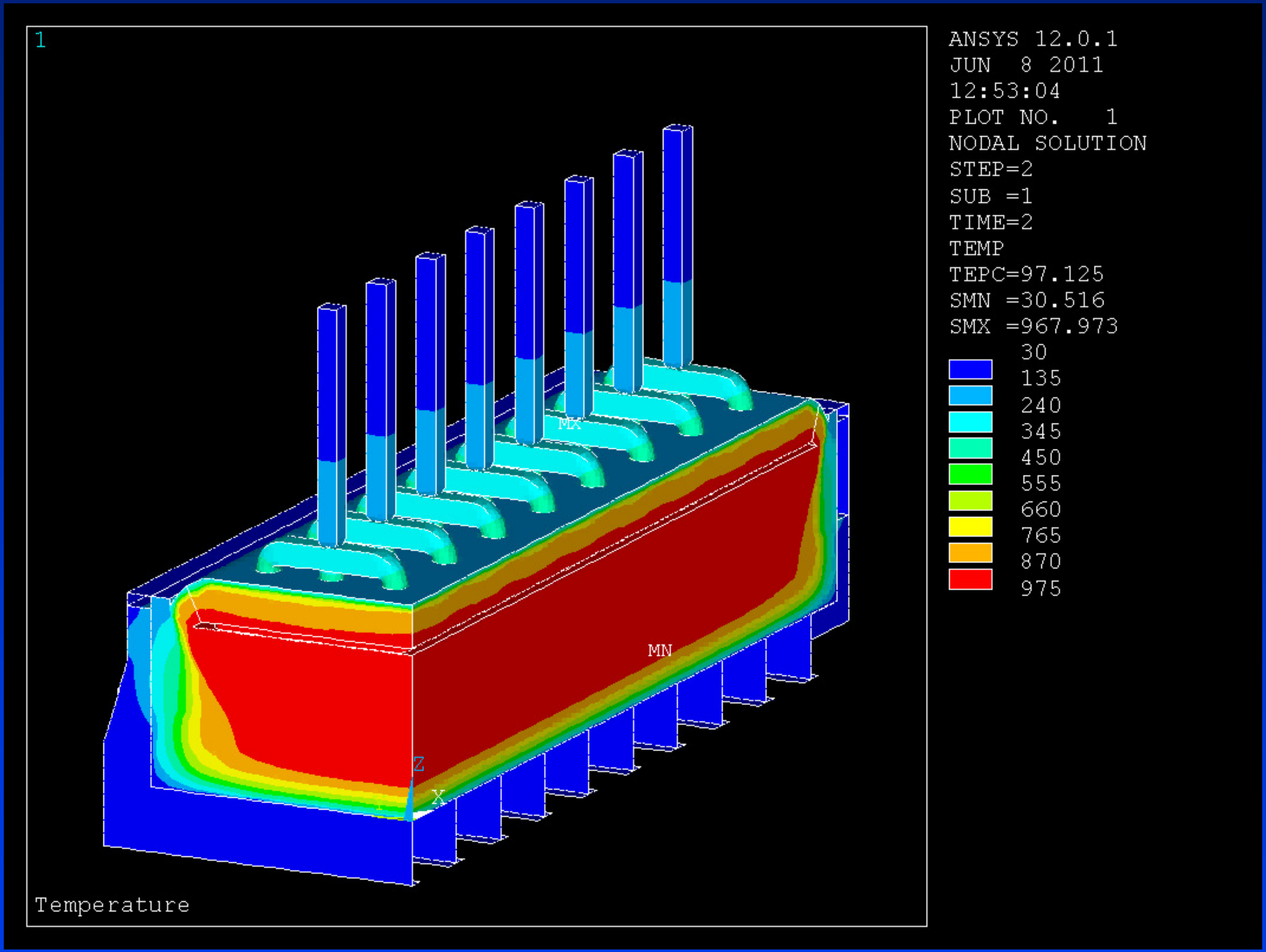

GENISIM

2012: Cathode Cooling Model

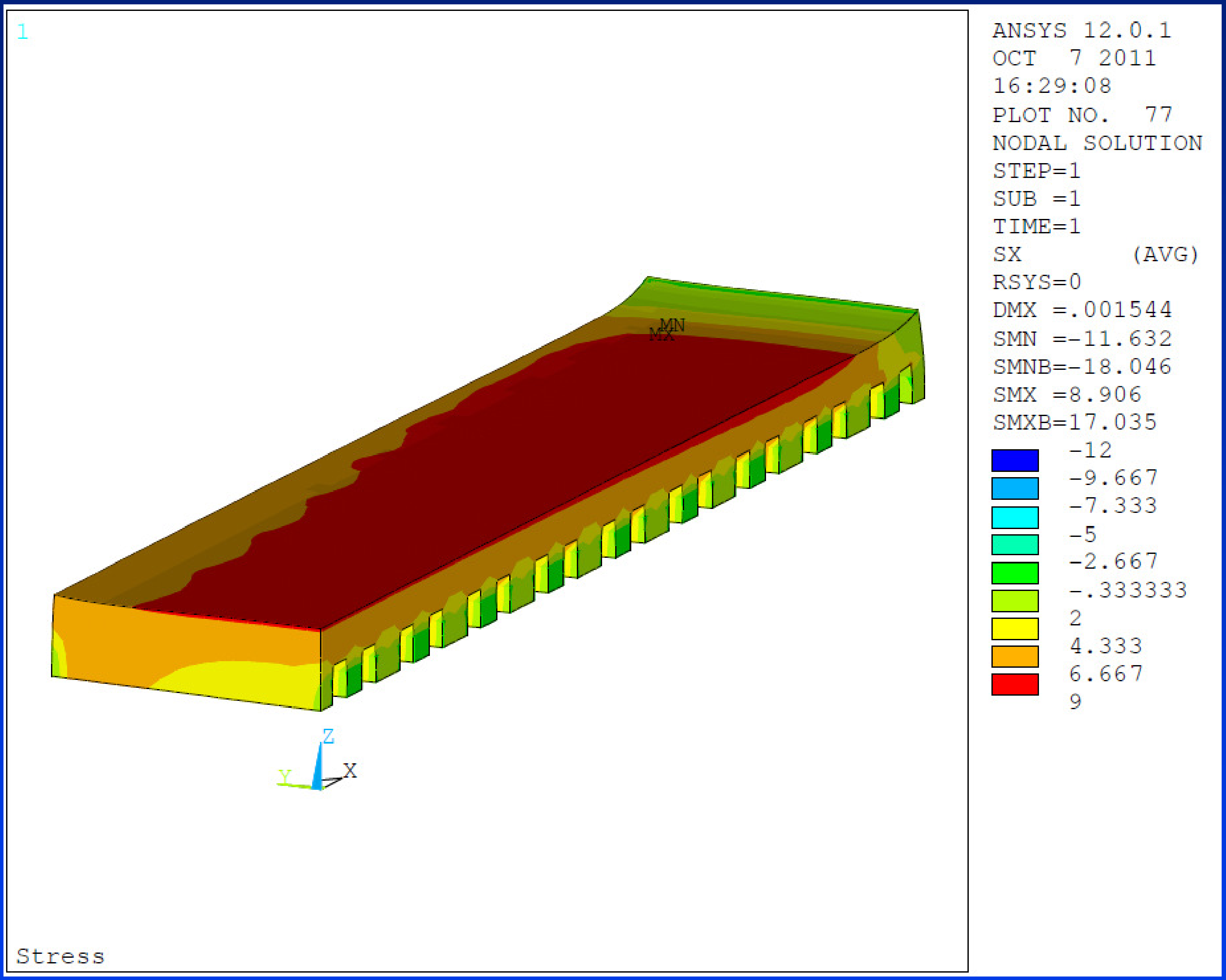

Longitudinal stress component obtained using the 3D quarter cathode panel model assuming that the collector bars are preventing the vertical carbon faces in the slots to move longitudinally

GENISIM

Impact of magnetohydrodynamic and bubbles driving forces on the alumina concentration in the bath of an Hall-Heroult cell

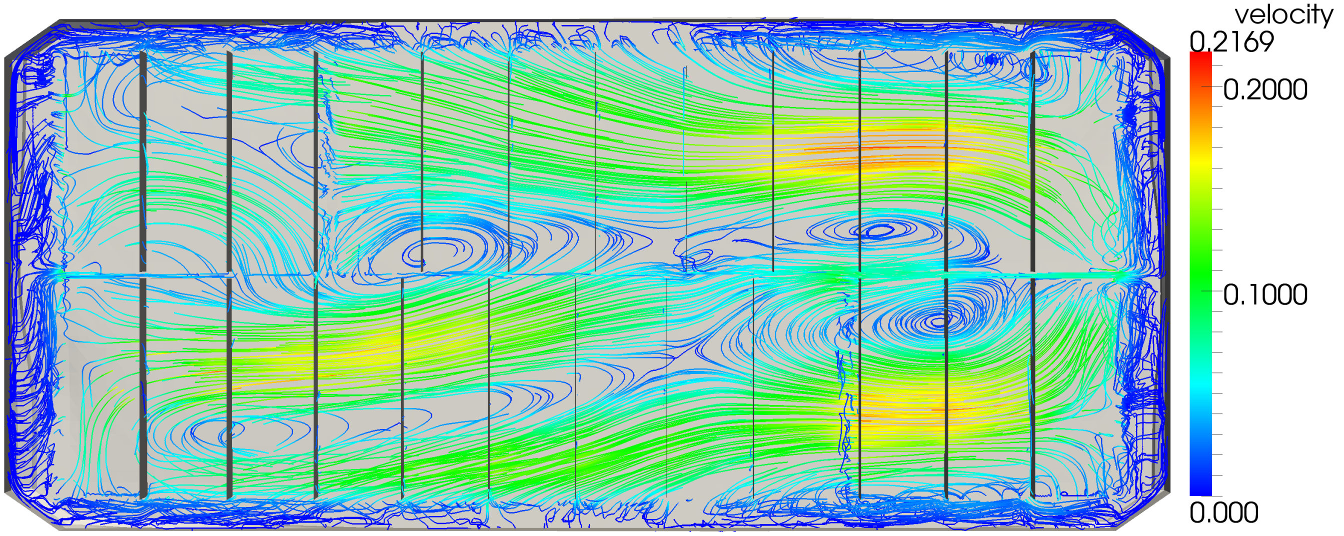

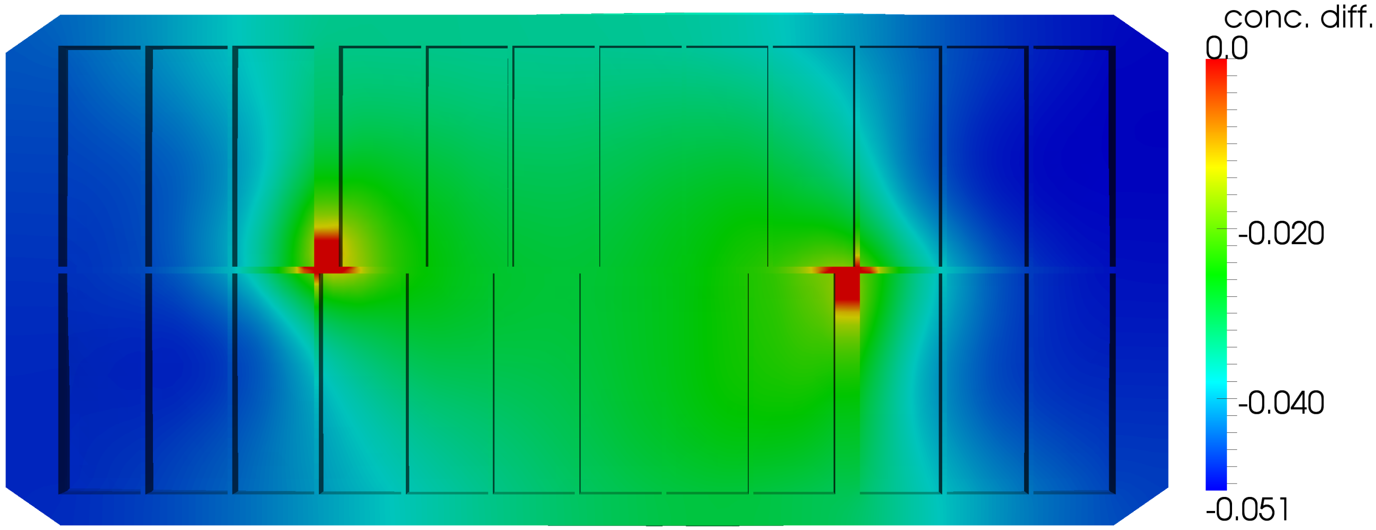

March 3-7, 2013 – San Antonio Texas

中南大學 CENTRAL SOUTH UNIVERSITY

A Virtual Aluminum Reduction Cell

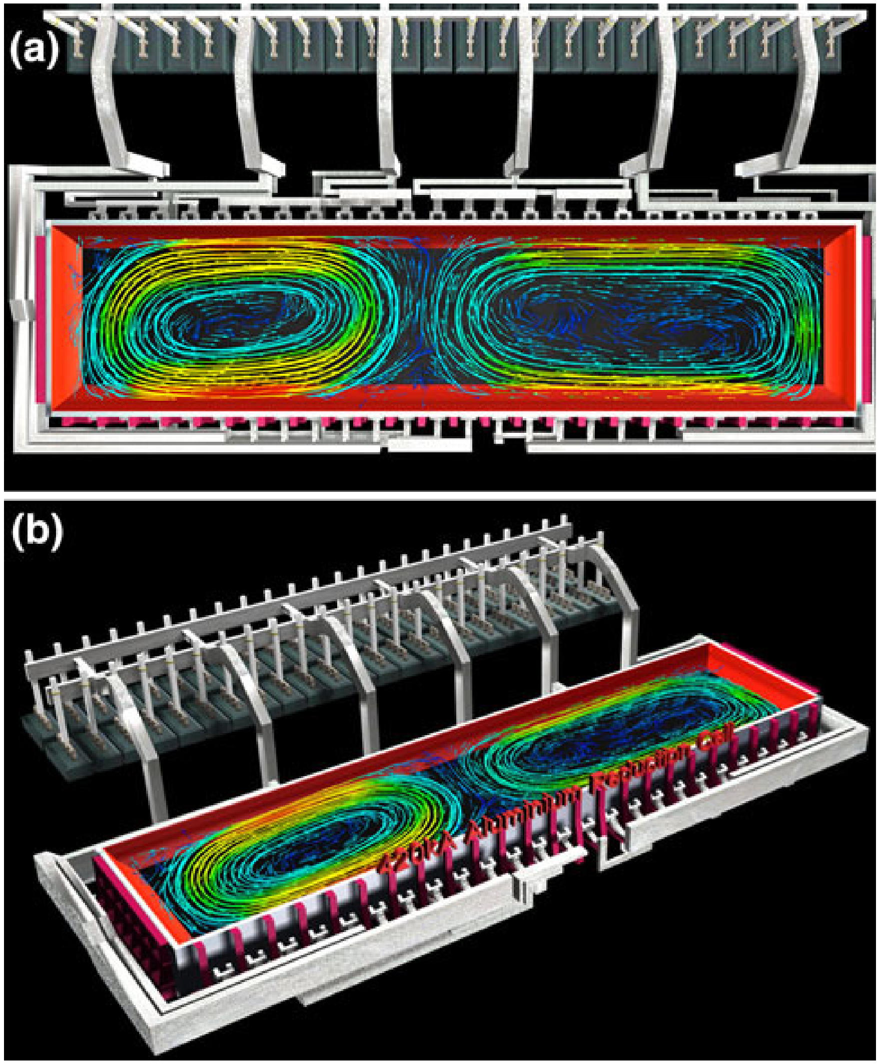

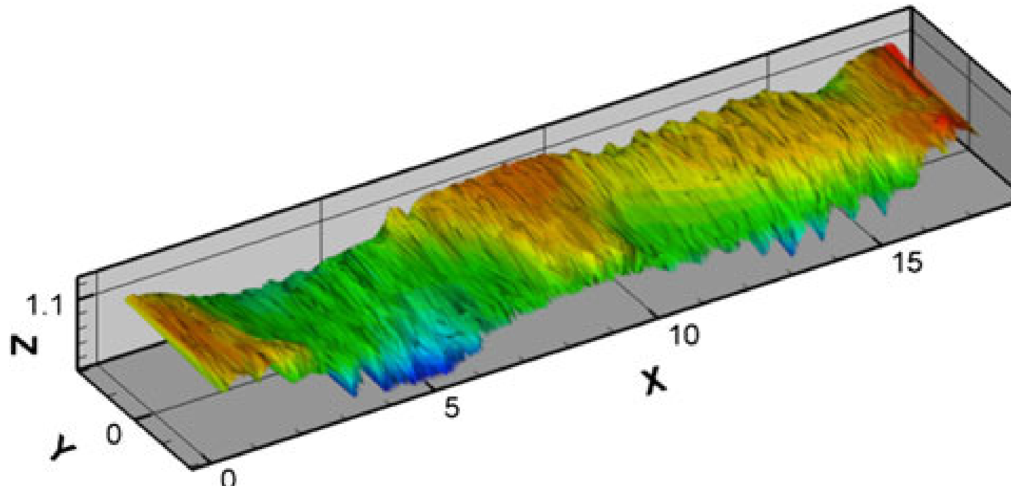

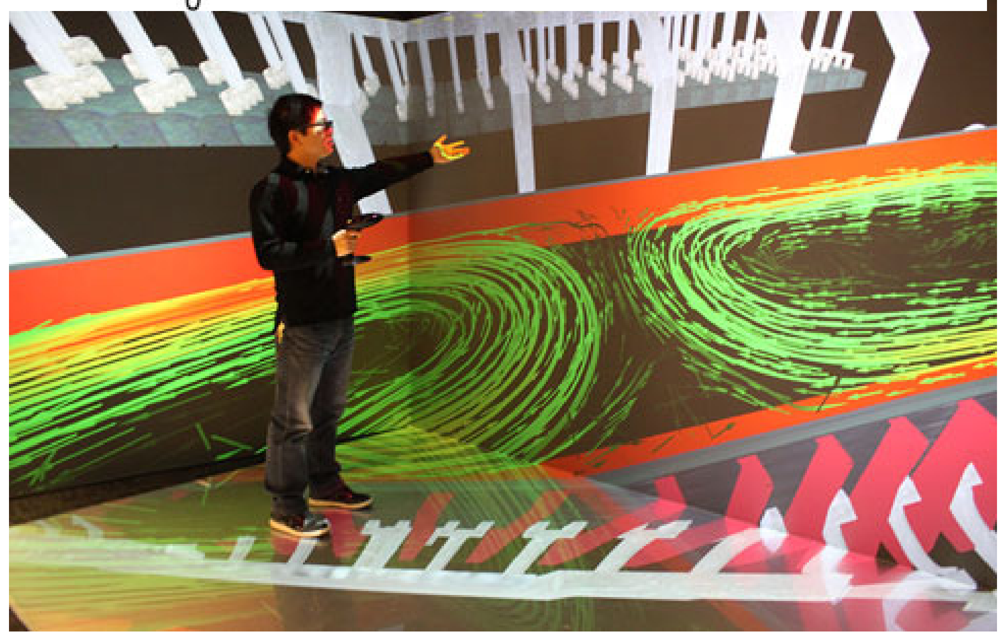

JOM, Vol. 65, No. 11, 2013

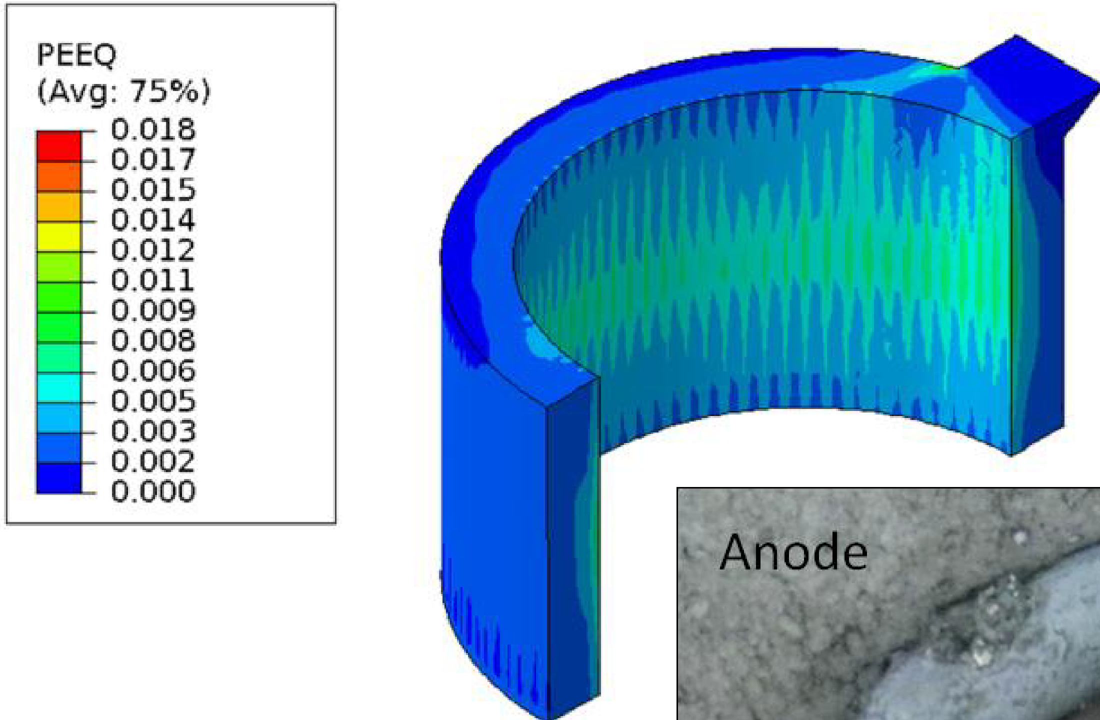
PEEQ
(Avg: 75%)
0.018
0.017
0.015
0.014
0.012
0.011
0.009
0.008
0.006
0.005
0.003
0.002
0.000


Anode
Crack on thimble
Stub

CFD simulation of dissolution process of alumina in an aluminum reduction cell with two-particle phase population balance model

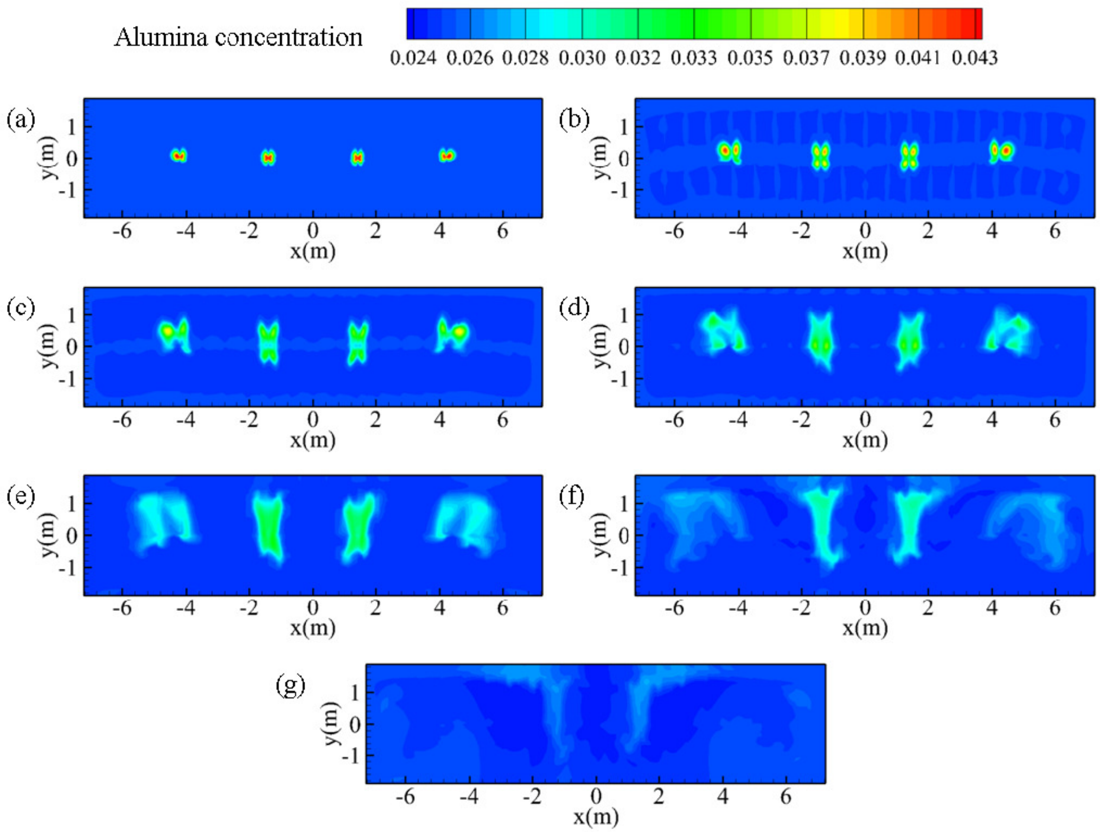

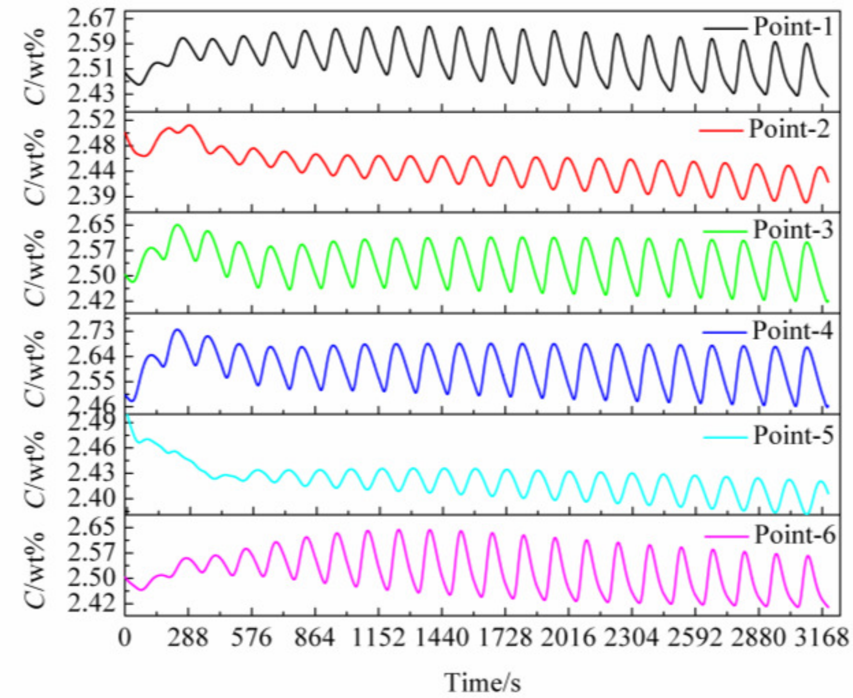

Applied Thermal Engineering, December 2014